ELIANA MARIA BARBOSA SOUTO

SLN AND NLC AS DRUG CARRIERS OF CLOTRIMAZOLE FOR HYDROGEL TOPICAL FORMULATIONS

Faculdade de Farmácia
Universidade do Porto
2003

ELIANA MARIA BARBOSA SOUTO

SLN AND NLC AS DRUG CARRIERS OF CLOTRIMAZOLE FOR HYDROGEL TOPICAL FORMULATIONS

FACULDADE DE FARMACIA
U. P.
BIBLIOTECA
Data 31 / 05 / 2004
Reg. 2656
Cota

FFM
SOU

Faculdade de Farmácia
Universidade do Porto
2003

ELIANA MARIA BARBOSA SOUTO

SLN AND NLC AS DRUG CARRIERS OF CLOTRIMAZOLE FOR HYDROGEL TOPICAL FORMULATIONS

TESE APRESENTADA PARA A OBTENÇÃO DO GRAU DE MESTRE
MESTRADO EM TECNOLOGIA FARMACÊUTICA

Faculdade de Farmácia
Universidade do Porto
2003

To my Parents and Grandparents

To my dearest Selma

To João

Acknowledgements.....xii

Abstract.....xiv

Resumo.....xvii

Zusammenfassung.....xx

Aim and organization of the thesis.....xxiii

Table index.....xxv

Figure index.....xxvii

Publications list.....xxxviii

Abbreviations.....xl

CHAPTER I – INTRODUCTION.....1

CHAPTER II – COLLOIDAL DRUG CARRIERS FOR TOPICAL ROUTE.....11

2.1. Structure, properties and functions of the skin.....13

2.2. Drug absorption through the skin.....15

2.3. Innovative drug carrier systems for topical administration.....18

2.3.1. Liposomes.....18

2.3.2. Niosomes.....20

2.3.3. Sphingosomes.....20

2.3.4. Microemulsions.....20

2.3.5. Multiple emulsions.....21

2.3.6. Polymeric nanoparticles.....22

2.3.7. Solid lipid nanoparticles (SLN).....23

2.3.7.1. Preparation methods of SLN.....25

2.3.7.1.1. High pressure homogenization technique.....25

2.3.7.1.1.1. Hot HPH.....26

2.3.7.1.1.2. Cold HPH.....26

2.3.7.1.2. Microemulsions based SLN preparations.....29

2.3.7.1.3. Solvent emulsification-evaporation technique.....31

2.3.7.1.4. Solvent displacement technique.....31

2.3.7.1.5. Emulsification-diffusion technique.....34

2.3.7.2. Models for incorporation of active compounds into SLN.....34

2.3.8. Nanostructured lipid carriers (NLC).....37

2.4. Lipid polymorphism.....41

CHAPTER III – MATERIALS.....45

3.1. Lipids.....47
3.1.1. *Dynasan*®112, 114, 116 and 118.....47
3.1.2. *Softisan*®154.....48
3.1.3. *Witepsol*®H5, S55, E75 and E85.....48
3.1.4. *Imwitor*®900 and 191.....49
3.1.5. *Compritol*®888 ATO.....49
3.1.6. *Precirol*® ATO 5.....49
3.1.7. *Precifac*® ATO 5.....50
3.1.8. *Apifil*®.....50
3.1.9. *Miglyol*®812.....51
3.2. Emulsifying agents.....51
3.2.1. *Tween*®80.....51
3.2.2. *Span*®85.....52
3.2.3. *Lutrol*®F68.....52
3.2.4. *Lipoid*®S75.....52
3.2.5. *Tego Care*®450.....53
3.2.6. *Tyloxapol*®.....53
3.2.7. *Lanette*®N.....53
3.3. Gel-forming agents.....54
3.3.1. Xanthan gum.....54
3.3.2. Hydroxyethylcellulose 4000.....54
3.3.3. *Carbopol*®934.....55
3.3.4. Chitosan.....55
3.4. Water.....56
3.5. Clotrimazole.....56
3.6. Other materials.....57
3.6.1. Glycerol 85%.....57
3.6.2. Sodium hydroxide.....58
3.6.3. Acetic acid.....58

CHAPTER IV – METHODS.....59

4.1. Preparation of SLN and NLC.....61
4.2. Preparation of hydrogels-loaded SLN and NLC.....62
4.3. Measurement of particle size and zeta potential.....63
4.3.1. Laser light diffraction.....63
4.3.2. Photon correlation spectroscopy.....64
4.3.3. Zeta potential and electrophoretic mobility.....66
4.4. Measurement of crystallinity and lipid modification.....68
4.4.1. Differential scanning calorimetry.....68
4.4.2. X-ray diffraction.....70
4.5. Light microscopy.....71
4.6. Assay of clotrimazole.....72
4.6.1. Assay of clotrimazole in SLN and NLC aqueous dispersions.....73
4.6.2. Assay of clotrimazole in the release studies.....74
4.7. Determination of the encapsulation parameters.....75
4.8. Evaluation of clotrimazole release profile from SLN and NLC aqueous dispersions.....76
4.9. Evaluation of rheological properties of SLN and NLC formulations.....77
4.9.1. Oscillation frequency sweep test.....81
4.9.2. Continuous shear investigations.....83
4.10. Evaluation of the occlusive properties of SLN and NLC formulations.....83

CHAPTER V – RESULTS AND DISCUSSION.....85

5.1. Clotrimazole-containing SLN and NLC preliminary studies.....87
5.1.1. Lipid screening for clotrimazole solubilization.....87
5.1.2. Surfactant selection for SLN and NLC preparation.....87
5.1.3. Preparation of different clotrimazole-containing SLN and NLC formulations.....92
5.1.4. Optimizing the homogenization conditions.....93
5.2. Physicochemical characterization of developed SLN and NLC formulations.....97
5.2.1. Encapsulation parameters.....97
5.2.2. Particle size.....98
5.2.3. Zeta potential.....99

5.2.4. DSC studies.....99
5.2.4.1. Crystalline status of bulk material.....100
5.2.4.2. Crystalline status of lipid matrix.....100
5.2.5. X-ray diffraction studies.....103
5.3. Stability of developed SLN and NLC formulations.....108
5.3.1. Encapsulation parameters.....108
5.3.2. Particle size.....115
5.3.2.1. Particle size stability of clotrimazole-free SLN and NLC formulations.....115
5.3.2.2. Particle size stability of clotrimazole-loaded SLN and NLC formulations.....117
5.3.2.3. Particle size stability of clotrimazole-free and clotrimazole-loaded SLN and NLC formulations as function of temperature of storage.....118
5.3.3. Zeta potential.....125
5.3.4. DSC studies.....126
5.3.4.1. Maintenance of crystalline status at room temperature.....127
5.3.4.2. Maintenance of crystalline status at different temperatures.....131
5.4. Clotrimazole release profiles of developed SLN and NLC formulations.....135
5.5. Incorporation of SLN and NLC into hydrogels.....139
5.6. Characterization of developed hydrogel formulations.....141
5.6.1. Particle size of SLN and NLC.....141
5.6.2. Zeta potential of SLN and NLC.....142
5.6.3. DSC studies.....144
5.7. Stability of developed hydrogel formulations.....149
5.7.1. Particle size of SLN and NLC.....149
5.7.1.1. SLN-containing hydrogel formulations.....149
5.7.1.2. NLC-containing hydrogel formulations.....158
5.7.2. Zeta potential of SLN and NLC.....163
5.7.3. DSC studies.....166
5.8. Rheological properties of SLN and NLC aqueous dispersions and hydrogels.....172
5.8.1. Oscillation frequency sweep test.....173
5.8.2. Continuous shear rheometry.....177
5.9. Occlusive properties of SLN and NLC aqueous dispersions and hydrogels.....182
5.9.1. Dependency upon the number of homogenization cycles.....182
5.9.2. Dependency upon sample mass.....186
5.9.3. Dependency upon lipid formulation type and presence of clotrimazole.....186

5.9.4. Dependency upon hydrogel type.....188

CHAPTER VI – CONCLUSIONS AND FUTURE TRENDS.....191

REFERENCE LIST.....201

ACKNOWLEDGEMENTS

As minhas primeiras palavras de agradecimento são dirigidas ao meu orientador, Prof. Dr. Carlos Maurício Barbosa, por me ter ministrado os seus conhecimentos e a sua visão científica. Desde o início do meu curso de Mestrado, todas as suas sugestões foram de um valor inqualificável para assegurar a profundidade e o nível científico de todo o trabalho que foi realizado. Devo ainda reconhecer-lhe todo o apoio pessoal que recebi, sempre que o meu futuro se apresentou agreste e hostil.

Die vorliegende Arbeit entstand am Fachbereich Pharmazie der Freien Universität Berlin unter Anleitung vor Herrn Prof. Dr. Rainer H. Müller. Er hat mir jeglichen zeitlichen, materiellen und inhaltlichen Spielraum gewährt. Hierfür bin ich ihm zu großem Dank verpflichtet. Ohne seinen großem persönlichen Einsatz wäre die vorliegende Arbeit in dieser Form nicht möglich gewesen.

Ao Prof. Dr. Sousa Lobo, agradeço-lhe o elevado valor pedagógico e nível de excelência que sempre qualificaram as suas aulas. Assim, não posso deixar de agradecer-lhe por ter sido aceite como aluna do IV Mestrado em Tecnologia Farmacêutica da Faculdade de Farmácia da Universidade do Porto. Agradeço-lhe pela amizade, imaginação e dedicação que sempre dispensou ao meu grupo.

Ebenso gilt mein besonderer Dank meiner Betreurin Dr. Sylvia Wissing für die motivierende Betreuung, die zahlreichen Anregungen im Rahmen dieser Arbeit sowie ihre Heranführung an die Themeatik des interessanten Themas und die sehr guten Arbeitsmöglichkeiten. Bei Dr. Sylvia Wissing möchte ich mich auch für ihre persönliche und fachliche Unterstützung und ihre große Hilfsbereitschaft während meiner gesamten Zeit am Institut danken.

Den Kolleginnen und Kollegen des Arbeitskreises, insbesondere Anne Saupe, Norma Hernandez, Dr. Silke Templin, Illona Buttle, Francesco Lai, Andreas Lemke, Cornelia Keck, Mario Fichera, Jan Möschwitzer, Boris Petri, Torsten Göppert, Felix Troester, Nadiem Bushrab, Aslihan Akkar, Marc Muchow, Katia Jores und Erol Yilmaz, danke ich für die ausgesprochen angenehme Arbeitsatmosphäre. Allen anderen mir nahestehenden Menschen im Arbeitskreis,

insbesondere Fr. Karsubke, Fr. Schmidt und Fr. Albrecht, danke ich für die mir entgegengebrachte Geduld und Ausdauer in der Zeit der Erstellung dieser Arbeit.

Das Land Berlin hat diese Arbeit mit einem Stipendium nach des Deutschen Akademischen Austauschdienstes (DAAD) unterstüzt. Ohne diese finanzielle Unterstützung wäre die Arbeit nicht in so kurzer Zeit möglich gewesen. Hierfür möchte ich meinen besonderen Dank aussprechen.

Aos meus colegas do Mestrado, Paulo Santos, Rui Gabriel, Margarita Dominguez, Carla Gomes e Gustavo Dias, quero expressar-lhes a minha sincera gratidão pela amizade, pelo afecto e bom humor que sempre caracterizou o nosso grupo. Agradeço, em especial, ao meu querido colega e amigo Paulo, por partilhar comigo os seus mais variados e interessantes pontos de vista.

Um agradecimento muito especial à Dra. Maribel Teixeira pelo seu profissionalismo, sugestões e apoio consistentes que sempre me dispensou.

Much of the credit of this work goes to the people that have made this thesis possible, directly or indirectly. I have no doubt that they were many and this manuscript is only a part of their help. The most important one is not visible because it is written itself across my face. Therefore, I am thankful to my dearest friends and family.

To Ana, Guida, Cris and Ana Maria, I thank you for your understanding and patience every time I deny your company. I thank you for your spontaneous generosity, friendship, trust and joy.

To Pedro Hugo, I thank you for your help every time I asked, for your promptitude to make people's life easier and for your friendship.

To my Grandparents, I thank you for your sincere and generous devotion, and for entrust me the task of responsibility since my childhood.

To my dearest sister Selma, I thank you for your dedicate and poetic life, and for your capability to influence the reality of my days. To you I have the greatest debt of gratitude, your unexpected truth!

To João, I thank you for my name, my position, my happiness, and my freedom. And, whatever is a mystery to you, it is a grater one your capability to surpass yourself.

And, Mum and Dad, I want to thank you for teaching me the highest of all duties, the one we owe to our selves!

ABSTRACT

In the last years, different carrier systems – liposomes, niosomes, sphingosomes, microemulsions, multiple emulsions, nanoparticles, etc. – are being used for pharmaceutical application, cosmetics, agricultural and food products, with the aim of modifying the release profile of the incorporated substances.

With regard to pharmaceutical application, new drug delivery systems have been developed in order to improve the therapeutic index of drugs, to optimize their therapeutic efficacy and to limit their side effects. The selection of a particular drug delivery system should be determined according to several considerations regarding, for instance, the *in vivo* therapeutic behaviour and interactions with the biological surroundings, the administration route, the use of excipients of accepted status, the possibility of industrial scale production and the costs.

Solid lipid nanoparticles (SLN) and nanostructured lipid carriers (NLC) are new drug delivery systems composed of a lipid matrix that is solid both at room and body temperature. SLN and NLC represent alternative colloidal carrier systems, combining many advantages of other carriers reported above. For instance, unlike lipid emulsions, which have a fluid core, the solid core of SLN and NLC reduces the mobility of incorporated drug molecules, thus preventing their leakage from the carrier. Nevertheless, in comparison to the solid matrix of polymeric nanoparticles, the drug release from SLN and NLC is usually faster.

One possible application of SLN and NLC aqueous dispersions is the topical administration, where these systems can be used for controlled drug release and stabilization against chemical degradation. Thus, these systems have been already used for incorporation of several drug substances for the treatment of skin and mucosal diseases.

Fungal infections are one of the main dermatological disorders. In general, their treatment is based on the use of imidazole-containing conventional formulations. However, the risk of skin and mucosal irritation and, especially, the lack of a prolonged release profile are disadvantages related to the use of conventional topical formulations.

The aim of the present thesis was the development and characterization of clotrimazole--containing SLN and NLC aqueous dispersions, as well as clotrimazole-loaded SLN and NLC containing hydrogels, for topical administration.

Clotrimazole is an imidazole drug with an effective broad spectrum against many fungi, and it was chosen as a model drug due to its high lipophilic character.

After a screening study using 15 different lipids, *Dynasan*®116 was chosen as the lipid matrix for SLN and NLC preparation by the hot high pressure homogenization technique, using *Tyloxapol*® as emulsifying agent.

Two different SLN aqueous dispersions [containing 10% and 20% (*m/m*) of lipid matrix] and one NLC aqueous dispersion [containing 20% (*m/m*) of lipid matrix] containing 5% of clotrimazole (*m/m*, with regard to the lipid matrix) were developed and characterized.

In order to characterize all developed formulations, the particle size, zeta potential and lipid crystallinity were determined using different approaches, such as photon correlation spectroscopy (PCS), light diffraction (LD), polarized light microscopy, differential scanning calorimetry (DSC) and x-ray diffraction. In addition, encapsulation efficiency and loading capacity of SLN and NLC, as well as clotrimazole release profiles, were also determined.

Results obtained by LD showed the colloidal size of prepared SLN and NLC. PCS analysis confirmed the presence of a mean particle size in nanometer range (between 180 and 215 nm), low polydispersity indices (between 0.175 and 0.225) and negative electric charge. Polarized light microscopy studies allowed excluding the existence of clotrimazole crystals insoluble in *Dynasan*®116. The presence of crystalline lipid in SLN and NLC was confirmed by DSC and x-ray diffraction. Obtained encapsulation efficiencies were higher than 64% and drug loading capacities were higher than 2.5%. In addition, all three developed formulations revealed the ability of controlling the drug release profile of clotrimazole.

The stability study of formulations was carried out during a period of three months at 4ºC, 20ºC and 40ºC. All developed SLN and NLC aqueous dispersions showed good physically and chemically stability. The presence of clotrimazole does not interfere either with particle size or with chemical stability of formulations. Encapsulation efficiencies remained higher than 50% and drug loading capacities higher than 2% for SLN and NLC formulations, after 21 days of storage at room temperature (20ºC).

SLN and NLC aqueous dispersions have been incorporated into four different hydrogels, prepared with different gel forming agents: xanthan gum, hydroxyethylcellulose, *Carbopol*®934 and chitosan.

After incorporation in semi-solid formulations, nanoparticles maintained their colloidal dimensions (between 170 and 330 nm) and their negative charge. SLN and NLC of chitosan hydrogels showed the highest mean particle size (330 nm) and presented a positive electric charge.

During the three months of storage period at room temperature (20ºC) SLN and NLC incorporated in the different hydrogels maintained their colloidal size. By DSC studies, it was observed that clotrimazole does not interfere with the gel forming agents during the same period of time.

With regard to rheological properties of semi-solid preparations, it was observed that the increase of lipidic content was responsible for the increase of elastic properties of formulations (increase of G' in comparison to G'').

Oclusive properties of SLN and NLC aqueous dispersions confirmed the importance of these carriers for increasing the occlusive and hydrating effects of semi-solid preparations for topical administration.

According to the obtained results in the present work, SLN and NLC appear to be useful carriers for topical delivery of clotrimazole and, therefore, will constitute a promising approach for controlling the release of this drug in the treatment of antifungal skin and mucosal disorders. In addition, some of semi-solid developed formulations – especially hydrogels prepared with xanthan gum and *Carbopol*®934 – showed appropriate properties for being good therapeutic systems for topical administration of clotrimazole.

RESUMO

Nos últimos anos têm sido desenvolvidos diferentes vectores de substâncias activas – lipossomas, niossomas, esfingossomas, microemulsões, emulsões múltiplas, nanopartículas, etc. – para utilização nas áreas farmacêutica e cosmética e também na agricultura e em produtos alimentares, com a finalidade de controlar o perfil de libertação das substâncias incorporadas.

No que se refere à área farmacêutica, estes novos sistemas visam essencialmente proporcionar um aumento do índice terapêutico e da eficácia terapêutica das substâncias incorporadas e reduzir os seus efeitos secundários. A selecção do vector mais adequado é determinada por um conjunto de factores, designadamente o seu comportamento *in vivo* e as interacções estabelecidas com o meio biológico, a via de administração pretendida, a utilização de excipientes aceites pelas autoridades, a possibilidade de produção do produto em escala industrial e os custos envolvidos.

As nanopartículas lipídicas sólidas (*Solid Lipid Nanoparticles*, SLN) e os vectores lipídicos nanoestruturados (*Nanostructured Lipid Carriers*, NLC) constituem sistemas muito recentes, formados por uma matriz lipídica que se apresenta no estado sólido, quer à temperatura ambiente, quer à temperatura corporal. As SLN e os NLC constituem alternativas vantajosas em relação aos restantes vectores, uma vez que conjugam algumas vantagens inerentes a cada um deles. Por exemplo, contrariamente às emulsões lipídicas, que comportam um núcleo interno líquido, o núcleo sólido das SLN e dos NLC reduz a mobilidade das substâncias incorporadas, evitando a sua difusão rápida para o exterior. No entanto, comparativamente às nanopartículas poliméricas, a libertação das substâncias activas a partir das SLN e dos NLC é, em regra, mais rápida.

Uma das possíveis aplicações das dispersões aquosas de SLN e de NLC consiste na administração tópica, em que estes sistemas são usados para controlar o perfil de libertação das substâncias activas incorporadas e para as proteger contra a degradação química. Assim, estes sistemas têm vindo a sido utilizados para vectorizar diversas substâncias activas, com vista ao tratamento tópico de patologias quer da pele quer das mucosas.

As infecções fúngicas constituem uma das principais dermatoses. Em geral, o seu tratamento é efectuado com base em formas farmacêuticas convencionais, contendo, designadamente, derivados imidazólicos. No entanto, o risco potencial de irritação da pele e das mucosas e,

especialmente, a impossibilidade de obtenção de uma libertação prolongada das substâncias activas constituem dificuldades inerentes às formas farmacêuticas convencionais.

O objectivo da presente tese consistiu no desenvolvimento e na caracterização de dispersões aquosas de SLN e de NLC contendo clotrimazol e também de hidrogeles contendo clotrimazol incorporado em SLN e em NLC, para administração cutânea.

O clotrimazol é um derivado imidazólico com um espectro alargado de acção contra numerosos fungos, tendo sido seleccionado como substância activa modelo para a realização do presente trabalho devido à sua lipofilia.

Após uma série de estudos preliminares, envolvendo 15 lípidos quimicamente distintos, o *Dynasan*®116 foi seleccionado para a preparação das SLN e dos NLC por homogeneização a alta pressão, realizada a quente, utilizando-se o *Tyloxapol*® como agente tensioactivo.

Foram desenvolvidas e caracterizadas duas dispersões aquosas de SLN [contendo 10% e 20% (*m/m*) de matriz lipídica] e uma dispersão aquosa de NLC [contendo 20% (*m/m*) de matriz lipídica], contendo 5% de clotrimazol (*m/m*, em relação à matriz lipídica).

A caracterização das formulações desenvolvidas consistiu na avaliação das dimensões das partículas, do seu potencial zeta e da cristalinidade, utilizando diferentes técnicas, como a espectroscopia de correlação fotónica (PCS), a difracção laser (LD), a microscopia de luz polarizada, a calorimetria diferencial de varrimento (DSC) e a difracção de raios X. Além disso, procedeu-se à determinação da eficácia de encapsulação e da capacidade de carga das SLN e dos NLC preparados e também ao estudo dos respectivos perfis de libertação do clotrimazol.

Os resultados obtidos por LD evidenciaram as dimensões coloidais das SLN e dos NLC preparados. A análise por PCS confirmou a obtenção de partículas com diâmetros médios nanométricos (entre 180 e 215 nm), baixos índices de polidispersão (entre 0,175 e 0,225) e carga eléctrica negativa. Os estudos de microscopia de luz polarizada permitiram excluir a existência de cristais de clotrimazol insolúveis no *Dynasan*®116. A presença de lipído cristalino nas SLN e nos NLC foi confirmada por DSC e por difracção de raios X. A eficácia de encapsulação apresentou-se superior a 64% e a capacidade de carga superior a 2,5% para todas as formulações. Além disso, as três formulações desenvolvidas evidenciaram capacidade para controlar o perfil de libertação do clotrimazol.

O estudo da estabilidade das formulações desenvolvidas decorreu durante um período de três meses, às temperaturas de 4ºC, 20ºC e 40ºC. Todas as dispersões aquosas de SLN e de NLC evidenciaram boa estabilidade, quer do ponto de vista físico, quer do ponto de vista químico. Verificou-se ainda que a presença de clotrimazol não interfere nas dimensões das partículas nem

na estabilidade química das formulações. Ao fim de 21 dias de armazenamento à temperatura ambiente (20°C), a eficácia de encapsulação manteve-se superior a 50% e a capacidade de carga superior a 2%, quer para as SLN, quer para os NLC.

As dispersões aquosas de SLN e NLC desenvolvidas foram, em seguida, incorporadas em quatro tipos de hidrogeles, preparados com diferentes agentes gelificantes: goma xantana, hidroxietilcelulose, *Carbopol*®934 e quitosano.

Imediatamente após a incorporação das dispersões aquosas de SLN e de NLC contendo clotrimazol nas formulações semi-sólidas, verificou-se que as nanopartículas mantinham as suas dimensões coloidais (entre 170 e 330 nm) e apresentavam-se carregadas negativamente. As SLN e os NLC incorporados nos hidrogeles preparados com quitosano apresentaram o diâmetro médio mais elevado (330 nm) e carga eléctrica positiva.

Durante o período de três meses, em que decorreu o estudo da estabilidade dos diferentes hidrogeles conservados à temperatura ambiente (20°C), verificou-se que as SLN e os NLC mantinham dimensões coloidais. Os estudos de DSC realizados durante este mesmo período demonstraram que o clotrimazol não estabelece interacções com os agentes gelificantes.

Em relação às propriedades reológicas das preparações semi-sólidas desenvolvidas, verificou-se que o aumento do conteúdo lipídico era acompanhado por um aumento das propriedades elásticas das preparações (aumento de G' comparativamente a G'').

As propriedades oclusivas das dispersões aquosas de SLN e de NLC confirmaram a sua capacidade para aumentar os efeitos oclusivo e hidratante das formulações semi-sólidas para aplicação tópica.

De acordo com os resultados obtidos no presente trabalho, as SLN e os NLC demonstraram constituir vectores adequados para a cedência do clotrimazol a nível tópico, podendo proporcionar uma estratégia promissora para a obtenção de uma libertação controlada desta substância activa no tratamento tópico de infecções fúngicas da pele ou das mucosas. Além disso, algumas das formulações desenvolvidas – em especial as correspondentes aos hidrogeles preparados com goma xantana e com *Carbopol*®934 – evidenciaram propriedades adequadas para constituírem sistemas terapêuticos apropriados para a aplicação tópica do clotrimazol.

ZUSAMMENFASSUNG

Während der letzten Jahre wurden verschiedene innovative Wirkstoffträgersysteme wie Liposomen, Niosomen, Sphingosomen, Mikroemulsionen, multiple Emulsionen und polymer Nanopartikel entwickelt, um eine kontrollierte oder verzögerte Wirkstofffreisetzung zu verbessern. Diese Systeme sollen es ermöglichen, den inkorporierten Arzneistoff nach der Applikation freizusetzen.

Die Wahl eines bestimmten Wirkstoffträgersystems sollte entsprechend einigen betreffend Betrachtungen, zum Beispiel, ihrer *in vivo* therapeutischen Leistung, dem Leitung Weg und ihren Abhängigkeiten mit den biologischen Umlagerungen, dem Gebrauch der Bindemittel des geltenden Status und der Möglichkeit der Produktion der industriellen Skala und ihrer Kosten festgestellt werden.

Die Entwicklung hochpotenter Wirkstoffe und deren Einführung in die Therapie lösten in den letzten Jahren intensive Forschungen auf dem Gebiet der pharmazeutische Technologie aus. Eine Einarbeitung dieser Stoffe in die klassischen Arzneiformen kann Überdosierungen und toxische Nebenwirkungen zur Folge haben. Probleme ergeben sich ebenfalls aus der Anreicherung von Wirktoffen in Organen und Geweben entsprechend ihres Verteilungsverhaltens. Aus dieser Problematik resultieren neue innovative Strategien bei der Optimierung von Arzneizubereitungen.

Feste Lipid-Nanopartikel (*Solid lipid nanoparticles*, SLN) und nanostrukturierte Lipidcarrier (*Nanostructured Lipid Carriers*, NLC) stellen alternative Trägersysteme zu Liposomen und Emulsionen zur topischen Anwendung dar. Sie bestehen aus festen Lipiden bzw. aus Mischungen von festen und flüssigen Lipiden oder lipidähnlichen Substanzen wobei vorwiegend physiologisch gut verträgliche Lipide verwendet werden. Im Vergleich zu nanopartikulären Carriersystemen aus Polymeren zeigen SLN und NLC eine relativ geringe Zytotoxizität. Gegenüber den Liposomendispersionen, die bezüglich als problematisch zu betracheten sind, haben SLN und NLC Dispersionen bei geeigneter Zusammensetzung den Vorteil der hohen physikalischen Stabilität auch nach einer Lagerung von über drei Jahren. Durch Inkorporation in die Lipidmatrix können chemisch instabile Wirkstoffe vor Zersetzung geschützt werden. Eine Variation der Wirkstofffreisetzung ist durch Inkorporation der SLN oder NLC in verschiedene halbfeste Grundlagen möglich. Neben einer verzögerten Freisetzung im Vergleich zu Nanoemulsionen besteht die Möglichkeit einer beschleunigten Freisetzung.

Im Rahmen der vorliegenden Arbeit beschäftigte ich mich mit der Entwicklung und Charakterisierung von SLN und NLC flüssigen Dispersionen. Um die Eignung von SLN und NLC zur verzörgerten Arzneistoffreisetzung zu untersuchen, wurde Clotrimazol als lipophiler Modellarzneistoff eingesetzt. Clotrimazol ist ein Chlor-substituiertes Triphenylmethylimidazol mit einem Breitspektrum in einem sehr hohen Prozentsatz bei verschiedenen Pilzerkrankungen wirksam. Als Lipidmatrix zur Herstellung von SLN und NLC wurde von 15 verschiedene Lipide *Dynasan*®116 ausgewählt. Zur Herstellung der clotrimazolhaltigen und Placebo SLN und NLC wurde das Verfahren der Heißhomogenisation eingesetzet. *Tyloxapol*® wurde als Emulgator ausgewählt.

Zur Messung der Partikelgröße von SLN und NLC können unterschiedliche Verfahren zum Einsatz kommen, wie Photonenkorretationsspektroskopie und Laserdiffraktometrie. Die Partikelladdung gibt Aufschuß über die Stabilität einer Dispersion gegenüber Lagerung, Elektrolyteinfluß oder Scherkraft. Daher wurde Zetapotential der hergestellten SLN und NLC und der weiterverarbeiteten halbfesten Zubereitungen mittels Laser-Doppler-Anemometrie bestimmt. Zur Charakterisierung des Wirkstoffeinschlusses in SLN und NLC wurden ergänzend dynamische Differenz-Wärmestrom-Kalorimetrie, Röntgendiffraktometrie und Mikroskopie mit polarisiertem Licht durchgeführt.

Nach Vorbereitung clotrimazol-geladener SLN und NLC, wurden von eines E.E. stark als 64% und von der Wirkstoff, die stark als 2,5% lädt, für alle Proben erreicht. Außerdem könnte ein E.E. stark als 50% für alle nachgeforschten Formulierungen nach 21 Tagen Ablage bei Raumtemperatur beobachtet werden, ein kontrolliertes Freisetzungsprofil für clotrimazol wurde mit diesen Formulierungen erzielt. Auch hier konnte festgestellt werden, dass bei den SLN und NLC Dispersionen die Freisetzungsprofile fast identisch waren. Beide konnten die Freisetzung verlangsamen.

Nach eingehender Entwicklung und Charakterisierung der flüssigen Dispersionen wurden diese zu halbfesten Endprodukten weiterverarbeitet. Eine einfache topische Arzneiform stellen Hydrogele dar. Diese enthalten notwendigerweise einen Gelbildner, in der Regel ein Polymer. Vier verschiedene Hydrogele (Xanthan Gum, Hydroxyethylcellulose, *Carbopol*®934 und Chitosan) wurden produziert. Aufgrund der bekannten Instabilität der SLN und NLC Dispersionen in Gegenwart von Elektrolyten oder nach mechanischem Energieeintrag, musste zunächst die nanopartikuläre Struktur der SLN in diesen Gelen sichergestellt werden. Es zeigte sich, dass SLN und NLC in Gelen keine Aggregatbildung aufweisen. Auch zeigten die SLN und

NLC in Hydrogele keine nennenswerten polymorphen Transformationen innerhalb von Lagerungszeiten bis zu 3 Monaten. Die untersuchten SLN und NLC erwiesen sich somit in den Hydrogelegrundlagen als physikalisch stabil. In der weiteren Entwicklung wurden die okklusive Eigenschaften von SLN und NLC untersucht.

Zusammenfassend ist es in dieser Arbeit gelungen, Clotrimazol SLN und NLC für eine topische Applikation zu entwickeln. Die Ergebnisse zeigen weiterhin, dass SLN und NLC als Trägersysteme für eine verzörgerte Arzneistofffreisetzung geeignet sind. Andererseits ermöglicht diese Dynamik der Systeme, dass gezielt Freisetzungseigenschaften über bestimmte Trigger beeinflußt werden können. Diese Systeme zeigten sich aufgrund ihrer physikalischen Stabilität und ihrer rheologischen Eigenschaften als gut geeignet für das Versprühen mittels eines Pumpzerstäubers.

AIM AND ORGANIZATION OF THE THESIS

The aim of the present thesis was the investigation of the promising potential of lipid nanoparticles, such as solid lipid nanoparticles (SLN) and nanostructured lipid carriers (NLC), as new carrier systems for clotrimazole for the treatment of fungal infections of the skin and mucosa.

Concerning the organization of the present dissertation, it has been divided in 6 different chapters.

In Chapter I a characterization of SLN and NLC as new drug delivery systems, as well as their importance for site-specific drug delivery, is provided. In this chapter the most important lipids and emulsifying agents used for the preparation of these systems are presented, as well as some examples of compounds that have been incorporated in these carriers.

Chapter II comprises a theoretic outfit of the main theme of this dissertation. The physiological characteristics of the topical route are described in terms of structure, properties and functions of the skin and mucosa, and the main aspects concerning drug absorption through this route are also presented. In this chapter the most important innovative systems available for topical drug delivery are reviewed. It is emphasized the use and the development of SLN and NLC and their advantages over other drug carrier systems. An introduction to lipid polymorphism is presented, in order to understand the main thermodynamic modification that the lipid material can suffer during particle preparation and storage time.

Chapter III describes all the materials used during this present study. This chapter is devoted to the physicochemical characteristics of the different lipids and emulsifying agents used for SLN and NLC preparation, as well as the characterization of clotrimazole, purified water, gel forming agents and other materials used in the research study.

In Chapter IV the adopted preparation methods of SLN and NLC aqueous dispersions and hydrogels, as well as the analytical procedures used to characterize the developed formulations, are described in detail.

In Chapter V all the results obtained are reunited and discussed. This chapter was chronologically organized in order to describe the development and the characterization of the formulations containing SLN and NLC as drug carriers of clotrimazole for topical administration.

Finally, Chapter VI is devoted to the main conclusions of these investigations and opens the future fields and perspectives for further investigations using SLN and NLC as drug delivery systems.

TABLE INDEX

Table I Examples of the most frequently used lipids for the preparation of SLN and NLC.

Table II Examples of the most frequently used emulsifying agents for the preparation of SLN and NLC.

Table III Examples of drugs and other substances incorporated into SLN and/or NLC.

Table IV Potential advantages of lipid suspensions over lipid emulsions due to the solid state properties.

Table V Characterization of the crystal systems.

Table VI Three dimensional structure of the crystal order in the three main polymorphs from monoacid triacylglycerols.

Table VII Main typical properties of some *Witepsol* bases.

Table VIII Solubility studies of clotrimazole in different lipids at 90°C and at 20°C.

Table IX First SLN formulations tested with 20% of lipid and the obtained results one day and one week after preparation.

Table X Composition of the prepared SLN formulations.

Table XI Composition of the prepared NLC formulations.

Table XII E.E. and loading capacity of clotrimazole into SLN and NLC one day after preparation.

Table XIII PCS diameter, PI and d99% diameter of SLN formulations on day 1 of storage at 20°C.

Table XIV PCS diameter, PI and d99% diameter of NLC formulations on day 1 of storage at 20°C.

Table XV Zeta potential of SLN formulations on day 1 of storage at 20°C.

Table XVI Zeta potential of NLC formulations on day 1 of storage at 20°C.

Table XVII DSC results of clotrimazole-free SLN and NLC aqueous dispersions, as a function of storage time at room temperature (20°C).

Table XVIII DSC results of clotrimazole-loaded SLN and NLC aqueous dispersions, as a function of storage time at room temperature (20°C).

Table XIX DSC results of clotrimazole-free SLN and NLC aqueous dispersions as a function of storage temperature, obtained after 90 days of storage.

Table XX DSC results of clotrimazole-loaded SLN and NLC aqueous dispersions as a function of storage temperature, obtained after 90 days of storage.

Table XXI Composition of the investigated SLN-containing hydrogels formulations.

Table XXII Composition of the investigated NLC-containing hydrogels formulations.

Table XXIII PCS diameter, PI and LD (d99%) diameter of SLN-containing hydrogel formulations on day 1 of storage at 20°C.

Table XXIV PCS diameter, PI and LD (d99%) diameter of NLC-containing hydrogel formulations on day 1 of storage at 20°C.

Table XXV Zeta potential of SLN-containing hydrogel formulations on day 1 of storage at room temperature (20°C).

Table XXVI Zeta potential of NLC-containing hydrogel formulations on day 1 of storage at room temperature (20°C).

Table XXVII DSC results of clotrimazole-free SLN and NLC aqueous dispersions before and after incorporation into different four hydrogels recorded after 1 day of storage at room temperature (20°C).

Table XXVIII DSC results of clotrimazole-loaded SLN and NLC aqueous dispersions before and after incorporation into different four hydrogels recorded after 1 day of storage at room temperature (20°C).

Table XXIX DSC results of clotrimazole-loaded SLN and NLC aqueous dispersions after their incorporation into different hydrogel formulations, obtained on day 1 and 90 after production.

FIGURE INDEX

Figure 2.1 Schematic representation of the skin structure, showing its many components in an ideal arrangement.

Figure 2.2 Schematic procedure of SLN prepared by hot HPH technique.

Figure 2.3 Schematic procedure of SLN prepared by cold HPH technique.

Figure 2.4 Schematic procedure of SLN preparation by microemulsion technique.

Figure 2.5 Schematic procedure of SLN preparation by solvent emulsification-evaporation technique.

Figure 2.6 Schematic procedure of SLN preparation by solvent displacement technique.

Figure 2.7 Schematic procedure of SLN preparation by emulsification-diffusion technique.

Figure 2.8 Models of incorporation of active compounds into SLN.

Figure 2.9 Differences between a perfect crystal in SLN in comparison to a structure with imperfections in NLC.

Figure 2.10 The three types of NLC compared to the relatively ordered matrix of SLN.

Figure 2.11 Triggered drug release and supersaturation effect.

Figure 3.1 Structural formula of clotrimazole.

Figure 4.1 The principle of HPH.

Figure 4.2 Discontinuous *APV Micron Lab 40* used for the production of SLN and NLC.

Figure 4.3 Principle of operation of a laser diffractometer.

Figure 4.4 Schematic representation of a laser diffractometer.

Figure 4.5 Principal set up of PCS.

Figure 4.6 Schematic representation of different surface potentials associated to the particle in aqueous medium.

Figure 4.7 Schematic representation of x-ray diffraction.

Figure 4.8 Calibration curve of clotrimazole in diethyl ether.

Figure 4.9 Calibration curve of clotrimazole in a solution of 100 mM acetate buffer, pH 6.0 with 35% (*V/V*) of dioxane.

Figure 4.10 Schematic representation of a Franz diffusion cell.

Figure 4.11 Schematic model for demonstrating the components of classic viscous flow.

Figure 4.12 The four basic types of rheograms.

Figure 4.13 Schematic representation of a cone-and-plate rheometer.

Figure 5.1 Micrographical picture of 1% (*m/m*) of clotrimazole-containing *Witepsol*®85 at 20°C, (a) without using polarized light, and (b) using polarized light.

Figure 5.2 Particle size of the first SLN formulations measured by LD (d99%) on day 1 and day 7 after preparation.

Figure 5.3 Particle size of SLN formulation D10% measured by LD (d95%) after 1 to 5 homogenization cycles, on day 0 and after 7, 14 and 30 days of storage at 20°C.

Figure 5.4 Mean particle size and PI of SLN formulation D10% measured by PCS after 1 to 5 homogenization cycles, on day 0 and after 7, 14 and 30 days of storage at 20°C.

Figure 5.5 Particle size of SLN formulation D20% measured by LD (d95%) after 1 to 5 homogenization cycles, on day 0 and after 7, 14 and 30 days of storage at 20°C.

Figure 5.6 Mean particle size and PI of SLN formulation D20% measured by PCS after 1 to 5 homogenization cycles, on day 0 and after 7, 14 and 30 days of storage at 20°C.

Figure 5.7 Particle size of NLC formulation DM20% measured by LD (d95%) after 1 to 5 homogenization cycles, on day 0 and after 7, 14 and 30 days of storage at 20°C.

Figure 5.8 Mean particle size and PI of NLC formulation DM20% measured by PCS after 1 to 5 homogenization cycles, on day 0 and after 7, 14 and 30 days of storage at 20°C.

Figure 5.9 DSC curves of glyceryl tripalmitate (*Dynasan*®116) bulk material and of a mixture of *Dynasan*®116 with 5% (*m/m*) of clotrimazole.

Figure 5.10 DSC curves of D10% (clotrimazole-free) and D10%C (clotrimazole-loaded) SLN formulations, after 7 days of storage at 20°C.

Figure 5.11 DSC curves of D20% (clotrimazole-free) and D20%C (clotrimazole-loaded) SLN formulations, after 7 days of storage at 20°C.

Figure 5.12 DSC curves of DM20% (clotrimazole-free) and DM20%C (clotrimazole-loaded) NLC formulations, after 7 days of storage at 20°C.

Figure 5.13 WAXS curve of glyceryl tripalmitate (*Dynasan*®116) bulk material.

Figure 5.14 WAXS curve of SLN formulation D10%.

Figure 5.15 WAXS curve of SLN formulation D10%C.

Figure 5.16 WAXS curve of SLN formulation D20%.

Figure 5.17 WAXS curve of SLN formulation D20%C.

Figure 5.18 WAXS curve of NLC formulation DM20%.

Figure 5.19 WAXS curve of NLC formulation DM20%C.

Figure 5.20 Variation of E.E. of clotrimazole in D10%C, measured after 1, 3, 7, 14 and 21 days of storage at room temperature (20°C).

Figure 5.21 Variation of drug loading capacity of D10%C, measured after 1, 3, 7, 14 and 21 days of storage at room temperature (20°C).

Figure 5.22 Variation of E.E. of clotrimazole in D20%C, measured after 1, 3, 7, 14 and 21 days of storage at room temperature (20°C).

Figure 5.23 Variation of drug loading capacity of D20%C, measured after 1, 3, 7, 14 and 21 days of storage at room temperature (20°C).

Figure 5.24 Variation of E.E. of clotrimazole in DM20%C, measured after 1, 3, 7, 14 and 21 days of storage at room temperature (20°C).

Figure 5.25 Variation of drug loading capacity of DM20%C, measured after 1, 3, 7, 14 and 21 days of storage at room temperature (20°C).

Figure 5.26 E.E. of clotrimazole-loaded lipid nanoparticles (D10%C, D20%C and DM20%C) on day 21 of storage at room temperature (20°C), as a function of E.E. obtained on day 1.

Figure 5.27 Loading capacity of clotrimazole-loaded lipid nanoparticles (D10%C, D20%C and DM20%C) on day 21 of storage at room temperature (20°C), as a function of loading capacity obtained on day 1.

Figure 5.28 Triggered release of active compounds by controlling the transformation from β and β' to β.

Figure 5.29 Particle size of clotrimazole-free SLN and NLC formulations (D10%, D20% and DM20%) measured by LD (d99%), after 1, 30, 60 and 90 days of storage at room temperature (20°C).

Figure 5.30 Mean particle size and PI of clotrimazole-free SLN and NLC formulations (D10%, D20% and DM20%) measured by PCS, after 1, 30, 60 and 90 days of storage at room temperature (20°C).

Figure 5.31 Particle size of clotrimazole-loaded SLN and NLC formulations (D10%C, D20%C and DM20%C) measured by LD (d99%), after 1, 30, 60 and 90 days of storage at room temperature (20°C).

Figure 5.32 Mean particle size and PI of clotrimazole-loaded SLN and NLC formulations (D10%C, D20%C and DM20%C) measured by PCS, after 1, 30, 60 and 90 days of storage at room temperature (20°C).

Figure 5.33 Particle size of clotrimazole-free SLN formulation D10% measured by LD (d99%), after 1, 7, 14, 30, 60 and 90 days of storage at 4°C, 20°C and 40°C.

Figure 5.34 Mean particle size and PI of clotrimazole-free SLN formulation D10% measured by PCS, after 1, 7, 14, 30, 60 and 90 days of storage at 4°C, 20°C and 40°C.

Figure 5.35 Particle size of clotrimazole-loaded SLN formulation D10%C measured by LD (d99%), after 1, 7, 14, 30, 60 and 90 days of storage at 4°C, 20°C and 40°C.

Figure 5.36 Mean particle size and PI of clotrimazole-loaded SLN formulation D10%C measured by PCS, after 1, 7, 14, 30, 60 and 90 days of storage at 4°C, 20°C and 40°C.

Figure 5.37 Particle size of clotrimazole-free SLN formulation D20% measured by LD (d99%), after 1, 7, 14, 30, 60 and 90 days of storage at 20°C and 40°C.

Figure 5.38 Mean particle size and PI of clotrimazole-free SLN formulation D20% measured by PCS, after 1, 7, 14, 30, 60 and 90 days of storage at 20°C and 40°C.

Figure 5.39 Particle size of clotrimazole-loaded SLN formulation D20%C measured by LD (d99%), after 1, 7, 14, 30, 60 and 90 days of storage at 20°C and 40°C.

Figure 5.40 Mean particle size and PI of clotrimazole-loaded SLN formulation D20%C measured by PCS, after 1, 7, 14, 30, 60 and 90 days of storage at 20°C and 40°C.

Figure 5.41 Particle size of clotrimazole-free NLC formulation DM20% measured by LD (d99%), after 1, 7, 14, 30, 60 and 90 days of storage at 4°C, 20°C and 40°C.

Figure 5.42 Mean particle size and PI of clotrimazole-free NLC formulation DM20% measured by PCS, after 1, 7, 14, 30, 60 and 90 days of storage at 4°C, 20°C and 40°C.

Figure 5.43 Particle size of clotrimazole-loaded NLC formulation DM20%C measured by LD (d99%), after 1, 7, 14, 30, 60 and 90 days of storage at 4°C, 20°C and 40°C.

Figure 5.44 Mean particle size and PI of clotrimazole-loaded NLC formulation DM20%C measured by PCS, after 1, 7, 14, 30, 60 and 90 days of storage at 4°C, 20°C and 40°C.

Figure 5.45 Zeta potential of clotrimazole-free and clotrimazole-loaded SLN and NLC formulations, after 1, 30 and 90 days of storage at room temperature (20°C).

Figure 5.46 DSC curves of clotrimazole-free SLN formulation D10% after 7 and 90 days of storage at room temperature (20°C).

Figure 5.47 DSC curves of clotrimazole-loaded SLN formulation D10%C after 7 and 90 days of storage at room temperature (20°C).

Figure 5.48 DSC curves of clotrimazole-free SLN formulation D20% after 7 and 90 days of storage at room temperature (20°C).

Figure 5.49 DSC curves of clotrimazole-loaded SLN formulation D20%C after 7 and 90 days of storage at room temperature (20°C).

Figure 5.50 DSC curves of clotrimazole-free NLC formulation DM20% after 7 and 90 days of storage at room temperature (20°C).

Figure 5.51 DSC curves of clotrimazole-loaded NLC formulation DM20%C after 7 and 90 days of storage at room temperature (20°C).

Figure 5.52 DSC curves of clotrimazole-free SLN formulation D10% after 90 days of storage at 4°C, 20°C and 40°C.

Figure 5.53 DSC curves of clotrimazole-loaded SLN formulation D10%C after 90 days of storage at 4°C, 20°C and 40°C.

Figure 5.54 DSC curves of clotrimazole-free SLN formulation D20% after 90 days of storage at 4°C, 20°C and 40°C.

Figure 5.55 DSC curves of clotrimazole-loaded SLN formulation D20%C after 90 days of storage at 4°C, 20°C and 40°C.

Figure 5.56 DSC curves of clotrimazole-free NLC formulation DM20% after 90 days of storage at 4°C, 20°C and 40°C.

Figure 5.57 DSC curves of clotrimazole-loaded NLC formulation DM20%C after 90 days of storage at 4°C, 20°C and 40°C.

Figure 5.58 *In vitro* release profiles of clotrimazole from SLN and NLC formulations containing 5% of drug, with regard to the lipid matrix.

Figure 5.59 Partitioning effects on drug during the production of SLN by the hot HPH technique.

Figure 5.60 DSC curves of clotrimazole-free SLN formulation D10% as pure aqueous dispersion and when incorporated into four different hydrogels recorded after 1 day of storage at 20°C.

Figure 5.61 DSC curves of clotrimazole-loaded SLN formulation D10%C as pure aqueous dispersion and when incorporated into four different hydrogels recorded after 1 day of storage at 20°C.

Figure 5.62 DSC curves of clotrimazole-free SLN formulation D20% as pure aqueous dispersion and when incorporated into four different hydrogels recorded after 1 day of storage at 20°C.

Figure 5.63 DSC curves of clotrimazole-loaded SLN formulation D20%C as pure aqueous dispersion and when incorporated into four different hydrogels recorded after 1 day of storage at 20°C.

Figure 5.64 DSC curves of clotrimazole-free NLC formulation DM20% as pure aqueous dispersion and when incorporated into four different hydrogels recorded after 1 day of storage at 20°C.

Figure 5.65 DSC curves of clotrimazole-loaded NLC formulation DM20%C as pure aqueous dispersion and when incorporated into four different hydrogels recorded after 1 day of storage at 20°C.

Figure 5.66 Particle size of clotrimazole-free and clotrimazole-loaded SLN formulations D10% and D10%C incorporated into XG hydrogels measured by LD (d50%, d95% and d99%), after 1, 30, 60 and 90 days of storage at room temperature (20°C).

Figure 5.67 Mean particle size measured by PCS and PI of clotrimazole-free and clotrimazole-loaded SLN formulations D10% and D10%C incorporated into XG hydrogels, after 1, 30, 60 and 90 days of storage at room temperature (20°C).

Figure 5.68 Particle size of clotrimazole-free and clotrimazole-loaded SLN formulations D10% and D10%C incorporated into HEC hydrogels measured by LD (d50%, d95% and d99%), after 1, 30, 60 and 90 days of storage at room temperature (20°C).

Figure 5.69 Mean particle size measured by PCS and PI of clotrimazole-free and clotrimazole-loaded SLN formulations D10% and D10%C incorporated into HEC hydrogels, after 1, 30, 60 and 90 days of storage at room temperature (20°C).

Figure 5.70 Particle size of clotrimazole-free and clotrimazole-loaded SLN formulations D10% and D10%C incorporated into PA hydrogels measured by LD (d50%, d95% and d99%), after 1, 30, 60 and 90 days of storage at room temperature (20°C).

Figure 5.71 Mean particle size measured by PCS and PI of clotrimazole-free and clotrimazole-loaded SLN formulations D10% and D10%C incorporated into PA hydrogels, after 1, 30, 60 and 90 days of storage at room temperature (20°C).

Figure 5.72 Particle size of clotrimazole-free and clotrimazole-loaded SLN formulations D10% and D10%C incorporated into CH hydrogels measured by LD (d50%, d95% and d99%), after 1, 30, 60 and 90 days of storage at room temperature (20°C).

Figure 5.73 Mean particle size measured by PCS and PI of clotrimazole-free and clotrimazole-loaded SLN formulations D10% and D10%C incorporated into CH hydrogels, after 1, 30, 60 and 90 days of storage at room temperature (20°C).

Figure 5.74 Particle size of clotrimazole-free and clotrimazole-loaded SLN formulations D20% and D20%C incorporated into XG hydrogels measured by LD (d50%, d95% and d99%), after 1, 30, 60 and 90 days of storage at room temperature (20°C).

Figure 5.75 Mean particle size measured by PCS and PI of clotrimazole-free and clotrimazole-loaded SLN formulations D20% and D20%C incorporated into XG hydrogels, after 1, 30, 60 and 90 days of storage at room temperature (20°C).

Figure 5.76 Particle size of clotrimazole-free and clotrimazole-loaded SLN formulations D20% and D20%C incorporated into HEC hydrogels measured by LD (d50%, d95% and d99%), after 1, 30, 60 and 90 days of storage at room temperature (20°C).

Figure 5.77 Mean particle size measured by PCS and PI of clotrimazole-free and clotrimazole-loaded SLN formulations D20% and D20%C incorporated into HEC hydrogels, after 1, 30, 60 and 90 days of storage at room temperature (20°C).

Figure 5.78 Particle size of clotrimazole-free and clotrimazole-loaded SLN formulations D20% and D20%C incorporated into PA hydrogels measured by LD (d50%, d95% and d99%), after 1, 30, 60 and 90 days of storage at room temperature (20°C).

Figure 5.79 Mean particle size measured by PCS and PI of clotrimazole-free and clotrimazole-loaded SLN formulations D20% and D20%C incorporated into PA hydrogels, after 1, 30, 60 and 90 days of storage at room temperature (20°C).

Figure 5.80 Particle size of clotrimazole-free and clotrimazole-loaded SLN formulations D20% and D20%C incorporated into CH hydrogels measured by LD (d50%, d95% and d99%), after 1, 30, 60 and 90 days of storage at room temperature (20°C).

Figure 5.81 Mean particle size measured by PCS and PI of clotrimazole-free and clotrimazole-loaded SLN formulations D20% and D20%C incorporated into CH hydrogels, after 1, 30, 60 and 90 days of storage at room temperature (20°C).

Figure 5.82 Particle size of clotrimazole-free and clotrimazole-loaded NLC formulations DM20% and DM20%C incorporated into XG hydrogels measured by LD (d50%, d95% and d99%), after 1, 30, 60 and 90 days of storage at room temperature (20°C).

Figure 5.83 Mean particle size measured by PCS and PI of clotrimazole-free and clotrimazole-loaded NLC formulations DM20% and DM20%C incorporated into XG hydrogels, after 1, 30, 60 and 90 days of storage at room temperature (20°C).

Figure 5.84 Particle size of clotrimazole-free and clotrimazole-loaded NLC formulations DM20% and DM20%C incorporated into HEC hydrogels measured by LD (d50%, d95% and d99%) after 1, 30, 60 and 90 days of storage at room temperature (20°C).

Figure 5.85 Mean particle size measured by PCS and PI of clotrimazole-free and clotrimazole-loaded NLC formulations DM20% and DM20%C incorporated into HEC hydrogels, after 1, 30, 60 and 90 days of storage at room temperature (20°C).

Figure 5.86 Particle size of clotrimazole-free and clotrimazole-loaded NLC formulations DM20% and DM20%C incorporated into PA hydrogels measured by LD (d50%, d95% and d99%), after 1, 30, 60 and 90 days of storage at room temperature (20°C).

Figure 5.87 Mean particle size measured by PCS and PI of clotrimazole-free and clotrimazole-loaded NLC formulations DM20% and DM20%C incorporated into PA hydrogels, after 1, 30, 60 and 90 days of storage at room temperature (20°C).

Figure 5.88 Particle size of clotrimazole-free and clotrimazole-loaded NLC formulations DM20% and DM20%C incorporated into CH hydrogels measured by LD (d50%, d95% and d99%), after 1, 30, 60 and 90 days of storage at room temperature (20°C).

Figure 5.89 Mean particle size measured by PCS and PI of clotrimazole-free and clotrimazole-loaded NLC formulations DM20% and DM20%C incorporated into CH hydrogels after 1, 30, 60 and 90 days of storage at room temperature (20°C).

Figure 5.90 Zeta potential of clotrimazole-free and clotrimazole-loaded SLN containing 10% of lipid matrix when incorporated into four different hydrogels, measured on day 1 and day 90 after production and stored at room temperature (20°C).

Figure 5.91 Zeta potential of clotrimazole-free and clotrimazole-loaded SLN containing 20% of lipid matrix when incorporated into four different hydrogels, measured on day 1 and day 90 after production and stored at room temperature (20°C).

Figure 5.92 Zeta potential of clotrimazole-free and clotrimazole-loaded NLC containing 20% of lipid matrix when incorporated into four different hydrogels, measured on day 1 and day 90 after production and stored at room temperature (20°C).

Figure 5.93 DSC curves of D10%C SLN formulation incorporated into XG hydrogel after 1 and 90 days of storage at room temperature (20°C).

Figure 5.94 DSC curves of D10%C SLN formulation incorporated into HEC hydrogel after 1 and 90 days of storage at room temperature (20°C).

Figure 5.95 DSC curves of D10%C SLN formulation incorporated into PA hydrogel after 1 and 90 days of storage at room temperature (20°C).

Figure 5.96 DSC curves of D10%C SLN formulation incorporated into CH hydrogel after 1 and 90 days of storage at room temperature (20°C).

Figure 5.97 DSC curves of D20%C SLN formulation incorporated into XG hydrogel after 1 and 90 days of storage at room temperature (20°C).

Figure 5.98 DSC curves of D20%C SLN formulation incorporated into HEC hydrogel after 1 and 90 days of storage at room temperature (20°C).

Figure 5.99 DSC curves of D20%C SLN formulation incorporated into PA hydrogel after 1 and 90 days of storage at room temperature (20°C).

Figure 5.100 DSC curves of D20%C SLN formulation incorporated into CH hydrogel after 1 and 90 days of storage at room temperature (20°C).

Figure 5.101 DSC curves of DM20%C NLC formulation incorporated into XG hydrogel after 1 and 90 days of storage at room temperature (20°C).

Figure 5.102 DSC curves of DM20%C NLC formulation incorporated into HEC hydrogel after 1 and 90 days of storage at room temperature (20°C).

Figure 5.103 DSC curves of DM20%C NLC formulation incorporated into PA hydrogel after 1 and 90 days of storage at room temperature (20°C).

Figure 5.104 DSC curves of DM20%C NLC formulation incorporated into CH hydrogel after 1 and 90 days of storage at 20°C.

Figure 5.105 Storage modulus (G'), loss modulus (G'') and complex viscosity (η*) of clotrimazole-free SLN formulation D10%, as a function of the frequency at a constant stress amplitude of 5 Pa.

Figure 5.106 Storage modulus (G'), loss modulus (G'') and complex viscosity (η*) of clotrimazole-loaded SLN formulation D10%C, as a function of the frequency at a constant stress amplitude of 5 Pa.

Figure 5.107 Storage modulus (G'), loss modulus (G'') and complex viscosity (η*) of clotrimazole-free SLN formulation D20%, as a function of the frequency at a constant stress amplitude of 5 Pa.

Figure 5.108 Storage modulus (G'), loss modulus (G'') and complex viscosity (η*) of clotrimazole-loaded SLN formulation D20%C, as a function of the frequency at a constant stress amplitude of 5 Pa.

Figure 5.109 Storage modulus (G'), loss modulus (G'') and complex viscosity (η*) of clotrimazole-free NLC formulation DM20%, as a function of the frequency at a constant stress amplitude of 5 Pa.

Figure 5.110 Storage modulus (G'), loss modulus (G'') and complex viscosity (η*) of clotrimazole-loaded NLC formulation DM20%C, as a function of the frequency at a constant stress amplitude of 5 Pa.

Figure 5.111 Shear rate of XG hydrogels containing clotrimazole-free lipid nanoparticles D10%, D20% and DM20%, as a function of shear stress.

Figure 5.112 Shear rate of XG hydrogels containing clotrimazole-loaded lipid nanoparticles D10%C, D20%C and DM20%C, as a function of shear stress.

Figure 5.113 Shear rate of HEC hydrogels containing clotrimazole-free lipid nanoparticles D10%, D20% and DM20%, as a function of shear stress.

Figure 5.114 Shear rate of HEC hydrogels containing clotrimazole-loaded lipid nanoparticles D10%C, D20%C and DM20%C, as a function of shear stress.

Figure 5.115 Shear rate of PA hydrogels containing clotrimazole-free lipid nanoparticles D10%, D20% and DM20%, as a function of shear stress.

Figure 5.116 Shear rate of PA hydrogels containing clotrimazole-loaded lipid nanoparticles D10%C, D20%C and DM20%C, as a function of shear stress.

Figure 5.117 Shear rate of CH hydrogels containing clotrimazole-free lipid nanoparticles D10%, D20% and DM20%, as a function of shear stress.

Figure 5.118 Shear rate of CH hydrogels containing clotrimazole-loaded lipid nanoparticles D10%C, D20%C and DM20%C, as a function of shear stress.

Figure 5.119 Effect of the number of homogenization cycles on occlusion factor F for D10% clotrimazole-free SLN aqueous dispersion.

Figure 5.120 Effect of the number of homogenization cycles on occlusion factor F for D20% clotrimazole-free SLN aqueous dispersion.

Figure 5.121 Effect of the number of homogenization cycles on occlusion factor F for DM20% clotrimazole-free NLC aqueous dispersion.

Figure 5.122 Model of film formation on the skin for 2 μm and 200 nm lipid particles.

Figure 5.123 Effect of the applied sample mass of NLC aqueous dispersions containing 20% of lipid matrix on occlusion factor F.

Figure 5.124 Effect of the lipid formulation (D10%, D20% and DM20%) and presence of clotrimazole on occlusion factor F.

Figure 5.125 Effect of the type of hydrogel on occlusion factor F.

Figure 5.126 Effect of the type of hydrogel on occlusion factor F of NLC formulation containing 20% of lipid matrix.

PUBLICATIONS LIST

The present dissertation includes results, which have been partially used to write the following publications. The author co-operated in the development of the scientific project, in the carrying out of the laboratory programme, in the interpretation and discussion of the results and in the writing of the publications, under the name Souto, E.B..

Refereed Journals:

Souto, E.B., Wissing, S.A., Barbosa, C.M., Müller, R.H., Development of a controlled release formulation based on SLN and NLC for topical clotrimazole delivery, *Int. J. Pharm.*, submitted.

Souto, E.B., Wissing, S.A., Barbosa, C.M., Müller, R.H., Evaluation of the physical stability of SLN and NLC before and after incorporation into hydrogel formulations, *Eur. J. Pharm. Biopharm.*, submitted.

Souto, E.B., Wissing, S.A., Barbosa, C.M., Müller, R.H., SLN and NLC – Definition and Preparation Methods, *Rev. Port. Farm.*, submitted.

Proccedings:

Souto, E.B., Wissing, S.A., Barbosa, C.M., Müller, R.H., Preparation of clotrimazole-loaded NLC and SLN, *Proceed. Int. Symp. Control. Rel., Bioact. Mater.*, 30 (2003) P321.

Souto, E.B.,Wissing S.A., Barbosa, C.M., Müller, R.H., Preparation of topical formulations containing an antimycotic agent, *Proceed. Int. Symp. Control. Rel., Bioact. Mater.*, 30 (2003) P322.

Abstracts:

Souto, E.B., Wissing, S.A., Müller, R.H., Barbosa, C.M., HEC and Carbopol hydrogels containing clotrimazole loaded SLN, *Rev. Port. Farm.* LII Suppl. (2003) 25.

Souto, E.B., Wissing, S.A., Müller, R.H., Barbosa, C.M., Incorporation of clotrimazole in SLN - Evaluation of drug-lipid interaction, *Rev. Port. Farm.* LII Suppl. (2003) 117.

Souto, E.B., Wissing, S.A., Barbosa, C.M., Müller, R.H., Preparation of clotrimazole-loaded solid lipid nanoparticles for topical use, *AAPS Annual Meeting and Exposition,* Salt Lake City, Utah, USA, 2003.

Souto, E.B., Wissing, S.A., Müller, R.H., Barbosa, C.M., NLC as new carrier systems for dermal and cosmetic preparations, Congresso Nacional dos Farmacêuticos, Lisbon 27th to 29th Nov 2003.

Souto, E.B., Wissing, S.A., Müller, R.H., Barbosa, C.M., Comparative study of the physicochemical properties of SLN and NLC based glyceryl behenate, Congresso Nacional dos Farmacêuticos, Lisbon 27th to 29th Nov 2003.

Oral Presentation:

Souto, E.B., Wissing, S.A., Müller, R.H., Barbosa, C.M., HEC and Carbopol hydrogels containing clotrimazole loaded SLN, *1º Congresso da Sociedade Portuguesa de Ciências Farmacêuticas*, Lisboa, 14 a 16 de Abril, 2003.

ABBREVIATIONS

AFM	atomic force microscopy
CH	chitosan
DNA	deoxyribonucleic acid
DSC	differential scanning calorimetry
ΔH	molar melting enthalpy
η*	complex dynamic viscosity
E.E.	entrapment efficiency
ESR	electron spin resonance
*G**	complex modulus
G'	storage modulus
G''	loss modulus
GC	gas chromatography
GRAS	generally regarded as safe
HEC	hydroxyethylcellulose
HLB	hydrophilic-lipophilic balance
HPLC	high performance liquid chromatography
HPH	high pressure homogenization
LD	light diffraction
LDA	laser Doppler anemometry
LHDH	luteinizing hormone-releasing hormone
MRT	magnetic resonance tomography
MW	molecular weight
NLC	nanostructured lipid carriers
NMR	nuclear magnetic resonance

PA	polyacrylate (*Carbopol*®934)
Pa	pascal
PCS	photon correlation spectroscopy
PEG	polyethylene glycol
PI	polydispersity index
PM	photomultiplier
ppb	parts per billion
ppm	parts per million
RI	recrystallization index
rpm	rotations per minute
SAXS	small-angle x-ray scattering
S.D.	standard deviation
SLN	solid lipid nanoparticles
TEM	transmission electron microscopy
UV	ultraviolet
WAXS	wide-angle x-ray scattering
ζ	zeta potential
XG	xanthan gum

CHAPTER I

INTRODUCTION

CHAPTER I

INTRODUCTION

The concept of site-specific drug delivery is an old one [1]. Nevertheless, only recently full consideration has been given to the way in which this might be achieved in practice. Clearly, a drug's therapeutic index, as measured by its pharmacological response and safety, relies on the access and specific interaction of the drug with its candidate receptor, whilst minimizing its interactions with non-target tissues.

Site-specific drug delivery may be achieved by using carrier systems, where reliance is placed on exploiting both the innate pathway of the carriers, and the protection that they can afford to drugs during transit through the body. The use of a carrier opens up the range of opportunities for adjusting both drug access to its site of action and its pharmaceutical response.

The strategy for site-specific drug delivery should be based on consideration of the disease and drug access, retention and timing in its interaction with the target [2]. Thus, in the treatment of a disease with a carrier system one needs to have a clear understanding of the inherent anatomical and physiological characteristics of the site-specific drug delivery, the location of the target, the pharmacology of the drug and the target site response. Furthermore, the potential side-effects and the clinical utility of the therapeutic system need to be well defined.

Promising examples of drug delivery systems are the solid lipid nanoparticles (SLN). These systems have been introduced in 1991 as a new generation of carrier systems, combining the advantages of existing carriers such as liposomes, niosomes, sphingosomes, microemulsions, multiple emulsions and polymeric nanoparticles, while avoiding some of their specific disadvantages [3-7].

Similar to emulsions and liposomes, SLN consist of physiologically well tolerated excipients, like acylglycerols and phospholipids, allowing the transport of lipophilic substances molecularly dispersed in the lipid matrix [5-7]. Due to the solid character of the SLN matrix, physical instabilities which have been observed when incorporating liposomes into creams can be minimized or completely avoided.

Similar to polymeric nanoparticles, SLN can protect incorporated drug substances against chemical degradation and the drug can be released in a time-controlled manner [8-11]. However, for the production of SLN biodegradable raw materials such as acylglycerols, hard fats and waxes are used.

In contrast to polymeric nanoparticles, SLN can be produced at low costs and under sterile conditions [12,13]. Note that due to the low transition temperature of synthetic polymers, these later tend to be temperature sensitive, which means that they tend to stick at elevated temperatures and cannot be heated, sterilized or autoclaved. In contrast, SLN can be autoclaved or sterile filtered depending on the composition of the formulation [14-16]. SLN also have the advantage of industrial production by hot high pressure homogenization (HPH) [17,18]. They can be lyophilized [15,19-22], spray-dried [19,21] and sterilized [5,19], reflecting the high stability of these systems. In addition, sterically stabilized SLN can be prepared using polyethylene glycol (PEG) lipid conjugates as stealth agents [23-25].

More recently, a novel type of lipid nanoparticles called the nanostructured lipid carriers (NLC) was developed [26-29]. NLC are prepared from lipid blends, mixing solid and liquid lipids, while SLN are only made from solid lipids. Therefore, the former shows a new morphology, which affords an improvement of the loading capacity and the physical and chemical long-term stability in comparison to SLN.

The toxicity is the governing factor deciding if a product has the possibility to be introduced to the pharmaceutical market. Ideally, the product should contain only excipients which are already accepted in formulations by the regulatory authorities. This is possible when using SLN and NLC for ophthalmic, oral or peroral administration, as well as for cosmetics and pharmaceuticals intended for topical route. The materials used are excipients already present in cosmetical and pharmaceutical products accepted by the regulatory authorities, the full range of GRAS[1] substances and substances of recognized GRAS status are available. The list of these substances includes also compounds with surface activity or surfactants suibable for particle stabilization. The most frequently used lipids and emulsifying agents for the preparation of SLN and NLC are listed in Table I and II, respectively.

Many lipophilic and hydrophilic compounds (including some peptides) have been incorporated into SLN and NLC using different approaches [6,7,30,31]. Several examples of drugs and other substances incorporated into SLN and/or NLC are given in Table III.

[1] Generally regarded as safe.

Table I: Examples of the most frequently used lipids for the preparation of SLN and NLC.

Lipids	References
Triacylglycerols	
Tricaprin[a]	[32,33]
Trilaurin[a]	[9,20,34-49]
Trimyristin	[13,35,36,42,44,46-48,50-61]
Tripalmitin	[35,36,42,44,46-48,54,56,61-82]
Tristearin	[13,34-36,44,54,56,62,67,83-87]
Hydrogenated coco-acylglycerols	[31,44,48,49,85,86,88]
Mono, di and triacylglycerols mixtures	
Witepsol®W35	[54,62,63,68]
Witepsol®H35	[43,53,54,88]
Witepsol®H42	[44,89]
Witepsol®E85	[31,50,53]
Glyceryl monostearate (*Imwitor*®900)	[13,26,28,48,56,59,70,90,91]
Glyceryl behenate (*Compritol*®888 ATO)	[9,11-13,20,21,28,41-43,48,50-52,54,56,57,59,70,75,83,84,92-110]
Glyceryl palmitostearate (*Precirol*®ATO 5)	[48,50,57,84]
Acidan®N12	[15]
Diacylglycerol monocitrate monostearate	[15,30]
Waxes	
Cetyl palmitate	[9,12,13,18,21,42,43,47,51,59,67,70,75,84-86,95,99,102,111-119]
Beeswax	[48,56,70]
Hard fats	
Capric acid	[120]
Palmitic acid	[120]
Stearic acid	[13,15,23-25,30,48,71,89,90,121-140]
Behenic acid	[15,30]
Other lipids	
Cholesterol	[41,50,93]
Miglyol®812	[28,48,56,75,76,81,103,104,106,107,114-117]
Parafin	[13,56,75,108]

[a] These lipids create supercooled melts.

Table II: Examples of the most frequently used emulsifying agents for the preparation of SLN and NLC.

Emulsifiers	References
Soybean lecithin (*Lipoid*®S75, *Lipoid*®S100)	[9,13,20,34-36,41-46,48,50,52,53,55,57,58,62,63,66,68,69,73,77, 78,83,84,129,134,141]
Egg lecithin (*Lipoid*®E80)	[26,33,50,60,66,67,115]
Phosphatidylcholine (*Epikuron*®)	[15,23-25,65,71,72,88,90,91,123,124,126,127,130,131,135-140, 142]
Poloxamer 188	[9,11-13,20,21,31,41,42,48-51,54,56-60,62,63,65,68,69,77,78,84, 88,92,94-100,102,106,115,129,132,134]
Poloxamer 182	[31]
Poloxamer 184	[52]
Poloxamer 235	[52]
Poloxamer 335	[52]
Poloxamer 407	[42,52,58-61,66,67,84,87,92,99]
Poloxamine 908	[42,58,66,84,92,99]
Tyloxapol®	[35,36,44,47-49,53,64-66,73,76,79-82,141]
Polysorbate 20 (*Tween*®20)	[77,121,125,127]
Polysorbate 60 (Tween®60)	[125]
Polysorbate 80 (*Tween*®80)	[31,33,48,52,56,58-60,67,70,84,91,101,105,108-110,117,142]
Sorbitan esthers	[59,105,108]
Sodium cocoamphoacetate	[28,86,106]
Sodium cholate	[31,42,50,51,58-61,67,84,91]
Sodium glycocholate	[22-24,35,36,44-46,53,55,62,63,65,66,73,141,142]
Taurocholic acid sodium salt	[23-25,71,72,130,131,135-140,142]
Taurodeoxycholic acid sodium salt	[15,89,91,120-128]
Butanol	[71,90,121,124-128]
Butiric acid	[72,123,128]
Monooctylphosphoric acid sodium	[125]
Cholesterol hemissuccinate	[71,72]
Polyoxyethylene alquil ethers	[132]
Cetylpyridinium chloride	[46,58,60,108]
Sodium dodecyl sulphate	[59,60]
Sodium dioctyl sulfosuccinate	[58,128]
Polyglycerol methylglucodistearate (*Tego Care*®450)	[18,47,59,85,86,114,116,117]

Table III: Examples of drugs and other substances incorporated into SLN and/or NLC.

Incorporated drug or substance	References
Aciclovir	[111,143,144]
Albumin	[24,84]
Amphotericin B	[145,146]
3'-Azido-3'-deoxythymidine palmitate	[38,39]
Azidothymidine palmitate	[40]
Betamethasone valerate	[53]
Benzocain	[147]
Calixarenes	[148-151]
Camptothecin	[129,134]
Chloramphenicol	[147]
Cholesteryl acetate	[65,142,152]
Cholesteryl butyrate	[153]
Clotrimazole	[79-82]
Cortisone	[53]
Cyclodextrins	[154,155]
Cyclosporin A	[29,133,135,156-161]
Deoxycorticosterone acetate	[121]
Dexamethasone	[162]
Diazepam	[15,53,115]
3'-5'-dioctanoyl-5-fluoro-2'-deoxyuridine	[87]
DNA	[84,108]
Doxorubicin	[71,122,136,137]
Etomidate	[9,41,43]
Fenotiazin	[30]
Gadolinium (III) complexes	[128]
^{99m}Tc-HMPAO [a]	[101,110]
Hydrocortisone	[90]
Idarubicin	[122]
Insect repellents	[48,163-165]
Iotrolan	[84]
[D-Trp-6]LHRH [b]	[123]
Lysozyme	[31]
Menadione	[36,53]

[a] DL-hexamethylpropileneamine oxime
[b] Luteinizing hormone-releasing hormone

Table III: Examples of drugs and other substances incorporated into SLN and/or NLC. (Continuation)

Incorporated drug or substance	References
Nifedipine	[30]
Nile red	[166]
Nimesulide	[167]
Ovalbumin	[168]
Oxazepam	[53]
Oxytetracycline	[34]
Paclitaxel	[71,72,132,169]
Perfumes	[48,170,171]
Pilocarpine	[124]
Piribedil	[109]
Polycyclic aromatic hydrocarbons	[127]
Prednicarbate	[57]
Prednisolone	[11,41,50,53,93,100,172]
Progesterone	[90]
Retinoids	[33,53,56,70,75,103,104,106,107,173-175]
Rhodamine B	[23]
Somatostatin acetate	[74]
Spin-labelled compounds	[68,69,77,78,176-178]
Sunscreens	[48,76,114,117,179-181]
Tetracaine	[9,41,43]
Timolol	[89,120]
Thymopentin	[126]
Tobramycin	[138-140]
Tocopherol	[47,48,85,116,182,183]
Tributyrin	[184]
Ubidecarenone	[18,53,63,73,85,141,185]
Vitamin K	[186]

As reported before, SLN and NLC have been used for a variety of pharmaceutical applications, such as oral, peroral, parenteral, ophthalmic and also topical administration [10,48,57,85]. Recently, these systems have also been introduced as a novel topical carrier for cosmetics [56,185,187].

Due to the small size of these particles (nanometer range), they are not perceptible when applied to the skin. Since SLN and NLC aqueous dispersions are stable at high temperatures, they can be easily incorporated into hydrogels or creams, i.e. the water phase of a gel or cream

can be partly substituted by the aqueous dispersion during the production process, and can act as carriers for active ingredients which proved to be chemically unstable in aqueous formulations such as creams or lotions [185]. SLN and NLC can act as a drug reservoir providing controlled drug release and might also act as penetration enhancers, increasing the drug concentration in the upper skin layer [56,57]. Similar to liposomes they also can form a protective film [185,187]. Due to their small size a penetration into gaps between *stratum corneum* cells might be feasible.

These properties can be used for the delivery of antifungal agents into skin and mucosa for the treatment of fungal infections, such as yeast infections. *Candida albicans* is a yeast that, in addition to its many systemic manifestations, can cause cutaneous mycoses, often on body sites where excessive moisture accumulates [188]. Candida infections frequently occur in skin folds of obese individuals, under pendulous breasts, in armpits, in the crotch, and on nails and hands that spend a lot of time immersed in water or covered with nonporous gloves. The yeast multiplies in the cutaneous layers and causes local skin lesions. Persons with impaired immunologic or cellular defences may develop lesions that cover the entire body surface and the mucous membranes [189].

The azoles are a group of synthetic compounds used as antifungal agents because they interfere with the cell membrane growth of fungi by inhibiting the synthesis of ergosterol [188]. One group of azoles, – the imidazoles –, are effective broad spectrum antifungal drugs with few or no serious side effects. Clotrimazole and miconazole, for example, are found in topical ointments such as those used for vaginal yeast infections [190]. These antifungal agents are also effective against dermatophytes, when applied topically. Ketoconazole has been used successfully for treating systemic infections caused by several pathogenic moulds, yeast infections and dermatophytes [188].

It is well known that poor solubility of a drug in the carrier matrix results in a low affinity of the molecule for the carrier and is accompanied by a poor *in vivo* bioavailability. In order to develop SLN and NLC formulations for the treatment of fungal infections, clotrimazole was chosen as a model drug because of its lipophilic character and large spectrum against several pathogenic fungi. This drug was first entrapped into SLN and NLC using the hot high pressure homogenization technique and the obtained aqueous dispersions were incorporated in hydrogels. The developed formulations were characterized concerning the particle size and polydispersity index, particle crystallinity, entrapment efficiency, drug loading capacity and drug release profile. Rheological and occlusive properties of the obtained topical formulations were also investigated.

CHAPTER II

COLLOIDAL DRUG CARRIERS FOR TOPICAL ROUTE

CHAPTER II

COLLOIDAL DRUG CARRIERS FOR TOPICAL ROUTE

2.1. Structure, properties and functions of the skin

The skin is the largest organ in the body, occupying almost 2 m^2 (21,5ft^2) of surface area [191]. It varies in thickness on different parts of the body, from less than 0.5 mm on the eyelids to more than 5 mm on the middle of the upper back. A typical thickness is 1 to 2 mm.

According to some authors [192], the structure of the skin can be divided in three main parts, as it is represented in Figure 2.1. The *epidermis* is the outermost layer of epithelial tissue, the *dermis* is a thicker layer of connective tissue beneath the *epidermis* and the *hypodermis* is a layer of loose, fibrous connective tissue beneath the *dermis* [48,193,194].

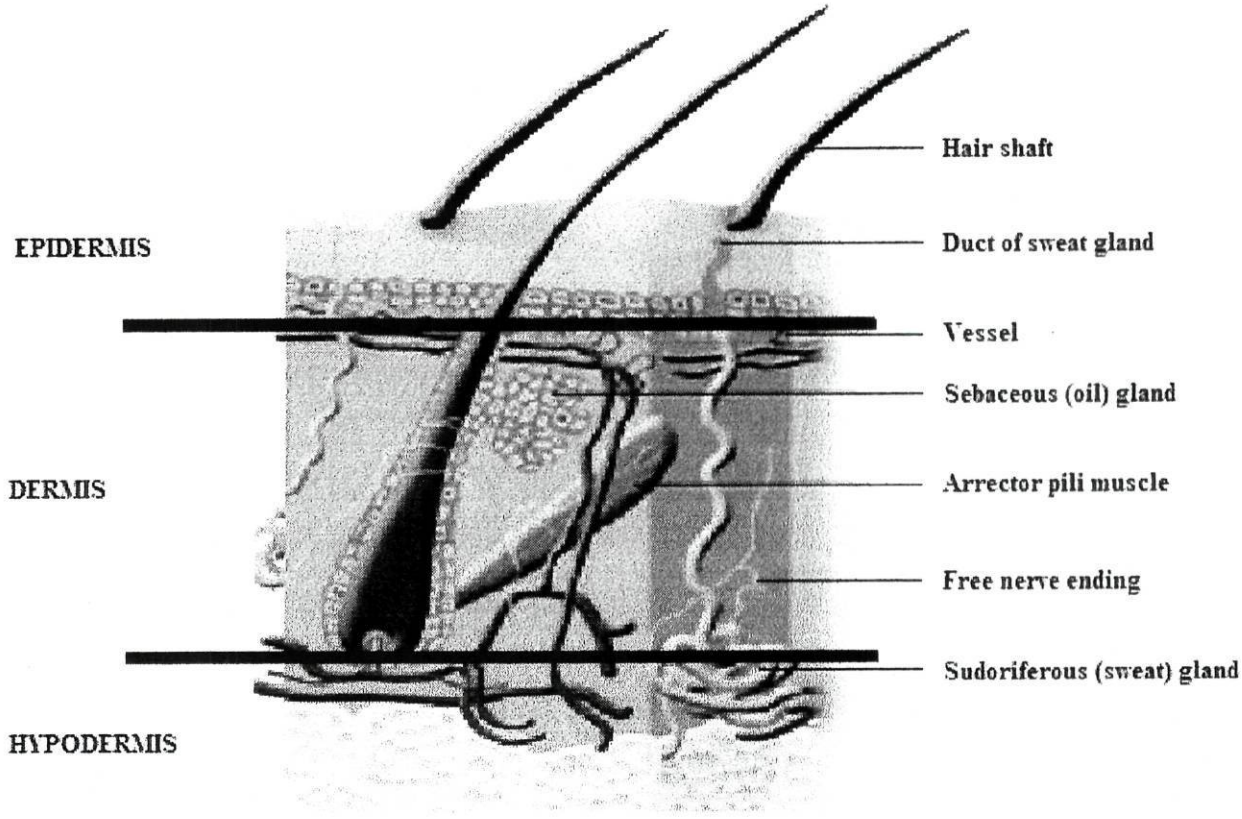

Figure 2.1: Schematic representation of the skin structure, showing its many components in an ideal arrangement. (Adapted from Wissing [48]).

The *epidermis* (from the Greek *epi* meaning over and *derma* meaning skin) is a stratified squamous epithelium and has an average thickness of 30 μm to 4 mm [192]. The *epidermis* contains no blood vessels, but most of it is so thin that even minor cuts can reach the *dermis* and draw blood. In the thick *epidermis* of the palms of the hand and soles of the feet, there are five

typical layers (*strata*). Starting with the outermost layer, they are *stratum corneum*, *stratum lucidum*, *stratum granulosum*, *stratum spinosum* and *stratum basale*. The *stratum spinosum* and *stratum basale* together are known as the *stratum germinativum* because they generate new cells. In parts of the body other than the palms and soles, only the *stratum corneum* and *stratum germinativum* are regularly present.

The *stratum corneum* is a flat, relatively thick layer of dead cells arranged in parallel rows [192]. It is a keratinized layer, consisting of soft keratin compared to the one existing in fingernails and toenails, which helps keeping the skin elasticity. This soft keratin also protects living cells underneath from being exposed to the air and drying out. The cells in the *stratum corneum* are constantly being renewed [195]. They are replaced by new cells that are formed by cell division and pushed up from the germinative layers below. It has been estimated that the equivalent of the full epidermal mass turns over through cell proliferation with a frequency of 1 or 2 months. Environmental and disease factors accelerate the turnover, but not without leaving an imprint on the skin's membrane attributes [196].

The *stratum lucidum* consists of flat, translucent layer of dead cells that contain a protein called eleidin, which is probably a transitional substance between the soft keratin of the *stratum corneum* and the precursor of soft keratin, keratohyaline, of the layer below [192]. The *stratum lucidum* appears only in the palms of the hands and soles of the feet, acting as a protective shield against the ultraviolet (UV) rays of the sun and preventing sunburns.

The *stratum granulosum* lies just below the *stratum lucidum* [192]. It is usually two to four cells thick. These cells also contain granules of keratohyaline and, therefore, the process of keratinization, which is associated with the dying cells, begins in this layer.

The *stratum spinosum* is composed of several layers of polyhedral cells that have delicate spines protruding from their surface [192]. The interlocking spine-like projections help support this binding layer. Active protein synthesis takes place in the cells of the *stratum spinosum*, indicating that cell division and growth are occurring. Some new cells are formed here and are pushed to the surface to replace the keratinized cells of the *stratum corneum*.

The *stratum basale* rests on the basement membrane next to the *dermis* [192]. It consists of a single layer of columnar or cuboidal cells. Like the *stratum spinosum*, it undergoes cell division to produce new cells to replace those being shed in the exposed superficial layer.

Most of the skin is composed of *dermis* (average thickness of 0.04 to 1.6 mm), which is called "true skin", because it is a strong, flexible connective tissue meshwork of collagenous reticular and elastic fibres [192]. Collagenous fibres, which are formed from protein collagen, are very thick and give the skin much of its toughness. Although reticular fibres are thinner, they

provide a supporting network, while elastic fibres give the skin flexibility. The cells of the *dermis* are mostly fibroblasts, fat cells and macrophages. These later cells are responsible for digesting foreign substances. Blood vessels, lymphatic vessels, nerve vessels, nerve endings, hair follicles and glands are also present. The *dermis* is composed of two layers that are not clearly separated. The thin papillary layer is directly beneath the *epidermis* and the deeper, thicker layer is called reticular layer.

Beneath the *dermis* lies the *hypodermis* (from the Greek *hipo* meaning under) or subcutaneous layer [192]. It is composed of loose, fibrous connective tissue, is generally much thicker than the *dermis* and is richly supplied with lymphatic and blood vessels and nerves. Also within the *hypodermis* are the coiled ducts of sudoriferous seat gland and the bases of hair follicles. While the boundary between the *epidermis* and *dermis* is distinct, the one which is between the *dermis* and the *hypodermis* is not.

Where the skin is freely movable, *hypodermis* tissue fibres are scarce. Where it is attached to underlying bone or muscle, the *hypodermis* contains tightly woven fibres. In some areas of the *hypodermis* where extra padding is desirable, as in the breast or the heels, thick sheets of fat cells are present.

An obvious function of the skin is to cover and protect the inner organs [191]. However, this is only one of its many functions. Other functions include protection against harmful microorganisms and foreign material from entering the body, defending the organism against disease [192]. It is also responsible for temperature regulation and for excretion of small amounts of waste materials. The skin helps screen out harmful excessive UV rays from the sun, but it also lets in some necessary UV rays for its synthesis property. This organ is an important sensory receptor that responds to heat, cold, touch, pressure and pain.

2.2. Drug absorption through the skin

The aim of topical drug delivery is to produce a desired therapeutic action at specific sites on the skin and mucosa [197]. While certain topical substances such as emollients, antimicrobials and deodorants act primarily on the surface of the skin, the target area for most topical disorders lies in the viable *epidermis* or upper *dermis*. This requires diffusive penetration into the skin and/or mucosa or percutaneous absorption.

Diffusion is a process involving the random movement of molecules among the past one another as often and as fast as the void space between molecules allows [198]. Physiological membranes may be regarded as molecular and/or macromolecular diffusion regimes that are

fixed and compositionally distinct from phases they separate. Passive diffusion takes place when a solute's thermodynamic activity is unequal on each side of the membrane, i.e. when a concentration gradient is present. The random movements of molecules lead to drug penetration into and through the membrane, always from regions where the molecules are concentrated (at high activity) to where they are sparsely concentrated. A gradient develops across the membrane, which reflects the existing difference of concentration (activity) through the membrane. The rate of transport across any chosen plane within the membrane of diffusion reflects the number of molecules moving forward and back across that plane in an instant of time. The factors determining the transport rate are the difference of concentration between the two sides of the membrane and the ease of positional relocation of the diffusing species. Diffusion of substances is spontaneous and irreversible and continues until the activity of the permanent is level throughout the membrane. Note that drug substances cannot be returned to their original place without doing any work.

The natural and irreversible tendency toward diffusive randomness of substances among one another arises as the result of increased entropy [198]. At constant temperature and pressure and when there is no other work except pressure-volume work, the thermodynamic driving force can be put in terms of the decrease in Gibbs' free energy of the system. Under isothermal conditions the Gibbs' equation is given by:

$$\Delta G = \Delta H - T\Delta S$$

which indicates that the free energy change of a system "ΔG" is equal to the increase or decrease in its enthalpy "ΔH" less the product of the absolute temperature "T" and the system's entropy change "ΔS". If the change in ΔG is negative under the conditions specified, the process under consideration will be spontaneous via diffusion [198].

For components that form an ideal solution when applied to the skin, there is no enthalpy change associated with the diffusive movement [198]. On the contrary, the entire decrease in free energy arises from increased entropy. However, some enthalpy figures into the free energy change in all real situations (Gibbs' equation). The diffusive process is invariably driven by increased system entropy. Although an individual molecule's movements are without preferred direction, a so-called random-walk process, their random movements eventually lead to the alluded to evenness of distribution.

When a drug delivery system is applied topically, the drug diffuses out of the system onto the surface tissues according to their concentration gradient and can enter through the follicular

region, through the sweat ducts or through the unbroken *stratum corneum* between these appendages [198]. It seems that eccrine glands do not play any significant role in cutaneous permeability. Substances may enter the ducts, and even the glands, but there appears to be no penetration from these areas to the *dermis*.

In contrast to deeper skin layers, the lipid layers of the *stratum corneum* contain no phospholipids [192]. They are substituted by ceramides, which only have small head groups and therefore allow only limited hydration of the skin. The formation of small water pores is therefore prevented and the organism is protected against evaporation of water. The ceramides of the skin differ from those in other tissues, e.g. in the brain by impair length of their lipid side chains. The lipid mono-layers are therefore interdigitated to complex multi-layers, which are partially covalently coupled to the dead horny cells. The high degree of saturation of the ceramides and other *stratum corneum* lipids like cholesterol, cholesterol esters, cholesterol sulfates and free fatty acids, result in a gel-like lipid superstructure with low fluidity, which supports the low permeability of the skin [197].

By the transepidermal route, penetration of substances is fairly rapid, although slower than intestinal tract absorption, and is almost always accompanied by some degree of pilosebaceous penetration as well [197]. For substances that are absorbed through both pathways, the transepidermal route is the principal portal of entry because of the total, relatively small, absorbing surface offered by the pilosebaceous units. The *epidermis* presents a surface area 100 to 1000 times grater than the other routes of absorption, such as intestinal route. The appendages, sweat glands and hair follicles are scattered throughout the skin in varying numbers, but are comparatively sparse, i.e. their total cross-sectional area is probably between 0.1 and 1.0% of the skin area.

The particular route that the drug may take, and the relative importance of one in contrast to the other, depends almost entirely on the physicochemical properties of the drug and the conditions, each of the contending routes of permeability may change and be overwhelmingly dominant. In particular, the transient diffusion that occurs shortly after the application of a substance to the surface of the skin is shown to be potentially far grater through the appendages than through the matrix of the *stratum corneum* [197]. After steady-state diffusion has been established, the dominant diffusion mode is probably no longer intra-appendageal, but occurs through the matrix of the *stratum corneum*. Flux through shunts is difficult to measure experimentally, except possibly through hair. The recognition of transient diffusion, occurring primarily via follicles and ducts and steady-state diffusion occurring primarily through the intact

stratum corneum, results in a considerably more self-consistent and ordered treatment of the process of percutaneous absorption.

Once a substance passes through the *stratum corneum*, there is apparently no significant further hindrance to penetration of the remaining epidermal layers [197]. There is then a rapid entry into the circulation via the capillaries. The concentration gradient essentially ends in the dermal layer at the beginning of the circulation. The systemic circulation acts as a reservoir for the drug. Once in the general circulation, the drug is diluted and distributed rapidly with little systemic build-up.

Diffusion through the horny layer is a passive process [197]. There is a little evidence to support specialized active transport systems for cells of the *stratum corneum*. The passive process is affected only by the substance being absorbed, by the medium in which the substance is dispersed, and by ambient conditions. On the other hand, percutaneous absorption is a more complicated process, of which epidermal diffusion is the first phase, and clearance from the *dermis* the second. This latter depends on effective blood flow, interstitial fluid movement, lymphatic, and perhaps other factors related to dermal constituents [197].

2.3. Innovative drug carrier systems for topical administration

Different drug delivery systems have been suggested as promising vehicles for enhancing the activity of several compounds into the skin and mucosa. This chapter pays a special attention to the main drug delivery systems for topical administration such as liposomes, niosomes, sphingosomes, microemulsions, multiple emulsions, polymeric nanoparticles, SLN and NLC.

2.3.1. Liposomes

Liposomes are vesicular carriers comprising a hydrophilic core surrounded by one or more lipid bilayer membranes [199,200]. The membranes normally consist of a bilayer of amphiphilic lipids, like phospholipids (lecithins), cholesterol and glycolipids. The hydrophilic parts of lipids, i.e. the head groups, are oriented to the aqueous side, while the lipophilic parts, i.e. the tails, of the molecules of both lipid layers (mono-layers, leaflets) face each other and form the hydrophobic inner space of the membrane [200]. The bilayer thickness is about 5 nm [201].

Liposomes are one of the most extensively investigated drug delivery systems [199]. These carriers can be produced in sizes from below 50 nm up to several μm. Lipophilic drugs can be

incorporated into the lipid bilayers while hydrophilic drugs are solubilized in the inner aqueous core or between the layers.

The New York Academy of Science has defined small unilamellar vesicles (SUV), large unilamellar vesicles (LUV) and multilamelar vesicles (MLV) as the three basic types of liposomes differing in their size and number of lamellae [202]. This definition has been expanded in the meantime.

The advantages of these systems are its high drug loading capacity, the low inherent toxicity and immunogenicity and its biodegradability [199]. Drug release, *in vivo* stability and biodistribution are determined by size, surface hydrophobicity and membrane fluidity. Chemical and physical stability problems can lead to liposome aggregation and drug degradation or expulsion during storage and limit the performance of liposome based drug carriers.

Liposomes were first introduced to the cosmetic market by Dior in 1986 and they were considered a major innovative carrier system in the dermal area [27,182]. After some years later, liposomes appeared on the market in pharmaceutical products. Although, their high costs and up-scaling problems still are a great obstacle for the broad introduction of these carriers to the market.

It was shown in many studies that conventional liposomes as intact hydrophilic vesicles do not penetrate through the skin and therefore do not possess a transepidermal carrier function for active substances [203,204]. In spite of electron microscopical investigations could demonstrate vesicles in deeper *stratum corneum* after topical liposome application [205], it resulted probably from vesiculation by *stratum corneum* lipids. Identical phenomena could be shown after application of non-ionic liposomes [206]. Nevertheless, a certain penetration supporting effect of liposomal preparations is probable. For the distribution of liposomal formulations it could be shown that lipophilic drugs like cortisol are held for a long time in high concentrations in the *stratum corneum* (drug localizing effect) without reaching the systemic circulation [207]. A possible explanation is the occlusive effect of drying lecithin lamellae resulting in an increasing water content which supports penetration of both hydrophilic and lipophilic drugs into the upper skin layers. Another explanation is a facilitated penetration by formation of low molecular complexes of drug and liposomal lipid. Furthermore, poorly soluble drugs can be incorporated into the inner area of the liposome bilayer. Upon topical application these carriers are able to form a drug depot and facilitate the release into the skin through a large surface.

A new development are the so-called transfersomes [208], which make possible the penetration of larger quantities of even large and hydrophilic active substances. Their mode of action is still under discussion. The large amount of contained emulsifying agents and skin lipids

are probably responsible for fluidization of the liposomes during the penetration of these drug delivery systems. Also the osmotic gradient over the *stratum corneum* seems to be involved.

Examples of registered preparations and trademarks for liposomes and lipid-based formulations already in the pharmaceutical market are *AmBisome*®, *Abelcet*®, *Alveofact*®, *Amphocil*®, *DaunoXome*®, *Pevaryl*®-Lipogel, *HeparinPur*®, *HeparinPur*®-forte, *Doxil*® and *Caelix*®.

2.3.2. Niosomes

Niosomes are vesicles formed via the self-assembly of synthetic non-ionic surfactants [209]. These spherical vesicles with lipid bilayers like liposomes are designated as Non-ionic Surfactant Vesicles (NSV) [210]. They consist of synthetic non-ionic lipids, such as polyglycerolalkylether, polyoxyethylenalkylether and polyoxyethylenalkylester [211], which have a high chemical stability due to the saturated hydrocarbon chains and intramolecular ether bonds.

2.3.3. Sphingosomes

Sphingosomes are vesicles with a structure similar to liposomes but their membranes consist of sphingolipids and/or derivates, such as ceramides [212]. These structures present the advantage of being composed of physiologic lipids from the *stratum corneum*.

2.3.4. Microemulsions

Microemulsions represent a surfactant-containing multiple component system consisting of a lipophilic and a hydrophilic component, as well as at least one surfactant, mostly applied together with a co-surfactant. First positive results have been published regarding physiologically compatible mixtures of the components with an optimized release of selected drugs [213,214].

These systems are close to spontaneous formed nanoparticles in terms of preparation, as well as to micellar systems in terms of properties. Due to ratio of oil and water, they cannot be considered micellar solutions [215]. Macroscopically, they appear as clear, one phase isotropic systems. The dispersed phase consists of very small particles (5-140 nm [216]) and its properties resemble those of a bulk phase rather than an inner emulsion phase. The enormous reduction in interfacial tension, enabling the large interface, is provided by high amounts of surfactant and co-surfactant. This low interfacial tension also supports the spontaneous formation of such systems,

not requiring any energy input. Consequently, as thermodynamically stable systems, microemulsions do not exhibit stability problems such as phase separation or increase in particle size. Generally, with some exceptions [216], no single component alone is capable to provide the required low interfacial tension. A surfactant has to be mixed with another amphiphilic substance like low molecular alcohols or glycols to stabilize the interface. Besides, low molecular liquids as co-surfactants reduce the viscosity of the overall system. Depending on the volume ratio of the two immiscible liquids and molecular length, surface area and volume of the surfactants, microemulsions can be classified to be of either oil-in-water (O/W) or water-in-oil (W/O) type. However, many authors suggest a bicontinuous structure, especially if oil and water are present in similar amounts [216]. With an excess of either oil or aqueous phase, no transparent microemulsion is formed, but an opaque conventional emulsion, although without energy input. These preparations are also referred as self-emulsifying systems.

Microemulsions have the advantages of being transparent, thermodynamically stable, fluid and they can be prepared applying simple production methods. They can also improve the solubility and the stability of incorporated drugs, increase the bioavailability and prolong drug effect. A special advantage of microemulsions is an improvement of the corneal permeability resulting in increased intensity and duration of drug action. At present, microemulsions are been investigated as potential carrier systems for topical use [214,217-220].

The use of these systems is also associated with some drawbacks, limiting their use to the application of problematic drugs rather than being universal tools [216]. These drawbacks are the required high amount of surfactant, which can decrease the *in vivo* tolerability, and the stability problems that can arise with the use of alcohols (because of their volatility) and oils (risk of rancidity). Incompatibilities between the oil phase and emulsifying agents can also be observed, possible incomplete solubilization of drug can lead to drug precipitation and only a limited amount of drug, approximately 10-15% can be incorporated. These systems are also susceptible to qualitative and quantitative changes in composition.

Examples of commercially available microemulsions on the pharmaceutical market are *Contrafungin*®, *Capsoft*®, *Capsoft*® Cream and *Sandimmun*® Neoral.

2.3.5. Multiple emulsions

Multiple emulsions are complex systems where droplets of the dispersed phase themselves contain even smaller droplets, identical with or different from the continuous phase [221]. There

are two basic types of multiple emulsions: water-in-oil-in-water (W/O/W) and oil-in-water-in-oil (O/W/O).

Multiple emulsions are a challenge to the cosmetic and pharmaceutical technology [222]. To obtain optimum skin care effects that are as long-lasting as possible, well-formulated bases are needed that not only meet the requirements for the stability, purity and safety of the chosen ingredients imposed by quality management but additionally achieve a perceptible and measurable caring effect on the skin. Owing to their structure, multiple emulsions of the W/O/W type combine the classical properties of W/O emulsions with those of the lighter O/W emulsions and hence protect the skin's barrier and provide long-lasting care while actively moisturizing the skin. Immediately after application of a W/O/W emulsion to the skin, the water of the external aqueous phase is absorbed by the skin, cooling it and providing the same moisturizing care as that of a moisturizing cream with an O/W base. At the same time a protective film of coalescing oil droplets covers the skin, gradually releasing additional entrapped water droplets and thus moisturizing the skin long-term. A significant moisturizing effect can still be detected 18-24 hours even after a single application of these products.

This type of emulsion can also significantly improve the skin's moisture binding capacity [222]. For example, in long-term studies over an application period of 12 weeks a significant improvement in the water balance of the upper skin layers could be demonstrated. Regular application of W/O/W emulsions steadily increased the skin's moisture, with the maximum effect being reached after approximately 8 weeks and kept at this high level with continued use. Due to the variable electrolyte content, W/O/W technology also has a normalizing effect on extremely dry skin conditions as well as on sensitive but healthy skin. In addition, multiple emulsions especially of the W/O/W type can be used as dermal sustained release systems or to protect sensitive drugs. Hence lipophilic (e.g. some vitamins) and hydrophilic active substances of different origin can be incorporated in multi-lamellar phases in the internal or external aqueous phase. Also, incompatible drugs can be separated in different phases.

Examples of commercially available multiple emulsions on the pharmaceutical market are *Nivea*® Visage Optimale 3, *Nivea*® Visage Optimale Eye Care, *Eucerin*® Hydro balance, *Rejuven*® Q10 and *Rejuven*® Q10 eye.

2.3.6. Polymeric nanoparticles

Almost 30 years of intensive research have been invested in nanoparticles since their development by Speiser *et al.* in the middle of the seventies [223]. Many review and research

articles report about the benefits of these systems for controlled drug delivery. However, as market products, they are practically non-existing.

The reasons for the lack of products based on polymeric nanoparticles are many, such as the lack of large scale production methods yielding a product being acceptable by the regulatory authorities and simultaneously cost-effective, the organic solvent residues that can appear in the final product (depending on the method of preparation), the cytotoxicity of polymers and problems with polymer chemistry, as well as the need of γ-irradiation for production of sterile formulations, which can cause decomposition of incorporated drug and/or polymer and formation of potentially cancerogenic radicals [224].

Several synthetic polymers, such as poly(lactic acid), poly(β-hydroxybutyrate) and poly(lactide-*co*-glycolide), have shown good histocompatibility and biodegradability, and their safety has been extensively documented. But even the ones which are accepted for use as microparticles and implants, can show cytotoxic effects when delivered as nanoparticles or as very small microparticles [225]. There are interesting data in academic research; however, they still fail as a benefit for the patient.

The research and development of polymer-based formulations for controlled drug release is responsible for some registered preparations and trademarks for microparticles and implants approved for therapeutic use. Examples of commercially available polymer-based formulations on the pharmaceutical market are *Enantone Depot®*, *Decapeptyl Depot®*, *Parlodel LA®*, *Parlodel LAR®*, *Profact Depot®*, *Suprefact Depot®* and *Zoladex®*. Concerning nanoparticulate products, just one – a diagnostic for magnetic resonance tomography (MRT) imaging – has been recently introduced on the market.

2.3.7. Solid lipid nanoparticles (SLN)

The first lipid microparticles were described by Speiser *et al.* at the beginning of the eighties [226]. The production method of these particles consisted of dispersing the melted lipid in a hot surfactant solution applying high speed stirring. The obtained emulsion was then cooled down and the lipid formed solid microparticles. Disadvantages of stirring techniques are the relatively broad size distribution, requiring high concentrations of surfactants to obtain a mean particle diameter in the nanometer range. The obtained products were called "Lipid nanopellets" and they have been developed for oral administration [3].

Similar systems have been described by Domb, as Lipospheres, which were produced by sonication [34,227,228]. The patent obtained by Speiser was not followed up by the owner

Rentschler and in a number of countries patent protection does not longer exist. The lipospheres found also no broad application in pharmaceutical products.

At the beginning of the nineties, SLN have been developed as an alternative to the traditional systems, such as emulsions, liposomes and polymeric nanoparticles [5]. SLN are nanoparticles with a mean average size in the nanometer range, which means approximately between 50 nm and 1000 nm. They consist of a matrix composed of a lipid being solid at room temperature and at body temperature.

The first patents for SLN were filed in 1991, one by Müller and Lucks [229] describing the production of SLN by high pressure homogenization, and another by Gasco [230] describing the production via microemulsions.

As reported in Chapter I, a clear advantage of these particles is the fact that the lipid matrix is composed by physiological lipids (e.g. GRAS status for oral and topical administration), which decreases the danger of acute and chronic toxicity. The choice of the emulsifying agent depends on the administration route and is more limited for parenteral administration [5].

A major disadvantage of emulsions and liposomes is the lack of protection for chemically labile drugs, in addition drug release takes place as a burst (emulsions) or at least relatively fast (from liposomes). In contrast, SLN possess a solid lipid matrix identical to polymeric nanoparticles. In fact, SLN were idealized by simply exchanging the liquid lipid (oil) of the emulsions by a solid lipid [6], which can bring many advantages in comparison to a liquid core (Table IV) [231].

Table IV: Potential advantages of lipid suspensions over lipid emulsions due to the solid state properties. (Adapted from Siekmann and Westesen [231]).

Solid state properties	Potential advantages
Solid particle core	No particle coalescence; Improved physical stability.
Strongly reduced mobility of incorporated drug	Reduced drug leakage; Avoidance of drug protruding into emulsifying agent film; Sustained/controlled drug release.
Static interface solid/liquid	Facilitated surface modification.

It can be stated that SLN possess major advantages over the previous carriers, and they also avoid some of their major disadvantages. In addition, SLN are "low cost" products. Excipients and production lines are relatively cheap and production costs are not much higher than to parenteral emulsion manufacture.

For topical delivery of SLN, the full range of excipients in cosmetic and pharmaceutical topical products can be exploited. For oral SLN, all lipids and surfactants used for tablets, capsules and other oral products, such as microemulsions can be used (see Tables I and II, Chapter I). For parenteral administration, the lipid matrix can be produced from acylglycerols being composed of fatty acids contained in the acylglycerols of parenteral nutrition emulsions.

2.3.7.1. Preparation methods of SLN

There are three main production methods for SLN described in scientific literature. These methods are the high pressure homogenization technique, the microemulsions based SLN preparations and the solvent emulsification-evaporation technique [232]. Recently, the solvent displacement and the emulsification-diffusion techniques, which have been used to prepare polymeric nanoparticles, where also tested for SLN preparation.

2.3.7.1.1. High pressure homogenization technique

As it has been reported before, the high pressure homogenization (HPH) technique was developed by Müller and Lucks [229].

HPH is a technique broadly used in different areas and it is also established in pharmaceutical production, e.g. the production of emulsions for parenteral nutrition (*Intralipid*®, *Lipofundin*®) [5]. This technique overcomes a major problem of other nanoparticles, i.e. the large scale production line is possible. This technology also leads to nanoparticles having a relatively homogeneous size distribution, which increases the physical stability of the aqueous dispersion.

The dispersion grade depends on the power density and the power distribution in the dispersion volume [7]. High power densities result in more effective particle disruption. High pressure homogenizers reach by far the highest power densities (10^{12} – 10^{13} W/m^3). A homogeneous distribution of the power density is necessary to obtain narrow size distribution. Otherwise, particles localized in different volumes of the sample will experience different dispersing forces and therefore, the degree of particle disruption will vary within the sample volume. Inhomogeneous power distributions are observed in high-shear homogenizers and ultrasonifiers. High pressure homogenizers are characterized by a homogeneous power distribution due to the small size of the homogenizing gap (25 – 30 μm).

Production of SLN by HPH can be done using either the hot or the cold homogenization technique. For both techniques, the active compound is dissolved or dispersed in the melted lipid prior to HPH [5,6].

2.3.7.1.1.1. Hot HPH

Figure 2.2 represents the schematic procedure of SLN preparation by hot HPH technique. The active compound-containing melted lipid (1) is dispersed in the hot surfactant solution (2) at the same temperature by high-speed stirring (3) [54,233,234] or by ultrasound (4) [36,54,233,234]. These procedures involve the break-up of large drops into smaller ones [54].

The obtained pre-emulsion (5) is then passed through a high pressure homogenizer (6). Typical production conditions are 500-1500 bar and 3 to 5 homogenization cycles. The obtained nanoemulsion is cooled down, solidifies and forms a SLN aqueous dispersion (7).

This technique is the most frequently applied. It can be applied to lipophilic and insoluble drugs. In general, even temperature sensitive compounds can be processed because the exposure time to elevated temperatures is relatively short. The technique is not suitable for incorporating hydrophilic drugs into SLN. During the homogenization of the melted lipid phase the drug will partition to the water phase resulting in a too low encapsulation.

2.3.7.1.1.2. Cold HPH

In the cold HPH technique (Figure 2.3), the active compound-containing melted lipid (1) is cooled down by means of dry ice or liquid nitrogen (2). Dry ice or liquid nitrogen are used to increase the brittleness of the lipid and to ease the further milling procedure. The high cooling rate favours a homogeneous distribution of the drug within the lipid matrix [7]. After solidification, the lipidic mass is grounded by means of ball or mortar milling (3) [11,44,114] to yield lipid microparticles in a range between 50 and 100 μm (4) [6]. The lipid microparticles are then dispersed in cold surfactant solution by stirring, yielding a macro-suspension (5). This suspension is passed through a high-pressure homogenizer at/or below room temperature (6) and the microparticles are broken down to form SLN (7). The cavitation and shear forces in the homogenization gap are sufficiently high to break the microparticles and to yield SLN. These particles stay in their solid state. Note that low temperatures increase the fragility of the lipid and favour, therefore, particle comminution [7].

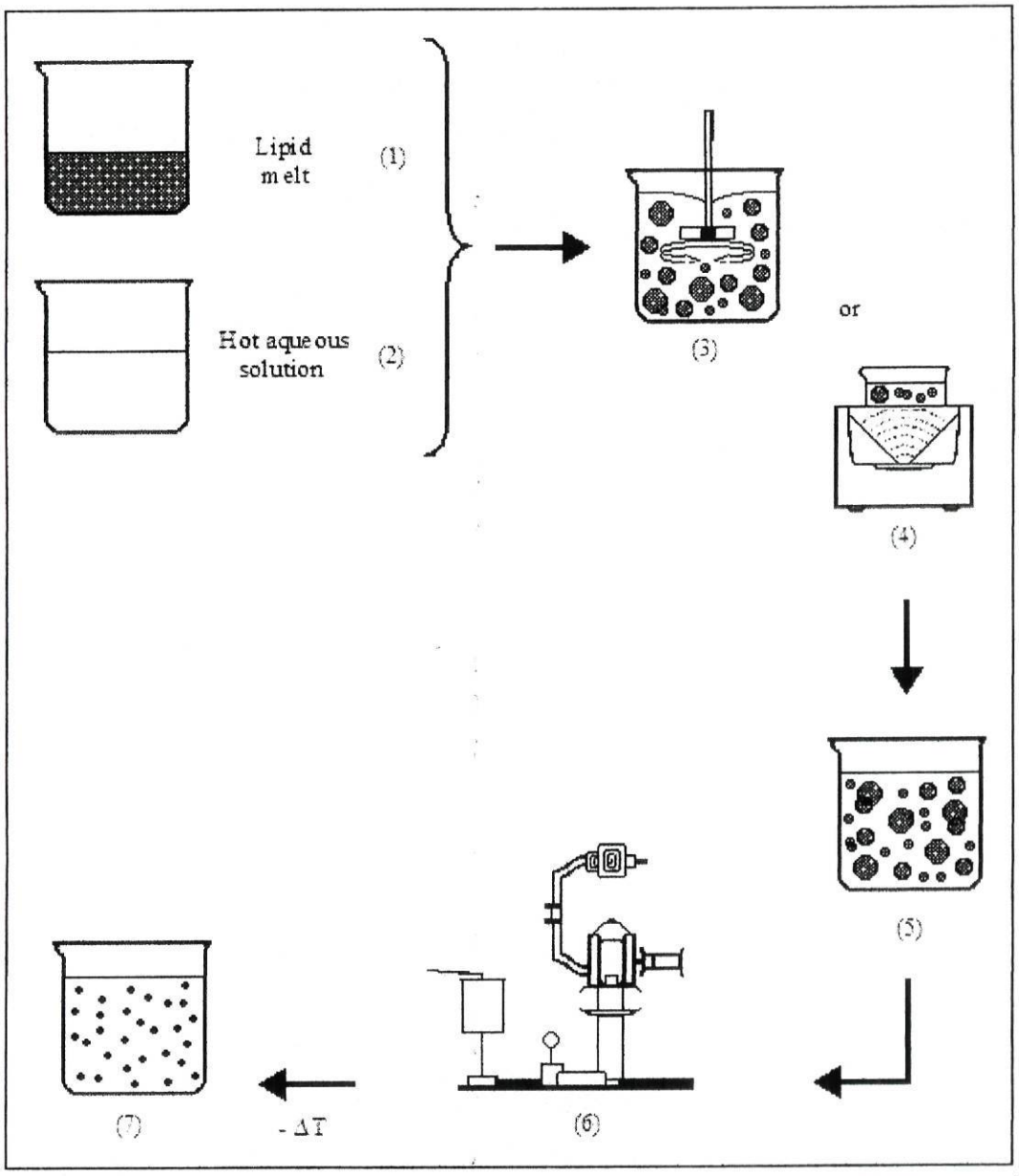

Figure 2.2: Schematic procedure of SLN preparation by hot HPH technique. (1) Active compound -containing melted lipid; (2) hot surfactant aqueous solution; (3) high-speed stirring; (4) ultrasounds; (5) O/W pre-emulsion; (6) HPH; (7) aqueous dispersion of lipid particles.

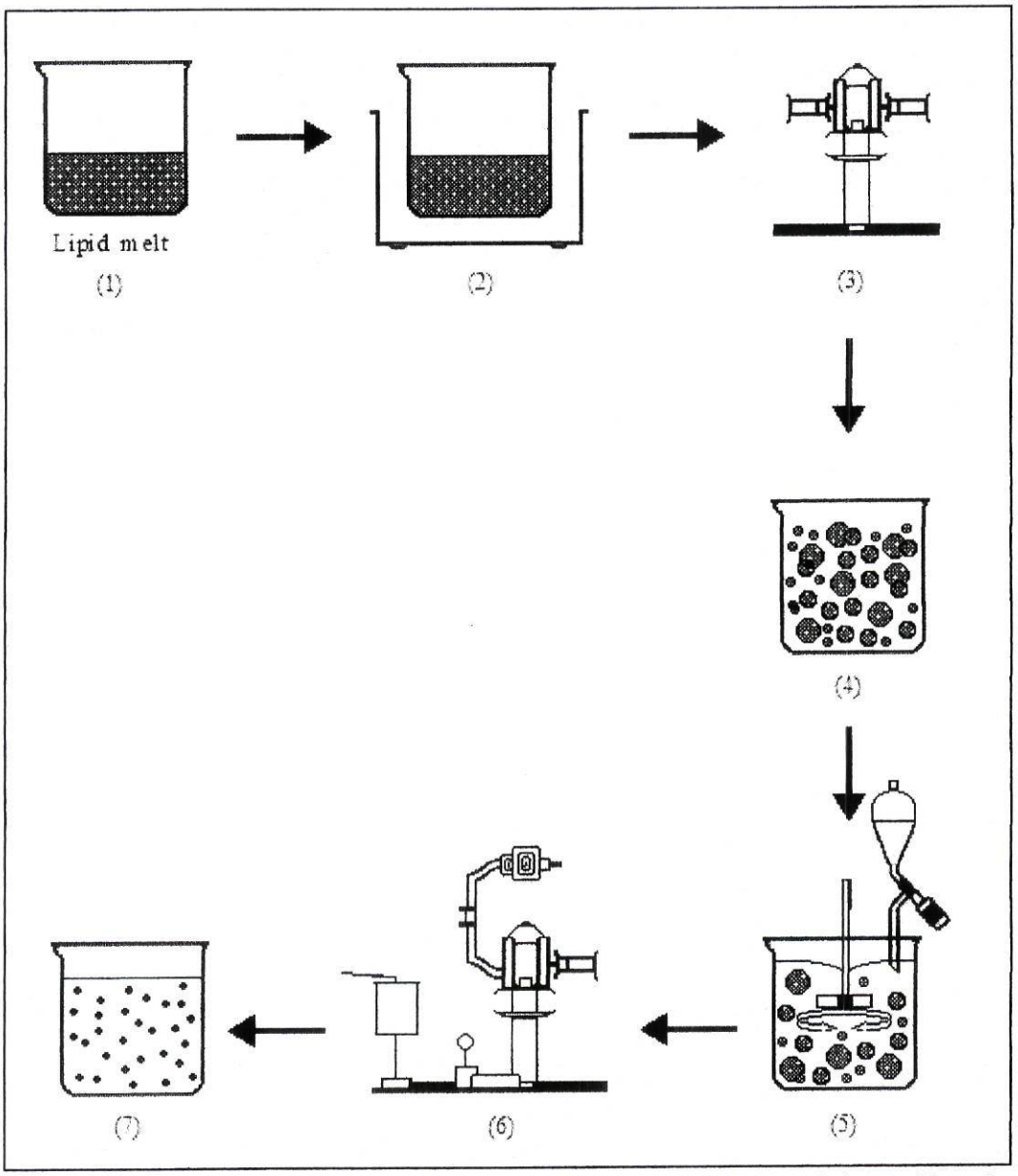

Figure 2.3: Schematic procedure of SLN preparation by cold HPH technique. (1) active compound-containing melted lipid; (2) cooling down; (3) mortar milling; (4) lipid microparticles; (5) dispersion of lipid micropaticles in cold surfactant solution; (6) HPH; (7) aqueous dispersion of SLN.

The cold HPH technique minimizes the thermal exposure of the sample, but does not avoid it completely due to the melting of the lipid in the initial step of the process. Therefore, this technique is recommended for extremely temperature sensitive compounds and hydrophilic compounds, which might partition from the liquid lipid phase to the water phase during the hot HPH. To further minimize the loss of hydrophilic compounds to the aqueous phase of SLN dispersion, water can be replaced by liquids with low solubility for the drug, such as oils and PEG 600 [6].

SLN prepared by this procedure possess a slightly higher polydispersity in size distribution compared to particles obtained by hot HPH technique, the mean particle sizes are also slightly higher compared to hot processing of the same lipid at identical homogenization parameters (pressure, temperature, number of homogenization cycles). To further reduce the mean particle size and to minimize the polydispersity, a higher number of homogenization cycles can be applied.

The cold HPH technique can be also employed when lipid matrix is composed by lipids with high melting points [93]. Note that this technique is less effective in dispersing the lipids. During the production process, the lipid matrix remains mainly in the solid state despite of possible high (but short) temperature peaks occurring in the high pressure homogenizer. The homogenization can be performed slightly below the melting point of the lipid (e.g. 5 to 10°C) which seems to lead to a softening of the lipid during the homogenization process. The softened lipid can be more easily dispersed leading to a more uniform product of smaller mean particle size. The homogenization temperature needs to be carefully selected because otherwise the loss of hydrophilic drugs to the water phase might be too high.

2.3.7.1.2. Microemulsions based SLN preparations

The microemulsion technique was developed by Gasco [230] and is represented in Figure 2.4. For the production of SLN by this technique, the matrix lipid is melted (1) and an O/W surfactant/co-surfactant containing aqueous phase is prepared at the same temperature (2), approximately 60-70°C [24,30,71,72,89,90,120-122,125-128]. Both organic and aqueous phases are added and mixed (3) in such a ratio that a microemulsion results (4) [127]. The size of the microemulsion region in the phase diagram is a function of temperature, which means that a microemulsion can convert to a different system when e.g. reducing the temperature. Therefore, the microemulsion needs to be kept at elevated temperatures during the production process. For nanoparticle formation, the hot microemulsion is poured into excess cold water (5)

[15,30,54,71,72,89,90,120-122,126,128]. This leads to a "breaking" of the microemulsion, converting it into an ultra-fine nanoemulsion, which recrystallizes forming SLN.

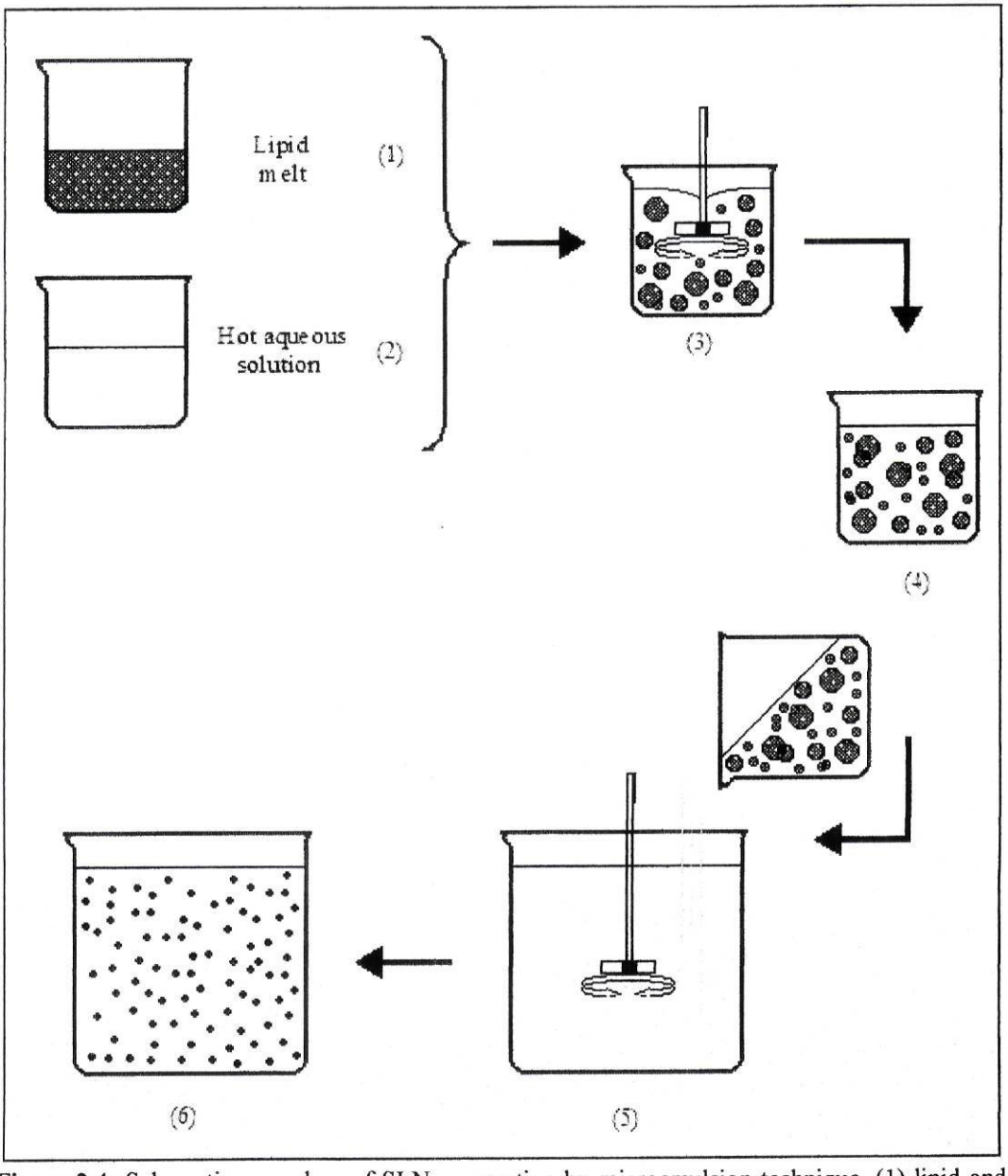

Figure 2.4: Schematic procedure of SLN preparation by microemulsion technique. (1) lipid and drug containing organic phase; (2) O/W surfactant containing aqueous phase; (3) emulsification between the organic phase and aqueous phase in order to prepare the microemulsion; (4) thermodynamically stable O/W microemulsion; (5) dilution of microemulsion in cold water under mechanical stirring; (6) aqueous dispersion of SLN.

Reasons for the breaking of the emulsion are the dilution with water and the reduction in temperature narrowing the microemulsion region. A typical microemulsion composition is 10-15% lipid, 15-25% surfactant, 2-10% co-surfactant and 50-73% water [127]. One disadvantage of the microemulsion method is the dilution of the particle suspension with water. Typically, the concentrations are distinctly below 1% particle content. In case of processing to a final dosage form, large amounts of water need to be removed, which is an inconvenient procedure.

2.3.7.1.3. Solvent emulsification-evaporation technique

Sjöström and Bergenståhl described a production method for preparing SLN dispersions by solvent evaporation in O/W emulsions [142]. This procedure is represented in Figure 2.5.

The lipid material is dissolved in a water-immiscible organic solvent, such as cyclohexane [65,142], chloroform [65] or methylene chloride [74], and then the drug is dissolved or dispersed producing an organic phase containing drug (1). This organic phase is emulsified in an O/W surfactant containing aqueous phase (2) by mechanical stirring (3). Upon evaporation of the organic solvent from the obtained O/W emulsion under mechanical stirring (4) [74] or reduced pressure (5) [65,142], a nanoparticle dispersion is formed by precipitation of the lipid in the aqueous medium (6). The solvent evaporation step must be quickly, in order to avoid particle aggregation [6].

This is a method analogous to the production of polymeric nanoparticles and microparticles by solvent evaporation [65]. The clear advantage of this procedure over the cold HPH technique described by Müller *et al.* [229], is the avoidance of any thermal stress. The major disadvantage is the use of organic solvents [7].

2.3.7.1.4. Solvent displacement technique

The solvent displacement technique was first described and patented by Fessi *et al.* [235], for the preparation of polymeric nanoparticles from pre-formed polymers. This method has also been recently used to prepare SLN [88,154,155] and is represented in Figure 2.6.

In this process, the lipid material is dissolved in a semi-polar water-miscible solvent, such as ethanol, acetone or methanol [88,154], and then the active compound is dissolved or dispersed in this phase (1). Simultaneously, an O/W surfactant containing aqueous phase is prepared (2). The organic phase is poured or injected into the aqueous phase under magnetic stirring (3). A violent spreading is observed because of the miscibility of both phases. Droplets of solvent of nanometer

size are torn from the O/W interface. These droplets are rapidly stabilized by the surfactant molecules presented in the aqueous phase, until diffusion of the solvent is complete and lipid precipitation has occurred. Removal of solvent can be performed by distillation (4). SLN are formed after total evaporation of the water miscible organic solvent (5).

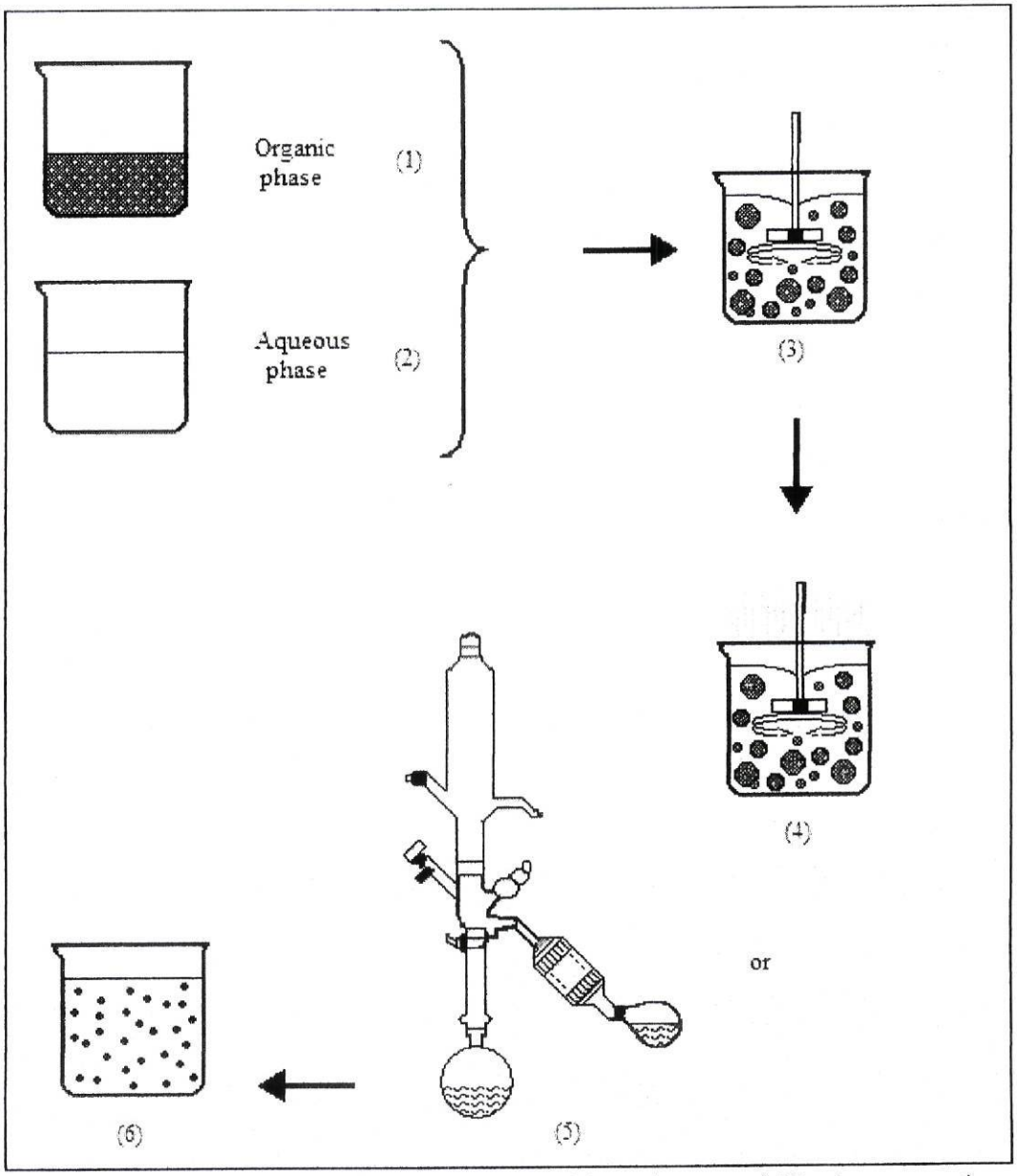

Figure 2.5: Schematic procedure of SLN prepared by solvent emulsification-evaporation technique. (1) lipid and drug containing organic phase; (2) O/W surfactant containing aqueous phase; (3) emulsification between the organic phase and aqueous phase; (4) evaporation of organic solvent under mechanical stirring; (5) evaporation of organic solvent under reduced pressure; (6) aqueous dispersion of SLN.

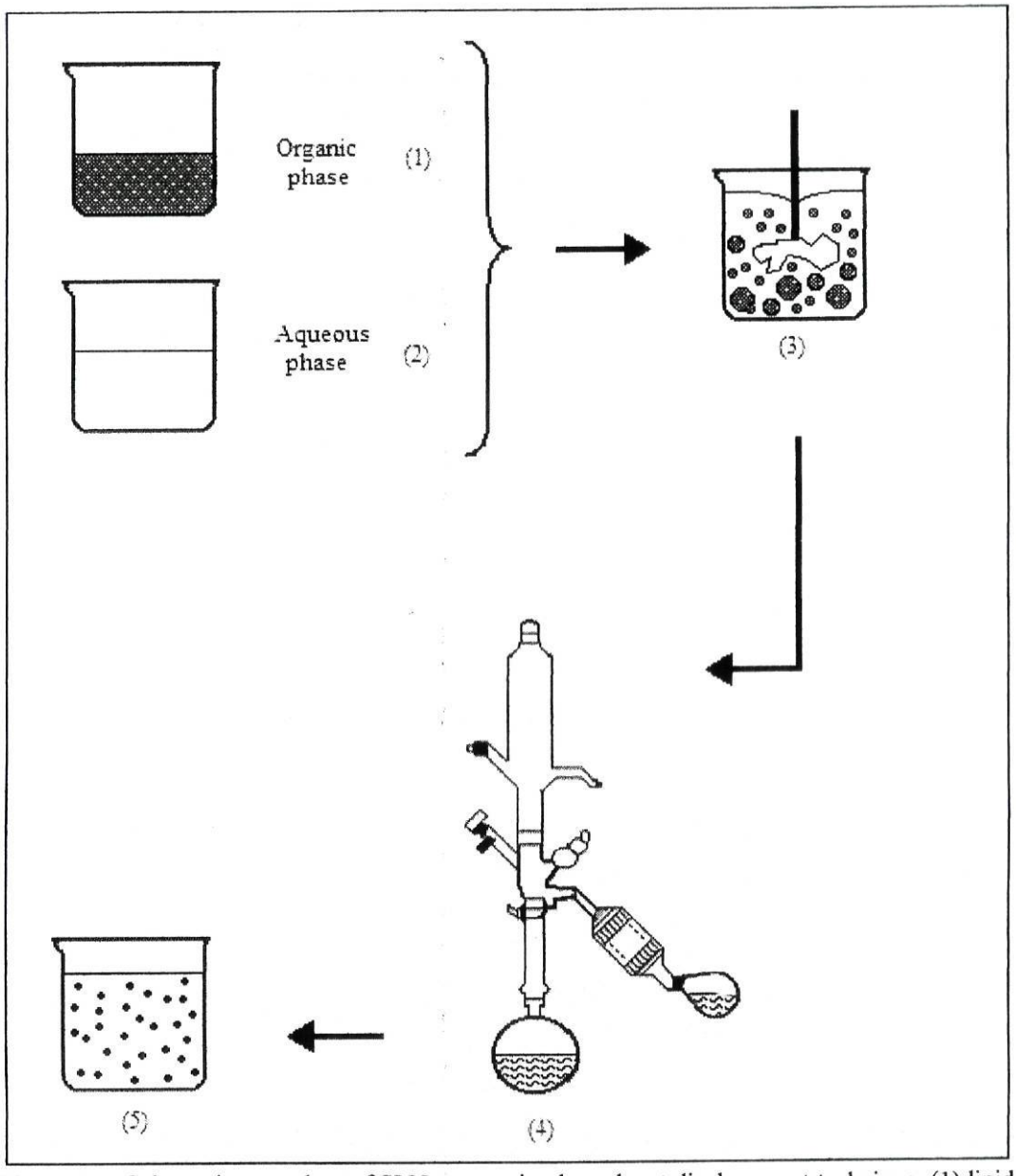

Figure 2.6: Schematic procedure of SLN preparation by solvent displacement technique. (1) lipid and drug containing organic phase; (2) O/W surfactant containing aqueous phase; (3) injection of the organic phase into the aqueous phase under magnetic stirring; (4) elimination of organic solvent by distillation; (5) aqueous dispersion of SLN.

2.3.7.1.5. Emulsification-diffusion technique

The emulsification-diffusion technique patented by Quintanar-Gerrero and Fessi in 1999 [236], is used to produce polymeric nanoparticles based on synthetic polymers. This method has also been recently used to prepare SLN [91,149] and is represented in Figure 2.7.

This procedure involves the use of a partially water soluble solvent (1), such as benzyl alcohol [91] or tetrahydrofuran [149], which is previously saturate with water (2) to ensure the initial thermodynamic equilibrium between the two liquids (water and solvent). The lipid is dissolved in the saturated solvent producing an organic phase where the drug is added. This organic phase is then emulsified, under vigorous agitation, in an aqueous solution containing a stabilizer agent obtaining an O/W emulsion (3). The subsequent addition of water to the system (4), under moderate mechanical stirring, causes solvent diffusion into the external phase and the lipid starts precipitating. Depending on its boiling point, the solvent can be eliminated by distillation (5) or ultrafiltration (6). After the organic solvent being totally eliminated, an aqueous dispersion of SLN is formed (7).

2.3.7.2. Models for incorporation of active compounds into SLN

According to Mehnert *et al.* there are three different models for the incorporation of active compounds into SLN [9]. These models are represented in Figure 2.8 and consist of a homogeneous matrix model, a drug-enriched shell model and a drug-enriched core model. The obtained structure depends on the formulation composition, i.e. the chemical nature of active compound, lipid and surfactant, and on the production method.

A homogeneous matrix with molecularily dispersed drug or drug being present in amorphous clusters (Figure 2.8, left) is thought to be mainly obtained when applying the cold HPH and when incorporating very lipophilic drugs in SLN with the hot HPH. In the former method, the bulk lipid contains the dissolved drug in molecularly dispersed form, mechanical breaking by HPH leads to nanoparticles having the homogeneous matrix structure. The same will happen when the oil droplets produced by the hot HPH is being cooled, crystallize and no phase separation between lipid and drug occurs during this cooling process. This model is assumed for drugs that can show prolonged release [27].

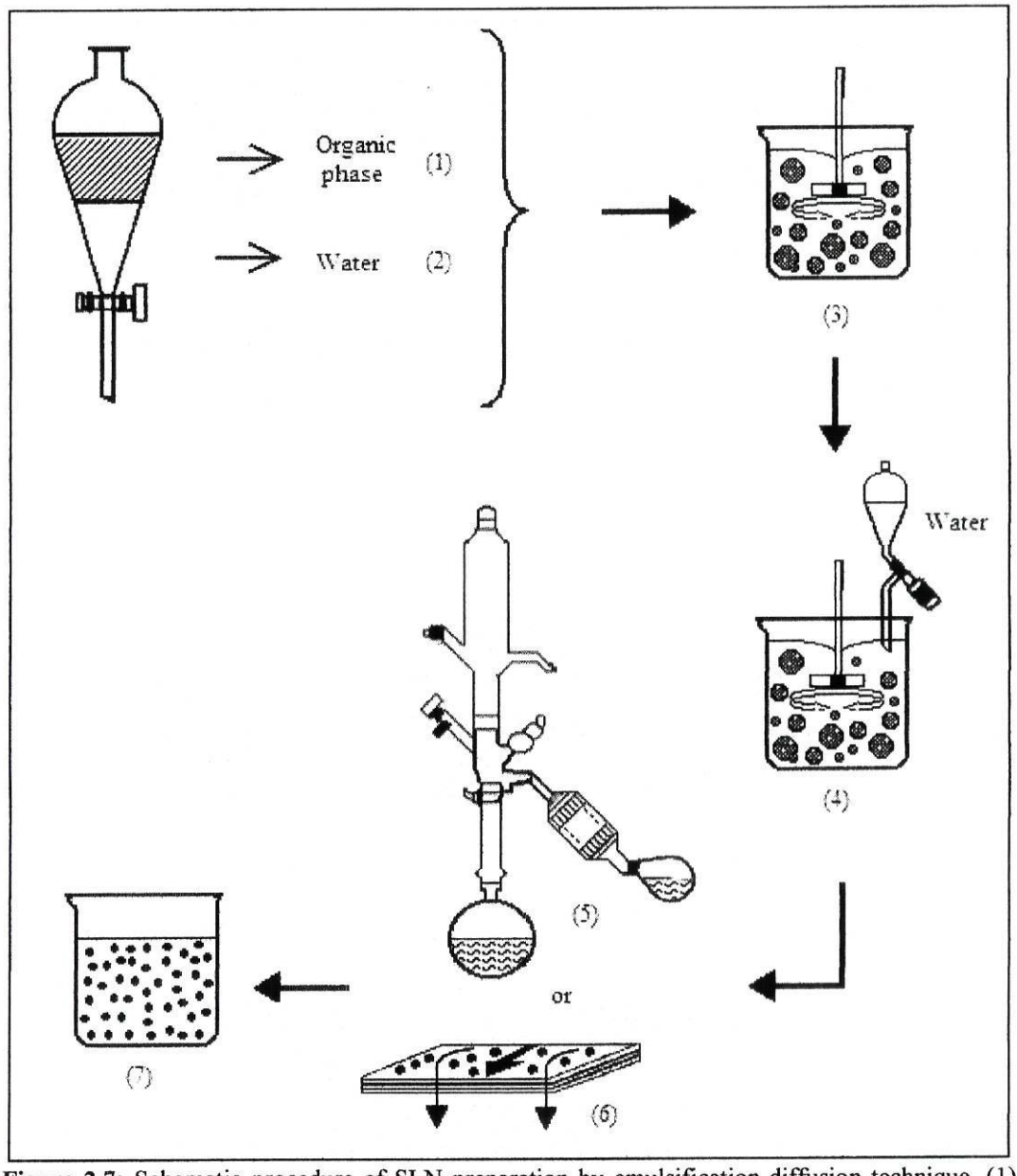

Figure 2.7: Schematic procedure of SLN preparation by emulsification-diffusion technique. (1) partially water soluble solvent; (2) water; (3) emulsification between the organic phase and an O/W surfactant containing aqueous phase; (4) addition of water under moderate mechanical stirring; (5) elimination of organic solvent by distillation; (6) elimination of organic solvent by ultrafiltration; (7) aqueous dispersion of SLN.

An outer shell enriched with active compound (Figure 2.8, middle) can be obtained when phase separation occurs during the cooling process from the liquid oil droplet to the formation of SLN when applying the hot HPH. The lipid can precipitate first forming a practically compound-free lipid core. At the same time, the concentration of active compound in the remaining liquid lipid increases continuously. Finally, the compound-enriched shell crystallizes. This model is valid for drugs that lead to a very fast release. A fast release can be highly desired when application of SLN to the skin should increase the drug penetration, especially when using the occlusive effect of SLN at the same time [27].

A core enriched with active compound (Figure 2.8, right) can be formed when the opposite occurs, which means the active compound starts precipitating first and the shell will have distinctly less drug. This leads to a membrane controlled release governed by the Fick law of diffusion [27]. This model is formed when the drug concentration is close to its saturation solubility in the lipid.

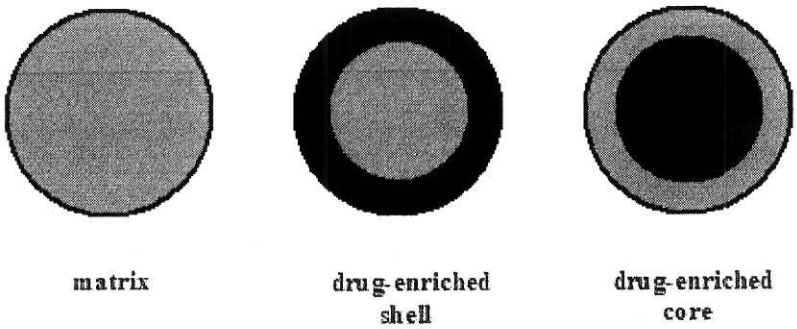

Figure 2.8: Models of incorporation of active compounds into SLN. (Adapted from Müller *et al.* [6]).

These three models of incorporation of active compounds into SLN described before represent ideal types. However, there are also mixed types which can be considered as a fourth type.

It has been reported that drugs can also be linked with the outer layer of SLN composed of phospholipids and steric stabilizers [69]. Distribution of the drug depends strongly on the physicochemical characteristics of the drug and components of the SLN. It is most influenced by the partition coefficient of the drug [68,78].

2.3.8. Nanostructured lipid carriers (NLC)

SLN were the first generation of a solid lipid nanoparticulate carrier. These systems can be considered as a solid development with interesting applications, however there was still some room for improvements which were realized in the next generation, the so-called "nanostructured lipid carriers" (NLC) [26-29].

The basic difference between SLN and NLC is that in the NLC concept controlled nanostructuring of the lipid matrix is performed, in order to increase drug-loading and to prevent drug expulsion, which gives more flexibility in modulation of drug release. This section describes the features of the novel NLC and the improvements compared to the first generation SLN.

SLN produced by hot HPH are formed during the cooling process of the hot O/W nanoemulsion as mentioned before. The solid nanoparticles are formed as a consequence of the lipid crystallization. As a result, a perfect crystal with little imperfections for drug accommodation can be formed immediately after production or during long-term storage leading to drug expulsion. To avoid this phenomenon, a less ordered lipid matrix with many imperfections is desirable. This approach was realized in the NLC. Figure 2.9 presents the differences between a perfect crystal in SLN in comparison to a structure with imperfections in NLC.

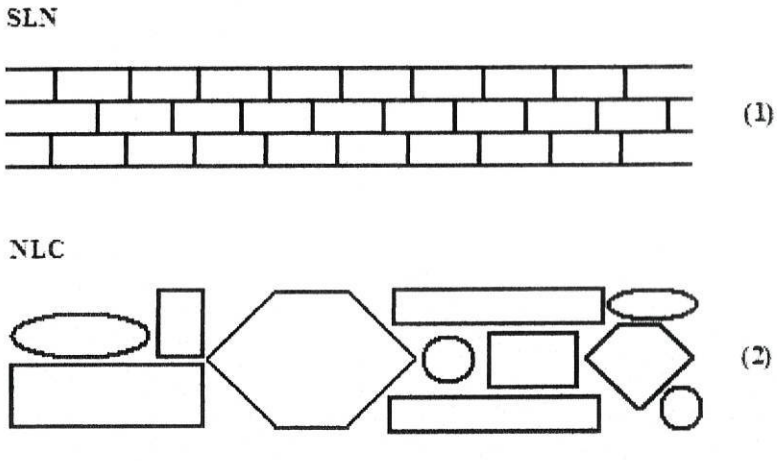

Figure 2.9: Differences between a perfect crystal in SLN in comparison to a structure with imperfections in NLC. Perfect crystal in SLN comparable with a brick all (1) and structure with imperfections due to spacially very different molecules in NLC (2). (Adapted from Müller *et al.* [27]).

Note that SLN are made from solid lipids and sometimes even highly purified lipids. This means that the lipid molecules are relatively similar, allowing the formation of structures with little imperfections [27]. In contrast to this, NLC are produced from lipid blends made from chemically very different molecules, which means mixing solid lipids with liquid lipids, such as oils. Figure 2.10 presents the three types of NLC compared to the relatively ordered matrix of SLN [27].

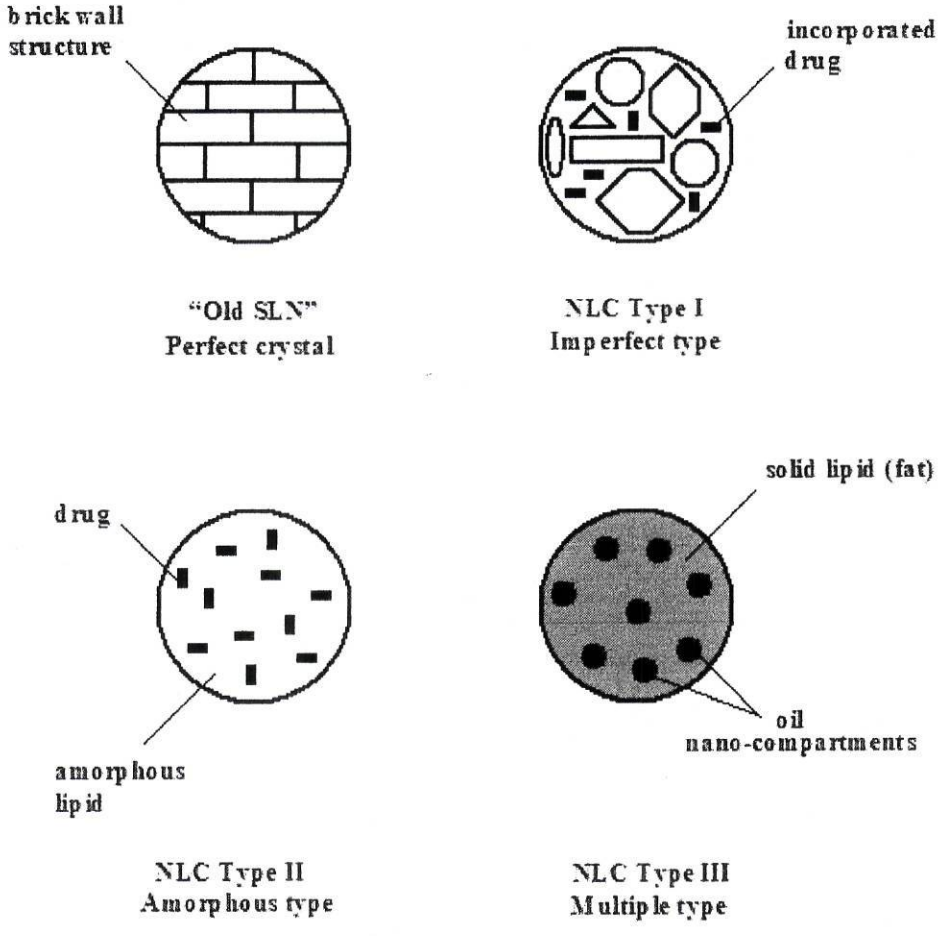

Figure 2.10: The three types of NLC compared to the relatively ordered matrix of SLN. (Adapted from Müller *et al.* [27]).

Due to the different chain lengths of the fatty acids and the mixture of mono-, di- and triacylglycerols, the matrix of NLC is not able to form a highly ordered structure [27]. There are many imperfections which are able to accommodate the drug. NLC based on this principle are called "imperfect crystal type" (type I, Figure 2.10 upper right) [27].

The occurrence of crystallization was identified as the basic mechanism to lead to drug expulsion. This phenomenon can be avoided by minimizing lipid crystallization, which means creating solid particles of amorphous lipid structure. This can be achieved by mixing special lipids which do not recrystallize anymore after homogenization and cooling down, like hydroxyoctacosanylhydroxystearate and isopropylmyristate [237]. This is the "amorphous type" of NLC (type II, Figure 2.10 lower left) [27].

For a number of drugs, the solubility in liquid lipids is higher than in solid lipids [56,107]. Therefore, the loading capacity for these drugs was improved by the development of the "multiple type" of NLC (type III, Figure 2.10 lower right). This type is derived from W/O/W emulsions, which consists of an oil-in-fat-in-water dispersion. In fact, tiny oil nanocompartments are created inside the solid lipid matrix of the lipid nanoparticles generated by a phase separation process [27]. A melted lipid and a hot oil are blended; therefore, the two lipids must show a miscibility gap at the used concentrations, approximately at 40°C. A hot O/W nanoemulsion is produced at higher temperature (80°C), the lipid droplets are cooled, when reaching the miscibility gap, the oil precipitates forming tiny oil droplets in the melted solid lipid. Subsequent solidification of the solid lipid as solid nanoparticle matrix leads to fixation of the oily nanocompartments. This is a procedure used to increase the solubility of a number of drugs in the particles [107].

Drug penetration into certain layers of the skin can be achieved using SLN or NLC as a consequence of the creation of a supersaturated system [27]. Supersaturation is a very useful method of enhancing the permeation of drugs across membranes such as skin, because unlike other methods, it does not interfere with the ultrastructure of the *stratum corneum*. Incorporation of lipid nanoparticles such as SLN and NLC into topical formulations (creams, ointments, emulsions, gels) can be performed to create supersaturated systems. The increase in saturation solubility will lead to an increased diffusion pressure of drug into the skin. Figure 2.11 shows the phenomenon of triggered drug release and supersaturation effect of NLC into a dermal preparation [27].

During storage, the drug remains in the NLC because these particles preserve their modification. After application to the skin, the increase in temperature and water loss observed lead to transformation to a more ordered lipid modification and are responsible for drug expulsion from the lipid matrix. The drug is expelled into the emulsion already saturated with drug and thus leading to supersaturation. This phenomenon increases the thermoactivity and leads to drug penetration into the skin.

In comparison to SLN, it can be stated that the novel NLC can be used for all purposes that the SLN have previously been exploited for. However, NLC can provide additional benefits such as higher drug loading capacity and avoidance or minimization of drug expulsion during storage. This is due to the less ordered structure of these new drug carrier systems.

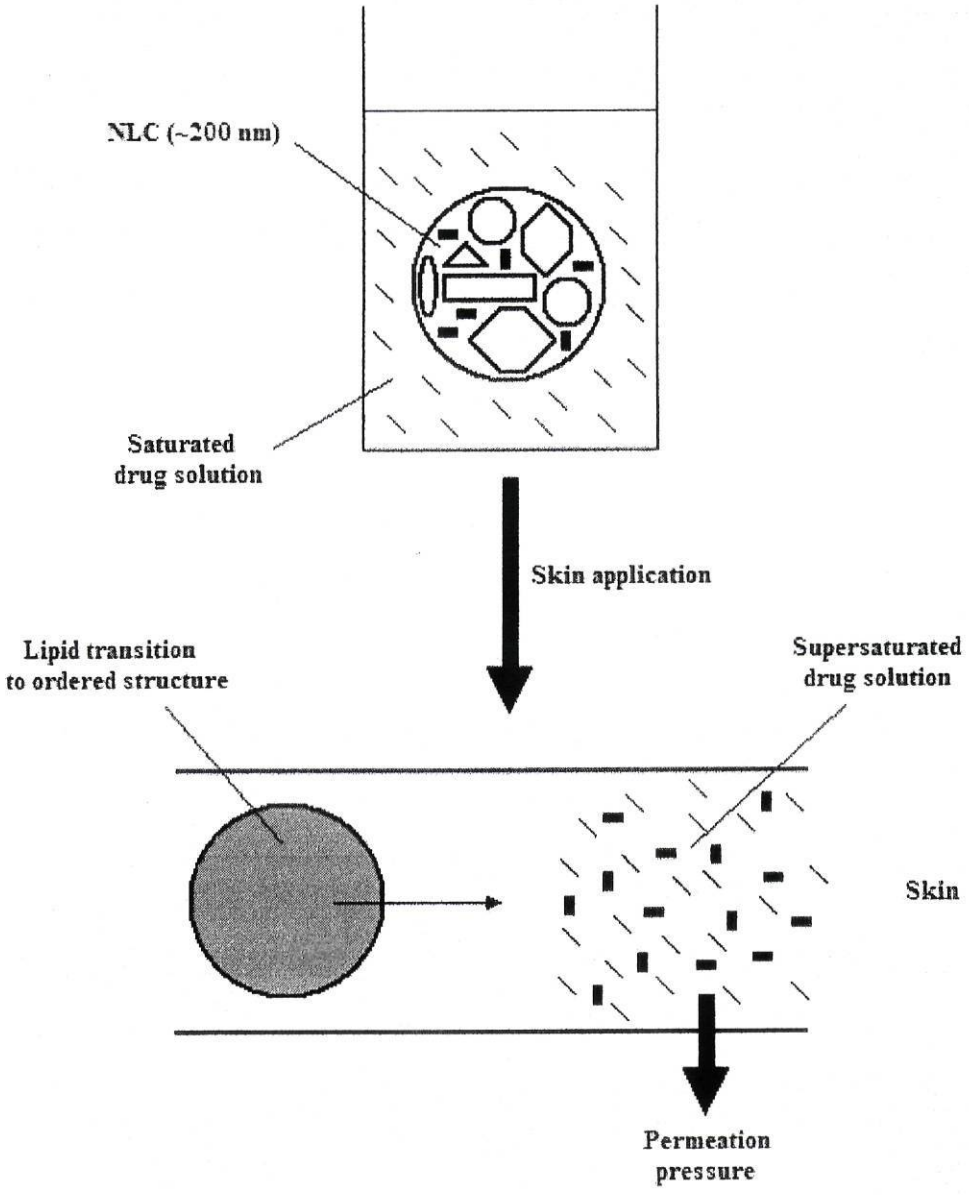

Figure 2.11: Triggered drug release and supersaturation effect. Drug-loaded NLC are incorporated into a dermal preparation. On the shelf the drug stays inside the NLC (upper); after application to the skin, the increase in temperature and water loss initiate transition to higher ordered structure in the lipid particle, drug is being expelled, supersaturation occurs increasing the thermodynamic activity and leading to increased penetration of the drug into the skin. (Adapted from Müller *et al.* [27]).

2.4. Lipid polymorphism

Polymorphism is the ability of a compound to crystallize in more than one distinct crystalline species with different internal lattices [238,239]. Lipid crystallization is an important point for the performance of the lipid nanoparticles. Therefore, polymorphism and the polymorphic transitions of acylglycerols are discussed in this section.

The internal structure of the lipid matrix can appear in a variety of ways, as shown in Table V. Lipids can crystallize in different three-dimensional structures, which are represented in Table VI [240].

According to Larsson [241], short spacings of triacylglycerols can be described as following:

1. α: Hexagonal (H) subcell with a lattice spacing of 0.415 – 0.42 nm;
2. β': Orthorhombic perpendicular ($O_{\perp}$) subcell with strong lattice spacings of 0.42 – 0.43 nm and 0.37 – 0.40 nm;
3. β: Triclin parallel ($T_{//}$) subcell with strong lattice spacings of 0.46 nm.

Further polymorphic forms are found with complex acylglycerols like mixed acid triacylglycerols or partial acylglycerols. Multiple β' and β, sub-α or intermediate forms, usually mentioned as β_i, have been described [242]. However, nomenclature and properties of monoacid triacylglycerols can also be used for these complex acylglycerols that have similar crystal packing [243].

Table V: Characterization of the crystal systems. (Adapted from Barrow [238]).

Crystal system	**Elementar lattice**	
	Axle	*Angle*
Cubic	a = b = c	$\alpha = \beta = \gamma = 90°$
Hexagonal	a = b, c	$\alpha = \beta = 90°$ $\gamma = 120°$
Rhomboedric	a = b = c	$\alpha = \beta = \gamma \neq 90°$
Tetragonal	a = b, c	$\alpha = \beta = \gamma = 90°$
Orthorhombic	a, b, c	$\alpha = \beta = \gamma = 90°$
Monoclinic	a, b, c	$\alpha = \beta = 90°$
Triclinic	a, b, c	α, β, γ

Table VI: Three-dimensional structure of the crystal order in the three main polymorphs from monoacid triacylglycerols. (Adapted from [243,244]).

	α - Modification	**β' - Modification**	**β - Modification**
Crystal system	Hexagonal	Monoclin	Triclin
Subcell	Orthorhombic	Orthorhombic	Triclin
b → a	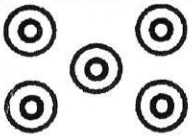		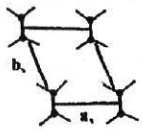
c → b			
c → a			

Crystallization of bulk triacylglycerols from the melt after rapid cooling usually occurs in the less stable α-form, which transforms via the β'-form, into the more stable β-form upon heating or during storage time [36].

In colloidal dispersions such as SLN, these transformations of triacylglycerols are faster than in the bulk material, which leads to a change in the relative fraction of the polymorphic forms [63]. Depending on the chemical nature of the lipid and the production conditions, different fractions of α and β' modifications may occur. This phenomenon can lead to a reduction of the melting point, or more precisely, changes in form and shift of the melting peak. These created polymorphic forms are not long-term stable, leading to a gradual transformation to more stable modifications, which means increasing content of β'/β_i and finally β. This is not desired because the change in lipid structure is responsible for drug expulsion during storage and changes in the release profile of incorporated drug.

Drug expulsion from suppository lipid matrices is a very well known phenomenon for many years [245]. There are many possibilities for incorporating drugs in the lipid matrix. In general, when a crystal is formed, foreign molecules can be incorporated by replacing host molecules in the lattice by a guest molecule or by being incorporated in between host molecules (however the guest molecule needs to be 20% smaller than the host molecule) [246].

In addition, drugs can be localized in between the lipid lamellae, resulting an increase in the lattice spacing "d", detectable by x-ray diffraction studies [247]. The drug can also be present in form of amorphous clusters, mainly localized in the imperfections of the crystal. In this case, drug accommodation is improved when the lipid crystal has more imperfections [247]. Thus, drug loading can be increased by using rather crude lipid mixtures or by controlled nanostructuring of the lipid matrix, i.e. creating as many imperfections as possible. Depending on the nature of the lipids used for blending the lipid matrix, different types of NLC will be obtained, as it has been reported in Chapter II.

It was found that the state of crystallinity of the lipid particles is also related to their physical stability in aqueous dispersions, i.e. absence or induction of particle aggregation and finally gel formation. It was observed that particle aggregation was accompanied, simultaneously, by transformation of high energetic polymorphic forms (i.e. mainly α) to more stable lipid modifications [98]. In general, the next step after particle aggregation is the increase of viscosity and the formation of soft and finally relatively rigid gels [66,97,248].

CHAPTER III

MATERIALS

CHAPTER III

MATERIALS

The raw materials used to prepare lipid nanoparticles represent a mixture of several chemical compounds [249].

In the context of this work, well-tolerated and *in vivo* biodegradable substances were selected for the preparation of lipid nanoparticles. The chosen lipids, emulsifying and gel-forming agents have GRAS status and are well accepted for human use.

3.1. Lipids

As matrix material for the lipid nanoparticles (either SLN or NLC) any lipid can be used since has a sufficiently high melting point, which normally should be higher than 37°C.

3.1.1. *Dynasan*®112, 114, 116 and 118

Dynasan are market products from *Sasol GmbH* (Witten, Germany). These products consist of lipid materials with a high content of microcrystalline triacylglycerols (approximately 90%) and monocarboxilic acids (approximately 10%). The triacylglycerols are glycerol esters of selected, even-numbered and unbranched fatty acids of natural origin, are free from antioxidants and other stabilizing agents. In the present work, *Dynasan*®112, 114, 116 and 118 have been used.

Dynasan®112 (triacylglycerol of lauric acid) is soluble in *n*-hexane and ether, and hardly soluble in ethanol [250].

Dynasan®114 (triacylglycerol of myristic acid) is slightly soluble in *n*-hexane and ether, and is also hardly soluble in ethanol [250].

Dynasan®116 (triacylglycerol of palmitic acid) and 118 (triacylglycerol of stearic acid) are hardly soluble both in *n*-hexane and ether as well in ethanol [250].

All *Dynasan* types are practically insoluble in water. If the individual *Dynasan* are rapidly cooled from the melt, glassy amorphous masses are initially formed which change on standing into crystalline modifications with volume expansion. The stable β-modification has a very sharp melting-point and is of triclinic structure. *Dynasan*®116 crystallizes in a β-modification (x-ray reflections at 4.6, 3.8 and 3.7 nm, long spacing $d_{001} = 4.5$ nm).

Dynasan should be stored in well-sealing containers and protected from light. Under these conditions, the product has a shelf life of at least 3 years. All products are stable against oxidation [251].

3.1.2. *Softisan*®154

Softisan®154 is a market product from *Sasol GmbH* (Witten, Germany), and belongs to the semi-synthetic acylglycerols, consisting of a mixture of di- (approximately 4%) and triacylglycerols (approximately 96%). It is defined as a special hard fat based on triacylglycerols with blends of natural, saturated even-numbered unbranched vegetable fatty acids with a chain length of C_{10}-C_{18}. It is free from antioxidants and stabilizers [150].

Softisan®154 is classified as "hydrogenated palm oil", with a melting point between 53 and 55°C and a drop point[2] between 53 and 55°C. It is characterized by an exceptional hardness at room temperature and a sharp melting range. The narrow interval between melting and solidification points allows a rapid and economic processing. This hard fat can be heated far beyond its melting point without its fast solidification and good contractibility being changed. It is exceptionally resistant against oxygen, so that there is no rancidity risk. This lipid is soluble in ether, toluol and acetone and is insoluble in water and ethanol.

3.1.3. *Witepsol*®H5, S55, E75 and E85

Witepsol bases are market products from *Hüls AG* (Witten, Germany), consisting mainly of mixtures of triacylglycerols of higher saturated fatty acids ($C_8H_{17}COOH$ to $C_{18}H_{37}COOH$) along with mono- and diacylglycerols [253]. They are white, odourless hard fats containing acylglycerols of vegetable origin and type specific additives.

In the present work, *Witepsol*®H5, S55, E75 and E85 have been used. Table VII shows the main typical properties of the used *Witepsol* bases.

Table VII: Main typical properties of some *Witepsol* bases. (Adapted from Kibbe [254]).

Witepsol base	Acid value	Hydroxyl value	Melting point (°C)	Saponification value	Solidification point
H5	≤ 0.2	5	34-36	235-245	33-35
S55	≤ 0.1	50-65	33.5-35.5	215-230	28-33
E75	≤ 1.3	5-15	37-39	220-230	32-36
E85	≤ 0.3	5-15	42-44	220-230	37-42

[2] Temperature at which the first drop of the melting substance to be examined falls from a cup under defined conditions [252].

3.1.4. *Imwitor*®900 and 191

Imwitor®900 and 191 are market products from *Hüls AG* (Witten, Germany), consisting of glyceryl stearate. *Imwitor*®900 has a content of 40-50% of this lipid, while *Imwitor*®191 has a content of 90%. They are soluble in acetone and diethyl ether, hardly soluble in heptan and insoluble in water [253]. *Imwitor*®900 is used as surfactant, co-surfactant and viscosifying agent in dermatological preparations [251].

3.1.5. *Compritol*®888 ATO

Compritol®888 ATO is a market product from *Gattefossé GmbH* (Weil am Rhein, Germany), based on glycerol esters of behenic acid (C_{22}). It consists of glycerol tribehenate (28-32%), glycerol dibehenate (52-54%) and glycerol monobehenate (12-18%). The main fatty acid is behenic acid (>85%) but other fatty acids (C_{16}-C_{20}) are also present [255].

Due to the presence of partial acylglycerols, *Compritol*®888 ATO has an amphiphilic character. Its hydrophilic-lipophilic balance (HLB) is approximately 2. The drop point is 69-74°C and the density is 0.94 g/cm^3 [256]. This lipid has a peroxide value lower than 6 meq O_2/kg, which gives a long stability character. It is soluble in chloroform, methylene chloride and xylene when heated and is insoluble in ethanol, ethyl ether, mineral oils and water.

It is used as lubricating agent for tablets and capsules, as a binding agent for direct compression and as a lipophilic matrix in sustained release formulations. In dermal preparations this lipid is used as viscosifying agent for oil phases in W/O or O/W emulsions and improves heat stability of emulsions. It has to be stored below 35°C because of the risk of caking, avoiding the contact with air, light, heat and moisture in its original packing [255].

3.1.6. *Precirol*® ATO 5

Precirol® ATO 5 (glycerol palmitostearate) is a market product from *Gattefossé GmbH* (Weil am Rhein, Germany). It is composed of a blend of mono- (8-17%), di- (approximately 54%) and triacylglycerols (approximately 30%) of saturated fatty acids of mainly natural origin ($C_{16}H_{32}O_2$) and ($C_{18}H_{36}O_2$) [255]. The main components are palmitic acid and stearic acid (approximately 48%).

This lipid has a melting point between 50 and 60°C, the HLB value is approximately 2 and the drop point is between 53 and 57°C [255]. It is soluble in chloroform and methylene chloride and is insoluble in mineral oils, ethanol and water.

Precirol® ATO 5 is a fine white powder used as taste-masking agent in wet granulation, melt granulation and hot-melt coating, as sustained release lipophilic matrix and as a lubricating agent with binding properties for tablets and powders filled into hard gelatine capsules. The storage must be below 35°C, avoiding the contact with air, light, heat and moisture. For storage above 1 month it must be between 2 and 15°C.

3.1.7. *Precifac*® ATO 5

Precifac® ATO 5 (cetyl palmitate) is a market product from *Gattefossé GmbH* (Weil am Rhein, Germany). Cetyl palmitate is a wax, composed of cetyl alcohol ester of palmitic acid, which chemically is hexadecyl hexadecanoate ($C_{32}H_{64}O_2$).

Differential scanning calorimetry (DSC) investigations showed for *Precifac*® ATO 5 an onset temperature of 51.9°C and a peak maximum at 55.9°C [178]. Its drop point is between 52 and 53°C. It is soluble in chloroform and acetone and practically insoluble in paraffin, water and ethanol [255].

In topical formulations, such as creams and fluid emulsions, *Precifac*® ATO 5 can be used as viscosifying agent [251].

3.1.8. *Apifil*®

Apifil® is non-ionic hydrophilic white beeswax obtained from *Gattefossé GmbH* (Weil am Rhein, Germany). The raw materials used in its production are waxes obtained from the honeycomb of the bee *Apis mellifera Linné* and polyethylene glycols from petrochemical origin.

Chemically, this beeswax consists of 70-80% of a mixture of various esters composed of straight-chain monohydric alcohols with even-number carbon chains from C_{24}-C_{36} esterified with straight-chain acids, which also have even-numbers of carbon atoms up to C_{26} together with some C_{18} hydroxyl acids [255]. The chief ester is myricyl palmitate. Also present are free acids (approximately 14%) and carbohydrates (approximately 12%), as well as approximately 1% of free wax alcohols and stearic esters of fatty acids.

Apifil® has a HLB lower than 5 and a drop point between 59 and 70°C [255]. Its peroxide value is below 6 meq O_2/Kg and its density is between 0.95 and 0.96 g/cm^3 [254]. This structural

self-emulsifying base is insoluble in ethanol and water, slightly soluble in vegetable oils and soluble in chloroform and methylene chloride when heated at 60°C [255].

This lipid is used as a non-ionic O/W emulsifying agent, stiffening agent and controlled-release vehicle. It is designed for emulsions in skincare, suncare and haircare, and for O/W masks in make-up applications. It can also be used as an additive for lipsticks and pencils due to its moisturizing and film forming properties [255]. During storage, the contact with air, light and heat must be avoided.

3.1.9. *Miglyol*®812

Miglyol®812 is a liquid triacylglycerol obtained from *Caelo GmbH* (Hilden, Germany). This lipid consists of middle-chain-triacylglycerols (C_8-C_{10}), having a density between 0.945 and 0.955 g/cm^3 [257]. It is used as skin oil and dissolution medium for many substances [251].

3.2. Emulsifying agents

The IUPAC[3] defines the properties of an emulsifying agent as a surfactant which is positively adsorbed at interfaces and lowers the interfacial tension. When present in small amounts, it facilitates the formation of an emulsion or enhances its colloidal stability by decreasing either or both of the rates of aggregation and coalescence [258].

These properties are primarily attributed to the traditional emulsifying agents. They are characterized by an amphiphilic structure and are capable to form micellar aggregates. Polymers can function in the same manner, if they are sufficiently surface-active. The use of polymers as primary emulsifying agents is widely spread in food products but plays a minor role in pharmaceutical and cosmetic formulations [259].

As referred before, SLN and NLC are stabilized by surfactants or by polymers in aqueous dispersions. In the present work, a full range of emulsifying agents used either in cosmetic products or in pharmaceutical products was selected.

3.2.1. *Tween*®80

Tween®80 or polyoxyethylene 20 sorbitan monooleate (polisorbate 80) is a market product from *ICI Surfactants* (Essen, Germany). It consists of a series of partial fatty acid esters of

[3] International Union of Pure and Applied Chemistry.

sorbitol and its anhydrides copolymerized with approximately 20 moles of ethylene oxide for each mole of sorbitol and its anhydrides [254]. The resulting product is therefore a mixture of molecules of varying sizes rather than an uniform mixture of a single chemical. It is miscible with water, alcohol, dehydrated alcohol, ethyl acetate and methyl alcohol and it is insoluble in liquid paraffin and fixed oils [260]. It has a HLB of 15.3 [261].

Tween®80 is a non-ionic surfactant widely used as emulsifying agent in the preparation of stable O/W pharmaceutical emulsions and can also be used as a solubilizing agent for a variety of substances, including essential oils and oil-soluble vitamins, and as wetting agents in the formulation of oral and parenteral suspensions. It is generally regarded as non-toxic and non-irritant material widely used in cosmetics and topical pharmaceutical formulations.

3.2.2. *Span*®85

Span®85 or sorbitan trioleate is a market product from *ICI Surfactants* (Essen, Germany). It consists of a series of mixtures of partial esters of sorbitol, and its mono- and dianhydrides with fatty acids [254]. It is widely used in cosmetics, food products and pharmaceuticals as lipophilic non-ionic surfactant. *Span*®85 is mainly used in pharmaceutical formulations as emulsifying agent in the preparation of creams, emulsions and ointments for topical application [261]. When used alone, produces stable W/O emulsions and microemulsions but is frequently used in combination with varying proportions of a polysorbate to produce either W/O or O/W emulsions or creams of varying consistencies. *Span*®85 has a HLB of 1.8.

3.2.3. *Lutrol*®F68

Lutrol®F68 or poloxamer 188 is a non-ionic surfactant obtained from *BASF AG* (Ludwigshafen, Germany). It consists of polyoxyethylene-polyoxypropylene block copolymer used primarily in pharmaceutical formulations as emulsifying or solubilizing agent [262]. The polyoxyethylene segments are hydrophilic while the polyoxypropylene segments are hydrophobic. It is freely soluble in water and alcohol and it has a HLB of 29 [263].

3.2.4. *Lipoid*®S75

Lipoid®S75 or soybean lecithin is a market product from *Lipoid KG* (Ludwigshafen, Germany). It is described as a complex mixture of acetone-insoluble phosphatides, which consist

chiefly of phosphatidylcholine, phosphatidylethanolamine, phosphatidylserine and phosphatidylinositol, combined with various amounts of other substances such as triacylglycerols, fatty acids and carbohydrates as separated from a crude vegetable oil source (soja) [254].

It is partially soluble in water, but readily hydrates to form emulsions. The oil-free phosphatides are soluble in fatty acids, but are practically insoluble in fixed oils [264]. When all phosphatide fractions are present, lecithin is partially soluble in alcohol and practically insoluble in acetone.

Lecithin is mainly used in food and pharmaceutical industry as dispersing, emulsifying and stabilizing agent [260].

3.2.5. *Tego Care*®450

Tego Care®450 or polyglycerol-methylglucose distearate is a market product from *Goldschmidt* (Essen, Germany). It is described as a PEG-free, non-ionic O/W-emulsifying agent, with a HLB value of 11.5 [265].

3.2.6. *Tyloxapol*®

Tyloxapol® is a polymer of 4-(1,1,3,3-tetramethylbutil)-phenol with ethylene oxide and formaldehyde obtained from *Caelo GmbH* (Hilden, Germany) [257]. It is described as a non-ionic surfactant which can be used to stabilize either O/W or W/O emulsions [260].

3.2.7. *Lanette*®N

Lanette®N is an anionic emulsifying wax obtained from *Gattefossé* (Weil am Rhein, Germany). It contains cetostearyl alcohol, purified water and either sodium lauryl sulphate or a sodium salt of similar sulfated higher primary aliphatic alcohol [254]. This wax is used in cosmetic and topical pharmaceutical formulations primarily as an emulsifying agent, and is added to fatty or paraffin bases in order to facilitate the production of O/W emulsions [255].

3.3. Gel-forming agents

Hydrogels are semi-solid systems consisting of highly swollen, hydrophilic polymer networks that can absorb large amounts of water and drastically increase in volume [266]. It is well known that physicochemical properties of the hydrogel depend not only on the molecular structure, the gel structure and the degree of cross-linking, but also on the content and state of water in hydrogel.

In the present work, four different types of hydrogels were prepared, in order to incorporate aqueous dispersions of SLN and NLC.

3.3.1. Xanthan gum

Xanthan gum (XG) was obtained from *Sigma Aldrich* (Deisenhofen, Germany). It is a high molecular weight polysaccharide gum (MW $\approx 2x10^6$ g/mol) produced by a pure-culture fermentation of a carbohydrate with *Xanthomonas campestris*, then purified by recovery with isopropyl alcohol, dried and milled [260]. It contains D-glucose and D-manose as the dominant hexose units, along with D-glucuronic acid [254].

The backbone of this polysaccharide consists of four β-D-glucose units linked at the 1 and 4 positions, and is therefore identical in structure to cellulose. Trisaccharide side chains on alternating anhydroglucose units distinguish XG from cellulose. Each side chain comprises a glucuronic acid residue between two manose units. At most of the terminal mannose units a pyruvate moiety is present; the mannose nearest the main chain carries a single group at C-6. The resulting stiff polymer chain may exist in solution, as a single, double or triple helix which interacts with other XG molecules to form complex, loosely bound network. It is soluble in hot and cold water [260].

This polymer is widely used in oral and topical pharmaceutical formulations, cosmetics and food products as suspending and stabilizing agent [267]. It is generally regarded as non-toxic and non-irritant at the levels usually employed.

3.3.2. Hydroxyethylcellulose 4000

Hydroxyethylcellulose (HEC) was obtained from *Sigma Aldrich* (Deisenhofen, Germany). It is a non-ionic, water-soluble polymer widely used in pharmaceutical formulations [254]. It is prepared by treating cellulose with NaOH and then reacted with ethylene oxide [260].

It is primarily used as a thickening agent in ophthalmic and topical formulations, although it is also used as a binder and film coating agent for tablets [267].

The concentration of HEC used in a formulation is dependent upon the solvent used and the MW of the grade [254]. It is available in several grades, carrying in viscosity and degree of substitution and some grades are modified to improve their dispersion in water. The grades are distinguished by appending a number indicative of the apparent viscosity, in mPa.s, of a 2% (*m/V*) solution measured at 20°C.

This polymer is soluble either in hot or cold water, forming clear, smooth, viscous and uniform solutions [260]. It is practically insoluble in acetone, ethanol, ether, toluene and most other organic solvents. In some polar organic solvents, such glycols, HEC swells or is partially soluble [254].

3.3.3. *Carbopol*®934

Carbopol®934 (polyacrylate, PA) was obtained from *BF Goodrich* (USA). It is a carbomer polymer, mainly used in liquid and semi-solid pharmaceuticals as a suspending or viscosifying agent [268]. It is a synthetic polymer with a high MW formed by repeating units of acrylic acid, crosslinked with either allylsucrose or allylethers of pentaerythritol [254]. It contains between 56 and 68% of carboxylic acid (-COOH) groups as calculated on the dry basis. It forms a gel like structure in water, alcohol and glycerine when neutralized with alkali hydroxides or amines [260].

3.3.4. Chitosan

Chitosan (CH, minimum 85% deacetylated) was obtained from *Sigma Aldrich* (Deisenhofen, Germany). It is a hydrophilic biopolymer, which chemically is β-(1,4)-2-amino-2-deoxy-D-glucose [267]. Chitosan is industrially obtained by hydrolysing the aminoacetyl groups of chitin, which is the main component of the exoskeleton of crustaceans, by an alkaline treatment [269,270]. This polymer is insoluble in water, but can be solubilized in dilute acetic acid due to the formation of the acetate salt [271].

CH has a MW between 500 000 and 800 000 g/mol and it is considered to be biocompatible, biodegradable and non-toxic [270]. Its cationic character and potential functional groups make it an attractive biopolymer for many biomedical and pharmaceutical applications. In an acidic environment, CH swells into a hydrogel and has also been used to slow drug release [269].

3.4. Water

The water used in all experiments was Purified Water (European Pharmacopoeia, 4th ed.) obtained from a *MilliQ Plus, Millipore* (Schwalbach, Germany). It is mainly characterized by an osmotic resistance of 18 MOhm.cm and a total organic content equal or lower than 10 ppb [252].

3.5. Clotrimazole

Clotrimazole, or (1-2-chlorphenyl-diphenylmethyl)-1-4-imidazole, was obtained from *Caelo GmbH* (Hilden, Germany). It is synthesized by the reaction of o-chlorotritylchloride with imidazole in the presence of a tertiary amine [257,272].

This drug is a synthetic derivative of imidazole with a broad-spectrum antifungal agent that inhibits growth of pathogenic dermatophytes [273], yeasts [188] and *Pityrosporon obiculare* (*Malassezia furfur*) [272]. It exhibits fungicidal activity *in vitro* against isolates of *Plasmodium falciparum* [274], *Fusarium solani* [275], *Triadelphia pulvinata* [276], *Thrichophyton rubrum* [277,278], *Thrichophyton mentagrophytes* [277], *Epidermophyton floccosum* [277], *Microsporum canis* [277,279] and *Candida albicans* [188]. It has a local antifungal effect, especially on the mucous membranes, which is widely used for the treatment of mycotic infections of the genitor-urinary tract [280]. It shares with econazole and miconazole the first choice status for topical treatment of *tinea pedis*, *tinea crusis* and *tinea corporis* due to any of the afore-mentioned organisms, *candidiasis* due to *Candida albicans* and *Tinea versicolor* due to *Pityrosporon obiculare*, as well as for local treatment of *oropharyngeal candidiasis* [190].

The structure of clotrimazole is represented in Figure 3.1.

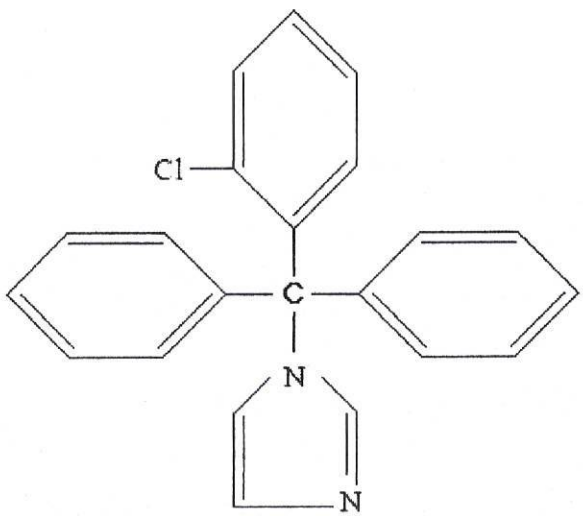

Figure 3.1: Structural formula of clotrimazole.

Clotrimazole is a colorless, odourless, tasteless and crystalline solid [272]. It is practically insoluble in water (<0.01 mg/ml), soluble in chloroform and methanol (>100 mg/ml), in ethanol (95 mg/ml) and in diethyl ether (14 mg/ml). It is freely soluble in acetone and methyl alcohol [260].

This drug is stable in the solid state under normal storage conditions [272]. It is unaffected by heat and by exposure to daylight for up two weeks. In solution, the stability of clotrimazole is pH dependent. It is stable in alkaline media, but it decomposes into o-chlorophenyl-diphenylmethanol and imidazole in acid media [272]. A relative hydrolytic stability in solution in ethanol-water and isopropanol-water mixtures under acidic, neutral and alkaline conditions has been reported.

DSC curve of clotrimazole shows a single sharp endotherm with an extrapolated onset temperature of 143°C and the molar melting enthalpy "ΔH" was calculated to be 7540 cal/mol [272]. A melting range between 141° and 145°C for this drug has been reported.

After topical administration, clotrimazole undergoes rapid biotranformation into inactive metabolites. It has been found that when clotrimazole was applied in the skin as a cream, the drug penetrated the skin to a depth of 2000 μm and no drug substance or metabolites were detected in the serum [281]. A small quantity of the material (up to 0.4%) was detected in the urine over a five-day period.

Several methods have been proposed for the identification of clotrimazole, such as titrimetric, spectrophotometric and chromatographic analysis [272]. Kráčmar *et al.* [282] have characterized the UV spectra of clotrimazole in methanol and in 0.1 N HCl as an aid to the identification of this drug substance.

3.6. Other materials

3.6.1. Glycerol 85%

Glycerol is an osmotic agent with lubricating and moisturising properties and has a wide range of pharmaceutical applications [260]. It is miscible with water and alcohol, slightly soluble in acetone, practically insoluble in chloroform, ether and in fixed and essential oils.

Glycerol 85% is an aqueous solution containing not less than 83.5% (*m/m*) and not more than 88.5% (*m/m*) of propane-1,2,3-triol [252]. In the present work, this product was used as humectant and emollient in the preparation of the hydrogels.

3.6.2. Sodium hydroxide

Sodium hydroxide (NaOH) is a dry, very deliquescent, white or almost white strongly alkaline powder. It is completely soluble in water and freely soluble in alcohol [260]. An aqueous solution of NaOH at 5% (*m/V*) was used as a neutralizing agent of the PA in order to form a gel.

3.6.3. Acetic acid

Acetic acid (CH_3COOH) is a clear colourless liquid with a pungent odour. This product is miscible with water, alcohol and glycerol [260]. An aqueous solution of CH_3COOH at 4% (*m/V*) was used to start gel formation of CH.

CHAPTER IV

METHODS

CHAPTER IV

METHODS

4.1. Preparation of SLN and NLC

The preparation of SLN and NLC was performed by the hot HPH technique, as described by Müller and Lucks [229]. The principle of HPH for the production of stable emulsions has been known for about 100 years [283]. The first homogenizer was introduced by Auguste Gaulin in 1890. In spite of the numerous modifications that this technique has suffered, the basic principle of high-pressure relief has not changed.

The high-pressure homogenizer consists of a high-pressure plunger pump with a subsequent relief valve [283]. The function of the plunger pump is to provide the energy level required for the relief. The relief valve (i.e. the homogenizing valve) consists of a valve seat, which is fixed, and an adjustable valve (Figure 4.1). Both parts form an adjustable radial precision gap. The gap conditions, the resistance and thus the homogenizing pressure, vary as a function of the force acting on the valve. An external impact ring forms a defined outlet cross section and prevents the valve casing from damage due to the flow.

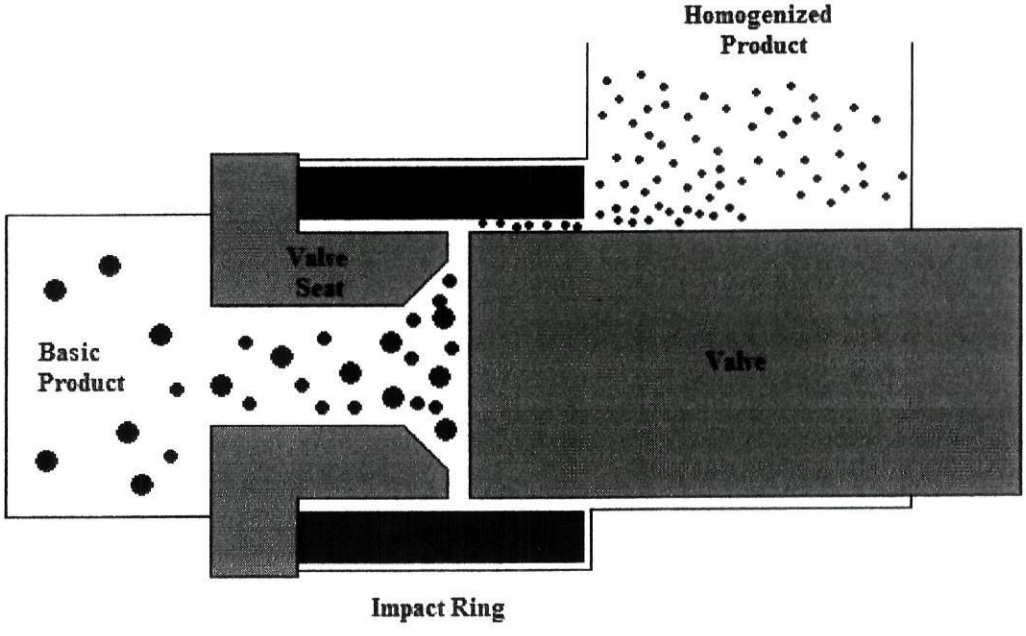

Figure 4.1: The principle of HPH. (Adapted from Jahnke [283]).

Briefly, in order to prepare SLN and NLC, in the present work the lipid phase was melted at 90°C. This hot lipid phase was dispersed in a hot surfactant aqueous solution (90°C), using an *Ultra-Turrax T25* (*Jahnke & Kunkel GmbH and Co KG*, Staufen, Germany) at 8000 rpm for 1 min. The obtained pre-emulsion was then homogenized at 90°C, using an *APV Micron Lab 40* (*APV Deutschland GmbH*, Lübeck, Germany) and applying a pressure of 500 bar. The obtained product was filled in siliconized glass vials, which were immediately sealed. Figure 4.2 shows a picture of the discontinuous *APV Micron Lab 40* used for the preparation of SLN and NLC.

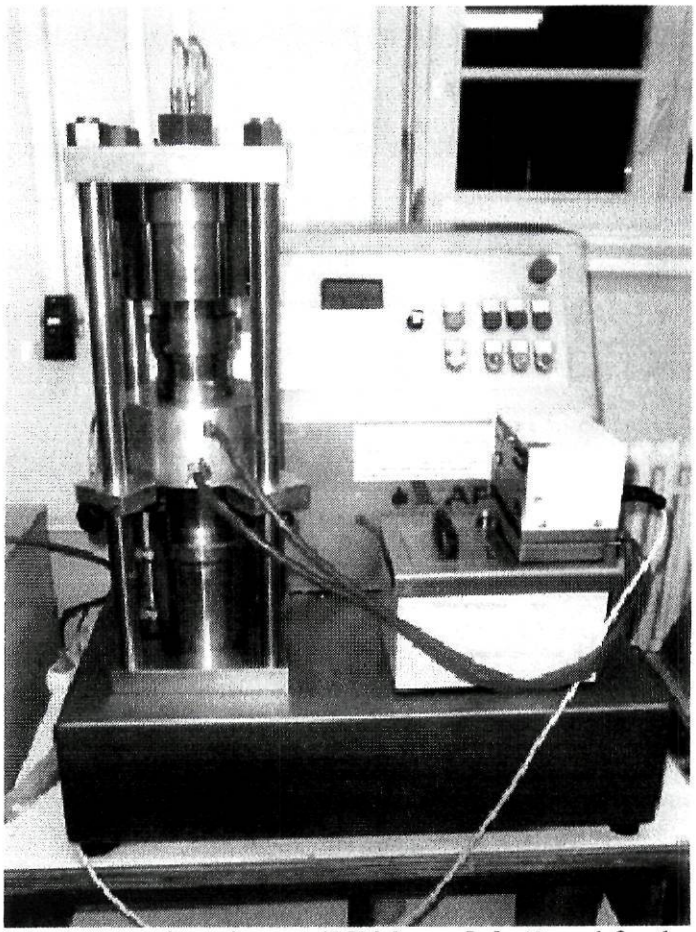

Figure 4.2: Discontinuous *APV Micron Lab 40* used for the production of SLN and NLC.

4.2. Preparation of hydrogels-loaded SLN and NLC

The SLN and NLC containing hydrogels were composed of 5% glycerol, 50% SLN or NLC aqueous dispersion, a sufficient amount of the gel-forming polymer and purified water.

Briefly, the gel-forming polymer, glycerol and water were weighed in a beaker and stirred with a high speed stirrer (*Cito Unguator Konictzko*, Bamberg, Germany) at approximately 1000 rpm for 5 min. Finally, the SLN or NLC aqueous dispersion was added under continuous stirring at 1000 rpm for 3 min.

4.3. Measurement of particle size and zeta potential

4.3.1. Laser light diffraction

Laser light diffraction (LD) is a technique used for determination of the sizes of particles in the range of 0.5 μm to 100 μm.

In order to calculate the size distribution, the instrument uses Fraunhofer diffraction of laser scattered from particles in dispersion. These particles cause diffraction of laser light through different angles and create a diffraction pattern of light rings with varying radii (Figure 4.3). The diffraction patterns created by differently sized particles are detected on a ring detector and are used to calculate the size distribution. The diffraction pattern depends on the particle size, i.e. small particles create a large diffraction angle, while large particles create a small diffraction angle [284].

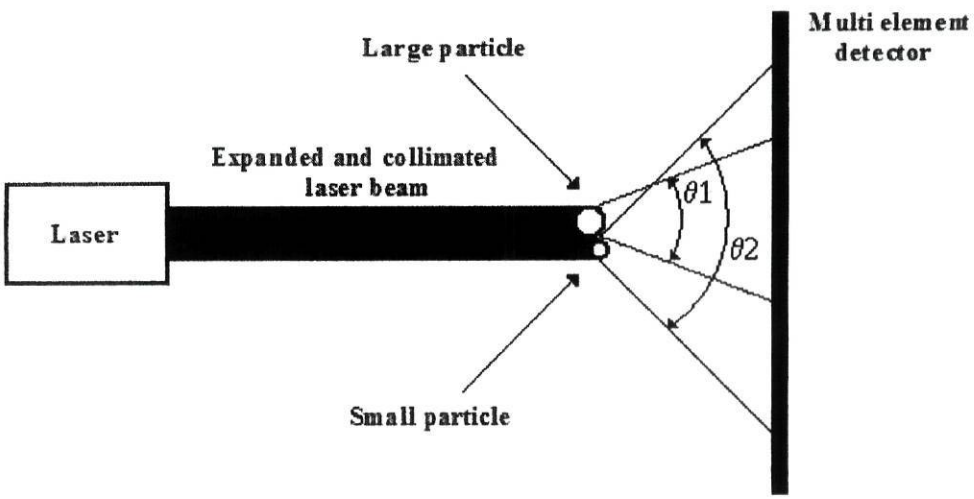

Figure 4.3: Principle of operation of a laser diffractometer. The diffraction angles and the diffraction pattern created are a characteristic function of particle size. The diffraction angle is small for large particles and large for small particles. (Adapted from Müller [2]).

The laser diffractometers are constituted by a laser, an optical unit to expand the beam, and a Fourier Transform lens for focussing the scattered light onto a ring detector (Figure 4.4).

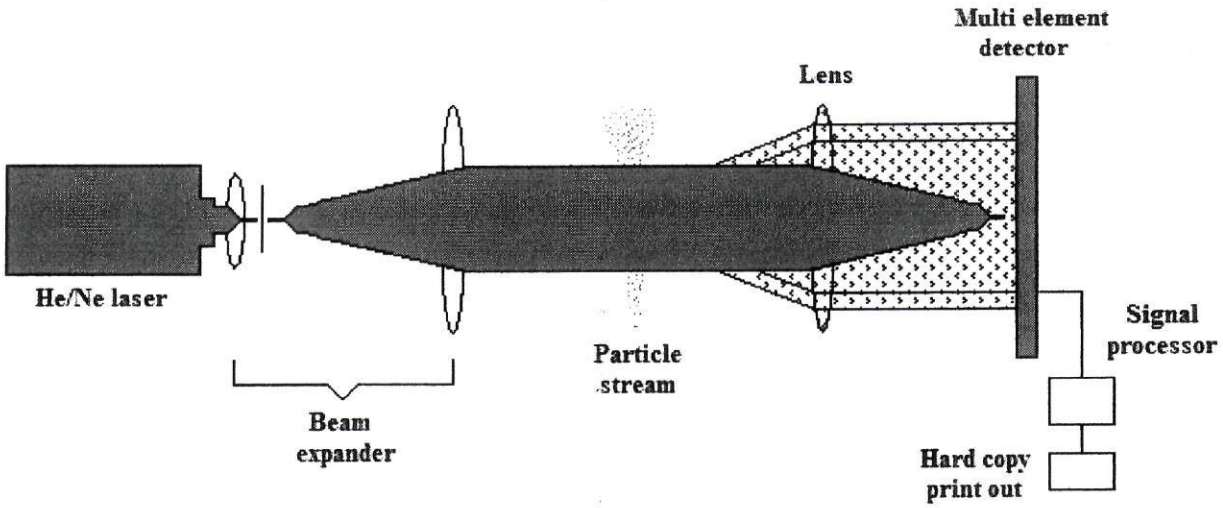

Figure 4.4: Schematic representation of a laser diffractometer. (Adapted from Müller [2]).

The particle dispersion is located in a measuring cell at a certain distance from the receiver lens. A great advantage of the laser diffractometers, is that any transparent dispersion medium can be used, such as aqueous or organic liquids and air. Size measurements can be performed maintaining the particles in their original dispersion medium, thereby minimizing changes in the sample due to modifications in the measurement conditions [2].

In the present work, LD was performed using a *Coulter®LS 230* (*Coulter Electronics*, Germany). LD data were evaluated using volume distribution, which means that a diameter 90% (d90%) value of 1 μm indicates that 90% of the particles possess a diameter of 1 μm or less. Note that larger particles are overestimated in a volume distribution.

In the case of hydrogels, prior to particle size analysis by LD, the semi-solid SLN and NLC formulations were diluted with double-distilled water to weak opalescence. All measurements were performed in triplicate.

4.3.2. Photon correlation spectroscopy

Photon correlation spectroscopy (PCS) is a technique employed to determine the mean particle size (PCS diameter) and size distribution (polydispersity index, PI) [2]. PCS consists of a laser light scattering technique suitable for application to particles ranging in size from 5 nm to approximately 3 μm. The light scattered from the particle dispersion is used to calculate the correlation function "G(τ)":

$$G(\tau) = 1 + e^{-2DK^2\tau}$$

where "D" is the diffusion coefficient of particles, "K" is the scattering vector of light and "τ" is the sample time.

The scattering vector of light "K" is given by:

$$K = \frac{4\pi n}{\lambda} \sin\frac{\theta}{2}$$

where "n" is the refractive index of the suspension medium, "λ" is the wavelength of the light and "θ" is the scattering angle.

The diffusion coefficient "D" obtained from the fit of the measured correlation function can be used to calculate the mean particle diameter "d" by application of the Einstein equation:

$$d = \frac{kT}{3\pi\rho D}$$

where "k" is the Boltzmann's constant, "T" is the absolute temperature and "ρ" is the viscosity of the medium.

The schematic set up of a PCS apparatus is represented in Figure 4.5. The apparatus consists of a laser, a temperature controlled sample cell and a photomultiplier (PM) for detection of the scattered light at a certain angle (for example 90°) [2]. The PM signal is transferred to a correlator for calculation of the "G(τ)". This "G(τ)" is relayed to a microprocessor for calculation of "D" and the correlated mean particle size.

PCS does not exploit the absolute intensity of the scattered light, but rather fluctuations in intensity. Small particles diffuse faster than large ones causing a stronger fluctuation in the scattering signal and a more rapid decaying "G(τ)". For a monodisperse particle population "G(τ)" is a single exponential, in the presence of more than one size the function is polyexponential.

Deviation from a single exponential is used to calculate the PI, as a measure of the width of the size distribution. An ideal, monodisperse formulation has a PI of zero.

PCS diameter gives information about the average particle size (z-ave). The measured PCS diameter is based on the intensity of scattered light and therefore is not identical to the numeric diameter except in case of monodisperse particle suspensions. For polydisperse samples, PCS diameter is larger because it is based on the scattering intensity of the particles. The scattering intensity does not linearly depend on the particle size but is proportionally related to the 6th power of the radius (Rayleigh scattering, $\Gamma \tilde{} r^6/\lambda^4$). Therefore, the broader the particle size distribution, the greater is the disparity between the PCS and number diameters. This phenomenon makes the measurements of PCS very sensitive for following aggregation or de-aggregation processes in suspensions.

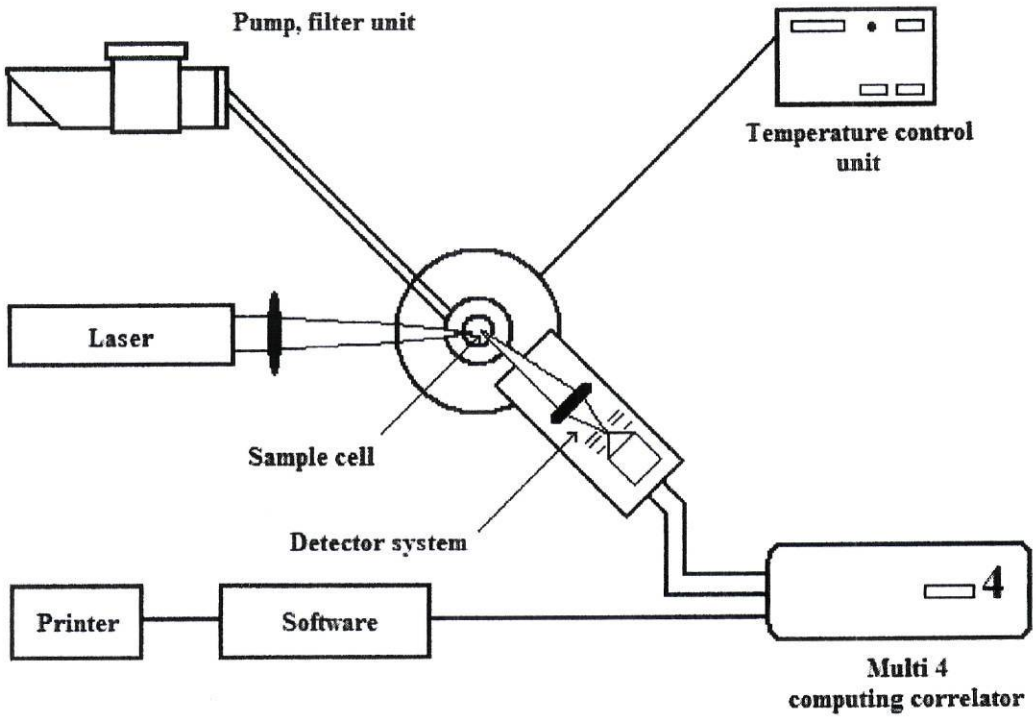

Figure 4.5: Principal set up of PCS. (Adapted from Müller [2]).

In the present work, for PCS measurements, all samples were diluted with double-distilled water to suitable concentration and measured by a *Malvern Zetasizer 4* apparatus (*Malvern Instruments*, UK).

In the case of hydrogels, prior to particle size analysis by PCS, the semi-solid SLN and NLC formulations were diluted with double-distilled water to weak opalescence. All measurements were performed in triplicate.

4.3.3. Zeta potential and electrophoretic mobility

Most of the solid particles are electrically charged in aqueous dispersion media, a property that can be due either to the process of dispersing the particles in water, the existence of charged groups on the surface and/or adsorption of ions from the dispersion medium [2]. In electrolytic solutions, particles possess an adsorbed monolayer of ions on their surface (Figure 4.6).

The adsorbed monolayer of ions at the particle surface consists of fixed, dehydrated and in most cases negatively charged ions (inner Helmholtz layer) [2]. These negative ions increase the surface potential (Nernst potential "Ψ_0") to the potential of the inner Helmholtz layer "Ψ_i". The next monolayer (outer Helmholtz plane) consists of fixed but hydrated positive ions reducing the

potential to the potential of the Stern plane "Ψ_δ" where "δ" is the thickness of the Stern plane. In the diffuse layer the potential drops towards zero. During the movement of the particle a part of the diffuse layer will be stripped to reveal a potential at the shear plane. This potential is called zeta potential "ζ" and is an indirect measurement of the surface charge because its magnitude depends on the Nernst potential.

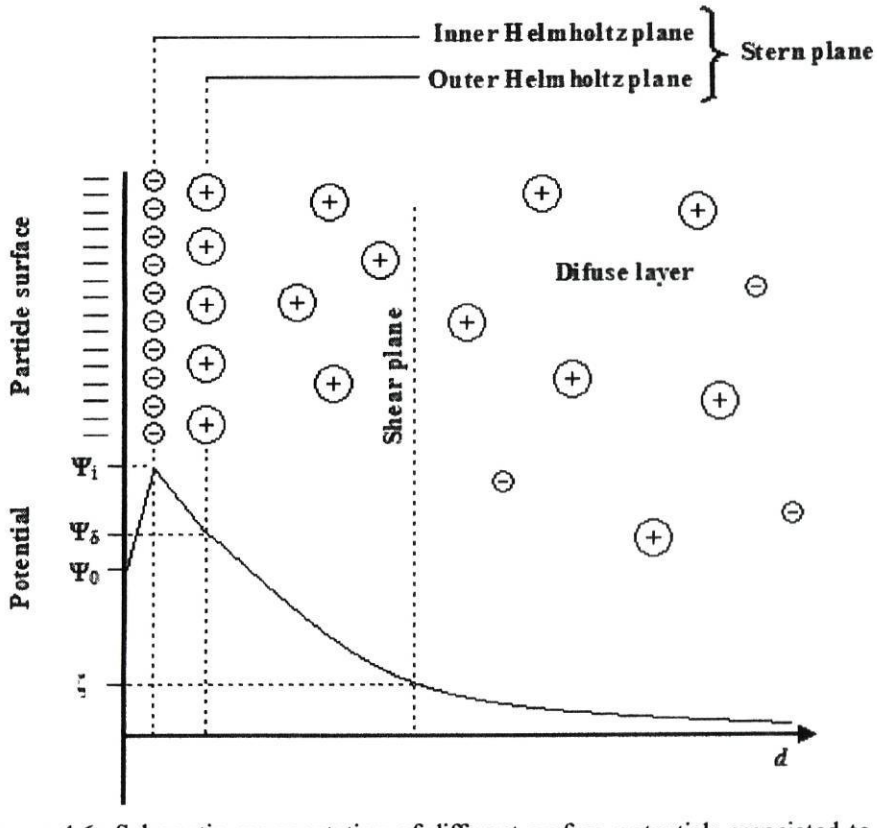

Figure 4.6: Schematic representation of different surface potentials associated to the particle in aqueous medium. Formation of Stern plane and diffuse layer on particle surface. Ψ_0, Nernst potential; Ψ_i, potential of inner Helmholtz plane, Ψ_δ, Stern potential; δ, thickness of Stern plane; ζ, zeta potential at the surface of shear; *d*, distance from the particle surface. (Adapted from Müller [2]).

The ζ can be measured by determination of the movement velocity of the particles in an electric field (electrophoresis measurements). Conventional instruments use a light microscope to observe the particle movement, whilst modern zetameters use laser Doppler anemometry (LDA) to determine the particle velocity.

A LDA set up consists of a laser, a beam splitter and a lens which focuses the beams into the measuring volume, forming a beam crossover. Particles move through the beam crossover and scatter laser light. The scattered light is detected in the forward direction and projected by collecting optics onto a PM. The frequency of the laser light scattered by the particles differs from the frequency of the incident beam. This frequency shift is caused by the Doppler effect

and it is a function of the particle velocity. As mentioned before, the *Malvern Zetasizer 4* apparatus uses the PM signal to calculate a "G(τ)", which is transferred via Fourier Transform to the frequency spectrum of the scattered light.

Particle velocity "v" is expressed in relation to the electrical field strength "E" as electrophoretic mobility "μ" (μm/s)/(V/cm):

$$\mu = \frac{v}{E}$$

where "v" is the particle velocity and "E" is the field strength. The electrophoretic mobility "μ" can be converted to a "ζ" by using the following equation of Helmholtz [285]:

$$\zeta = \frac{4v\pi\eta}{E\varepsilon}$$

where "η" is the viscosity of dispersion medium, "E" is the field strength and "ε" is the dielectric constant.

In the present work, for the ζ measurements a *Malvern Zetasizer 4* apparatus (*Malvern Instruments*, UK) was used. Samples were previously diluted with double-distilled water adjusted to a conductivity 50 μS/cm with a solution of 0.9% NaCl (if not otherwise stated).

4.4. Measurement of crystallinity and lipid modification

4.4.1. Differential scanning calorimetry

Differential scanning calorimetry (DSC) is frequently used in thermal analysis due to its ability to provide information on both physical and energetic properties of a compound [286]. DSC measures the heat loss or gain resulting from physical or chemical changes within a sample as a function of the temperature.

Examples of heat-absorbing processes (endothermic measurements) are fusion, boiling, sublimation, vaporization, desolvation and solid-solid transitions. Crysallization is usually an exothermic process, i.e. energy is liberated. Qualitative measurements of these processes have many applications, such as the study of purity, polymorphism, solvation, degradation and compatibility of substances.

If a thermodynamic event – either endothermic or exothermic – occurs, the power requirements for the coils maintaining a constant temperature will differ. This power difference is plotted as a function of the temperature recorded by the programming device [286].

DSC analysis has been used to characterize the state and the degree of crystallinity of lipid dispersions, semi-solid systems, polymers and liposomes [287]. DSC measurements offer a close look at the melting and crystallization behaviour of crystalline material like lipid nanoparticles [83,226,288,289]. The breakdown or fusion of the crystal lattice by heating or cooling the sample yields inside information on polymorphism, crystal ordering, eutectic mixtures or glass transition processes [287]. DSC experiments are useful in order to understand solid dispersions like solid solutions, simple eutectic mixtures or, as in the case of SLN and NLC, drug and lipid interactions and the mixing behaviour of solid lipids with liquid lipids, such as oils [5,35,53,289,290].

In general, a melting point depression is observed when transforming the bulk lipid to nanoparticulate form. This melting point depression is described in the Gibbs-Thomson equation which itself is derived from the Kelvin equation [291]:

$$\ln\left(\frac{T}{T_0}\right) = \frac{2\gamma V_s}{r\,\Delta H}$$

where "T" represents the melting point of the particle, and it is always smaller than the melting point of the bulk material "T_0". The molar volume of the substance is characterized by "V_s", "r" is the radius of the particle, "ΔH" is the molar melting enthalpy and "γ" is the interfacial energy at the solid-lipid interface. For characterizing crystal forms, "ΔH" can be obtained from the area under the DSC curve for the melting endotherm.

An additional melting point depression occurs when a foreign compound is dissolved in the lipid matrix, such as surfactant molecules that will partition from the water phase to the lipid phase. Therefore, drug-loaded SLN will show a melting point depression in case of a molecularly dispersed drug is present.

The recrystallization index (RI) is defined as the percentage of the lipid matrix that has recrystallized during storage time [98]. Its determination is useful for comparison of the crystallinity between the developed formulations. According to the literature [98], RI of the developed SLN and NLC formulations was calculated as follows:

$$RI(\%) = \frac{\Delta H_{\,SLN\ or\ NLC\ aqueous\ dispersion}}{\Delta H_{\,bulk\ material} \;\; x \;\; Concentration_{\,lipid\ phase}} \; x\,100$$

where "ΔH" is the molar melting enthalpy given by J/g^{-1} and the concentration is given by the percentage of lipid phase.

In the present work, DSC measurements were performed on a *Mettler DSC 821e* apparatus (*Mettler Toledo*, Gießen, Germany). Samples containing 1-2 mg of solid lipid were accurately weighed in 40 ml aluminium pans. DSC scans were recorded from 25°C to 85°C at a heating rate of 5 K/min, using an empty pan as reference. Melting points correspond to the maximum of the heating curve. Polymorphic forms were assigned by comparison with x-ray diffraction data.

4.4.2. X-ray diffraction

An important technique for establishing the reproducibility of a polymorphic form between different batches is x-ray diffraction, i.e. wide-angle x-ray scattering (WAXS) and small-angle x-ray scattering (SAXS). Figure 4.7 shows the schematic representation of this technique.

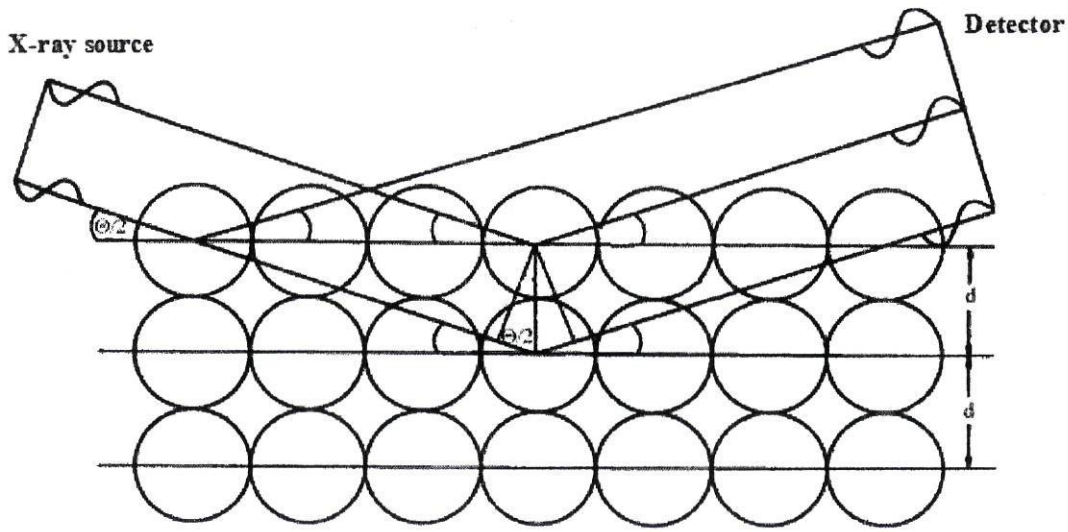

Figure 4.7: Schematic representation of x-ray diffraction. (Adapted from Krischner [292])

When a monochromatic x-ray beam is focused on a crystal, the scattered x-rays from the regularly placed atoms interfere with each other, giving strong diffraction signals in particular directions, since the interatomic distances are of the same order as the x-ray wavelength [292]. The directions of the diffracted beams are related to the shape and dimensions of the unit cell of the crystalline lattice. The diffraction intensity depends on the disposition of the atoms within the unit cell. This technique allows amorphous and crystalline materials to be differentiated. Crystalline materials display many diffractions bands whereas amorphous compounds present a more or less regular baseline.

The crystal diffracts x-rays similar to a diffraction grating, whose plane diffracts ordinary light. The three-dimensional crystal functions like a series of plane gratings stacked one above the other [292]. The wavelength of the x-rays "λ" is related to the angle of incidence "θ" and the interatomic distance "d" by Bragg's equation:

$$n.\lambda = 2d \sin\frac{\theta}{2}$$

where "n" is the order of the diffraction. For a single crystal, the diffracted x-rays consist of a few lines. With powder, due to a random distribution of crystals, the diffraction pattern consists of a series of concentric cones with a common apex on the sample. The atoms in a crystal possess the power of diffracting the x-ray beam. Each substance scatters the beam in a particular diffraction pattern, producing a fingerprint for each atom crystal or molecule.

If an unknown powder sample is to be identified, its diffraction pattern may be compared with those of known substances or its "d" values calculated from the diffraction diagram and compared with the "d" values of known compounds.

If the diffraction pattern of a single crystal is to be determined, the crystal is mounted on a thin glass capillary and the capillary is fastened to a brass pin. A substance in powder form can be ground finely and transformed into a small rod using collodion as a binder or held in a specific device with an open cup. Samples like aqueous dispersions can be transformed into a paste, using a thickening agent, such as locust bean gum [29] and xanthan gum [107].

X-ray diffraction has been used for the study of molecular structure and polymorphism of lipid nanoparticles [29,36,56,63,74,103,107,293,294].

In the present work, x-ray studies were performed by WAXS (2 Theta = 4-40°) on a *Philips PW 1830* x-ray generator (*Philips*, Amedo, The Netherlands) with a copper anode (Cu-Kα radiation, λ=0.15418 nm). SLN and NLC aqueous dispersions were previously transformed into a paste using locust bean gum as a thickening agent, and then mounted into a specific device before the measurement by WAXS.

4.5. Light microscopy

All substances that are transparent when examined under a microscope that has crossed polarizing filters are either isotropic or anisotropic [295]. Amorphous substances, such as supercooled melts and non-crystalline solid organic compounds, or substances with cubic crystal

lattices are isotropic materials, which have a single refractive index. Materials with more than one refractive index are anisotropic and appear bright with brilliant colours (birefringence) against a black polarized background. The interference colours depend upon the crystal thickness and the differences are either uniaxial, having two refractive indices, or biaxial, having three principal refractive indices.

Most drugs are biaxial, corresponding to either an orthorhombic, monoclinic or triclinic crystal system. Therefore, in the present work polarized light microscopy was employed to detect drug crystals in suspension, as suggested by Westesen *et al.* [53]. Investigations were performed using a *Leitz Orthoplan Microscope* (Wetzlar, Germany) at 100x, 400x and 1000x with an oil immersion objective, in order to determine the presence/absence of drug crystals in the melted lipid.

4.6. Assay of clotrimazole

In the present work, the quantitative determination of clotrimazole was performed by ultraviolet (UV).

As it is well known, UV and visible absorption bands are due to electronic transitions in the region of 200 nm to 800 nm [296,297]. In the case of organic molecules – such as clotrimazole –, the electronic transitions could be ascribed to a "σ", "π" or "n" electron transition from the ground state to an excited state (σ*, π* or n*). Since the "σ" electron is firmly involved in the construction of a single bond, its transition requires much more energy (usually in far UV) than the "n" electron (non-bonding electrons) or less tightly bonded "π" electrons [296].

According to Beer's law, the absorbance of a solution "*A*" is defined as the logarithm to base 10 of the reciprocal of the transmittance "*T*" for monochromatic light and is expressed by the following equation:

$$A = \log_{10}\left(\frac{1}{T}\right) = \log_{10}\left(\frac{I_0}{I}\right)$$

where "I_0" is the intensity of incident monochromatic light, "*I*" is the intensity of transmitted monochromatic light and "*T*" is the ratio I/I_0.

In the absence of other physicochemical factors, the measured absorbance "*A*" is proportional to the path length "*b*" through which the light passes and to the concentration "*c*" of the substance in solution, in accordance to the equation:

$$A = \varepsilon.c.b$$

where "ε" is the molar absorptivity, if "b" is expressed in centimetres and "c" is expressed in moles per litre.

The expression "$A_{1cm}^{1\%}$", representing the specific absorbance of a dissolved substance, refers to the absorbance of a 10 g/l solution in a 1 centimetre cell and measured at a defined wavelength, so that:

$$A_{1cm}^{1\%} = \frac{10\varepsilon}{Mr}$$

Spectrophotometers suitable for measuring in the UV and visible range of spectrum consist of an optical system capable of producing monochromatic light in the range of 200 nm to 800 nm and a device suitable for measuring the absorbance.

In the present work, two solutions of clotrimazole, using diethyl ether or a solution of 100 mM acetate buffer pH 6.0 with 35% (*V/V*) of dioxane as dissolution medium, were scanned from 300 nm to 200 nm, using an *Uvikon 940* double-beam spectrophotometer (*Kontron Instruments*, Eching, Germany). In both media, the wide-band of clotrimazole shows a typical absorption pattern with two peaks at approximately 243 nm and 270 nm.

4.6.1. Assay of clotrimazole in SLN and NLC aqueous dispersions

For the assay of clotrimazole in the developed SLN and NLC aqueous dispersions, UV measurements were performed at 243 nm in a path length of 1 cm at 20±1°C, using diethyl ether as dissolution medium of the samples.

Diethyl ether has shown to be an appropriate solvent for this assay, because it dissolves all the components of the formulations and the obtained peak at the prescribed wavelength (243 nm) is only due to the presence of clotrimazole, i.e. the excipients do not interfere with the measurement of the drug absorbance in this organic medium.

Calibration curves were obtained from a series of standard solutions of clotrimazole in diethyl ether ranging from 25 to 150 µg/ml. Diethyl ether was used as blank. Figure 4.8 shows an obtained typical calibration curve.

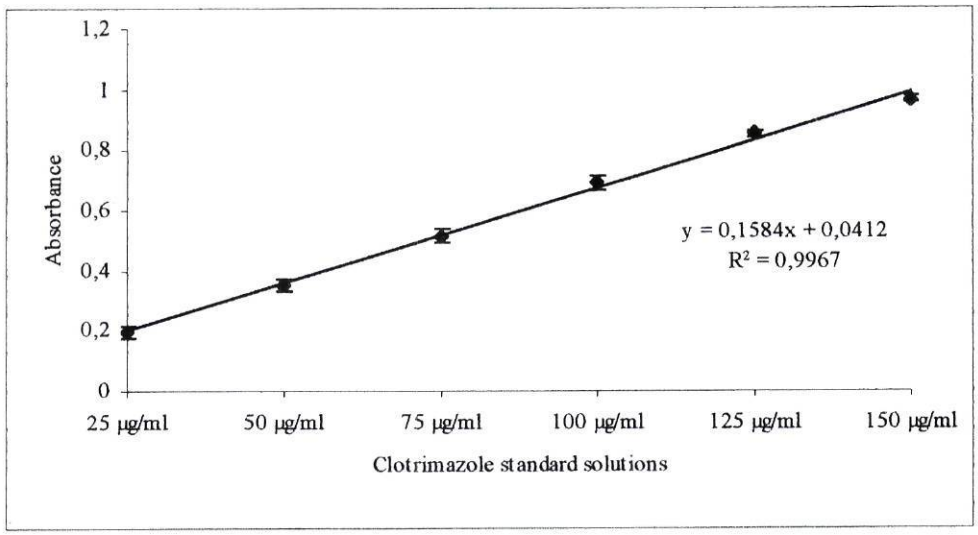

Figure 4.8: Calibration curve of clotrimazole in diethyl ether.

The total amount of clotrimazole was determined in the prepared aqueous dispersions of SLN or NLC, previously to the removal of non incorporated clorimazole. Briefly, 5 µl of an aqueous dispersion of SLN or NLC was introduced in a dilution-flask of 25 ml, completing the volume with diethyl ether in order to prepare a solution. The absorbance of the resulted solution was measured at 243 nm.

For the determination of incorporated clotrimazole, the amount of free drug was firstly assessed by assaying clotrimazole in the obtained supernatant, after centrifugation of the SLN or NLC aqueous dispersions. The difference between total clotrimazole and free clotrimazole gives the amount of incorporated clotrimazole. Briefly, 1 ml of an aqueous dispersion of SLN or NLC was centrifuged at 32 000 rpm. 5 µl of the obtained supernatant was introduced in a dilution-flask of 10 ml, completing the volume with diethyl ether in order to prepare a solution. The absorbance of the resulted solution was measured at 243 nm.

4.6.2. Assay of clotrimazole in the release studies

For the assay of clotrimazole in the release studies, UV measurements were also performed at 243 nm in a path length of 1 cm at 20±1°C, using a solution of 100 mM acetate buffer, pH 6.0 with 35% (*V/V*) of dioxane as receptor medium in Franz diffusion cells.

The 100 mM acetate buffer, pH 6.0 with 35% (*V/V*) of dioxane was chosen as receptor medium according to the studies carried out by Kast *et al.*, for the evaluation of the release profile of clotrimazole in bioadhesive systems based on chitosan-thioglycolic acid conjugates

[280]. The inclusion of 35% (*V/V*) of dioxane in the composition of the receptor medium is due to the insufficient solubility of clotrimazole in the 100 mM acetate buffer solution.

Calibration curves were obtained from a series of standard solutions of clotrimazole in the receptor medium ranging from 25 to 150 µg/ml. The 100 mM acetate buffer pH 6.0 with 35% (*V/V*) of dioxane was used as blank. Figure 4.9 shows an obtained calibration curve.

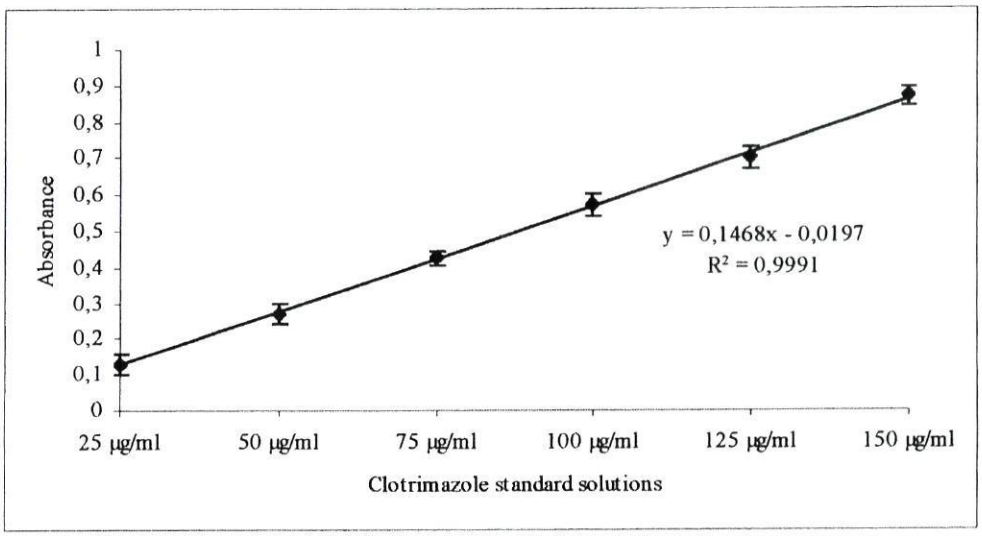

Figure 4.9: Calibration curve of clotrimazole in a solution of 100 mM acetate buffer, pH 6.0 with 35% (*V/V*) of dioxane.

The amount of released clotrimazole was assessed by measuring the absorbance of the samples directly after their collection from Franz cells.

4.7. Determination of the encapsulation parameters

The E.E. was calculated as the percentage of the initial amount of drug which has been incorporated into lipid nanoparticles. The drug loading capacity, also called payload or drug content, is generally expressed in percentage of incorporated drug related to the lipid matrix [6].

The determination of the E.E. of clotrimazole in SLN and NLC and the drug loading capacity were calculated using the following equations:

$$E.E. = \frac{amount\ of\ clotrimazole\ in\ lipid\ nanoparticles}{initial\ amount\ of\ clotrimazole} \times 100$$

$$Drug\ loading\ capacity = \frac{amount\ of\ clotrimazole\ in\ lipid\ nanoparticles}{amount\ of\ lipid\ material} \times 100$$

4.8. Evaluation of clotrimazole release profile from SLN and NLC aqueous dispersions

In matrix systems like lipid nanoparticles the drug is incorporated in the lipid matrix either in dissolved or in dispersed form [6,7]. Therefore, the solubility of the drug in the lipid matrix becomes a very important controlling factor of the drug release from SLN and NLC. When the initial drug loading is below the solubility limit, release is achieved by simple diffusion through the lipid. However, when the drug loading is above the solubility limit, dissolution of the drug in the lipid becomes the limiting factor [27].

In the present work, static Franz glass diffusion cells were used in order to evaluate the release profile of clotrimazole from SLN and NLC. Static Franz glass structure is schematically represented in Figure 4.10.

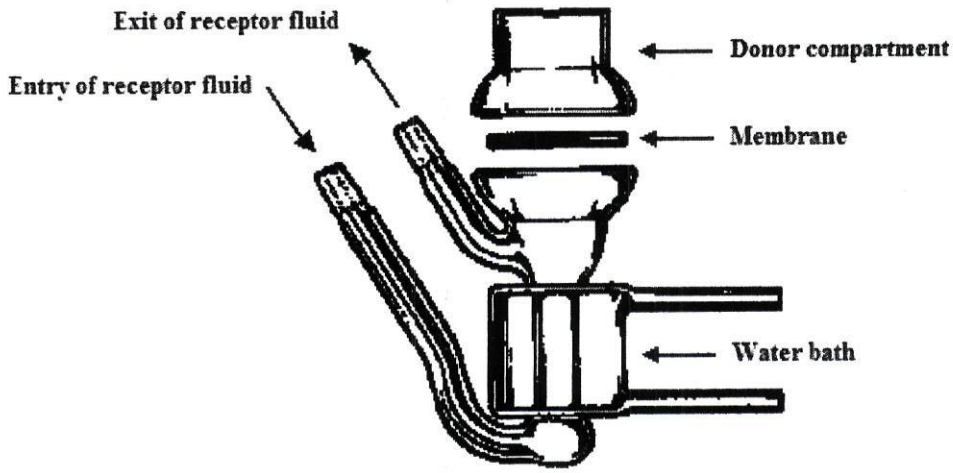

Figure 4.10: Schematic representation of a Franz diffusion cell. (Adapted from Jenning [56]).

These cells consist of donor and receptor chambers between which a membrane is positioned [298]. In the present work, the area for diffusion was 0.64 cm^2 and the receptor chamber volume was approximately 5.5 ml. Cellulose nitrate membranes with an average pore size of 0.1 μm were used. The receptor chamber was maintained at 37°C, in order to ensure the surface skin temperature of 32°C on the surface of the membrane.

As reported above, the receptor medium consisted of a solution of 100 mM acetate buffer, pH 6.0 with 35% (*V/V*) of dioxane. Since the receptor medium was not intended to mimic skin

conditions, it was suitable for the present *in vitro* investigations. Clotrimazole is well soluble in the chosen receptor medium.

Briefly, 100 µl of a SLN or NLC aqueous dispersion (containing 1% of clotrimazole) was applied to the donor compartment. Samples (250 µl) were collected over 24h and analysed by spectrophotometric determination at 243 nm as described before. After each sample taking, the Franz cells were filled up with receptor medium. For each formulation, the release studies were performed in triplicate.

4.9. Evaluation of rheological properties of SLN and NLC preparations

Rheology (from the Greek *rheos* meaning flow and *logos* meaning science) is the study of the flow or deformation under stress. Rheologic measurements are a valuable tool for quality control of ingredients and final products together with manufacturing processes, such as mixing, pumping, stirring, filling and sterilization [299].

Concerning liquid dispersions of lipid nanoparticles, they usually need to be incorporated in convenient topical dosage forms – like hydrogels or creams – to obtain a topical application form having the desired semi-solid consistency. However, when incorporated into a semi-solid base, the physicochemical characteristics of SLN and NLC can be modified as a result of interactions between the components of the final product, which can be evaluated using the so-called rheologic measurements [300,301].

Semi-solid systems are characterized as materials that retain their shape when unconfined, but flow or deform when an external force is applied. Essential components for a rheologic observation are the tangential application of a force to a body and the resultant deformation of that body [302]. If this force is applied for a short period of time and then withdrawn, the deformation is defined as *elastic* if the shape is restored or *flow* if the deformation remains. A fluid or liquid becomes a body that blows under the action of an infinitesimal force. In practice, gravity is generally regarded as the criterion of such a minimal force.

Figure 4.11 represents the model demonstrating the components of classic viscous flow [302]. Two parallel planes are a distance "x" apart, and between these planes the viscous body is confined. The top plane "A" moves horizontally with the velocity "v" because of the action of force "F". The lower plane "B" is motionless. As a consequence, there exists a velocity gradient between the planes "dv/dx". This gradient is given by the definition of rate of shear "*D*". The shear stress "*S*" is the force per unit of area creating the deformation.

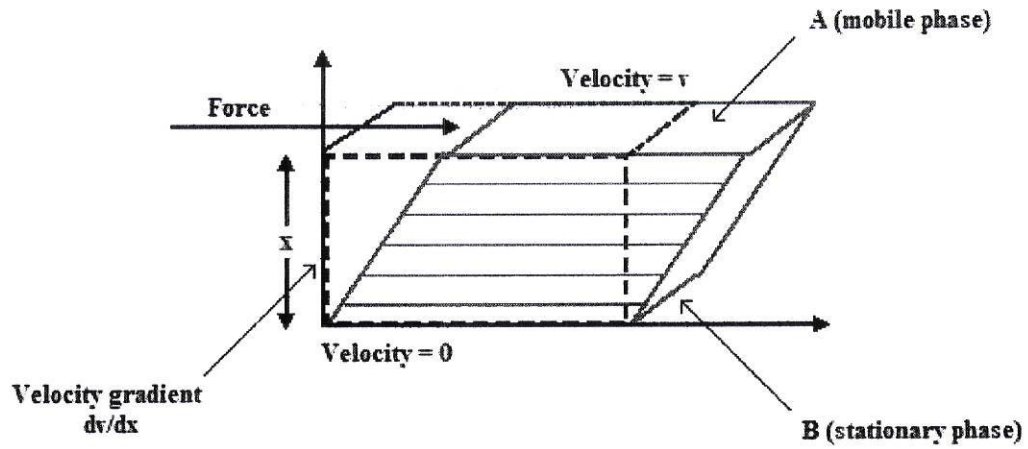

Figure 4.11: Schematic model for demonstrating the components of classic viscous flow. (Adapted from Wood [302]).

The shear stress may be applied either momentarily or continuously. *Elastic deformation* occurs if, as the force is applied, the upper plate moves in the direction of the force only momentarily and then stops but returns to its original position when the deforming force is removed. On the other hand, *pure viscous flow* occurs if there is continuous movement during the applied force, and no restorative motion follows removal of the deforming force.

Between the limits of *elastic deformation* and *pure viscous flow*, a continuum of combinations of these limits exists. Such behaviour is called *viscoelastic flow*. A *newtonian fluid* is a fluid in which a direct proportionality exists between shear stress and shear rate, for all values of shear.

Viscosity or coefficient of viscosity is the proportionality constant between shear stress "*S*" and shear rate "*D*". Conventionally, viscosity is represented by "η" and is given by:

$$\eta = \frac{S}{D}$$

Fluidity is the reciprocal of the viscosity, usually designed by the symbol "Φ". Kinematic viscosity "ν" is the Newtonian viscosity divided by density "d":

$$\nu = \frac{\eta}{d}$$

Non-newtonian fluids are those for which there is no direct linear relationship between shear stress and shear rate. Most systems of pharmaceutical interest fall into this category. A *pseudoplastic material* is one in which the stress increases at less than a linear rate with increasing shear rate, while a *dilatant material* is characterized by a more rapid increase. Thus, if viscosity is calculated at each of a series of shear rate points, by use of the ratio between shear rate and shear stress, then the resultant values decrease with increasing shear rate for

pseudoplastic materials and increase for *dilatant* ones. Measurements at such single points are frequently referred to as apparent viscosity to recognize clearly that the number quoted refers only to the condition of measurement. The fact that one number cannot characterize the viscous behaviour, however, requires the use of some equation of state. One such empiric one is the Power Law Equation:

$$S = AD^n$$

where "S" and "D" are the shear stress and shear rate, respectively, "A" is an appropriate proportionality constant and "n" is the Power Index.

In this form, "n" is less than 1 for *pseudoplastic materials* and grater than 1 for *dilatant materials*. The Power Law Equation is also used with the index "n" associated with shear stress rather than shear rate.

When the logarithm of both sides of the last equation is taken, the result is:

$$\log S = \log A + n \log D$$

Compared with the equation of a straight line, a plot of "log S" against "log D" results in a straight line of slope "n" and intercept "log A".

When an initial finite force is necessary before any rheologic flow can start, the initial stress is called *yield value*. A Bingham plastic is represented by a straight line or curve on the stress shear rate plot being displaced from the origin by a finite stress value. Thus, for Newtonian behaviour at stresses "S" greater than the yield value "f", it can be written:

$$S - f = UD$$

where "U" is the plastic viscosity and "D" is the shear rate. Similarly, both pseudoplastic and dilatant curves may appear to exhibit *yield values*. The dimensional units of the *yield value* must be those of the shear stress.

In general, *Newtonian liquids* are pure chemicals rather than of polymeric materials. All interactions are such that no structure is contributed to the liquid. Since by definition, shear stress and shear rate are directly proportional, a single viscometric point can characterize the liquid rheology. Increasing temperature decreases viscosity as it reduces intra-molecular forces of attraction. Such temperature viscosity relationships are quickly established, regardless of whether temperature is increased or decreased.

Pseudoplastic behaviour is exhibited by polymer solutions and by most semi-solid systems containing some polymer components.

Thixotropy is a phenomenon resulting from the time dependency of the breakdown or the rebuilding of structure. It is an empiric observation of good reliability that structure breakdown

or build-up is an exponential function time. Thus, if the observed shear stress for a given shear rate is followed with time, a plot of stress against time, both on the logarithmic scale, results in a straight line. A coefficient of thixotropic breakdown "B" can be calculated by the equation:

$$B = \frac{S_1 - S_2}{\ln(t_2/t_1)}$$

where "S_1" and "S_2" are the stress values at times "t_1" and "t_2" of continuous shear at any arbitrary shear rate chosen for comparison.

Dilatant systems are essentially the opposite of pseudoplastic thixotropic ones. In dilactancy as shear continued, the fluid components contributing to lubricity between the shear planes so that the resulting structure develops increasing friction. Thus, stress increases with time in a logarithmic manner similar to that with thixotropy. A similar hysteresis loop[4] of rheopexy is developed in dilatant systems. The last equation may be used with dilatant systems in the same way as with thixotropic ones to yield a coefficient of dilatant build-up.

To sum up, Figure 4.12 represents the four basic types of rheograms or flow curves.

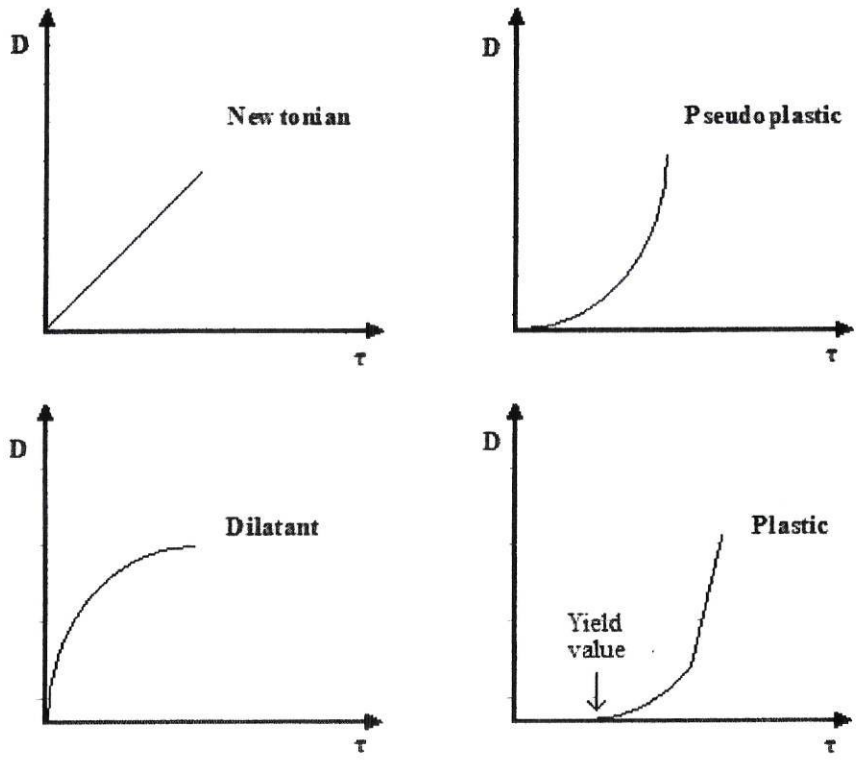

Figure 4.12: The four basic types of rheograms. (Adapted from Stricker [303]).

[4] Hysteresis loop is a measure of the thixotropy in area.

In the present work, evaluation of the rheological properties of SLN and NLC preparations were performed applying an oscillation frequency sweep test and continuous shear investigations.

4.9.1. Oscillation frequency sweep test

In the present work, oscillation tests were carried out in order to determine the rheological properties of the developed SLN and NLC aqueous dispersions.

Oscillation tests are dynamic methods for determining the rheological properties of the material in its rheological ground state without altering its static structure and providing a so-called fingerprint under non-destructive conditions [304,305].

In an oscillation experiment the material is subject to a sinusoidal stress, providing information on the inter-molecular and inter-particle forces in the material [306]. It can be used to differentiate between two samples which can not be distinguished by shear experiments, because this test is capable of separating elastic and viscous properties, while shearing leads to an integrated characterization only. The response of the tested material is measured as a function of frequency at constant stress amplitude.

The selection of frequency that is applied has a strong influence on the testing time. The reciprocal of the frequency is the required time to run through one cycle.

When applying stress "τ" to a sample, it will deform. Dependent on the relationship of viscous and elastic properties, the amplitude of deformation "γ_0" is not necessary reached at the same time as the stress amplitude "τ_0". There is a phase shift "δ" between stress and deformation.

Pure elastic materials have a phase shift of 0°. Note that for these materials as soon as the force is lowered or released the deformation recovers.

Pure viscous materials have a phase shift of 90° because when the applied force reaches its maximum, the material is pulled apart with its highest speed.

Viscoelastic materials show phase shifts between 0 and 90°.

For the evaluation of an oscillation experiment the following basic equation is used:

$$\tau_0 = G^* \gamma_0$$

where "G^*" is the complex modulus.

By setting the stress amplitude and measuring the deformation amplitude, "G^*" can be calculated. By knowing the frequency and measuring the time at which stress and strain (deformation) amplitudes are reached, the phase shift between both can be calculated, which is then used to determine the storage and the loss moduli.

The storage modulus "G'" gives information about the elastic component and it can be determined using the following equation:

$$G' = G^* \cos(\delta)$$

For a *purely elastic material* the phase shift is 0°, which makes "cos (δ)" equals to 1, and consequently, "G'" is 100%, reflecting the integral character "G^*".

The loss modulus "G''" is a measure of the viscous component and it can be determined using the following equation:

$$G'' = G^* \sin(\delta)$$

For a *purely viscous material* the phase shift is 90°, which makes "sin (δ)" equals to 1, and consequently, "G''" is 100%, reflects the integral character "G^*".

One might be interested in the ratio of viscous and elastic properties, which is given by the following equation:

$$\frac{G''}{G'} = \frac{\sin(\delta)}{\cos(\delta)} = \tan(\delta)$$

The complex dynamic viscosity "η^*" is given by the equation:

$$\eta^* = \frac{G^*}{\omega}$$

where "ω" is the frequency defined as sinus wave.

In the present work, oscillation tests were performed at 20±0.1°C on a rheometer *Rheo Stress RS 100* (*Haake Instruments*, Karlsruhe, Germany) equipped with a cone-and-plate test geometry (plate diameter 20 mm, cone angle 4°), schematically represented in Figure 4.13.

Oscillation stress sweep tests were carried out at a constant frequency of 1 Hz in a stress range of 100 Pa and the oscillation frequency sweep test was performed over a frequency range from 0 to 10 Hz at constant stress amplitude of 5 Pa.

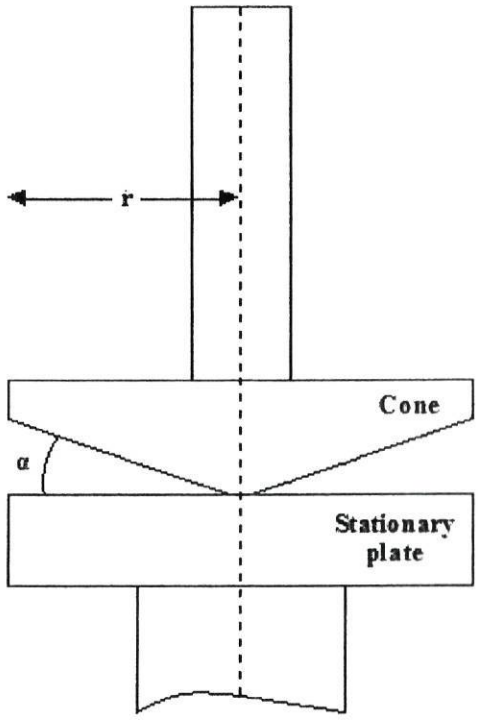

Figure 4.13: Schematic representation of a cone-and-plate rheometer. (Adapted from Reich [307]).

4.9.2. Continuous shear investigations

In the present work, the rheological properties of the developed hydrogels and hydrogels containing SLN and NLC were studied by continuous shear investigations which were performed in order to evaluate the shear rate as a function of shear stress. This study started applying 0 Pa up to a maximum shear stress of 50 Pa and the resulting shear rate was measured.

In the present work this investigation was carried out at 20±0.1°C on a rheometer *Rheo Stress RS 100* (*Haake Instruments*, Karlsruhe, Germany) equipped with a cone-and-plate test geometry (plate diameter 20 mm, cone angle 4°), schematically represented in Figure 4.13.

4.10. Evaluation of the occlusive properties of SLN and NLC preparations

It is well known that small particles, like lipid nanoparticles, possess an adhesive effect and this effect increases with the decrease of the diameter "*d*" of the particles [47]. But there are other factors influencing the adhesiveness, such as adhesion forces "F_H", van-der-Waals forces

"$\hbar\omega$", distance between adhesion partners "a", electric constant "ε_0", dielectric constant "ε", contact potential of electric conductors "U" and the surface charge density of adhesion partners "φ_1 φ_2". The adhesive forces can be calculated by [308]:

Van-der-Waals forces:

$$F_H = \frac{\hbar\omega}{16\pi}\frac{d}{a}$$

In case of a conductor:

$$F_H = \frac{\pi}{2}\varepsilon_0\varepsilon U^2\frac{d}{a}$$

In case of an isolator:

$$F_H = \frac{\pi}{2}\frac{\varphi_1\varphi_2}{\varepsilon_0\varepsilon}d^2$$

In the present work, the occlusivity of SLN and NLC aqueous dispersions, as well as SLN and NLC containing hydrogels, was quantified by an *in vitro* occlusion test adapted by de Vringer [309]. Briefly, beakers of 100 ml volume were filled with 50 ml of water, covered and sealed with cellulose acetate filters of 90 mm diameter and 4-7 µm cutoff size, obtained from *Schleicher* (Germany). Sample was spread with a spatula on the filter surface and then stored at 32°C (skin temperature) and 50-55% of room humidity for 48 hours.

After spreading the samples, the beakers were weighed after 6, 24 and 48 hours, giving the water loss due to evaporation at each time (water flux through the filter paper). Beakers were covered with filter paper but without applied sample served as reference values. Every experiment was performed in triplicate. The occlusion factor "F" was calculated according to the following equation:

$$F = 100*[(A-B)/A]$$

where "A" is the water loss in the absence of without sample (reference) and "B" is the water loss in the presence of sample. From this, an occlusion factor of 0 means no occlusive effect compared to the reference, the maximum occlusion factor is 100.

CHAPTER V

RESULTS AND DISCUSSION

CHAPTER V

RESULTS AND DISCUSSION

5.1. Clotrimazole-containing SLN and NLC preliminary studies

Solubility of drug in the material of the carrier is one of the main limiting factors in the design of new carrier systems [310]. Poor solubility of drug can be due to a lack of affinity to the carrier matrix or to a specific stability of the drug into self-organized structures, such as crystalline structures. In fact, at the equilibrium, systems orientate towards minimum free energy, i.e. lower thermodynamic activity, which sometimes corresponds to crystalline structures forming a separate phase from the carrier.

With regard to lipid nanoparticles – such as SLN and NLC –, the lack of affinity of the active compound to the lipid matrix is due to the increase of lipid packing density during the preparation process, resulting in a decrease of drug incorporation into the carrier, which is accompanied by a poor bioavailability [6].

The aim of the present preliminary studies was to assess the clotrimazole-lipid interaction, in order to select the best lipid or lipids for incorporating this drug in stable SLN and NLC formulations.

After lipid screening for clotrimazole, a range of emulsifying agents were tested for each selected lipid and the composition of SLN and NLC formulations has been established. In addition, the optimum homogenization conditions, i.e. the number of homogenization cycles, were also assessed for each investigated nanoparticle system.

5.1.1. Lipid screening for clotrimazole solubilization

The solubility of clotrimazole in 15 different lipids was screened by mixing the drug in different concentrations (1%, 5%, 10% and 20% *m/m*) with the lipid and melting the mixture at 90°C. The solubility was determined visually and microscopically at 90°C and at room temperature (20°C).

Table VIII reports the melting point of the selected lipids and the obtained results for the solubility studies of clotrimazole in different lipids at 90°C and at 20°C.

Table VIII: Solubility studies of clotrimazole in different lipids at 90°C and at 20°C.

Lipid	Melting point	Drug concentration %(*m/m*)	Solubility at 90°C	Solubility at 20°C
Dynasan®112	43-47°C	1%	+++	+++
		5%	++	-
		10%	-	-
		20%	-	-
Dynasan®114	55-58°C	1%	+++	+++
		5%	-	-
		10%	-	-
		20%	-	-
Dynasan®116	61-65°C	1%	+++	+++
		5%	-	-
		10%	-	-
		20%	-	-
Dynasan®118	70-73°C	1%	+++	+++
		5%	-	-
		10%	-	-
		20%	-	-
Softisan®145	53-58°C	1%	+++	+++
		5%	-	-
		10%	-	-
		20%	-	-
Witepsol®H5	34-36°C	1%	+++	+++
		5%	-	-
		10%	-	-
		20%	-	-
Witepsol®S55	33.5-35.5°C	1%	+++	+++
		5%	++	-
		10%	++	-
		20%	-	-
Witepsol®E75	37-39°C	1%	+++	+++
		5%	+++	-
		10%	-	-
		20%	-	-
Witepsol®E85	42-44°C	1%	+++	-
		5%	-	-
		10%	-	-
		20%	-	-
Imwitor®900	54-65°C	1%	-	-
		5%	-	-
		10%	-	-
		20%	-	-
Imwitor®191	66-71°C	1%	+++	+++
		5%	++	-
		10%	-	-
		20%	-	-
Compritol®888 ATO	72°C	1%	-	-
		5%	-	-
		10%	-	-
		20%	-	-
Precirol®ATO 5	52-55°C	1%	+++	-
		5%	-	-
		10%	-	-
		20%	-	-
Precifac®ATO 5	52-56°C	1%	++	-
		5%	-	-
		10%	-	-
		20%	-	-
Apifil®	59-70°C	1%	+++	+++
		5%	-	-
		10%	-	-
		20%	-	-

+++ soluble; ++ hardly soluble; - insoluble

Lipid screening showed that selection of the appropriated lipid for clotrimazole solubilization is extremely important. In order to ensure the success of incorporation process, the drug needs to be solubilized in the melted lipid, both at high and low temperatures. Therefore, microscopic observations were performed for confirming the presence/absence of drug crystals in the drug/lipid mixtures.

Figure 5.1 shows a micrographical picture of 1% (*m/m*) clotrimazole-containing *Witepsol*®E85 at 20°C, without using polarized light (a) and using polarized light (b). Crystals could be detected using polarized light (Figure 5.1, b). From this observation it could be concluded that clotrimazole is insoluble in this lipid at room temperature, in opposition to its solubility at 90°C (Table VIII).

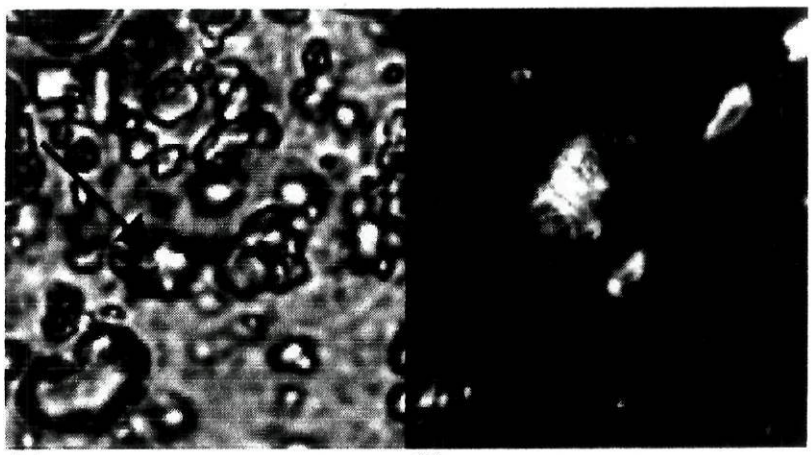

(a) (b)

Figure 5.1: Micrographical picture of 1% (*m/m*) of clotrimazole-containing *Witepsol*®85 at 20°C, (a) without using polarized light, and (b) using polarized light. The arrow identifies the presence of drug crystals.

According to the obtained results, *Dynasan*®116, *Softisan*®154, *Witepsol*®H5, *Witepsol*®S55, *Witepsol*®E75 and *Imwitor*®191 were selected for SLN preparation. Clotrimazole appeared to be soluble in all these lipids, both at high and low temperatures. Note that no crystals were observed after lipid screening for clotrimazole using these lipids.

5.1.2. Surfactant selection for SLN and NLC preparation

The selection of an appropriate surfactant for SLN and NLC preparation is a very important procedure due to the risk of gelation phenomenon or formation of gel-like systems, which is associated with unstable dispersions. This phenomenon describes the transformation of a low-

viscosity SLN or NLC dispersion into a viscous gel, which may occur very rapidly and unpredictably [7]. In most cases, gel formation is an irreversible process which involves the loss of the colloidal particle size and it can be stimulated by intense contact of the SLN or NLC dispersion with other surfaces and shear forces, such as the contact with the syringe needle during preparatory steps of particle characterization or sample shaking.

In the present work, several emulsifying agents were evaluated for the preparation of SLN containing 20% of lipid matrix, composed by different lipids, such as *Dynasan*®116, *Softisan*®154, *Witepsol*®H5, *Witepsol*®S55, *Witepsol*®E75 and *Imwitor*®191. The preparation of these systems was performed using a homogenization pressure of 500 bar and 3 homogenization cycles. The concentrations of lipid and emulsifying agent were selected according to the literature [48].

Table IX shows the first SLN formulations that were investigated and the obtained results on day 1 and day 7 after preparation.

Table IX: First SLN formulations tested with 20% of lipid and the obtained results one day and one week after preparation.

Lipid	**Emulsifiers**	**Results**	
% (*m/m*)	**% (*m/m*)**	**Day 1**	**Day 7**
Dynasan®116 20%	*Tween*®80 (1.2%)	-	-
	Tween®80/*Span*®85 (1.2%)	-	-
	Lipoid®S75/*Lutrol*®F68 (1.2%)	-	-
	Tego Care®450 (1.2%)	+	-
	Tyloxapol® (3%)	+	+
Softisan®154 20%	*Tween*®80 (1.2%)	-	-
	Tween®80/*Span*®85 (1.2%)	-	-
	Lipoid®S75/*Lutrol*®F68 (1.2%)	-	-
	Tego Care®450 (1.2%)	+	-
	Tyloxapol® (3%)	+	-
Witepsol®H5 20%	*Tween*®80 (1.2%)	-	-
	Tween®80/*Span*®85 (1.2%)	-	-
	Lipoid®S75/*Lutrol*®F68 (1.2%)	+	+
	Tego Care®450 (1.2%)	+	+
	Tyloxapol® (3%)	+	+

(-) gelation of aqueous dispersion of SLN; (+) production of aqueous dispersion of SLN.

Table IX: First SLN formulations tested with 20% of lipid and the obtained results one day and one week after preparation. (Continuation).

Lipid % (*m/m*)	Emulsifiers % (*m/m*)	Results	
		Day 1	Day 7
Witepsol®S55 20%	*Tween*®80 (1.2%)	-	-
	Tween®80/*Span*®85 (1.2%)	-	-
	Lipoid®S75/*Lutrol*®F68 (1.2%)	+	+
	Tego Care®450 (1.2%)	+	-
	Tyloxapol® (3%)	+	-
	Lanette®N (1.2%)	-	-
Witepsol®E75 20%	*Tween*®80 (1.2%)	-	-
	Tween®80/*Span*®85 (1.2%)	-	-
	Lipoid®S75/*Lutrol*®F68 (1.2%)	-	-
	Tego Care®450 (1.2%)	-	-
	Tyloxapol® (3%)	+	+
	Lanette®N (1.2%)	-	-
Imwitor®191 20%	*Tween*®80 (1.2%)	-	-
	Tween®80/*Span*®85 (1.2%)	-	-
	Lipoid®S75/*Lutrol*®F68 (1.2%)	-	-
	Tego Care®450 (1.2%)	-	-
	Tyloxapol® (3%)	-	-
	Lanette®N (1.2%)	-	-

(-) gelation of aqueous dispersion of SLN; (+) production of aqueous dispersion of SLN.

Regarding to the formulations showing gelation, this phenomenon was observed either directly on cooling after preparation or during storage at room temperature. For most investigated solid lipid/emulsifying agent combinations, SLN preparation resulted in gel-like systems.

It has been suggested that gelation phenomenon or formation of gel-like systems is associated to crystallization processes [36,289]. The crystal size of a modification of polycrystalline lipid aggregates is few microns or less [7]. A change of the α modification is associated with an increase in particle size (β' is less than 5 μm and β is between 20-100 μm) [294]. Westesen demonstrated by transmission electron microscopy (TEM) that tripalmitin and tristearin crystals have a spherical shape in α modification [66]. The β' modification is built up from stapled spheroids and the stable β modification is built up from long, coagulated platelets. Gelation process is connected with an increase of the particle surface due to the preferred formation of the more stable polymorph β, which is associated to a platelet form. The surfactant

molecules cannot longer provide sufficient coverage of the new surfaces and therefore, particle aggregation is observed. Gelation can be delayed or prevented by the addition of a co-surfactant agent with high mobility [66].

Other factors promoting gelation are the exposition to high temperatures, to the light and to mechanical stress [96]. Storage in darkness at 8°C can prevent particle growth for some SLN formulations. Freitas *et al.* found that fat samples stored under nitrogen atmosphere were more stable than samples filled under regular air [96]. This is attributed to the fact that nitrogen can inhibit the lipid hydrolysis [311]. High lipid concentrations and high ionic strengths can also promote gelation [97].

SLN obtained using *Dynasan*®116, *Witepsol*®H5, *Witepsol*®S55 and *Witepsol*®E75 were characterized by LD (d99% volume distribution) on day 1 and day 7 after preparation. The obtained results are shown in Figure 5.2.

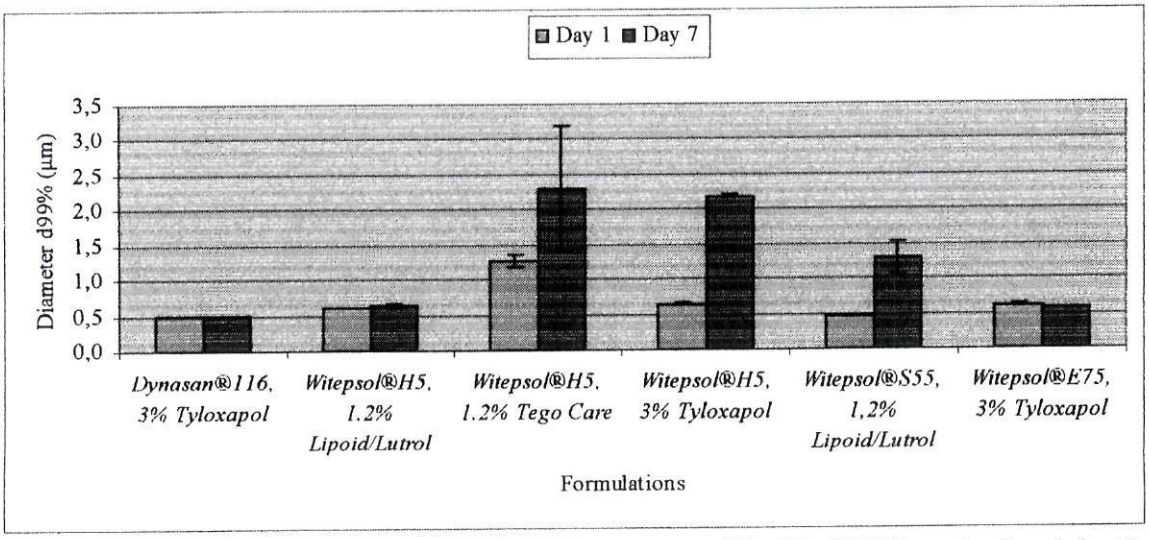

Figure 5.2: Particle size of the first SLN formulations measured by LD (d99%) on day 1 and day 7 after preparation.

Figure 5.2 shows that the best results, i.e. particle size below 500 nm, were obtained with 20% (*m/m*) of *Dynasan*®116 and 3% (*m/m*) of *Tyloxapol*®. *Witepsol*®H5 and *Witepsol*®S55 seem to be responsible for particle aggregation after 7 days of storage at 20°C. SLN obtained with *Witepsol*®E75 showed a mean particle size higher than 500 nm.

5.1.3. Preparation of different clotrimazole-containing SLN and NLC formulations

As observed before, the combination of 20% (*m/m*) of *Dynasan*®116 and 3% (*m/m*) of *Tyloxapol*® was responsible for the lowest particle size value measured by LD on day 1 and day

7 after SLN preparation, i.e. the SLN particle size remained lower than 490 nm during the first week.

According to the obtained results, *Dynasan*®116 appears to be the best lipid for preparation of SLN using *Tyloxapol*® as emulsifying agent. Therefore, this lipid and emulsifying agent were selected in order to prepare SLN and NLC containing 5% (*m/m*) of clotrimazole (with regard to the lipid matrix). The composition of the investigated SLN and NLC formulations are listed in Tables X and XI, respectively.

Table X: Composition of prepared SLN formulations.

Formulation code	*Dynasan*®116 % (*m/m*)	*Miglyol*®812 % (*m/m*)	*Tyloxapol*® % (*m/m*)	Clotrimazole % (*m/m*)	Water ad % (*m/m*)
D10%	10	-	3	-	100
D10%C	9.5	-	3	0.5	100
D20%	20	-	5	-	100
D20%C	19.5	-	5	1	100

Table XI: Composition of prepared NLC formulations.

Formulation code	*Dynasan*®116 % (*m/m*)	*Miglyol*®812 % (*m/m*)	*Tyloxapol*® % (*m/m*)	Clotrimazole % (*m/m*)	Water ad % (*m/m*)
DM20%	14	6	5	-	100
DM20%C	13.5	5.5	5	1	100

5.1.4. Optimizing the homogenization conditions

The optimum homogenization conditions need to be assessed for each nanoparticle system. It is known that the particle size distribution strongly depends on the amount and the type of emulsifying agent [233]. Therefore, the effect of the number of homogenization cycles on the particle size was investigated, keeping the homogenization pressure and the type of emulsifying agent constant.

In order to optimize the number of homogenization cycles, special batches D10%, D20% and DM20% were produced at 500 bar, applying 1 to 5 cycles and their diameter was evaluated by LD (d95%) and PCS on day 0 and after 7, 14 and 30 days of storage at 20°C.

Figures 5.3 and 5.4 show the results obtained by LD and PCS analysis, respectively, for D10% formulation.

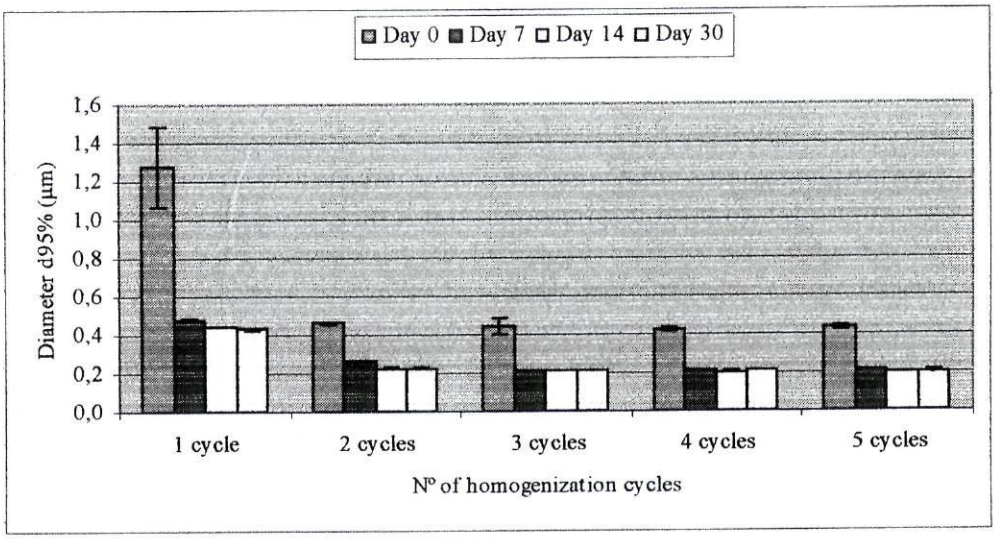

Figure 5.3: Particle size of SLN formulation D10% measured by LD (d95%) after 1 to 5 homogenization cycles, on day 0 and after 7, 14 and 30 days of storage at 20°C.

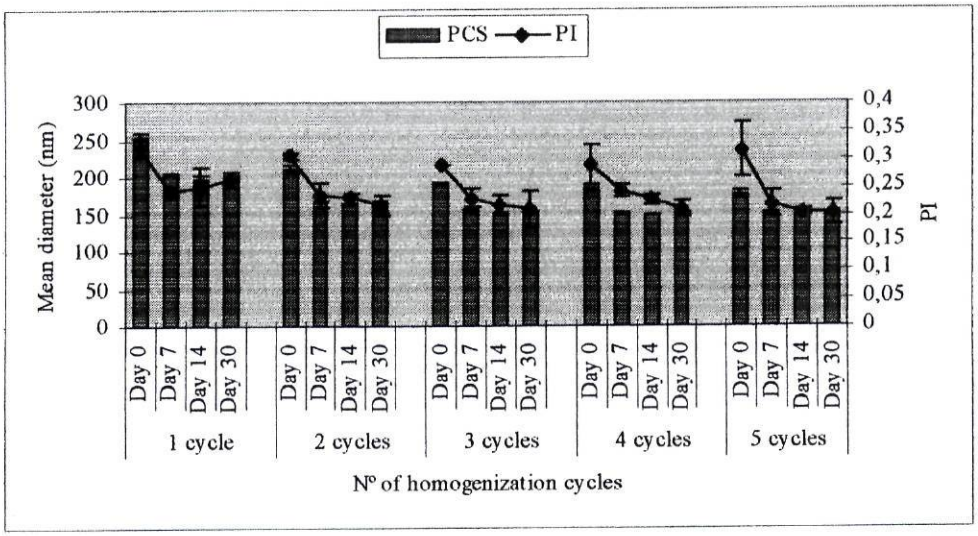

Figure 5.4: Mean particle size and PI of SLN formulation D10% measured by PCS after 1 to 5 homogenization cycles, on day 0 and after 7, 14 and 30 days of storage at 20°C.

Figures 5.5 and 5.6 show the results obtained by LD and PCS analysis, respectively, for D20% formulation.

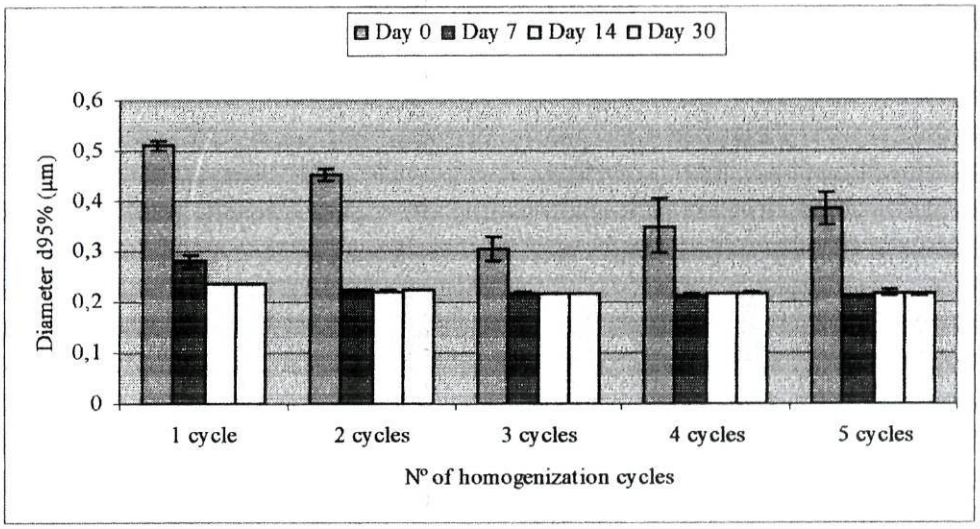

Figure 5.5: Particle size of SLN formulation D20% measured by LD (d95%) after 1 to 5 homogenization cycles, on day 0 and after 7, 14 and 30 days of storage at 20°C.

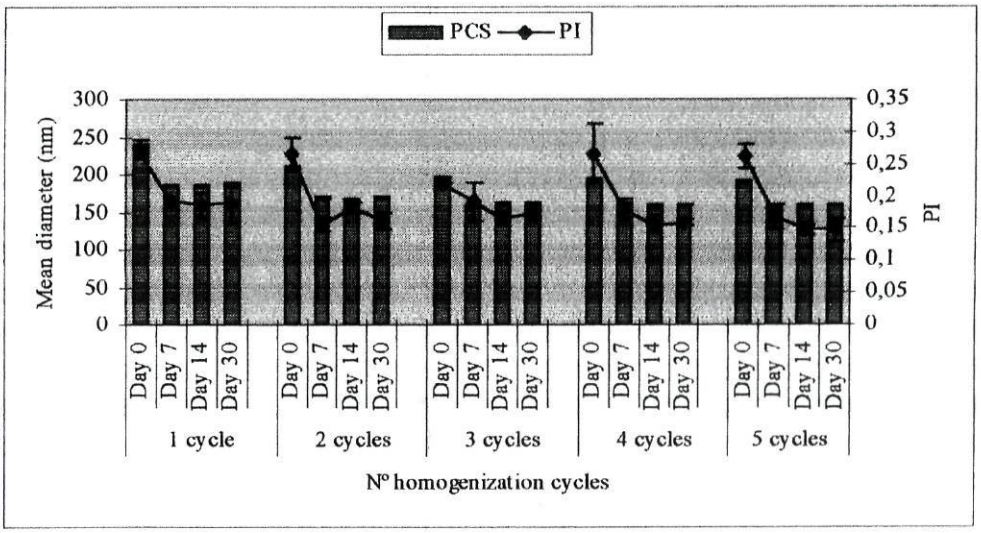

Figure 5.6: Mean particle size and PI of SLN formulation D20% measured by PCS after 1 to 5 homogenization cycles, on day 0 and after 7, 14 and 30 days of storage at 20°C.

Figures 5.7 and 5.8 show the results obtained by LD and PCS analysis, respectively, for DM20% formulation.

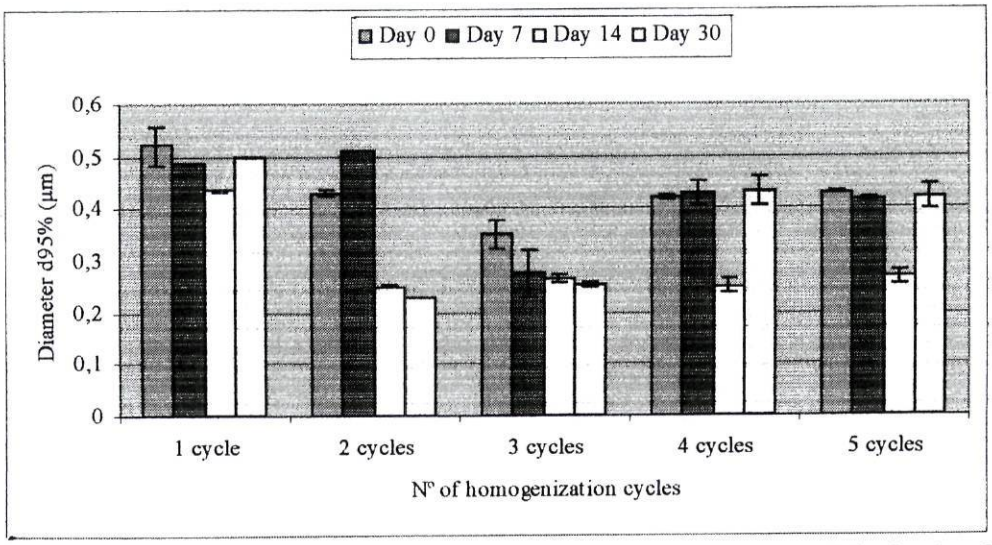

Figure 5.7: Particle size of NLC formulation DM20% measured by LD (d95%) after 1 to 5 homogenization cycles, on day 0 and after 7, 14 and 30 days of storage at 20°C.

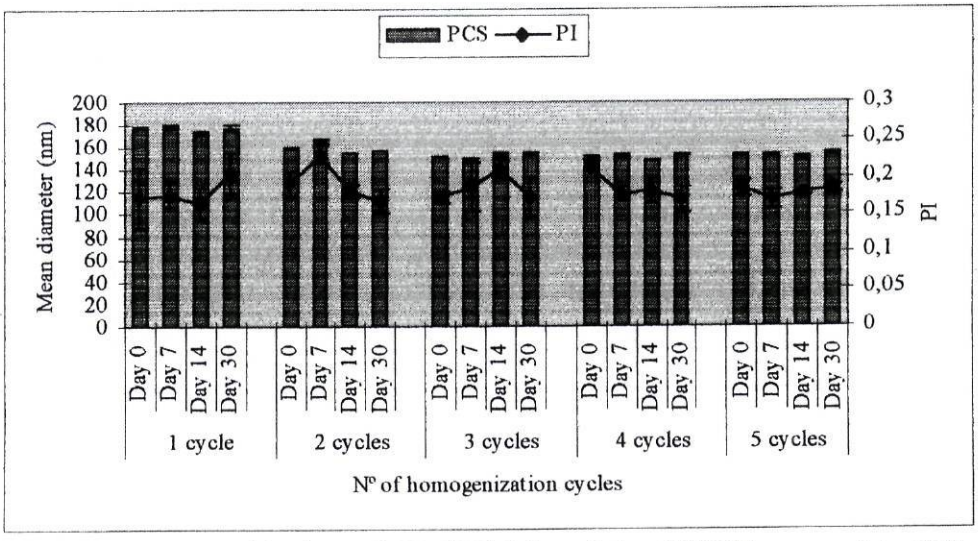

Figure 5.8: Mean particle size and PI of NLC formulation DM20% measured by PCS after 1 to 5 homogenization cycles, on day 0 and after 7, 14 and 30 days of storage at 20°C.

For all tested formulations LD and PCS measurements showed the decrease of the mean diameter by increasing the number of homogenization cycles from 1 to 3 cycles. Considering LD results, Figures 5.3, 5.5 and 5.7 show that SLN and NLC remain in their colloidal particle size during a period of 30 days. With regard to PCS results, Figures 5.4, 5.6 and 5.8 reveal similar

mean diameters from 3 to 5 homogenization cycles for all samples and a smallest PI after 3 homogenization cycles, which indicates a narrow size distribution. The observed particle growth after 4 and 5 homogenization cycles might be due to the high energy input originating particle fusion.

It is known that increasing the homogenization pressure or the number of homogenization cycles often results in an increase of the particle size due to particle coalescence, which occurs as a result of the high kinetic energy of the particle [64].

According to the obtained results, 3 homogenization cycles and a pressure of 500 bar were selected for preparation of all SLN and NLC formulations.

5.2. Physicochemical characterization of developed SLN and NLC formulations

Physicochemical characterization of formulations is an important tool used to assess the properties of the developed systems, considering the intended therapeutic purposes.

E.E. of clotrimazole in SLN and NLC formulations, as well as loading capacity were evaluated. In addition, particle size and zeta potential measurements, as well as DSC and X-ray analysis were performed for prepared SLN and NLC aqueous dispersions.

5.2.1. Encapsulation parameters

It was found that clotrimazole was successfully incorporated into physically stable lipid nanoparticle dispersions. Table XII shows the E.E. and the loading capacity of clotrimazole into SLN and NLC, one day after nanoparticles preparation.

Table XII: E.E. and loading capacity of clotrimazole into SLN and NLC one day after preparation.

Formulation	E.E. (%)	Loading capacity (%)
D10%C	64.189 ± 0.020	3.335 ± 0.004
D20%C	67.219 ± 0.040	2.623 ± 0.001
DM20%C	71.367 ± 0.004	3.860 ± 0.001

As Table XII shows, DM20%C revealed the highest E.E. (approximately 71.4%), probably due to the liquid oil content (*Miglyol*®812), which can better solubilize the clotrimazole. For

SLN samples, D10%C revealed a lower E.E. (approximately 64.2%) than D20%C (approximately 67.2%), which is probably due to the lower lipid content of the former.

With regard to drug loading capacity, Table XII shows the percentage of clotrimazole-loaded lipid nanoparticles (D10%C, D20%C and DM20%C), calculated on day 1 of storage at room temperature. Obtained results confirm the higher loading capacity of NLC samples (approximately 3.9% *m/m*) in comparison to SLN with the same lipid content (approximately 2.6% *m/m*). For SLN samples, D10%C revealed a higher loading capacity (approximately 3.3% *m/m*) in comparison to D20%C (approximately 2.6% *m/m*), in spite of being responsible for a lower E.E..

5.2.2. Particle size

Tables XIII and XIV show the PCS diameter, PI and d99% diameter of SLN and NLC formulations, respectively, on day 1 of storage at room temperature.

Table XIII: PCS diameter, PI and d99% diameter of SLN formulations on day 1 of storage at 20°C.

Formulation	PCS diameter (nm)	PI	d99% diameter (µm)
D10%	195.167 ± 1.150	0.224 ± 0.027	0.466 ± 0.007
D10%C	189.533 ± 4.750	0.208 ± 0.040	0.577 ± 0.002
D20%	203.600 ± 1.840	0.219 ± 0.004	0.492 ± 0.000
D20%C	214.400 ± 0.260	0.241 ± 0.024	0.725 ± 0.000

Table XIV: PCS diameter, PI and d99% diameter of NLC formulations on day 1 of storage at 20°C.

Formulation	PCS diameter (nm)	PI	d99% diameter (µm)
DM20%	181.167 ± 2.630	0.175 ± 0.027	0.573 ± 0.002
DM20%C	182.333 ± 1.930	0.182 ± 0.021	0.645 ± 0.002

On day 1 after preparation, both drug-free and drug-loaded SLN and NLC aqueous dispersions showed a narrow particle size distribution measured by LD (d99%), which was completely in the nanometer range (Tables XIII and XIV).

The presence of clotrimazole was not responsible for an increase in the mean particle size measured by PCS. NLC formulations revealed a lower PI (< 0.182) in comparison to SLN

formulations with the same lipid content (< 0.241). In addition, NLC showed a smaller mean particle size (approximately 180 nm).

5.2.3. Zeta potential

The determination of ζ was performed in SLN and NLC aqueous dispersions stored at room temperature. Tables XV and XVI show the ζ values of SLN and NLC formulations, respectively, one day after samples preparation. pH of all tested SLN and NLC aqueous dispersions ranged between 4 and 5.

Table XV: Zeta potential of SLN formulations on day 1 of storage at 20°C.

Formulation	ζ (mV)
D10%	-37.367 ± 0.057
D10%C	-11.333 ± 0.472
D20%	-23.400 ± 0.608
D20%C	-9.533 ± 0.208

Table XVI: Zeta potential of NLC formulations on day 1 of storage at 20°C.

Formulation	ζ (mV)
DM20%	-16.767 ± 0.153
DM20%C	-8.433 ± 0.379

On day 1 of storage at room temperature, ζ of drug-free samples was between -17 mV and -37 mV, while ζ of drug-loaded samples was between -8 mV and -11 mV. It could be observed that the clotrimazole-containing formulations showed ζ lowers than the drug-free formulations. In addition, drug-free NLC formulations also showed lower ζ values in comparison to SLN samples.

5.2.4. DSC studies

DSC investigations afford an insight into the melting point and recrystallization behaviour of crystalline materials, like SLN and NLC. The breaking down of the crystal lattice by heating the sample yields inside information on polymorphism and crystal ordering [287]. Therefore, the

bulk lipid (glyceryl tripalmitate), as well as clotrimazole-free and clotrimazole-loaded SLN and NLC were investigated by DSC.

DSC curves have been displaced along the ordinate for better visualization.

5.2.4.1. Crystalline status of bulk material

Figure 5.9 shows the DSC curves of glyceryl tripalmitate (*Dynasan*®116) bulk material and of a mixture of *Dynasan*®116 with 5% (*m/m*) of clotrimazole.

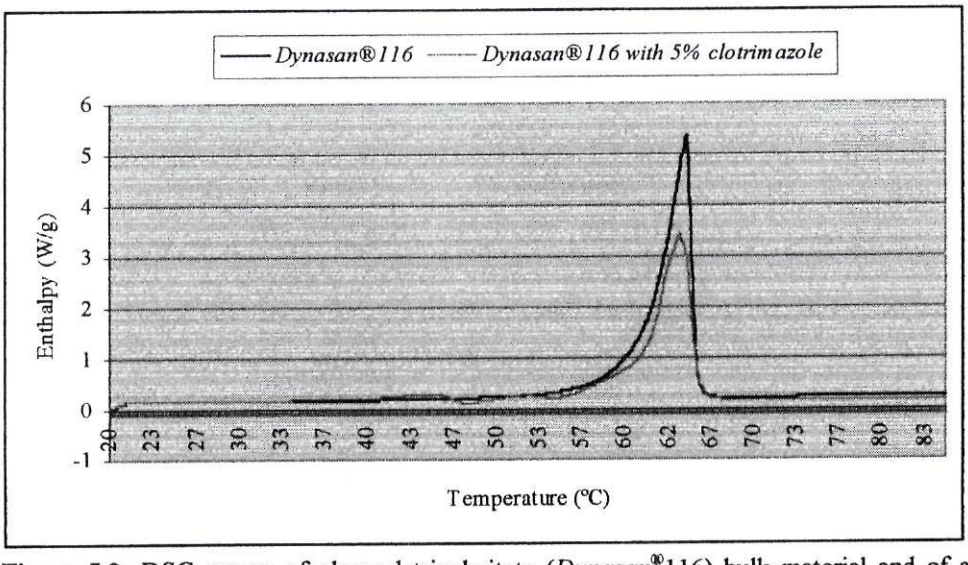

Figure 5.9: DSC curves of glyceryl tripalmitate (*Dynasan*®116) bulk material and of a mixture of *Dynasan*®116 with 5% (*m/m*) of clotrimazole.

The bulk material melted between 53°C and 68°C with the melting point at 63°C. When analysing Figure 5.9 it should be pointed out that a simple mixture of the *Dynasan*®116 with clotrimazole elicited only one thermal event at 63°C, indicating that the clotrimazole does not interfere with the melting point of the lipid.

The lower area under the curve observed for drug-lipid mixture is due to its lower solid lipid content in comparison to the bulk material. The transition temperature suggests that the endotherm is due to the melting of tripalmitin.

5.2.4.2. Crystalline status of lipid matrix

In order to assess possible interactions between clotrimazole and the lipid matrix of SLN and NLC aqueous dispersions DSC assays were performed for all tested formulations.

Figure 5.10 shows the DSC curves of D10% (clotrimazole-free) and D10%C (clotrimazole-loaded) SLN formulations, after 7 days of storage at 20°C. The sample containing 5% of clotrimazole (with regard to the lipid matrix) exhibited a thermal event at 59°C, exactly at the same value as the clotrimazole-free sample. This result indicates that clotrimazole does not interfere with the crystallinity of SLN containing 10% of *Dynasan*®116 as lipid matrix.

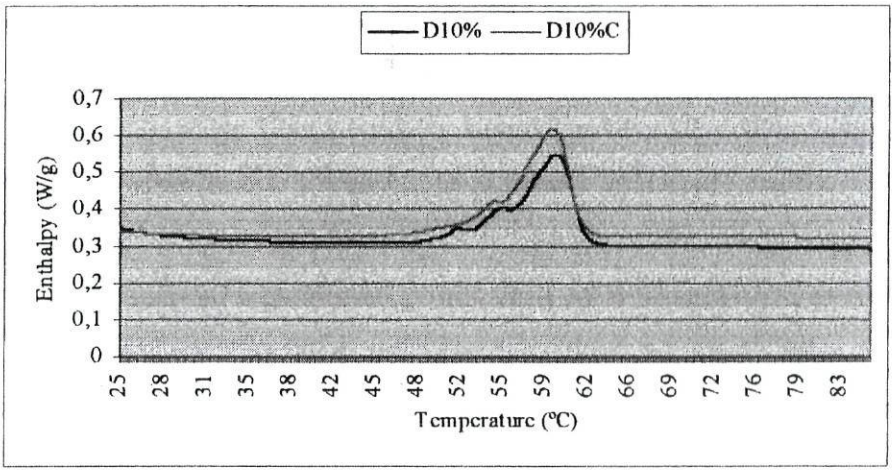

Figure 5.10: DSC curves of D10% (clotrimazole-free) and D10%C (clotrimazole-loaded) SLN formulations, after 7 days of storage at 20°C.

Figure 5.11 shows the DSC curves of D20% (clotrimazole-free) and D20%C (clotrimazole-loaded) SLN formulations, after 7 days of storage at 20°C. The sample containing 5% of clotrimazole (with regard to the lipid matrix) exhibited a thermal event at 60°C, exactly at the same value as the clotrimazole-free sample. This result also indicates that clotrimazole does not interfere with the crystallinity of SLN containing 20% of *Dynasan*®116 as lipid matrix.

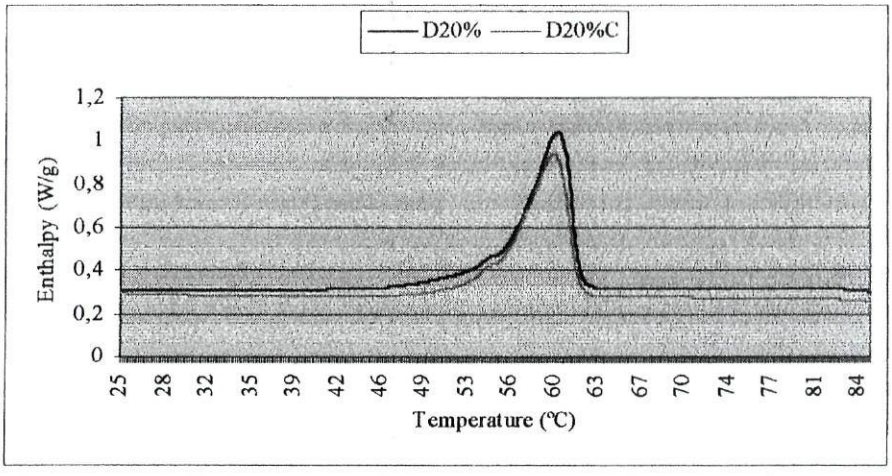

Figure 5.11: DSC curves of D20% (clotrimazole-free) and D20%C (clotrimazole-loaded) SLN formulations, after 7 days of storage at 20°C.

As it has been reported before, polymorphic transformations of triacylglycerols in colloidal dispersions, such as SLN, are faster than in the bulk material, leading to changes in the crystallinity of the lipid matrix [63]. Crystallization of the lipid in nanoparticles is different from the bulk material because the former recrystallizes at least in α form, whereas the bulk material tends to crystallize preferentially in the β' modification and transforming rapidly into the β form. Depending on the chemical nature of the lipid and on the production conditions, different fractions of α and β' modifications can be obtained in lipid nanoparticles. This phenomenon leads to a reduction of the melting point, i.e. changes in form and shift of the melting peak, which can be observed by DSC measurements.

Figure 5.12 shows the DSC curves of DM20% (clotrimazole-free) and DM20%C (clotrimazole-loaded) NLC formulations, after 7 days of storage at 20°C. The sample containing 5% of clotrimazole (with regard to the lipid matrix) exhibited a thermal event at 58°C, exactly at the same value as the clotrimazole-free sample. This result indicates that clotrimazole does not interfere with the crystallinity of NLC containing 14% of *Dynasan*®116 and 6% of *Miglyol*®812.

In comparison to SLN formulations, DM20% and DM20%C exhibited a lower melting point due to the liquid oil (*Miglyol*®812) inside their lipid matrix, indicating that a fat fraction might be liquid. The presence of liquid phases promotes the crystallization in the stable form because unstable crystals might redissolve and crystallize in the stable modification [312].

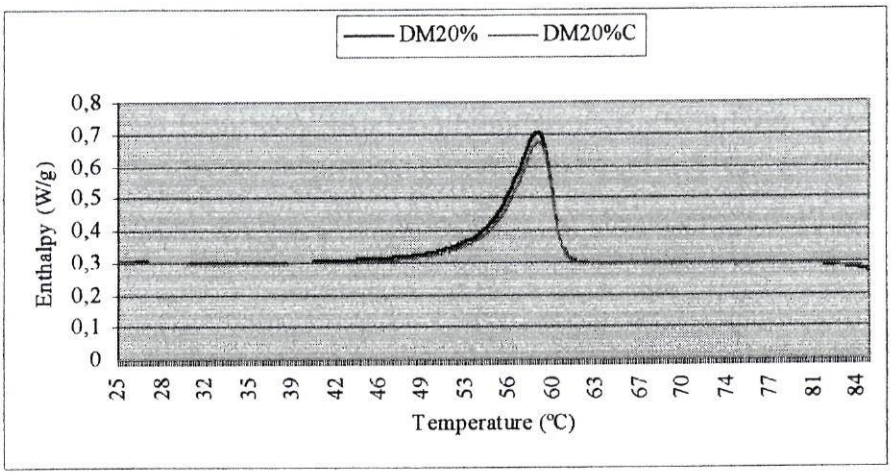

Figure 5.12: DSC curves of DM20% (clotrimazole-free) and DM20%C (clotrimazole-loaded) NLC formulations, after 7 days of storage at 20°C.

The obtained DSC data are in agreement with particle size and ζ measurements showing that clotrimazole has no effect on physicochemical stability of the lipid matrix. In comparison to the bulk material, the melting point of the lipid matrix of SLN and NLC formulations slightly decreased (from 63°C to 58°C).

The melting behaviour of triacylglycerol nanoparticles strongly depends on the particle size, irrespective of matrix material and stabilizer composition [44]. From thermodynamic point of view it is expected that the melting temperature of colloidal substances would decrease with particle size.

The Gibbs-Thompson equation (Chapter IV, section 4.4.1) has been used to explain the melting point depression of triacylglycerol nanoparticles compared to their bulk phase. The melting point of lipid nanoparticles (T) is always smaller than the melting point of the bulk material (T_0). When a foreign compound is dissolved in the lipid matrix, e.g. drug or surfactant molecules, the lipid nanoparticles will show a melting point depression. Defects in the crystal lattice may also contribute to the depression of the DSC melting temperature, and the small size of these nanoparticles may be an additional reason for their low melting temperature [53].

5.2.5. X-ray diffraction studies

The existence of only one additional, low-melting structure in very fine particles is, however, not sufficient to explain the complex melting behaviour of the solid lipid dispersions at higher temperatures [44]. According to the x-ray measurements, the complex melting behaviour is due to a stepwise melting of the β stable form. For the β modification of triacylglycerols, several sub-modifications, which differ in angle of chain tilt and thus in their long spacings, have been described.

Therefore, bulk material, as well as lipid nanoparticles without drug and clotrimazole-loaded were also characterized by WAXS-experiments. Scattering angles were transformed into short spacings using Bragg's equation (Chapter IV). These measurements were performed after 7 days of storage at room temperature.

By means of WAXS it is possible to assess the length of the long and short spacings of the lipid lattice. It is highly recommended to measure solid lipid dispersions themselves because solvent removal is able to lead to polymorphic changes [7].

The x-ray diffractograms of the bulk material display reflections due to the crystalline state of tripalmitin. The x-ray diffractograms of drug-free and drug-loaded dispersions also contain only the diffraction pattern of the stable β-polymorph of tripalmitin but no reflections of drug when incorporated [73].

In the following WAXS curves plots have been displaced vertically for better visualization. The units of intensity are arbitrary.

As it can be observed in Figure 5.13 bulk material (*Dynasan*®116) showed the typical signals of the β-modification of triacylglycerols [293,294].

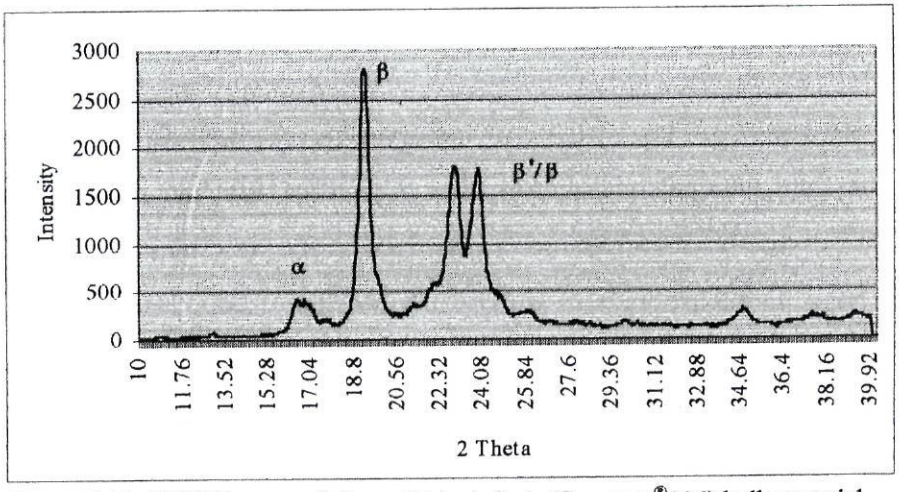

Figure 5.13: WAXS curve of glyceryl tripalmitate (*Dynasan*®116) bulk material.

Figures 5.14 and 5.15 show the WAXS curves of SLN prepared with 10% of lipid without drug and clotrimazole-loaded, respectively. These curves show the characteristic peaks for β'/β modifications, which are marked with arrows. They display x-ray peaks in the wide angle regions pointing to the crystalline nature of these particles.

These dispersions also exhibit melting endotherms in DSC heating runs. DSC and x-ray diffraction data indicate that solidification of the freshly O/W nanoemulsion under investigation results in crystalline material, i.e. SLN and NLC. The incorporation of drug into these particles did not influence lipid crystallinity, as reported after DSC analysis. Note that the position of the peak maxima did not change noticeably with the presence of clotrimazole.

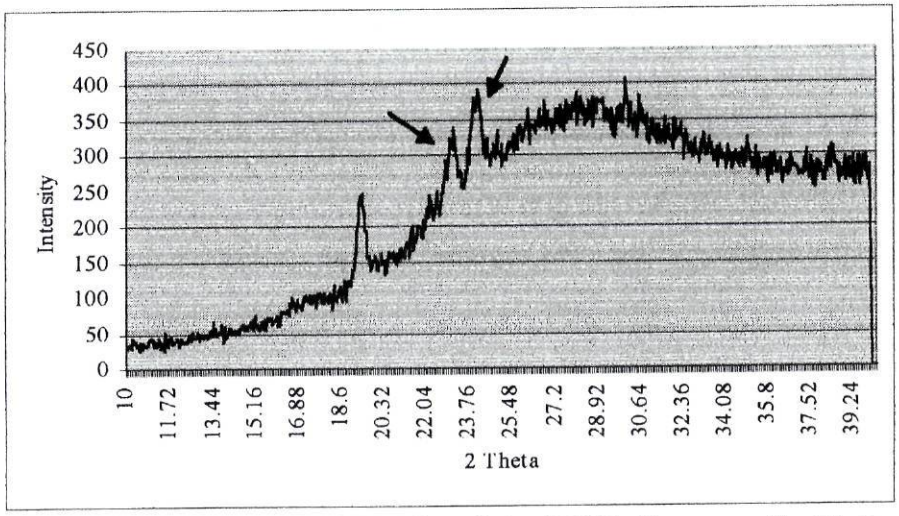

Figure 5.14: WAXS curve of SLN formulation D10%. The arrows identify the characteristic peaks of β/ β' modifications.

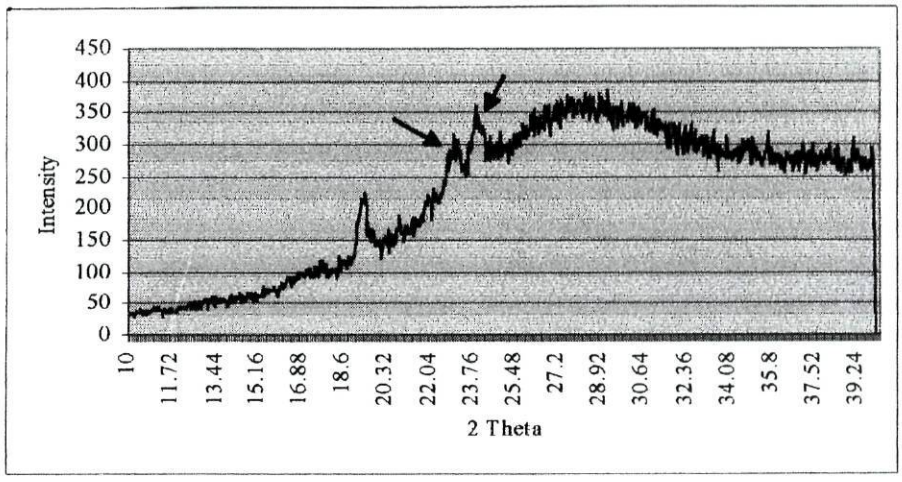

Figure 5.15: WAXS curve of SLN formulation D10%C. The arrows identify the characteristic peaks of β/ β' modifications.

Figures 5.16 and 5.17 show the WAXS curves of SLN prepared with 20% of lipid without drug and clotrimazole-loaded, respectively. As it could be observed for samples containing 10% of lipid matrix, these curves also show the characteristic peaks for β'/β modifications, which are marked with arrows, showing the crystalline nature of these particles. The incorporation of clotrimazole into these SLN did not influence the lipid crystallinity, as reported after DSC analysis.

In comparison to SLN formulations containing 10% of lipid matrix, the peak intensity is higher for SLN containing 20% of lipid matrix, as it could be expected.

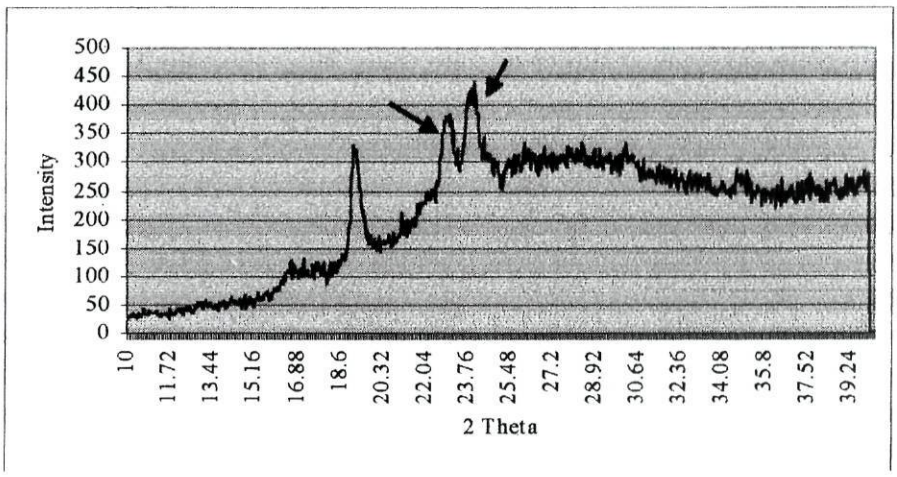

Figure 5.16: WAXS curve of SLN formulation D20%. The arrows identify the characteristic peaks of β/ β' modifications.

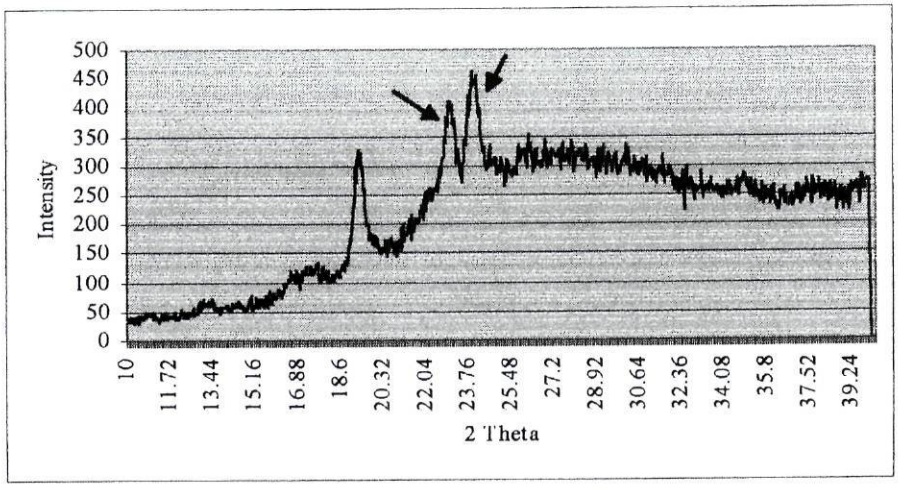

Figure 5.17: WAXS curve of SLN formulation D20%C. The arrows identify the characteristic peaks of β/ β' modifications.

Figures 5.18 and 5.19 show the WAXS curves of NLC formulations. No peak could be detected for both formulations, i.e. clotrimazole-free (Figure 5.18) and clotrimazole-loaded (Figure 5.19), which means that lipid might contain dissolved clotrimazole in the molecularly dispersed form.

None of the NLC formulations (clotrimazole-free and clotrimazole-loaded) displayed any wide angle reflection in their x-ray patterns. Although, these samples display a thermal event (melting endotherm) in DSC heating runs (Figure 5.12). Note that, whereas x-ray diffraction data only allow differentiation between crystalline data and amorphous material, DSC data can be used to differentiate between amorphous solids and liquids [53].

In comparison to SLN with the same lipid content, NLC formulations evidence lower lipid crystallinity in agreement with the obtained DSC data. These x-ray crystallization studies confirm that the transition rates of liquid oils are lower than solid lipids. These differences may be due to the more ordered structure of SLN in comparison to NLC.

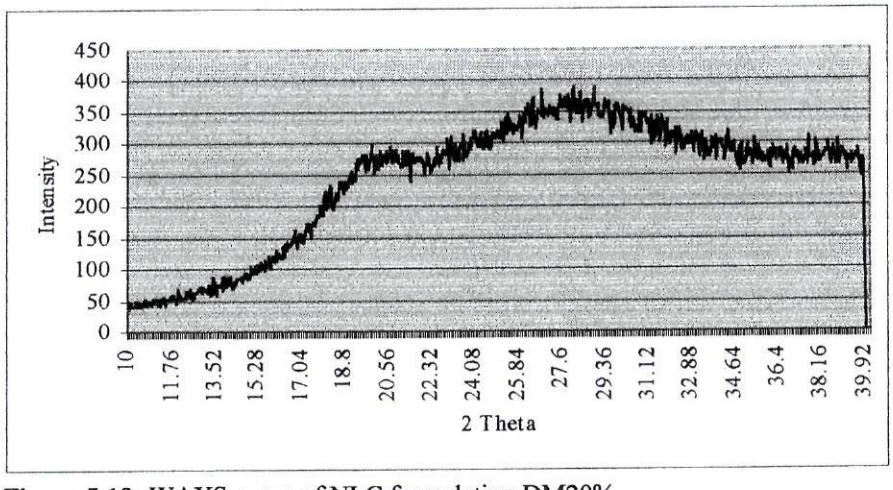

Figure 5.18: WAXS curve of NLC formulation DM20%.

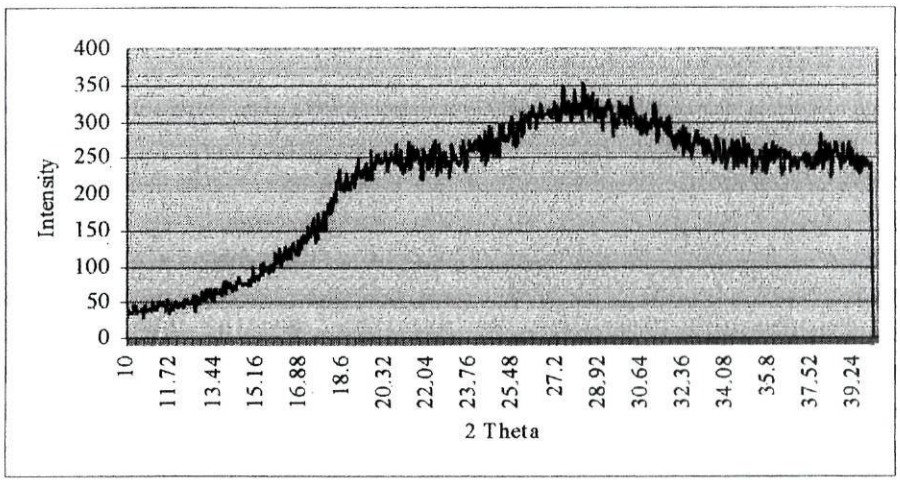

Figure 5.19: WAXS curve of NLC formulation DM20%C.

According to the x-ray results it can be stated that clotrimazole does not interfere with the lipid matrix. In fact, the incorporation of drug in SLN and NLC formulations led to similar results as the ones obtained without drug. In addition, no drug peaks are visible in WAXS curves of clotrimazole-loaded formulations; therefore, it can be concluded that drug is still inside the lipid nanoparticles.

In comparison to the bulk material, SLN and NLC seem to transform more rapidly into the stable β-polymorph, confirming the DSC data. The faster polymorphic transitions in lipid nanoparticles have been attributed to the presence of small crystallization nuclei [53,289]. Note that, x-ray peaks of SLN formulations are less intense in comparison to the bulk material pattern. This is due to lattice imperfections of incomplete crystallization of the dispersed lipid nanoparticles.

It has been reported that the degree of crystallinity has an effect on the long-term stability of aqueous dispersions of SLN [96]. In general, dispersions with a highly recrystallized lipid phase showed an increased particle size growth. SLN and NLC were produced by hot HPH of the melted lipid dispersed in a surfactant aqueous solution. The obtained O/W nanoemulsion was cooled down, recrystallized and formed the lipid particles. Depending on the nature of the lipid, this process can take place very quickly, in fact within minutes [98]. However, it has also been reported that the recrystallization of the lipid fraction can be retarded up to weeks or months [289]. In general, the degree of crystallinity of lipid nanoparticles is below the crystallinity of the bulk material used for SLN production and increases with increasing storage time [98].

5.3. Stability of developed SLN and NLC formulations

Ideally, SLN and NLC should be physically stable in aqueous dispersion. Optimized compositions of lipid nanoparticle aqueous dispersions proved to be stable for more than 3 years [48].

In the present work, the stability of prepared SLN and NLC formulations was evaluated concerning the encapsulation parameters, particle size, ζ and the crystalline status of SLN and NLC.

5.3.1. Encapsulation parameters

The evaluation of the E.E. of clotrimazole and the drug loading capacity during storage time are very important tools for the development of a colloidal carrier system [6]. Therefore, for all developed clotrimazole-containing SLN and NLC aqueous dispersions the E.E. and the loading capacity were evaluated over a period of 21 days.

Figures 5.20 and 5.21 show, respectively, the variation of E.E. of clotrimazole and drug loading capacity of D10%C, measured after 1, 3, 7, 14 and 21 days of storage at room temperature.

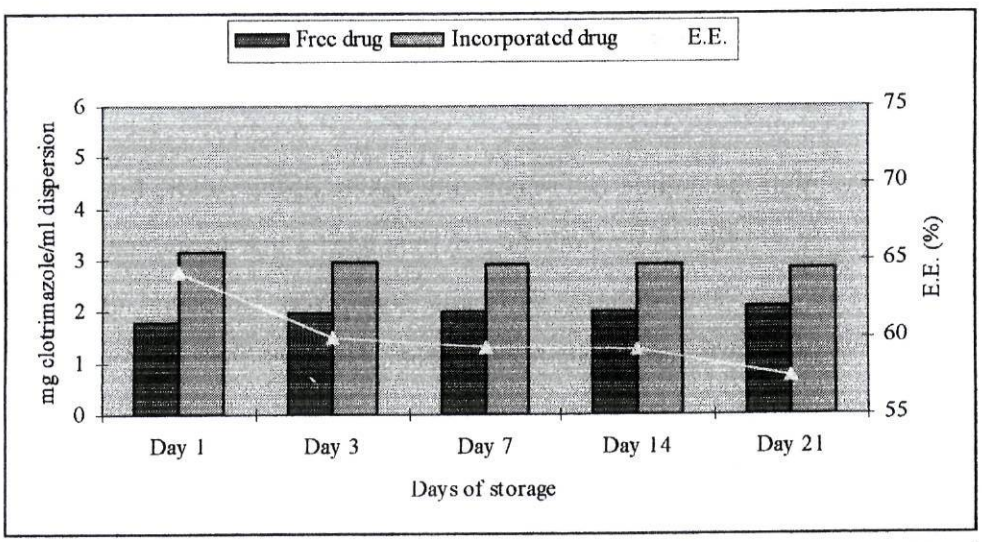

Figure 5.20: Variation of E.E. of clotrimazole in D10%C, measured after 1, 3, 7, 14 and 21 days of storage at room temperature (20°C).

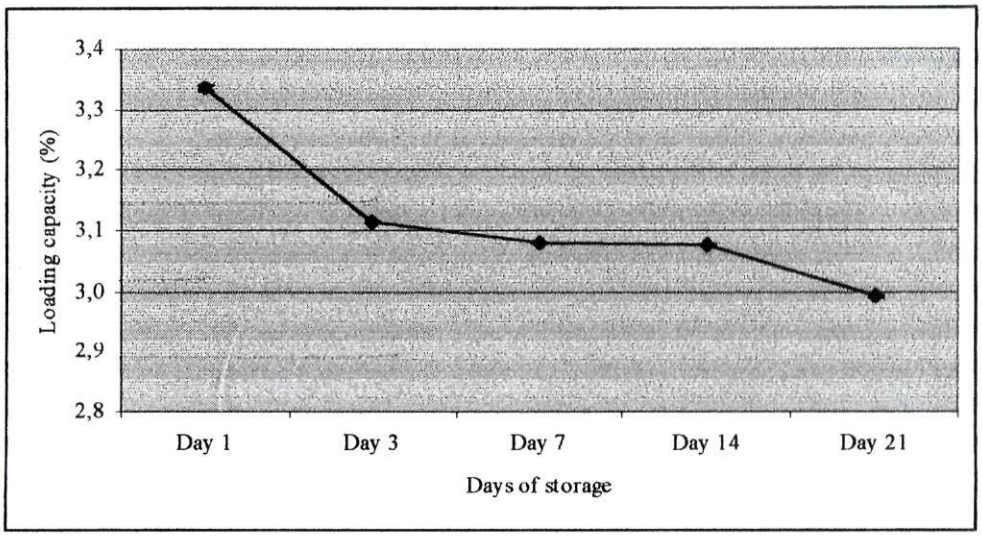

Figure 5.21: Variation of drug loading capacity of D10%C, measured after 1, 3, 7, 14 and 21 days of storage at room temperature (20°C).

Concerning the E.E., D10%C revealed a higher decrease between day 1 and day 3 of storage (approximately 7%), while from day 7 onwards, the decrease in E.E. became smaller. During 21 days the value of E.E. decreased from 60% to 58%. With regard to drug loading capacity, it was also observed a decrease of drug content in D10%C between day 1 and day 3 (approximately 0.3%). Between day 7 and day 21 the loss of drug was neglected.

Figures 5.22 and 5.23 show, respectively, the E.E. of clotrimazole and the drug loading capacity of D20%C, measured after 1, 3, 7, 14 and 21 days of storage at room temperature.

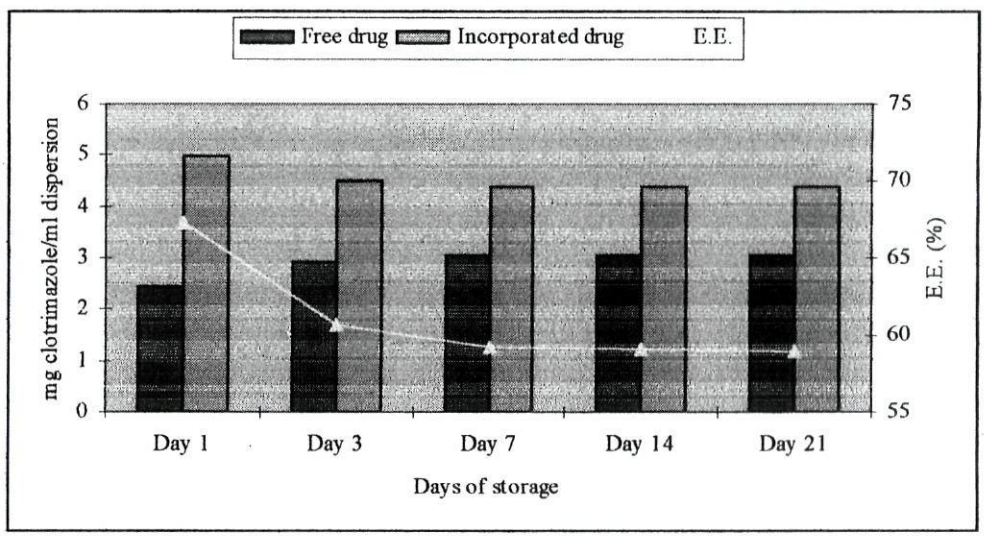

Figure 5.22: Variation of E.E. of clotrimazole in D20%C, measured after 1, 3, 7, 14 and 21 days of storage at room temperature (20°C).

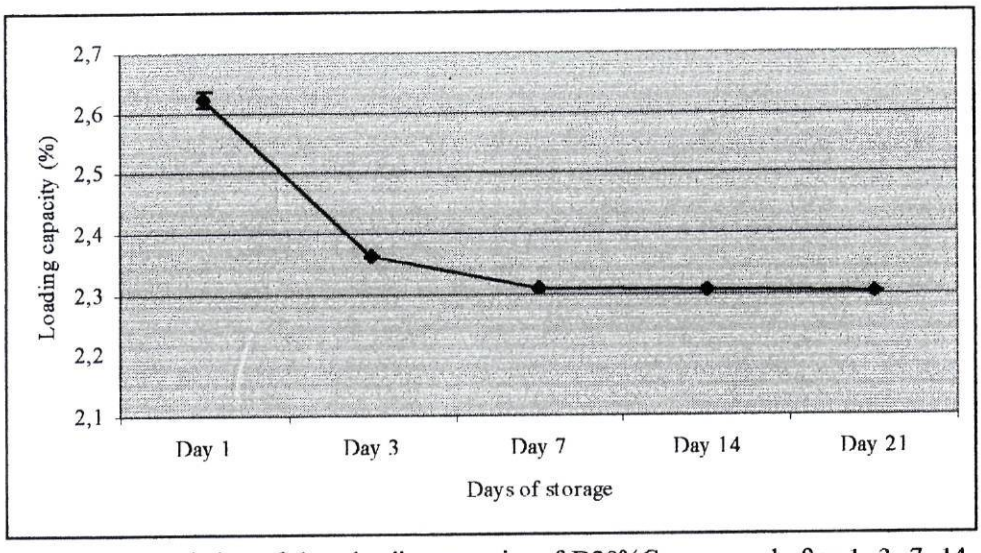

Figure 5.23: Variation of drug loading capacity of D20%C, measured after 1, 3, 7, 14 and 21 days of storage at room temperature (20°C).

Concerning the E.E., D20%C also revealed a higher decrease between day 1 and day 3 of storage (approximately 3%), in comparison to the period of time between day 7 and day 21. However, the decrease in E.E. during storage time was lower in D20%C than in D10%C. With regard to drug loading capacity, D20%C also showed drug loss during, approximately 0.3%, during 21 days of storage at room temperature.

Figures 5.24 and 5.25 show, respectively, the E.E. of clotrimazole and the drug loading capacity of DM20%C, measured after 1, 3, 7, 14 and 21 days of storage at room temperature.

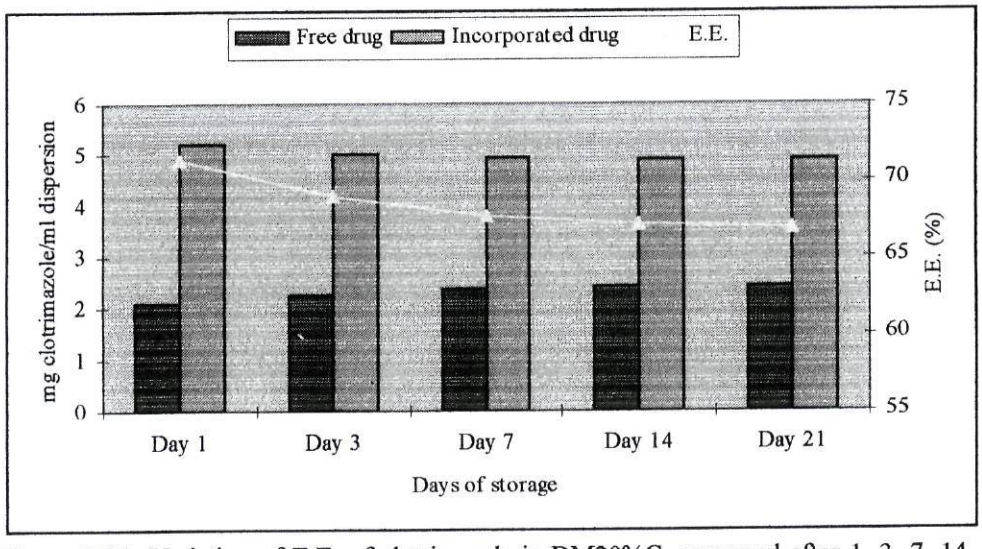

Figure 5.24: Variation of E.E. of clotrimazole in DM20%C, measured after 1, 3, 7, 14 and 21 days of storage at room temperature (20°C).

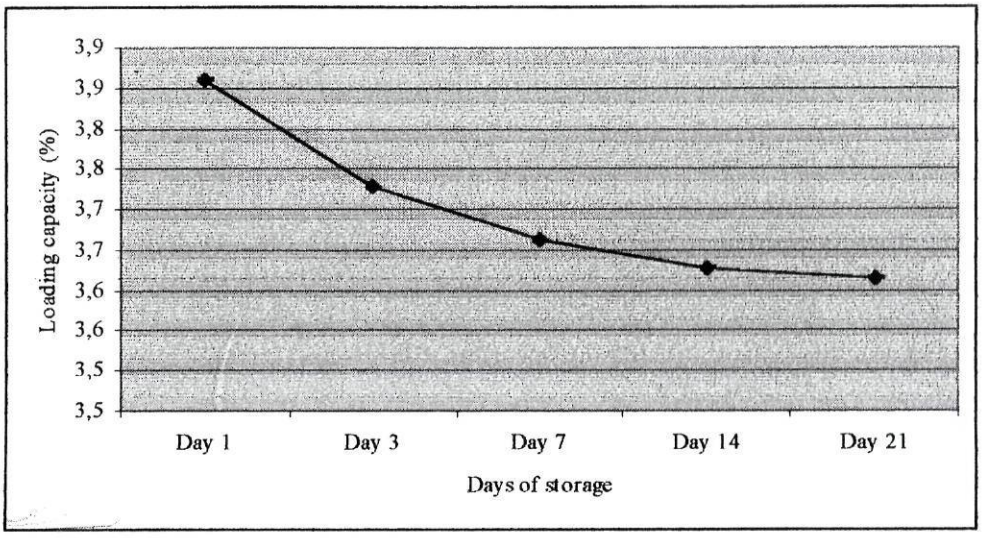

Figure 5.25: Variation of drug loading capacity of DM20%C, measured after 1, 3, 7, 14 and 21 days of storage at room temperature (20°C).

Concerning the E.E., DM20%C was responsible for the higher obtained value for E.E.. This formulation also revealed a decrease in E.E. between day 1 and day 3 of storage (approximately 2%), while from day 7 onwards, the decrease in E.E. became smaller. With regard to drug loading capacity, DM20%C also showed drug loss during, approximately 0.3%, during 21 days of storage at room temperature.

The obtained results confirm the higher loading capacity of NLC formulation (approximately 3.5% *m/m*) in comparison to SLN formulation prepared with the same lipid content (approximately 2.3% *m/m*).

For SLN formulations, D10%C revealed a higher loading capacity (approximately 3% *m/m*) in comparison to the D20%C (approximately 2.3% *m/m*), in spite of being responsible for a lower E.E..

According to Müller *et al.* [6], factors determining drug loading capacity are: (i) the solubility of drug in melted lipid, (ii) the miscibility of melted lipid and drug, (iii) the chemical and physical structure of solid lipid matrix, and (iv) the polymorphic state of the lipid material. The prerequisite for obtaining a sufficient loading capacity is a sufficiently high solubility of the drug in the melted lipid. Typically, the solubility should be higher than required because it decreases when cooling down the melt and might even be lower in the solid lipid. It needs also to be considered that during solidification of the lipid an expulsion of the drug from the lipid matrix might occur [5].

To enhance the solubility of the active compound in the melted lipid one can add solubilizers, emulsifying agents or use mono- and diacylglycerols as matrix material, which promotes drug

solubilization [6]. In addition, the presence of a liquid lipid can enhance both E.E. and drug loading capacity, which has been observed for DM20%C formulation.

The chemical nature of the lipid is also important, because lipids which form highly crystalline particles with a perfect lattice, such as monoacid triacylglycerols like *Dynasan*®116 [293], lead to drug expulsion [53]. In the present work, during 21 days of storage at room temperature, all SLN and NLC developed formulations showed some drug expulsion from the lipid matrix. During this period of time, all clotrimazole-loaded formulations revealed a drug loss of approximately 10% (*m/m*). More complex lipids, such as mixtures of mono-, di- and triacylglycerols form less perfect crystals with many imperfections, offering space to accommodate the drugs [9]. Also chemically polydisperse lipids, such as those used in cosmetics, show very good drug incorporation capabilities.

Figure 5.26 shows the E.E. of clotrimazole-loaded lipid nanoparticles (D10%C, D20%C and DM20%C) on day 21 of storage at room temperature (20°C), as a function of E.E. obtained on day 1.

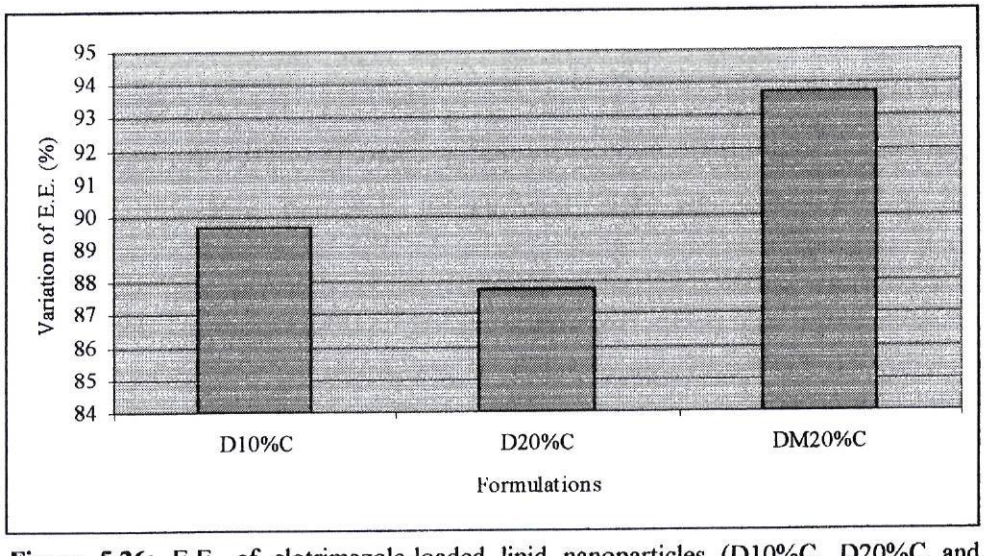

Figure 5.26: E.E. of clotrimazole-loaded lipid nanoparticles (D10%C, D20%C and DM20%C) on day 21 of storage at room temperature (20°C), as a function of E.E. obtained on day 1.

DM20%C showed the highest E.E. with regard to the results obtained on day 1 (approximately 94%), probably due to the liquid oil content, which can better solubilize the lipophilic drug. Although D10%C revealed a lower E.E., in comparison to D20%C after 21 days of storage at room temperature (Figures 5.20 and 5.22), the former was responsible for a lower loss of drug during this period of time. In fact, after 21 days of storage at room temperature the E.E. of D10%C was approximately 90% and of D20%C was approximately 88% (Figure 5.26).

With regard to drug loading capacity, Figure 5.27 shows loading capacity of clotrimazole-loaded lipid nanoparticles (D10%C, D20%C and DM20%C) on day 21 of storage at room temperature (20°C), as a function of loading capacity obtained on day 1.

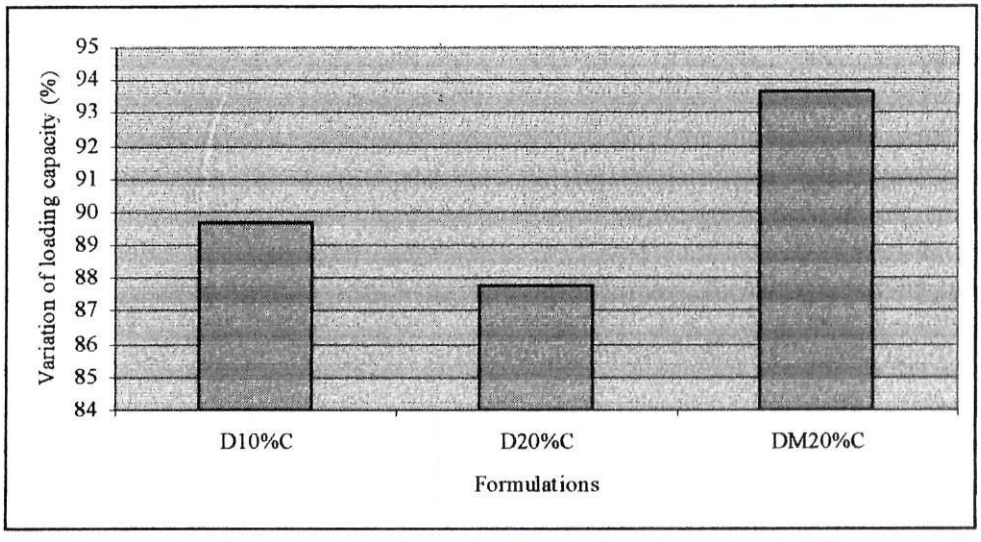

Figure 5.27: Loading capacity of clotrimazole-loaded lipid nanoparticles (D10%C, D20%C and DM20%C) on day 21 of storage at room temperature (20°C), as a function of loading capacity obtained on day 1.

The obtained results for loading capacity of clotrimazole-loaded lipid nanoparticles are in agreement with the obtained results for E.E. exposed above (Figure 5.26). Figure 5.27 shows that DM20%C is responsible for the lowest drug loss observed during 21 days of storage at room temperature. In comparison to NLC formulation, SLN formulations revealed a higher drug loss during storage time. The loading capacity of D10%C was higher than the value obtained for D20%C, probably due to the lower lipid content of the former in comparison to D20%C.

Crystalline structure which is related to the chemical nature of the lipid is the responsible factor to decide whether the drug will be expelled or firmly incorporated during long-term storage [6]. The polymorphic form is also a parameter determining drug incorporation. As reported before, crystallization of the lipid in nanoparticles is different from the bulk material. In fact, lipid nanoparticles recrystallize at least partially in the α-form, whereas bulk lipids tend to recrystallize preferentially in the β'-form and transforming rapidly into the β-form [63]. With increasing formation of the more stable modifications during storage, the lattice is getting more perfect and the number of imperfections decreases, which means the formation of β'/β-modifications and promotion of drug expulsion. In general, the transformation is slower for long-chain than for short-chain triacylglycerols [36].

In order to avoid drug loss during storage time, complex acylglycerols, like hard fats as lipid matrix, can be used because the incorporation of lipophilic drugs is facilitated [289]. However, these hard fats reveal tendency to form supercooled melts instead of solid nanoparticles. Even if they are solidified at room temperature, these particles melt at body temperature. Therefore, these later are not suitable for controlled release applications and could not be used for the purpose of the present work.

An optimal lipid nanoparticle carrier can be produced in a controlled way when a certain fraction of α-form can be created and preserved during the storage time [27]. This can be achieved by preparation of NLC aqueous dispersions. These later systems are characterized by having a built-in trigger mechanism to initiate transformation from α to β-forms and consequently controlled drug release upon application to the skin [103,106].

As reported before, SLN formulations revealed a higher drug loss that NLC formulation during storage time (Figures 5.26 and 5.27). A potential disadvantage of SLN over NLC is the transformation of the lipid matrix from a β'-modification to a more stable one, β, leading to drug expulsion. This triggered release theory described by Müller *et al.* [27] is schematically represented in Figure 5.28.

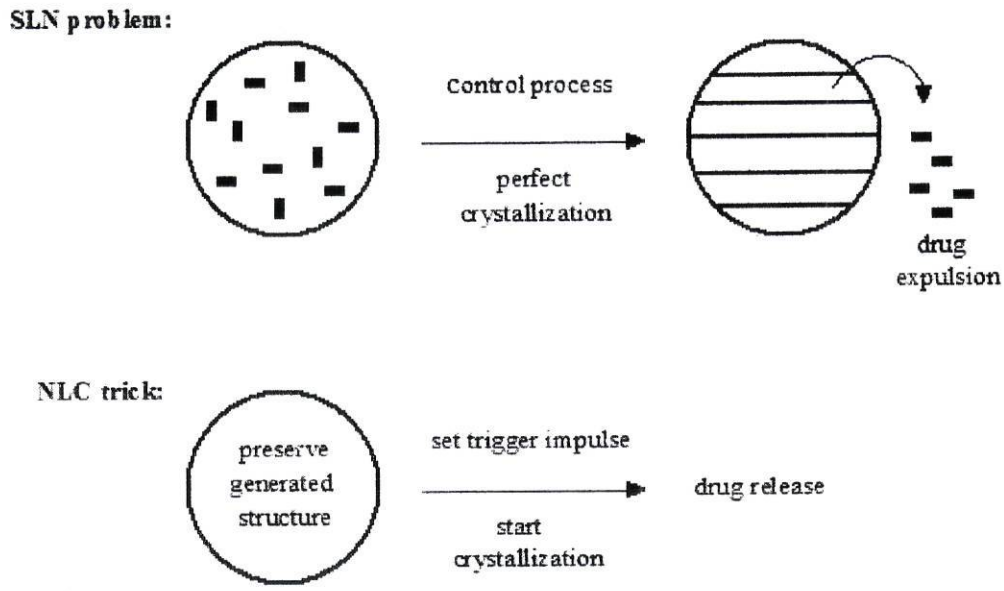

Figure 5.28: Triggered release of active compounds by controlling the transformation from β and β' to β. (Adapted from Müller *et al.* [27]).

In comparison to NLC, in spite of having lower E.E. and loading capacity SLN have a solid lipid matrix and should therefore theoretically be suitable for controlled release [107]. This property becomes important in dermal application, concerning to drugs that are irritating at high concentrations. Furthermore, it provides the possibility to supply an active compound over a period of time and can reduce systemic absorption. Controlled triggered release of drugs is feasible due to polymorphic transitions of the lipids induced by water evaporation from the dosage form after application to the skin. In addition, electrolytes present in the upper skin surface can initiate polymorphic transitions accompanied by drug expulsion due to the formation of a stable polymorph [103].

5.3.2. Particle size

Regarding to hot HPH technique, the parameters influencing the product quality are the power density, i.e. the homogenization pressure, the number of homogenization cycles, the percentage of solid content and the nature and concentration of the emulsifying agent.

Physical stability of SLN and NLC developed formulations was evaluated as a function of lipid concentration, presence of clotrimazole, and as a function of time and temperature of storage. The effect of the packing conditions was minimized and neglected. After production, aqueous dispersions were stored and sealed in siliconized glass vials. Immediate sealing avoids water evaporation from the freshly prepared aqueous dispersions, and siliconization of the vials almost eliminates particle growth [96,98]. By optimizing the storage conditions, the tendency of particle growth for each nanoparticle system can be achieved.

LD data were characterized by the diameter d99% and the mean particle size and PI were investigated by PCS during a period of 90 days.

5.3.2.1. Particle size stability of clotrimazole-free SLN and NLC formulations

It was possible to produce SLN and NLC dispersions having an extremely narrow particle size distribution, similar to emulsions for parenteral nutrition (*Lipofundin*®, *Intralipid*®). Note that commercial fat emulsions possess mean diameters ranging from about 200-400 nm [313].

Figure 5.29 shows that clotrimazole-free SLN and NLC dispersions revealed a narrow particle size distribution measured by LD analysis, which was completely in the nanometer range during 90 days of storage at room temperature. During the same period of time and storage conditions, the PI remained lower than 0.3 (Figure 5.30) for all drug-free formulations.

Figures 5.29 and 5.30 show that despite the increasing lipid content of the formulations, nanoparticles retained their colloidal particle size. Due to the narrow size distribution, their colloidal particle size can be maintained during storage time. If the particle size distribution was inhomogeneous, smaller particles would be able to dissolve and recrystallize on the surface of larger particles leading to an increase in particle size of already larger particles [117]. This phenomenon is based on the Kelvin equation (Chapter IV, section 4.4.1), which describes the increased vapour pressure over small liquid particles with a strong curvature of the surface.

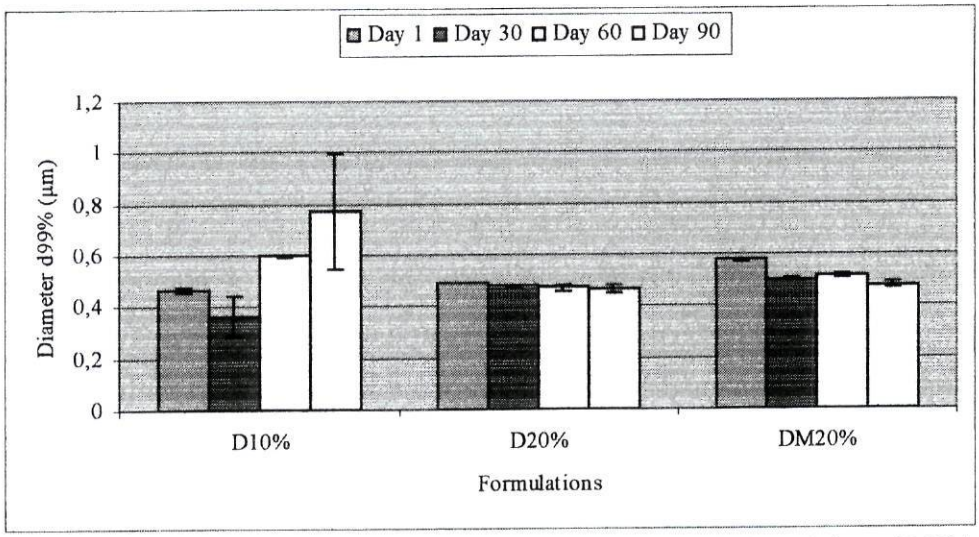

Figure 5.29: Particle size of clotrimazole-free SLN and NLC formulations (D10%, D20% and DM20%) measured by LD (d99%), after 1, 30, 60 and 90 days of storage at room temperature (20°C).

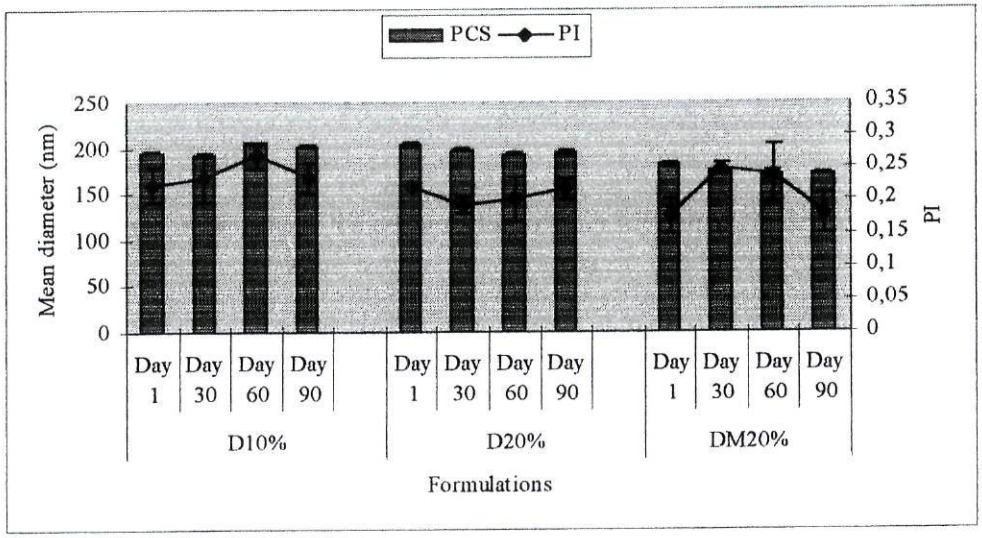

Figure 5.30: Mean particle size and PI of clotrimazole-free SLN and NLC formulations (D10%, D20% and DM20%) measured by PCS, after 1, 30, 60 and 90 days of storage at room temperature (20°C).

5.3.2.2. Particle size stability of clotrimazole-loaded SLN and NLC formulations

Figures 5.31 and 5.32 show the results obtained by LD and PCS analysis of SLN and NLC formulations containing clotrimazole, during a period of 90 days of storage at room temperature. Incorporation of the antifungal agent in the lipid matrix was successful in concentrations of 5% (*m/m*) with respect to the lipid content.

Figure 5.31 shows that 99% of clotrimazole-loaded SLN and NLC remained lower than 750 nm after three months of storage at room temperature. During this period, the particle size of the clotrimazole-loaded samples containing 20% of lipid matrix remained higher than drug-loaded samples containing 10% of lipid matrix.

It can also be observed that D10%C showed a decrease in particle size measured by LD during 3 months of storage at room temperature. This interesting observation might probably be due to the repartitioning effect of *Tyloxapol*® at the surface of the SLN and to the lower content of lipid in comparison to D20%C and DM20%C. One day after production, D20%C sample exhibited the highest particle size probably due to the higher solid lipid content of this formulation.

Figure 5.32 shows that the mean particle size of clotrimazole-loaded SLN and NLC remained between 150 and 250 nm, during 90 days of storage at room temperature. D20%C formulation showed a higher mean particle size (> 200 nm), in comparison to D10%C and DM20%C, during the investigation time.

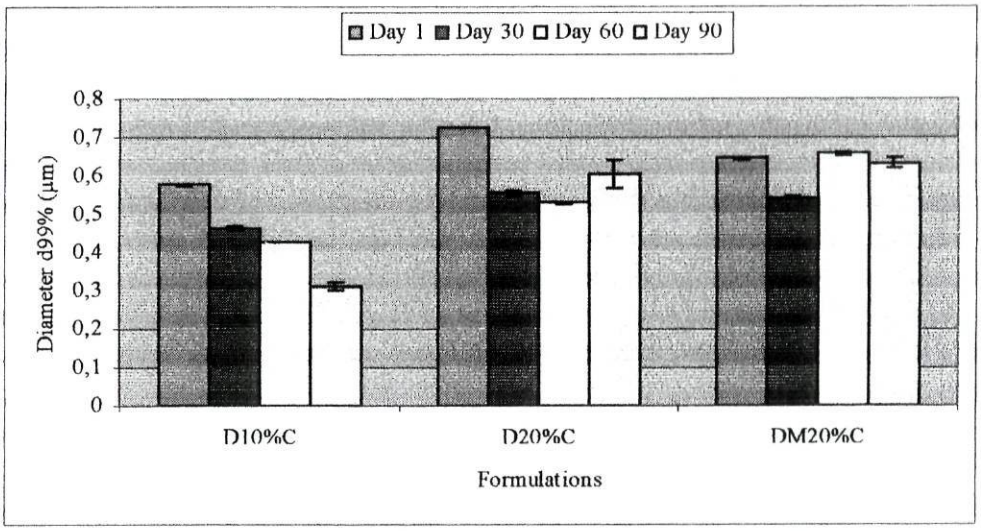

Figure 5.31: Particle size of clotrimazole-loaded SLN and NLC formulations (D10%C, D20%C and DM20%C) measured by LD (d99%), after 1, 30, 60 and 90 days of storage at room temperature (20°C).

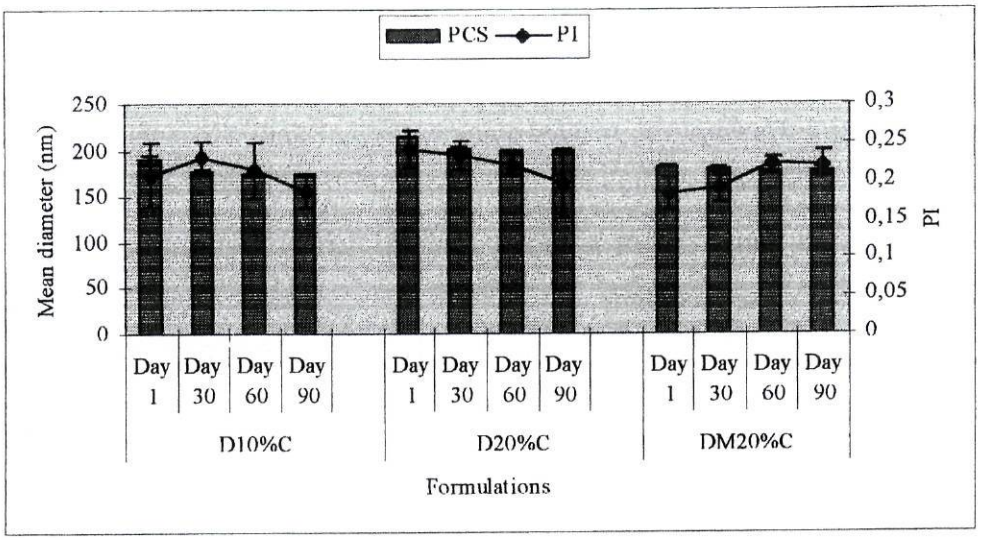

Figure 5.32: Mean particle size and PI of clotrimazole-loaded SLN and NLC formulations (D10%C, D20%C and DM20%C) measured by PCS, after 1, 30, 60 and 90 days of storage at room temperature (20°C).

5.3.2.3. Particle size stability of clotrimazole-free and clotrimazole-loaded SLN and NLC formulations as function of temperature of storage

When judging the suitability of SLN and NLC aqueous dispersion for therapeutic purposes, the long-term stability of these systems needs to be considered. It might be possible that a solid lipid formulation appears highly attractive with regard to toxicological aspects. However, it proves to be physically unstable during storage as aqueous dispersion. In such cases, lipid nanoparticles can be transferred to a dry product by lyophilization [15,20-22] or by spray-drying [21].

Physical integrity of SLN and NLC, i.e. absence or minimization of particle aggregation and quantitative preservation of solid lipid content during storage, has to be confirmed. However, a low extent of particle aggregation which is well below the perception limit has to be regarded as non-critical.

In the present work, storage stability of SLN and NLC aqueous dispersions was assessed by monitoring particle size as a function of time, for 3 months stored at 4°C, 20°C and 40°C.

Figures 5.33 and 5.34 show the results obtained for clotrimazole-free SLN formulation D10% analysed by LD and PCS, respectively.

For all three batches of this formulation, particle size remained below 0.8 μm during 90 days of storage at different temperatures. When stored at 4°C, a slight increase in particle size measured by LD could be observed. At 40°C particle size remained below 0.4 μm during 3 months, probably due to the lower viscosity of the medium in comparison to the samples stored

at 4°C and 20°C. Mean particle size measured by PCS was around 200 nm during the same period of storage. The PI obtained by PCS analysis remained around 0.3 throughout the observed storage time.

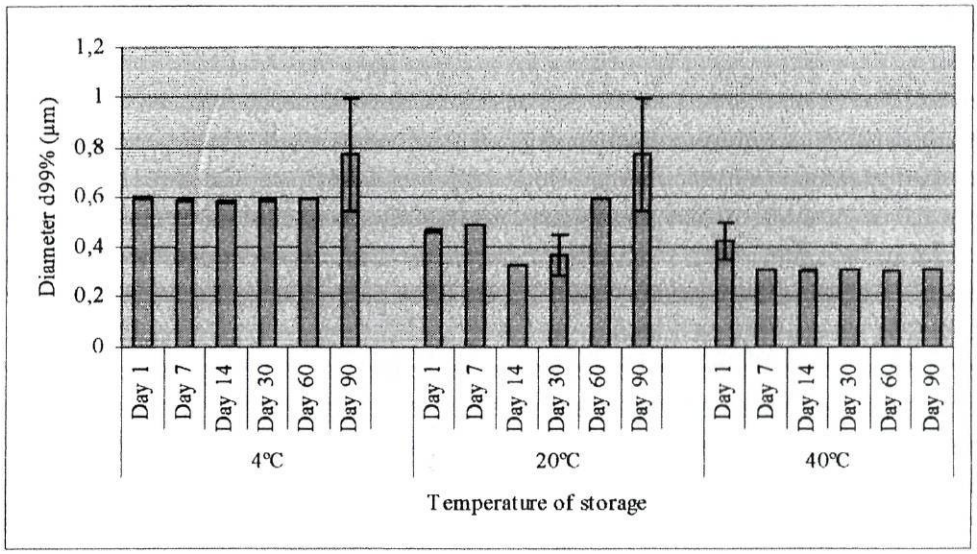

Figure 5.33: Particle size of clotrimazole-free SLN formulation D10% measured by LD (d99%), after 1, 7, 14, 30, 60 and 90 days of storage at 4°C, 20°C and 40°C.

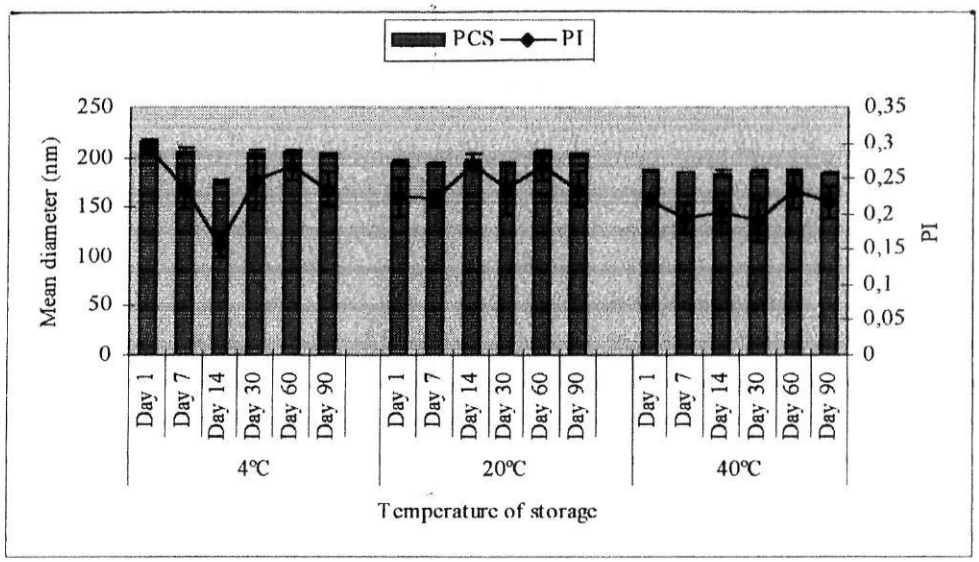

Figure 5.34: Mean particle size and PI of clotrimazole-free SLN formulation D10% measured by PCS, after 1, 7, 14, 30, 60 and 90 days of storage at 4°C, 20°C and 40°C.

Figures 5.35 and 5.36 show the results obtained for clotrimazole-loaded SLN formulation D10%C analysed by LD and PCS, respectively.

The incorporation of clotrimazole did not influence the particle size of the SLN aqueous dispersion when stored at different temperatures.

For all three batches of this formulation particle size remained below 0.7 µm during 90 days of storage at different temperatures. When stored at 4°C, a slight increase in particle size measured by LD could be observed. At 40°C the particle size remained below 0.6 µm during the first week but showed a decrease between 7 and 90 days of storage. Mean particle size measured by PCS was around 200 nm during the same period of storage. The PI obtained by PCS analysis remained around 0.3 throughout the observed storage time.

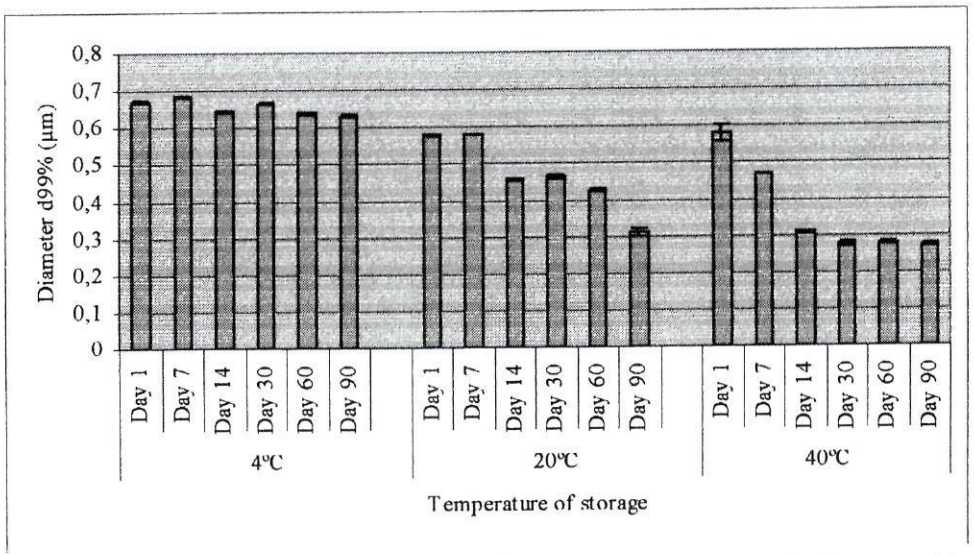

Figure 5.35: Particle size of clotrimazole-loaded SLN formulation D10%C measured by LD (d99%), after 1, 7, 14, 30, 60 and 90 days of storage at 4°C, 20°C and 40°C.

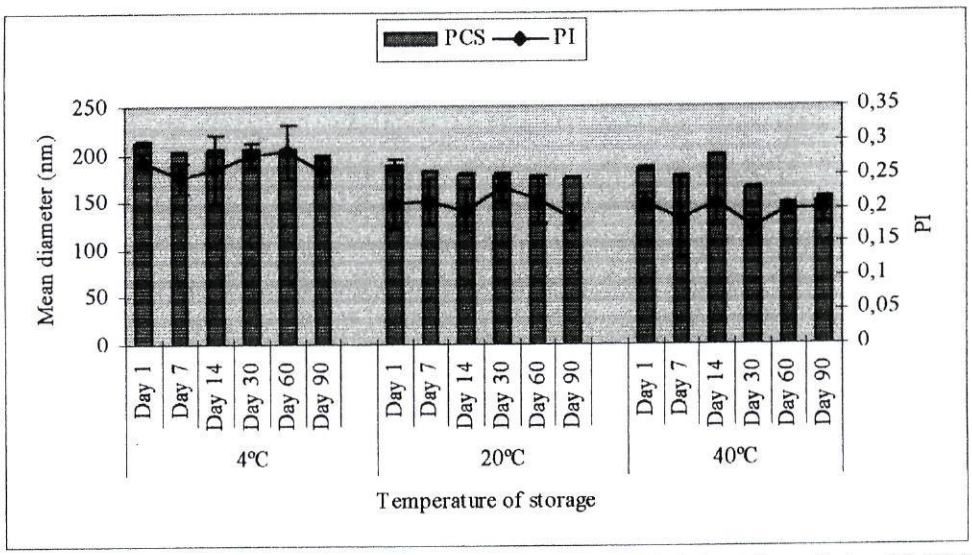

Figure 5.36: Mean particle size and PI of clotrimazole-loaded SLN formulation D10%C measured by PCS, after 1, 7, 14, 30, 60 and 90 days of storage at 4°C, 20°C and 40°C.

Figures 5.37 and 5.38 show the results obtained for clotrimazole-free SLN formulation D20% analysed by LD and PCS, respectively.

When stored at 4°C, samples were not able to be analysed by LD and PCS once they were congealed. Thus, particle size analysis was only performed for batches stored at 20°C and 40°C.

It could be observed that particle size remained below 0.5 µm during storage time and at 40°C from day 7 onwards it remained around 0.3 µm. The PI obtained by PCS analysis remained below 0.25 throughout the observed storage period.

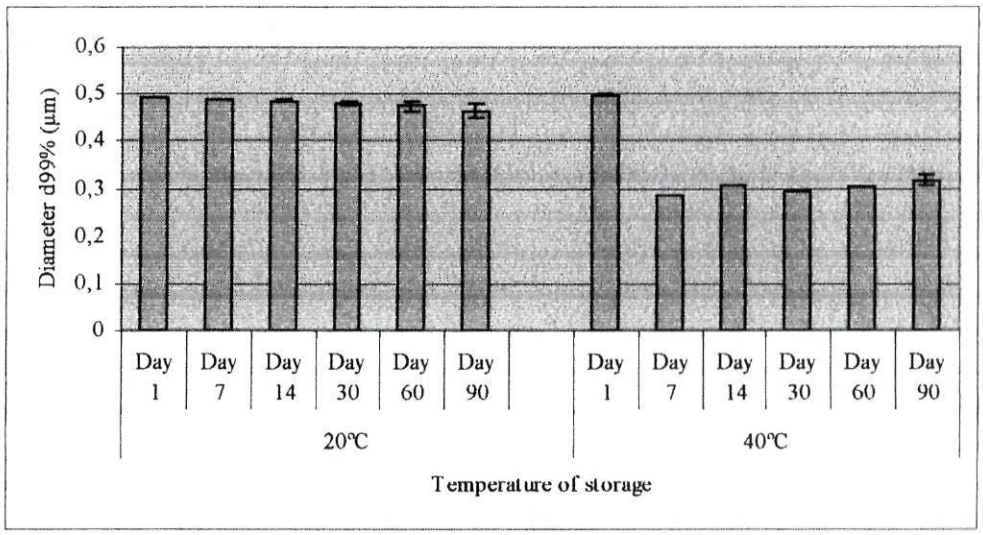

Figure 5.37: Particle size of clotrimazole-free SLN formulation D20% measured by LD (d99%), after 1, 7, 14, 30, 60 and 90 days of storage at 20°C and 40°C.

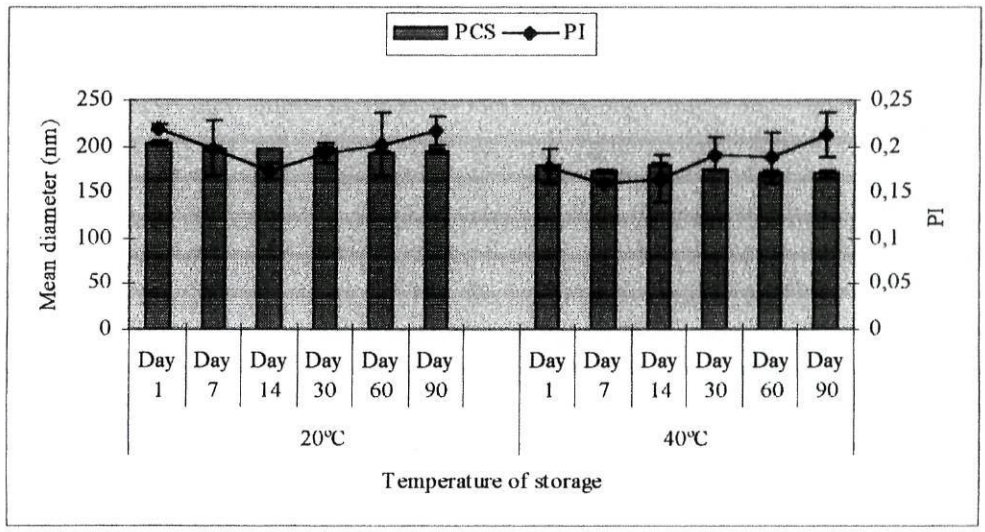

Figure 5.38: Mean particle size and PI of clotrimazole-free SLN formulation D20% measured by PCS, after 1, 7, 14, 30, 60 and 90 days of storage at 20°C and 40°C.

Figures 5.39 and 5.40 show the results obtained for clotrimazole-loaded SLN formulation D20%C analysed by LD and PCS, respectively.

As it can be observed, the presence of clotrimazole did not change significantly the particle size distribution. When stored at 20°C, particle size oscillated between 0.7 and 0.5 μm during the 3 months of storage. When stored at 40°C, a decrease in particle size, probably due to the lower viscosity of the medium, could be observed. For this sample (D20%C), the mean diameter remained approximately at 200 nm and the PI around 0.2.

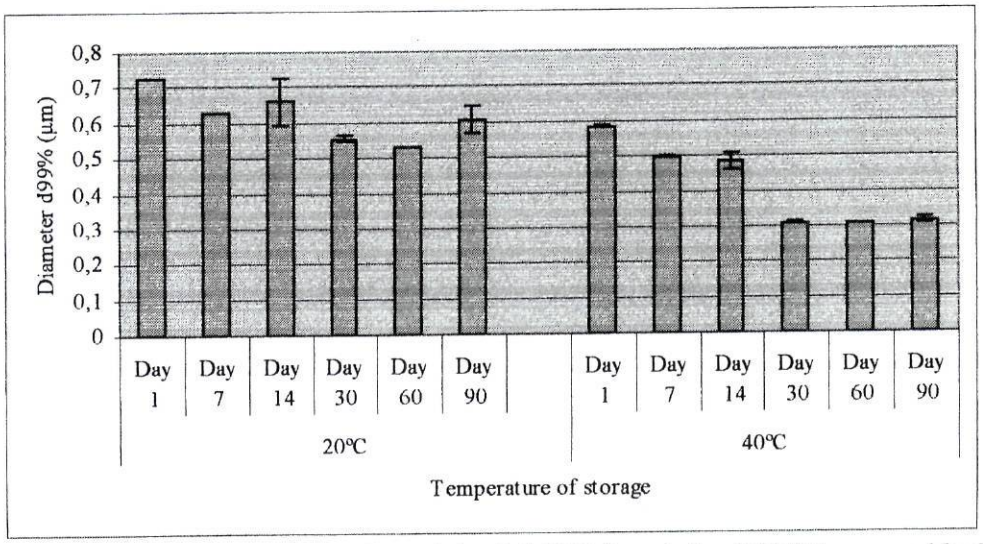

Figure 5.39: Particle size of clotrimazole-loaded SLN formulation D20%C measured by LD (d99%), after 1, 7, 14, 30, 60 and 90 days of storage at 20°C and 40°C.

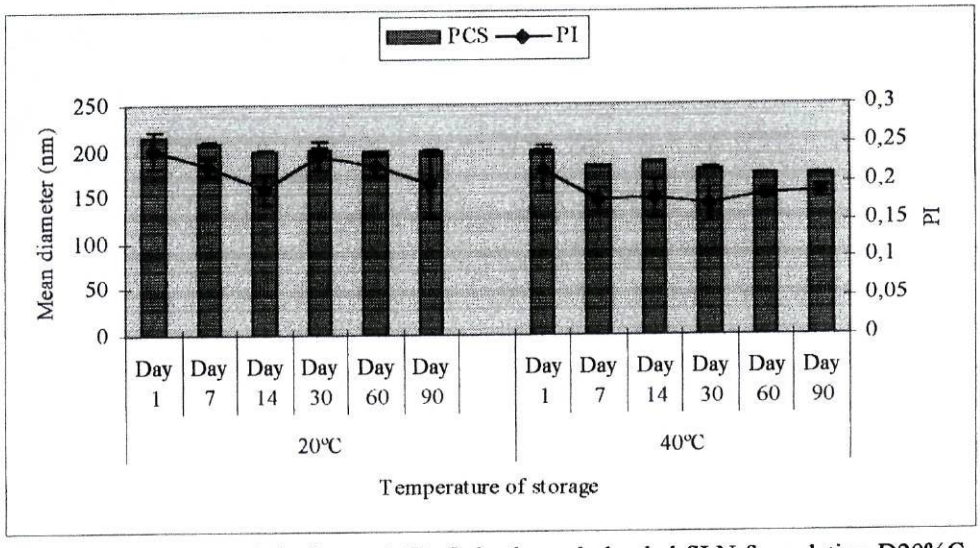

Figure 5.40: Mean particle size and PI of clotrimazole-loaded SLN formulation D20%C measured by PCS, after 1, 7, 14, 30, 60 and 90 days of storage at 20°C and 40°C.

Figures 5.41 and 5.42 show the results obtained for clotrimazole-free NLC formulation DM20% analysed by LD and PCS, respectively.

For all three batches of this formulation particle size measured by LD remained below 0.6 μm during 90 days of storage at different temperatures. Mean particle size measured by PCS was below 190 nm during the same period of storage. At 4°C a slight increase in mean diameter could be observed, although it remained below 190 nm. The PI obtained by PCS analysis was below 0.25 throughout the observed storage time.

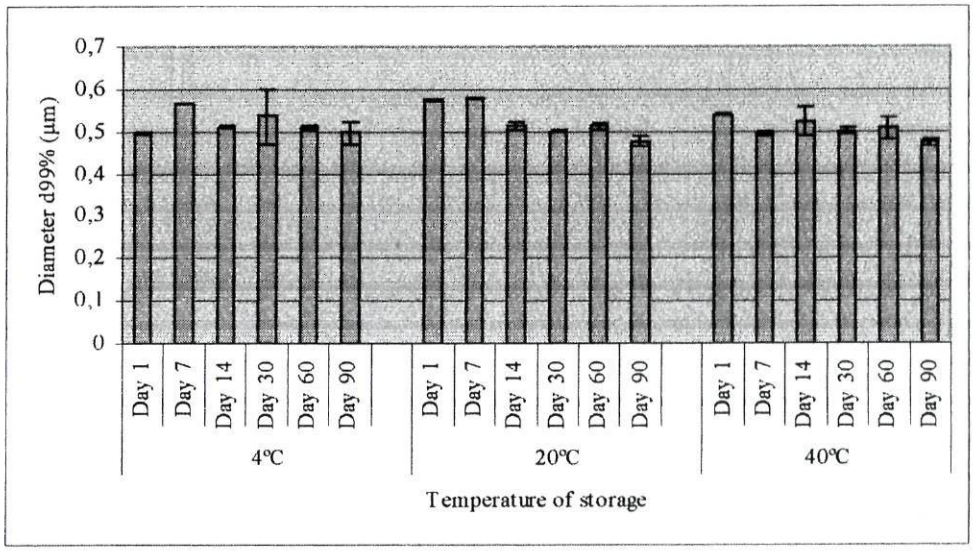

Figure 5.41: Particle size of clotrimazole-free NLC formulation DM20% measured by LD (d99%), after 1, 7, 14, 30, 60 and 90 days of storage at 4°C, 20°C and 40°C.

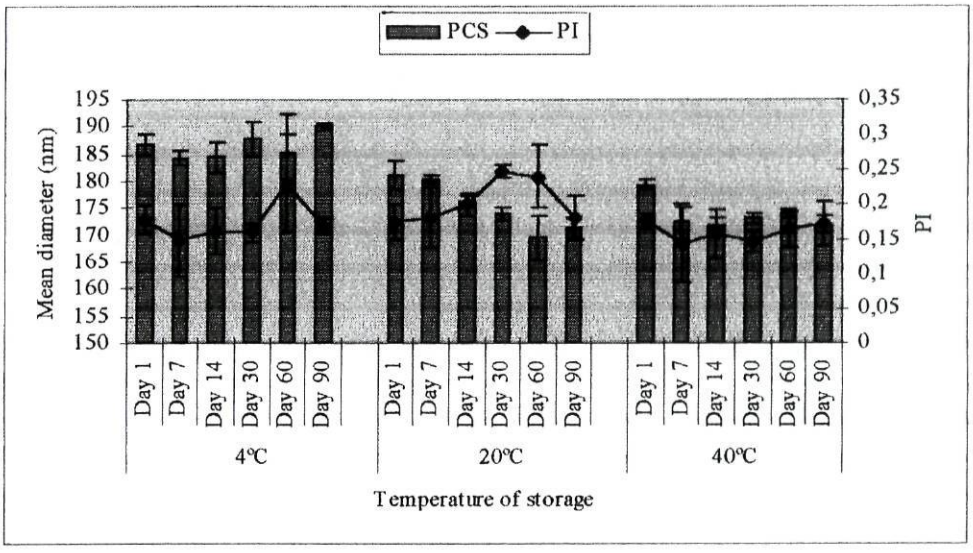

Figure 5.42: Mean particle size and PI of clotrimazole-free NLC formulation DM20% measured by PCS, after 1, 7, 14, 30, 60 and 90 days of storage at 4°C, 20°C and 40°C.

Figures 5.43 and 5.44 show the results obtained for clotrimazole-loaded NLC formulation DM20%C analysed by LD and PCS, respectively.

As expected, the presence of clotrimazole was not responsible for changes in particle size distribution. During 90 days of storage at different temperatures, particle size remained around 0.6 μm. Mean particle size measured by PCS was below 190 nm and the PI obtained by PCS analysis was below 0.25 throughout the observed storage time.

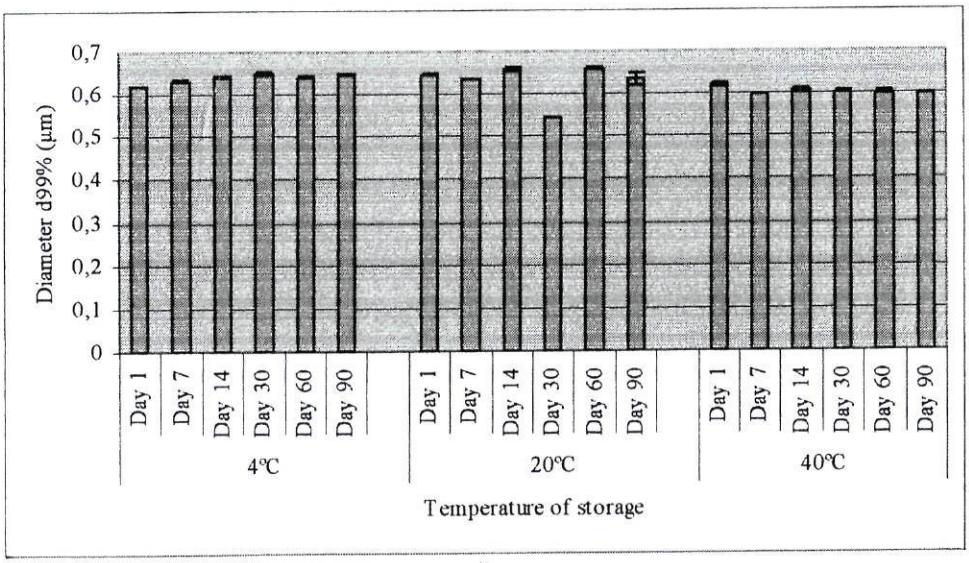

Figure 5.43: Particle size of clotrimazole-loaded NLC formulation DM20%C measured by LD (d99%), after 1, 7, 14, 30, 60 and 90 days of storage at 4°C, 20°C and 40°C.

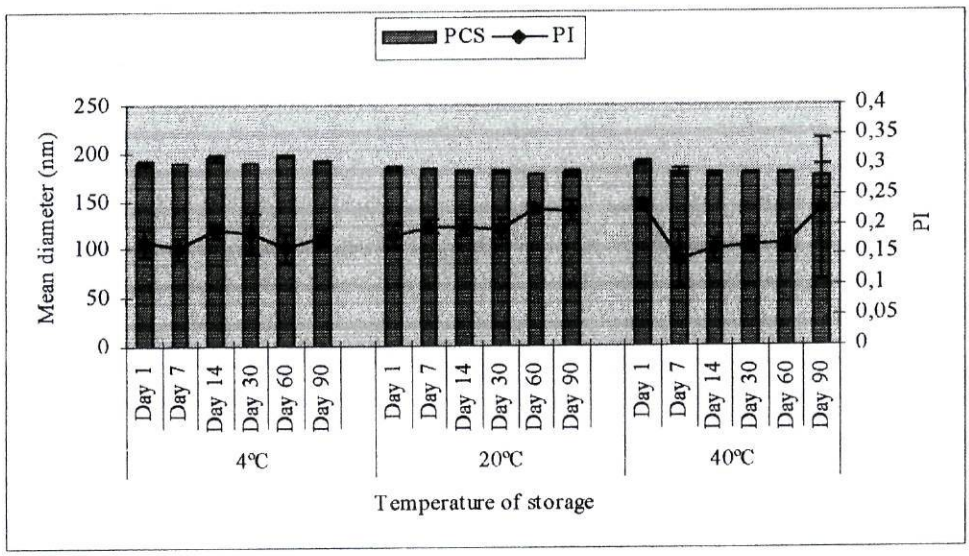

Figure 5.44: Mean particle size and PI of clotrimazole-loaded NLC formulation DM20%C measured by PCS, after 1, 7, 14, 30, 60 and 90 days of storage at 4°C, 20°C and 40°C.

In comparison to oil-free formulations (i.e. SLN formulations), samples containing *Miglyol*®812 (DM20% and DM20%C) showed a lower variation in size distribution during storage time.

5.3.3. Zeta potential

Determination of ζ was carried out in SLN and NLC aqueous dispersions stored at room temperature. Figure 5.45 shows the results after 1, 30 and 90 days of storage. All samples showed a pH between 4 and 5, during 3 months.

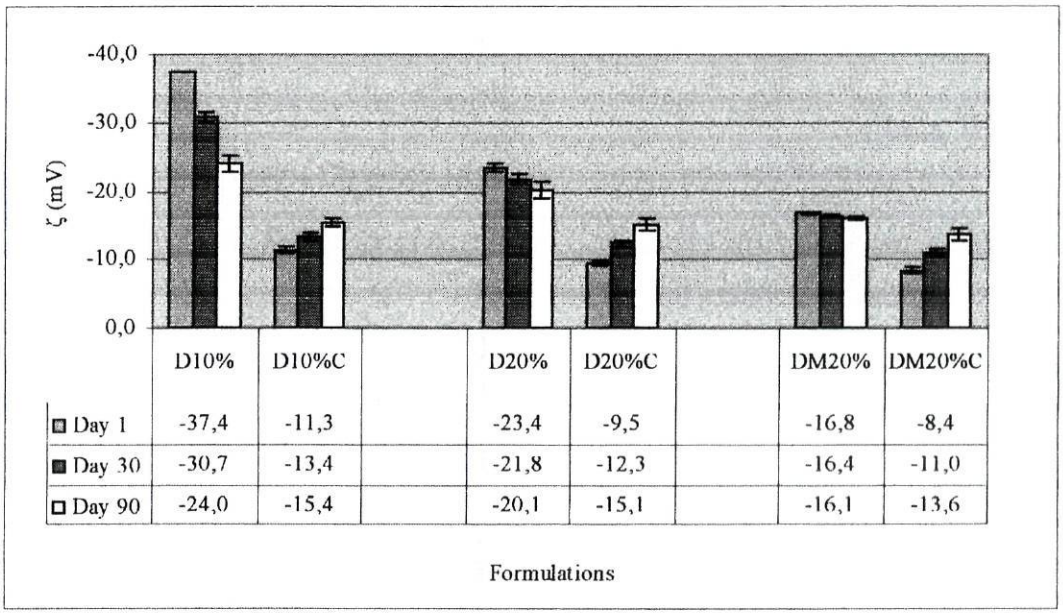

	D10%	D10%C	D20%	D20%C	DM20%	DM20%C
Day 1	-37,4	-11,3	-23,4	-9,5	-16,8	-8,4
Day 30	-30,7	-13,4	-21,8	-12,3	-16,4	-11,0
Day 90	-24,0	-15,4	-20,1	-15,1	-16,1	-13,6

Figure 5.45: Zeta potential of clotrimazole-free and clotrimazole-loaded SLN and NLC formulations, after 1, 30 and 90 days of storage at room temperature (20°C).

On day 1 of storage at room temperature, the ζ of drug-free samples was between -17 mV and -37 mV, while the ζ of drug-loaded samples was between -8 mV and -11 mV.

After 30 days of storage in the same conditions, the ζ of drug-free samples was between -16 mV and -31 mV, while the ζ of drug-loaded samples was between -12 mV and -13 mV.

After 90 days, the ζ of drug-free samples was between -16 mV and -24 mV, while the ζ of drug-loaded samples was between -14 mV and -15 mV.

It could be observed that samples with 10% of lipid matrix showed higher ζ than samples containing 20% of lipid. In addition, samples containing *Miglyol*®812 showed the lowest ζ value. On day 1 of storage, clotrimazole-loaded formulations showed lower ζ than drug-free formulations. On the contrary, after 3 months of storage, the ζ of the samples without drug was lower than clotrimazole-loaded systems.

A low ζ could be expected for all tested formulations, once these lipid particles are made of a non-ionic lipid and a non-ionic emulsifying agent. The ζ must be sufficiently high (in absolute value) for electrostatic stabilization of the nanoparticle dispersions [314]. In general, a ζ of

approximately -30 mV is considered as the lowest edge of the ζ range required for adequate stabilization [315].

Although all tested samples exhibited a ζ lower than -25 mV after 90 days of storage at room temperature, these samples remained physically stable during this period of time.

From these results it can be concluded that incorporated clotrimazole can take part in the improvement of long-term stability. Note that all produced clotrimazole-containing SLN and NLC aqueous dispersions presented higher ζ than clotrimazole-free aqueous dispersions.

5.3.4. DSC studies

Polymorphic transformations may occur during preparation of lipid drug delivery systems and during the subsequent storage time [53,83,226].

During solidification of the melt or the solution, the triacylglycerol can crystallize in different polymorphic forms (Chapter II), depending on the composition of the lipid and the cooling rate. Nanoparticles made from mixed triacylglycerols are characterized by more imperfections in the crystal lattice, while the ones made from monoacid triacylglycerols have a higher degree of crystalline order and are connected to lower loading capacities [9,53]. Concerning cooling rate, it is known that due to a fast solidification during the preparation of lipid nanoparticles the instable α modification is formed. During a slow process, the lipid molecules can arrange in the thermodynamically most stable β modification [294].

Thermodynamic stability and lipid packing density increase, while drug incorporation rates decrease in the following order: supercooled melt, α modification, β' modification and β modification [6].

Supercooled melts are not lipid suspensions, rather systems similar to O/W emulsions [7]. They describe a phenomenon that lipid crystallization may not occur although the sample is stored at temperature below the melting point of the lipid. These systems are not unusual in SLN preparation [316]. Therefore, special attention must be paid because the potential advantages of SLN over nanoemulsions are linked to the solid state of the lipid.

The main reason for the formation of supercooled melts is the size dependence of crystallization processes. Crystallization requires a critical number of crystallization nuclei to start [317]. This critical number of molecules is less likely to be formed in small droplets and therefore, the tendency of the formation of supercooled melts increase with decreasing droplet size. The range of supercooling (temperature difference between the melting and crystallization

points) can reach 30 to 40°C in lipid dispersions [35]. In addition to size, crystallization can be affected by surfactants, incorporated drugs and other factors.

Lipid nanoparticles, such as SLN and NLC, present a solid matrix and, therefore, are able to entrap drug molecules. On the contrary, supercooled melts immobilize more difficulty the active compound. Therefore it is necessary to evaluate the solid state of the lipid by DSC and by x-ray diffraction.

The phenomenon of crystallization may cause differences in solubility and melting point of active compounds and excipients, and especially the conversion of one polymorph to another may change the physical properties of the incorporated drug [83].

5.3.4.1. Maintenance of crystalline status at room temperature

It is not sufficient to describe the physical state of the lipid as crystallized or non-crystallized, because the crystallized lipid may be present in several modifications of the crystal lattice. In general, lipid molecules have higher mobility in thermodynamically unstable configurations, which are characterized by a lower density and a higher capacity for incorporation of active compounds [6,7].

The advantage of higher incorporation rates in unstable modifications is paid off by an increase mobility of the drug [7]. During storage, rearrangements of the crystal lattice might occur in favour of thermodynamically stable configurations and this is often associated to expulsion of the drug molecules. The performance of the system will be determined to a large extent by the lipid modification, because this parameter triggers drug incorporation and drug release. Aspects of reproducibility and drug safety demand the assurance of systems with defined and reliable characteristics. Therefore, DSC investigations during storage time are an important tool, in order to evaluate the performance of SLN and NLC as a function of time.

Figures 5.46 and 5.47 show the DSC curves of clotrimazole-free and clotrimazole-loaded, respectively, of SLN formulations containing 10% of lipid matrix, measured after 7 and 90 days of storage at room temperature.

It could be observed that during storage the crystallinity of lipid matrix increased, which is indicated by a higher melting point. On day 7 the clotrimazole-free and clotrimazole-loaded samples showed a melting point at 60°C while on day 90 the lipid matrix melted at 61°C. The melting enthalpy remained almost the same.

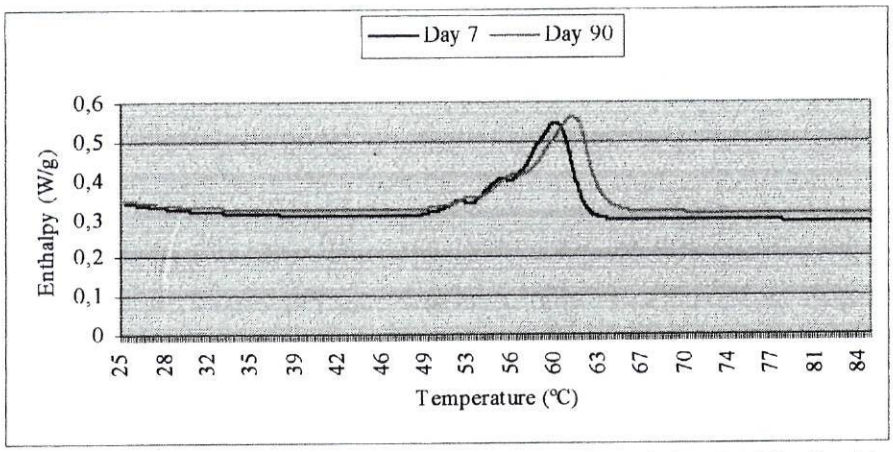

Figure 5.46: DSC curves of clotrimazole-free SLN formulation D10% after 7 and 90 days of storage at room temperature (20°C).

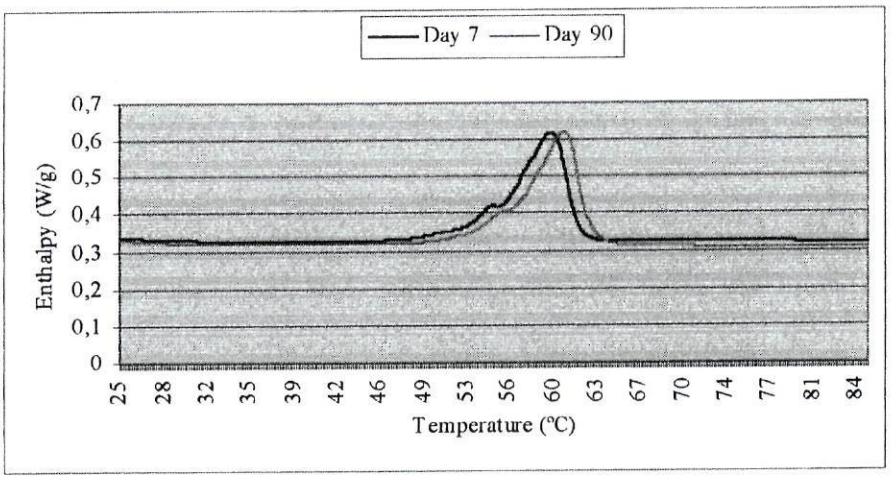

Figure 5.47: DSC curves of clotrimazole-loaded SLN formulation D10%C after 7 and 90 days of storage at room temperature (20°C).

Figures 5.48 and 5.49 show the DSC curves of clotrimazole-free and clotrimazole-loaded, respectively, of SLN formulations containing 20% of lipid matrix, measured after 7 and 90 days of storage at room temperature.

For these formulations an increase in lipid crystallinity during storage time could also be observed. On day 7 the clotrimazole-free and clotrimazole-loaded samples showed a melting point at 60°C while on day 90 the lipid matrix melted at 62°C. The melting enthalpy remained almost the same for clotrimazole-loaded sample, while it decreased for clotrimazole-free sample.

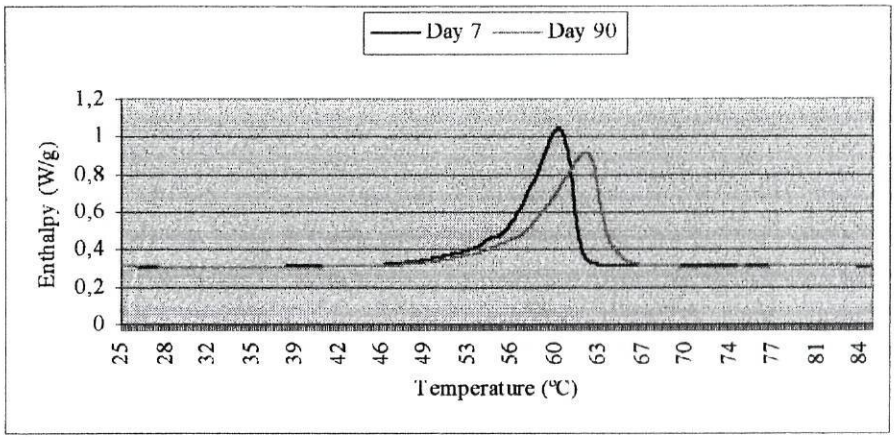

Figure 5.48: DSC curves of clotrimazole-free SLN formulation D20% after 7 and 90 days of storage at room temperature (20°C).

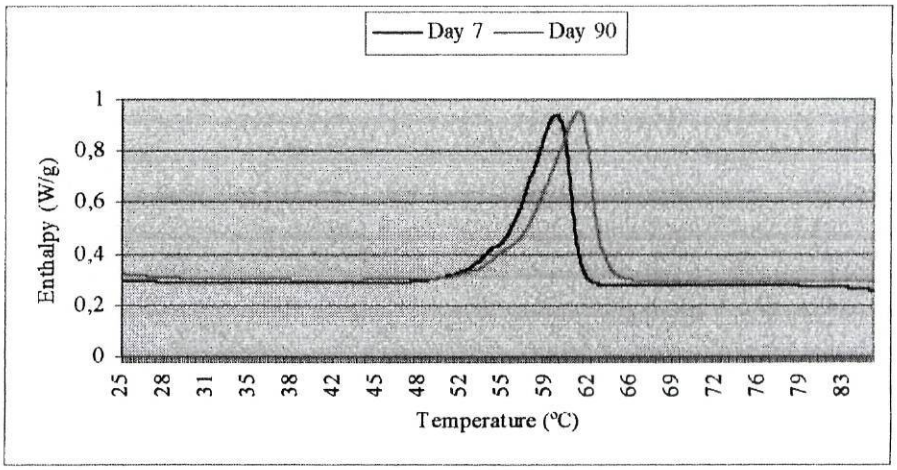

Figure 5.49: DSC curves of clotrimazole-loaded SLN formulation D20%C after 7 and 90 days of storage at room temperature (20°C).

Figures 5.50 and 5.51 show the DSC curves of clotrimazole-free and clotrimazole-loaded, respectively, of NLC formulations containing 20% of lipid matrix, measured after 7 and 90 days of storage at room temperature.

For both drug-free and drug-loaded NLC formulations the melting point increased from 58°C to 61°C upon 90 days of storage at room temperature. Similarly to the clotrimazole-loaded SLN formulations, clotrimazole-loaded NLC formulations also evidenced an increase in lipid crystallinity during storage time. However, this increase was higher than the registered for SLN formulations.

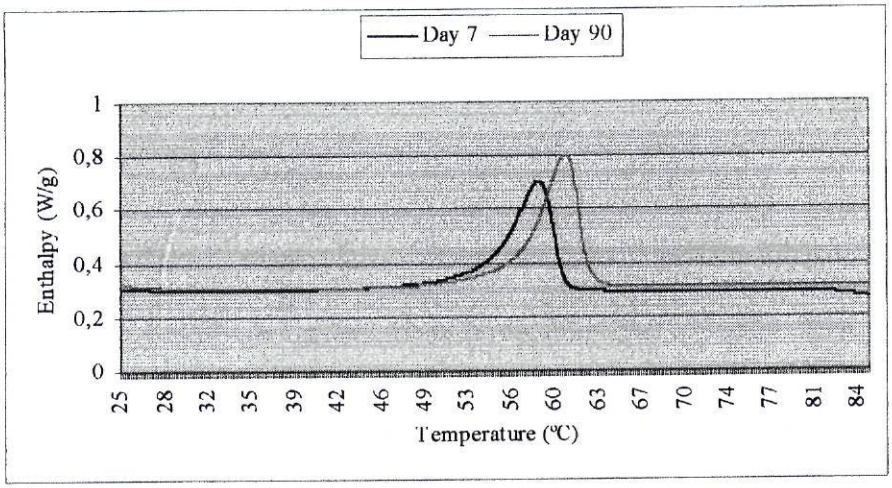

Figure 5.50: DSC curves of clotrimazole-free NLC formulation DM20% after 7 and 90 days of storage at room temperature (20°C).

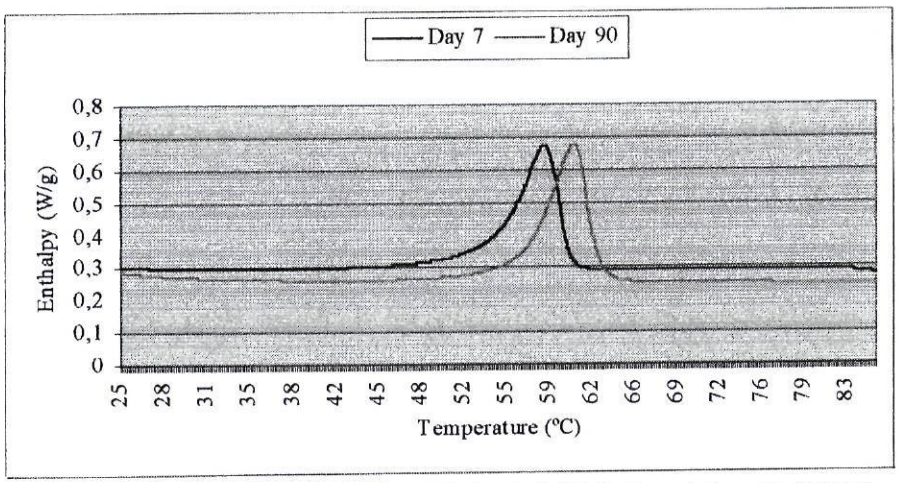

Figure 5.51: DSC curves of clotrimazole-loaded NLC formulation DM20%C after 7 and 90 days of storage at room temperature (20°C).

To sum up, for all studied samples, either clotrimazole-free or clotrimazole-loaded, it could be observed that crystallinity of the solid matrix increased during storage time. Tables XVII and XVIII show the DSC results of clotrimazole-free and clotrimazole-loaded SLN and NLC aqueous dispersions, respectively, as a function of storage time at room temperature.

Table XVII: DSC results of clotrimazole-free SLN and NLC aqueous dispersions, as a function of storage time at room temperature (20°C).

Formulation	Days of storage	Melting point (°C)	Onset (°C)	Integral (mJ)	Enthalpy (J/g)	RI (%)
D10%	7	59.33	55.12	479.25	13.51	69.8
	90	60.27	55.53	494.14	13.10	67.7
D20%	7	59.46	55.53	330.87	33.67	87.0
	90	60.69	55.74	362.64	30.70	79.4
DM20%	7	58.04	54.22	623.07	17.88	46.2
	90	59.83	56.54	665.00	16.74	43.3

Table XVIII: DSC results of clotrimazole-loaded SLN and NLC aqueous dispersions, as a function of storage time at room temperature (20°C).

Formulation	Days of storage	Melting point (°C)	Onset (°C)	Integral (mJ)	Enthalpy (J/g)	RI (%)
D10%C	7	58.95	54.65	411.36	15.86	81.2
	90	59.70	55.42	372.97	17.35	89.7
D20%C	7	59.07	54.97	339.08	32.85	84.9
	90	60.19	55.94	327.94	33.95	87.8
DM20%C	7	58.12	54.57	705.54	15.79	40.8
	90	60.21	56.53	576.80	19.32	49.9

The obtained results indicate that drug can be expelled from the lipid matrix during storage. Therefore, crystallinity of the lipid matrix is a parameter determining drug incorporation and it is also responsible for the drug release profile. As reported before, triacylglycerols are known to crystallize mainly in three polymorphic forms, which transform monotrophically from α to β via β' with increase of thermodynamic stability and lipid packing density and decrease of drug incorporation [244].

5.3.4.2. Maintenance of crystalline status at different temperatures

Figures 5.52 and 5.53 show the DSC curves of clotrimazole-free and clotrimazole-loaded SLN formulations containing 10% of lipid matrix, respectively, obtained after 90 days of storage at 4°C, 20°C and 40°C.

Lipid crystallinity remained practically as the same at the three different temperatures of storage. All clotrimazole-free and clotrimazole-loaded batches evidenced a thermal event between 60°C and 61°C, corresponding to melting of the lipid.

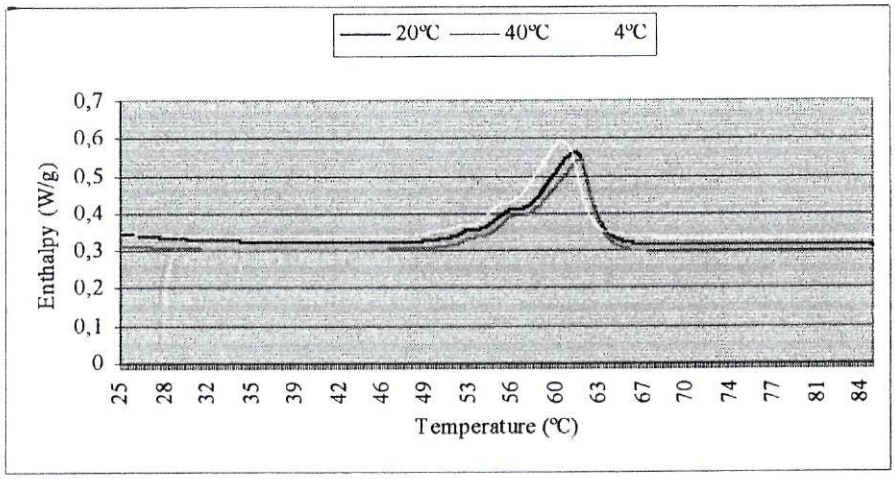

Figure 5.52: DSC curves of clotrimazole-free SLN formulation D10% after 90 days of storage at 4°C, 20°C and 40°C.

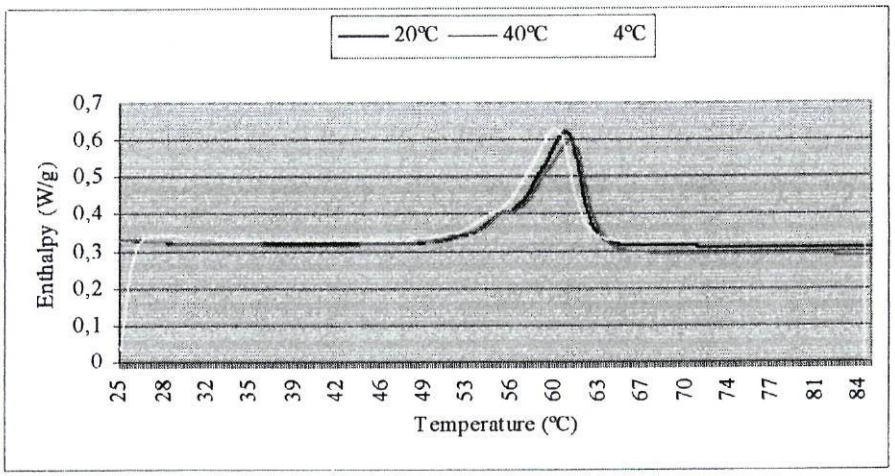

Figure 5.53: DSC curves of clotrimazole-loaded SLN formulation D10%C after 90 days of storage at 4°C, 20°C and 40°C.

Figures 5.54 and 5.55 show the DSC curves of clotrimazole-free and clotrimazole-loaded SLN formulations containing 20% of lipid matrix, respectively, obtained after 90 days of storage at 4°C, 20°C and 40°C.

For all these samples, it could also be stated that lipid crystallinity remained practically constant at the three different temperatures of storage. All clotrimazole-free and clotrimazole-loaded batches revealed a thermal event between 60°C and 62°C.

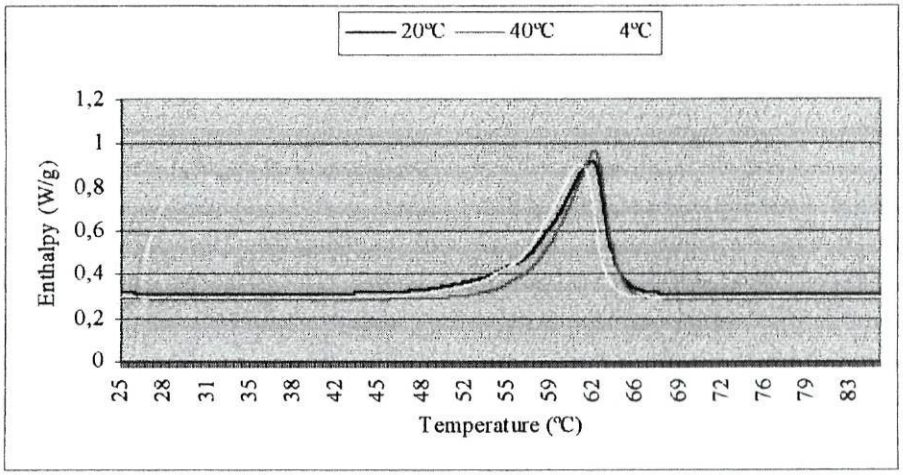

Figure 5.54: DSC curves of clotrimazole-free SLN formulation D20% after 90 days of storage at 4°C, 20°C and 40°C.

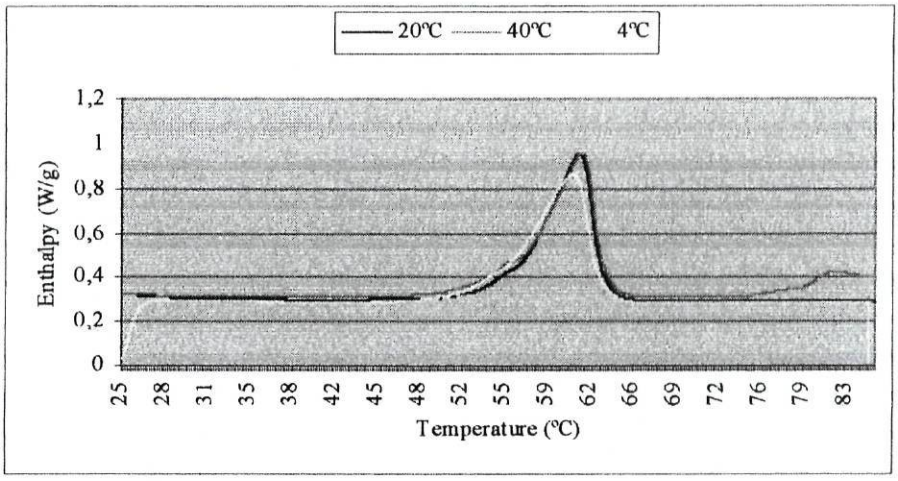

Figure 5.55: DSC curves of clotrimazole-loaded SLN formulation D20%C after 90 days of storage at 4°C, 20°C and 40°C.

Figures 5.56 and 5.57 show the DSC curves of clotrimazole-free and clotrimazole-loaded NLC formulations containing 20% of lipid matrix, respectively, obtained after 90 days of storage at 4°C, 20°C and 40°C.

For NLC formulations, thermal behaviour showed significant differences between samples stored at room temperature and samples stored at 4°C and 40°C. For both clotrimazole-free and clotrimazole-loaded formulations stored at 20°C, the matrix showed the highest crystallinity with a melting point at 61°C. When stored at 4°C and 40°C the melting point decreased to 58°C. At 40°C the observed melt enthalpy was lower than at 4°C.

These results may be due to the presence of the liquid oil inside the solid matrix, showing that NLC remain in a more unstable polymorph during storage, which can be associated to a higher drug payload in comparison to SLN prepared with the same lipid content.

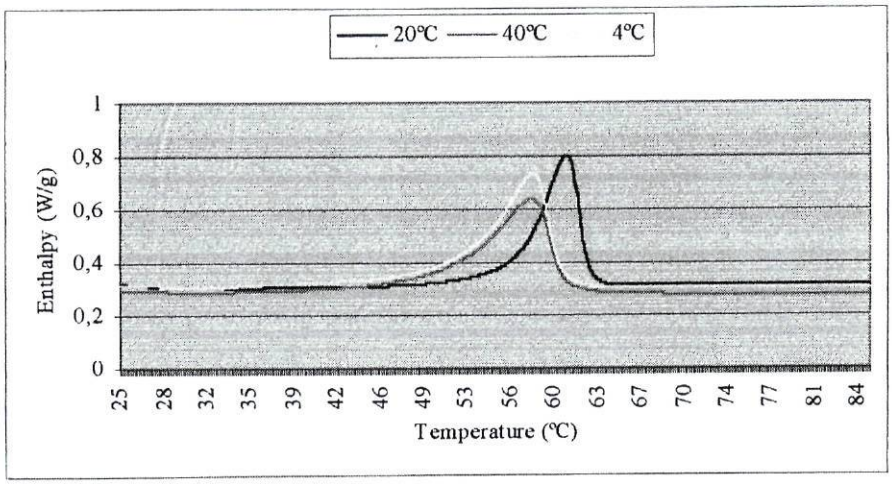

Figure 5.56: DSC curves of clotrimazole-free NLC formulation DM20% after 90 days of storage at 4°C, 20°C and 40°C.

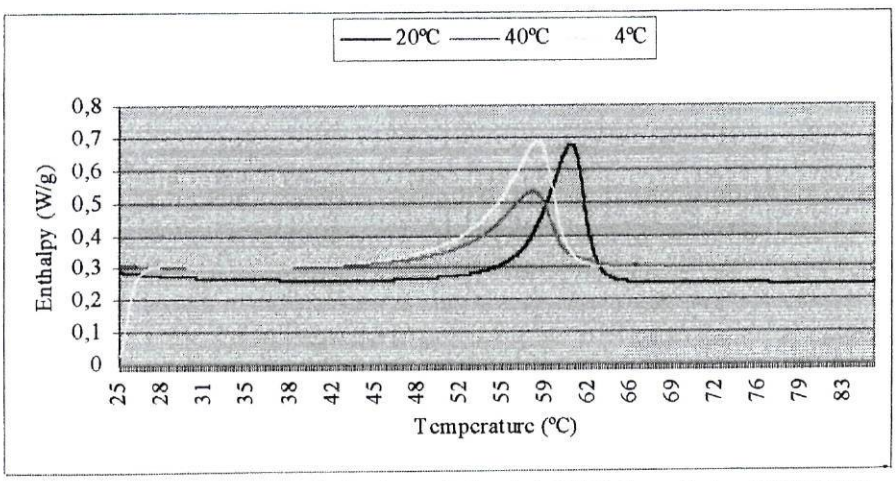

Figure 5.57: DSC curves of clotrimazole-loaded NLC formulation DM20%C after 90 days of storage at 4°C, 20°C and 40°C.

To summarise, for all studied samples, either clotrimazole-free or clotrimazole-loaded, it could be observed that crystallinity of the solid matrix did not change significantly when samples were stored at different temperatures, except for DM20% when stored at 4°C and 40°C. Tables XIX and XX show the DSC results of clotrimazole-free and clotrimazole-loaded SLN and NLC aqueous dispersions, respectively, as a function of storage temperature, obtained after 90 days of storage.

Table XIX: DSC results of clotrimazole-free SLN and NLC aqueous dispersions as a function of storage temperature, obtained after 90 days of storage.

Formulation	Temperature of storage (°C)	Melting point (°C)	Onset (°C)	Integral (mJ)	Enthalpy (J/g)	RI (%)
D10%	4	59.21	55.03	499.33	12.96	67.0
	20	60.27	55.53	494.14	13.10	67.7
	40	60.70	56.32	503.11	12.86	66.5
D20%	4	60.14	55.36	330.19	33.72	87.2
	20	60.69	55.74	320.95	34.70	89.7
	40	61.03	57.07	326.36	34.14	88.2
DM20%	4	57.45	52.29	594.67	18.74	48.4
	20	59.83	56.54	418.12	28.09	67,4
	40	58.27	56.78	660.49	16.85	43.6

Table XX: DSC results of clotrimazole-loaded SLN and NLC aqueous dispersions as a function of storage temperature, obtained after 90 days of storage.

Formulation	Temperature of storage (°C)	Melting point (°C)	Onset (°C)	Integral (mJ)	Enthalpy (J/g)	RI (%)
D10%C	4	59.22	54.73	374.61	17.28	89.3
	20	59.70	55.42	372.97	17.35	89.7
	40	60.10	55.72	368.84	17.55	90.7
D20%C	4	60.11	54.51	337.90	32.96	85.2
	20	60.19	55.94	327.94	33.95	87.8
	40	60.36	55.92	338.30	32.92	85.1
DM20%C	4	57.83	52.72	603.48	18.46	47.7
	20	60.21	56.53	400.43	27.81	71.9
	40	57.02	52.24	672.50	16.57	42.8

5.4. Clotrimazole release profiles of developed SLN and NLC formulations

Drug release profiles of clotrimazole from the developed SLN and NLC formulations were determined using static Franz glass diffusion cells. The receptor medium consisted on a solution of 100 mM acetate buffer, pH 6.0 with 35% (*V/V*) of dioxane. Samples were taken after 1, 2, 4, 6, 8, 10 and 24 h.

Figure 5.58 shows the release profiles of clotrimazole from three different SLN and NLC formulations containing 5% of drug, with regard to the lipid matrix.

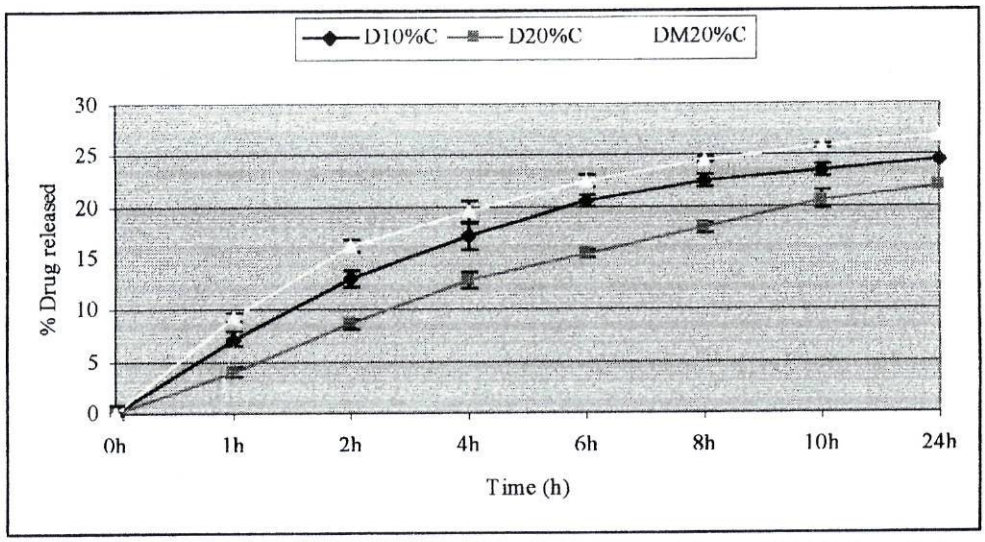

Figure 5.58: *In vitro* release profiles of clotrimazole from SLN and NLC formulations containing 5% of drug, with regard to the lipid matrix.

Clotrimazole is clearly more easily released from the NLC formulation (DM20%C). Regarding the SLN formulations – D10%C and D20%C –, it can be stated that after 1 hour the percentage of drug released from D10%C formulation (7% *m/m*) was almost doubled in comparison to D20%C (4% *m/m*). After the same period, the percentage of drug released from the NLC formulation was almost 10% (*m/m*).

As it was referred before, in NLC formulations lipid nanoparticles have a liquid core (*Miglyol*®812) and clotrimazole is incorporated in the oil less tightly in comparison to the solid lipid matrix of SLN formulations. In these later, drug molecules are incorporated into the crystalline matrix and their diffusional mobility is decreased.

It was also observed that the release rate of clotrimazole also depends on the E.E. of the systems. In fact, clotrimazole was faster released by the D10%C formulation, which showed the lowest E.E. (approximately 64%).

DSC measurements and x-ray diffraction studies demonstrated that the drug was present in the form of a solid solution in SLN formulations or dissolved in the oil core in NLC formulations. The existence of pure drug crystals inside the lipid nanoparticles could not be detected. Drug crystals in the water phase of the aqueous dispersions, a reason for fast release, could also be excluded. A possible explanation for the observed faster clotrimazole release from D10%C in comparison to D20%C is the enrichment of drug in the outer shell of the nanoparticle (Figure 2.8, Chapter II).

As it was referred in Chapter II, SLN formulations may present different drug incorporation and drug release mechanism models, such as the core-shell model with drug-enriched shell and the core-shell model with drug-enriched core [6]. The drug-enriched shell model is formed

during the production process when the drug in the melted lipid is well below its saturation solubility. During the cooling process after hot HPH, the lipid solidifies and the drug re-partitions into the shell of the particles. A drug-enriched core is formed when the drug in the melted lipid is close to its saturation solubility in the lipid. The cooling process leads to supersaturation of the drug and subsequently to drug crystallization prior to lipid crystallization [6].

In the present study, the SLN formulation D10%C corresponds to the drug-enriched shell model, while the SLN formulation D20%C corresponds to the drug-enriched core model. For SLN formulations corresponding to the drug-enriched shell model, burst release can be observed, whereas sustained release can be obtained by choosing a suitable formulation which forms drug-enriched core [6].

Generally, diffusion through the carrier is the main mechanism of controlled release as described by Fick's law of diffusion [27]. However, drug diffusion coefficient cannot be considered constant, but it is dependent upon drug concentration. Due to a large drug loading, the degree of diffusion can be decreased. There are too many molecules trying to diffuse and they limit their own permeation (hindering effects). Also, the previously described incorporation models for SLN (drug-enriched core or shell) underline these findings.

Drug loading is very important with regard to release characteristics [6]. Generally, the increase of drug loading leads to an acceleration of the drug release. However, in particular cases, increasing the drug loading may slow down the release, which can be explained by possible drug crystallization inside the nanoparticles, but in this particular investigation this phenomenon was not observed.

In the present work, it has been found that SLN and NLC are suitable systems for controlling the release of clotrimazole. The release profiles are determined by drug characteristics and the properties of the lipid carriers, i.e. particle size, loading capacity, structure of the lipid matrix and obviously the drug localization inside this matrix. Dominant factors for the shape of the profiles are the production parameters, such as the concentration of the emulsifying agent, the temperature and the nature of the lipid matrix [6].

Obtained profiles (Figure 5.58) could be explained by partitioning effects of the drug between the melted lipid phase and the aqueous surfactant solution during particle production, i.e. phase separation effect [11].

This phase separation effect is schematically represented in Figure 5.59. During hot HPH technique, drug moves from the liquid oil phase (melted lipid) to the aqueous phase. The amount of drug partitioning to the water phase will increase with the increase of drug solubility in this

phase, which happens when both temperature and surfactant concentration of the aqueous phase increase. The higher the temperature and the surfactant concentration, the greater is the saturation solubility of the drug in the water phase. During the cooling step of the produced O/W nanoemulsion solubility of the drug in the water phase decreases continuously with decreasing temperature of the water phase, which means a repartitioning of the drug into the lipid phase. When reaching the recrystallization temperature of the lipid, a solid lipid core starts forming including the drug, which is present at this temperature in the lipid phase. Reducing the temperature of the dispersion further increases the pressure on the drug because of its reduced solubility in water to further repartition into the lipid phase. The already crystallized core is not accessible anymore for the drug. As a consequence, drug concentrates in the still liquid outer shell of the SLN and/or on the surface of the particles.

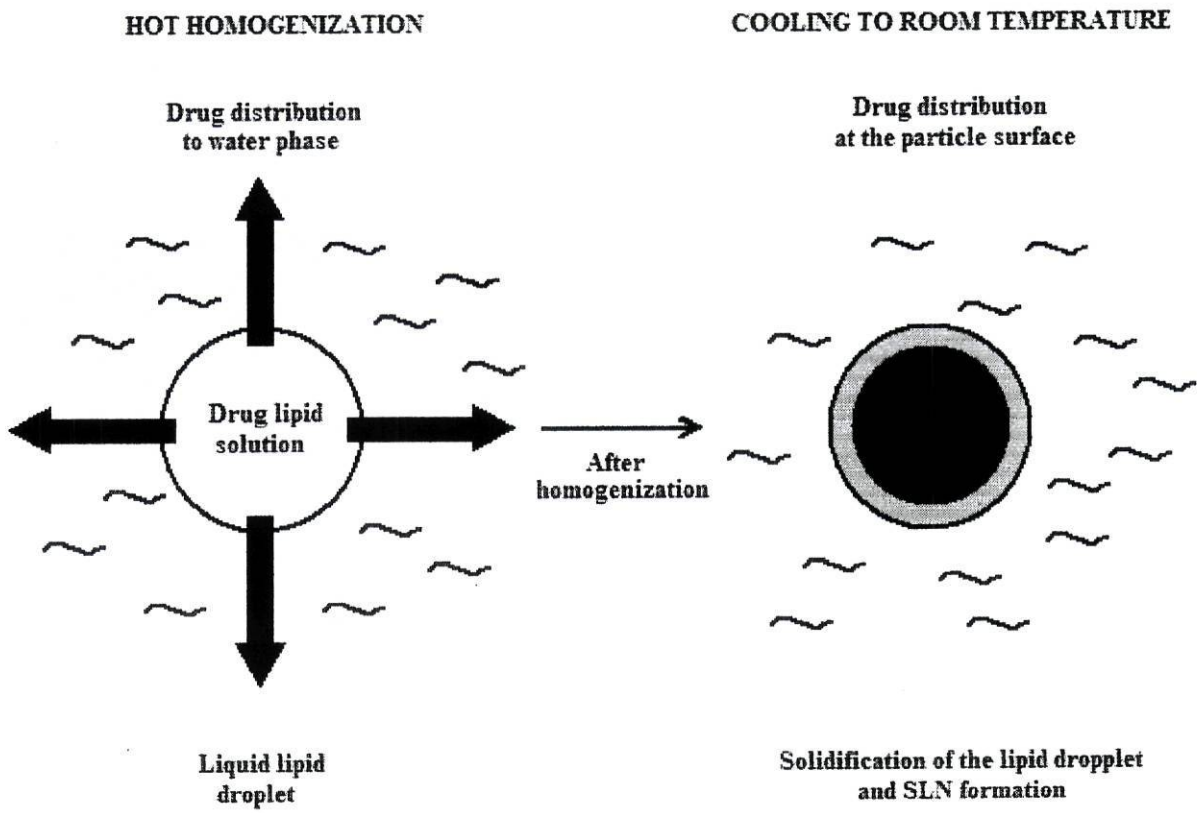

Figure 5.59: Partitioning effects on drug during the production of SLN by the hot HPH technique. Partitioning of drug from the lipid phase to the water phase at increased temperature, and repartitioning of the drug to the lipid phase during cooling of the produced O/W nanoemulsion. (Adapted from Müller *et al.* [6]).

Due to the morphological types of SLN, the amount of drug in the outer shell and on the particle surface is released in the form of a burst, while the drug incorporated into the particle core is released in a prolonged way [27].

This phenomenon of burst release of the drug has been described for a number of SLN formulations [6]. However, prolonged release is also possible as described by many examples in the literature [107,129,136]. Therefore, to achieve prolonged release, special production conditions are recommended [11]. The extent of burst release can be controlled via the solubility of the drug in the water phase during production, which means via the temperature employed and the surfactant concentration used. Higher temperatures and higher surfactant concentrations increase the burst. Thus, production at room temperature avoids partitioning of drug into the water phase and subsequently repartitioning from the oil phase [6]. If no initial dose is desired, the burst release can be avoided [50]. However, despite applying such production conditions for some drug and lipid mixtures the burst release cannot be avoided [29]. Applying the NLC technology, especially the imperfect type and amorphous type (Figure 2.10, Chapter II), provides much more flexibility to achieve the desired controlled drug release profile.

The reasons and the mechanism why certain drugs are very efficiently incorporated while others are not still remain poorly understood. One hypothesis that can be used to explain this phenomenon is based on different melting points of the drugs [318]. It is believed that drugs with higher melting points than the lipid precipitate first after the hot homogenization production process, and the drug, therefore, forms a core in the lipid phase. These systems show sustained release and a good E.E. [319]. In the case of drugs with lower melting points than the lipid, the lipid recrystallizes first and forms a lipid core, and the drug can only distribute to the surface. Thus, poor encapsulation and burst release results. However, this hypothesis, derived from release studies, was not investigated experimentally [75].

5.5. Incorporation of SLN and NLC into hydrogels

As reported before, SLN and NLC aqueous dispersions might be interesting systems in dermatological pharmaceutical formulations [9,47,56,104,107,113,119,175,177,183,187,320, 321]. These lipid particles are able to act as drug reservoirs, providing a controlled release profile of the incorporated drug. In addition, they can act as carriers for active substances, which prove to be chemically unstable in aqueous formulations, such as creams or lotions.

Therefore, in the present work clotrimazole-loaded SLN and NLC topical formulations were produced and investigated. Four different hydrogel types were prepared using an optimal

stabilizer combination of water, gel forming polymer (XG, HEC, PA and CH) and glycerol as hydrating agent, and finally adding the SLN and NLC aqueous dispersion into freshly prepared hydrogels. Table XXI and XXII resume the final composition of developed SLN and NLC-containing hydrogels formulations, respectively.

Table XXI: Composition of the investigated SLN-containing hydrogels formulations.

Formulation code	*Dynasan*®116 % (*m/m*)	*Tyloxapol*® % (*m/m*)	*Miglyol*®812 % (*m/m*)	Clotrimazole % (*m/m*)	Gel-forming agent % (*m/m*)	Glycerol % (*m/m*)	Water ad % (*m/m*)
D10%-XG	5%	1.5%	-	-	1% Xanthan gum	5%	100%
D10%-HEC	5%	1.5%	-	-	1.75% HEC 4000	5%	100%
D10%-PA	5%	1.5%	-	-	0.5% *Carbopol*®934	5%	100%
D10%-CH	5%	1.5%	-	-	1% Chitosan	5%	100%
D10%C-XG	4.75%	1.5%	-	0.25%	1% Xanthan gum	5%	100%
D10%C-HEC	4.75%	1.5%	-	0.25%	1.75% HEC 4000	5%	100%
D10%C-PA	4.75%	1.5%	-	0.25%	0.5% *Carbopol*®934	5%	100%
D10%C-CH	4.75%	1.5%	-	0.25%	1% Chitosan	5%	100%
D20%-XG	10%	2.5%	-	-	1% Xanthan gum	5%	100%
D20%-HEC	10%	2.5%	-	-	1.75% HEC 4000	5%	100%
D20%-PA	10%	2.5%	-	-	0.5% *Carbopol*®934	5%	100%
D20%-CH	10%	2.5%	-	-	1% Chitosan	5%	100%
D20%C-XG	9.5%	2.5%	-	0.5%	1% Xanthan gum	5%	100%
D20%C-HEC	9.5%	2.5%	-	0.5%	1.75% HEC 4000	5%	100%
D20%C-PA	9.5%	2.5%	-	0.5%	0.5% *Carbopol*®934	5%	100%
D20%C-CH	9.5%	2.5%	-	0.5%	1% Chitosan	5%	100%

Table XXII: Composition of the investigated NLC-containing hydrogels formulations.

Formulation code	*Dynasan*®116 % (*m/m*)	*Tyloxapol*® % (*m/m*)	*Miglyol*®812 % (*m/m*)	Clotrimazole % (*m/m*)	Gel-forming agent % (*m/m*)	Glycerol % (*m/m*)	Water ad % (*m/m*)
DM20%-XG	7%	2.5%	3%	-	1% Xanthan gum	5%	100%
DM20%-HEC	7%	2.5%	3%	-	1.75% HEC 4000	5%	100%
DM20%-PA	7%	2.5%	3%	-	0.5% *Carbopol*®934	5%	100%
DM20%-CH	7%	2.5%	3%	-	1% Chitosan	5%	100%
DM20%C-XG	6.75%	2.5%	2.75%	0.5%	1% Xanthan gum	5%	100%
DM20%C-HEC	6.75%	2.5%	2.75%	0.5%	1.75% HEC 4000	5%	100%
DM20%C-PA	6.75%	2.5%	2.75%	0.5%	0.5% *Carbopol*®934	5%	100%
DM20%C-CH	6.75%	2.5%	2.75%	0.5%	1% Chitosan	5%	100%

Clotrimazole-containing SLN and NLC hydrogels having a drug content of 5% (*m/m*) with regard to the lipid matrix could be prepared. In order to investigate the physicochemical stability of the lipid particles into hydrogels the mean particle size, the ζ and the state of crystallinity were

characterized and evaluated during a period of 3 months. Results will be presented in the following sections.

5.6. Characterization of developed hydrogel formulations

In order to physically characterize the developed SLN and NLC-containing hydrogel formulations particle size measurements, ζ and DSC studies were performed.

5.6.1. Particle size of SLN and NLC

For particle size measurement of SLN and NLC into hydrogels, aqueous dispersions were previously diluted with double-distilled water to weak opalescence and then the PCS diameter and PI and the LD diameter (d99%) were determined.

Table XXIII and XXIV show the PCS diameter, PI and LD (d99%) diameter of SLN and NLC-containing hydrogel formulations, respectively, one day after hydrogel preparation.

Table XXIII: PCS diameter, PI and LD (d99%) diameter of SLN-containing hydrogel formulations on day 1 of storage at 20ºC.

Formulation	PCS diameter (nm)	PI	LD (d99%) diameter (μm)
D10%-XG	191.000 ± 3.819	0.355 ± 0.015	0.504 ± 0.005
D10%-HEC	179.391 ± 0.666	0.246 ± 0.027	0.581 ± 0.002
D10%-PA	177.400 ± 3.955	0.217 ± 0.030	0.315 ± 0.003
D10%-CH	288.790 ± 7.262	0.427 ± 0.011	0.475 ± 0.006
D10%C-XG	182.788 ± 2.571	0.419 ± 0.009	0.610 ± 0.004
D10%C-HEC	169.098 ± 1.102	0.263 ± 0.031	0.510 ± 0.008
D10%C-PA	181.297 ± 1.677	0.186 ± 0.035	0.344 ± 0.058
D10%C-CH	230.500 ± 1.514	0.365 ± 0.024	0.458 ± 0.007
D20%-XG	239.600 ± 3.233	0.294 ± 0.020	0.574 ± 0.002
D20%-HEC	227.897 ± 6.782	0.239 ± 0.016	0.577 ± 0.001
D20%-PA	230.291 ± 0.300	0.240 ± 0.045	0.554 ± 0.028
D20%-CH	330.490 ± 11.310	0.416 ± 0.023	0.686 ± 0.058
D20%C-XG	201.100 ± 8,778	0.421 ± 0.035	1.937 ± 0.107
D20%C-HEC	171.400 ± 2.157	0.247 ± 0.044	0.554 ± 0.004
D20%C-PA	173.380 ± 1.789	0.235 ± 0.011	0.568 ± 0.006
D20%C-CH	257.890 ± 5.381	0.467 ± 0.017	0.568 ± 0.005

Table XXIV: PCS diameter, PI and LD (d99%) diameter of NLC-containing hydrogel formulations on day 1 of storage at 20°C.

Formulation	PCS diameter (nm)	PI	LD (d99%) diameter (μm)
DM20%-XG	192.100 ± 1.026	0.385 ± 0.031	0.703 ± 0.006
DM20%-HEC	185.769 ± 2.329	0.274 ± 0.038	0.643 ± 0.001
DM20%-PA	175.290 ± 0.611	0.191 ± 0.019	0.632 ± 0.007
DM20%-CH	207.900 ± 4.530	0.376 ± 0.011	0.607 ± 0.004
DM20%C-XG	169.311 ± 2.344	0.304 ± 0.004	0.731 ± 0.006
DM20%C-HEC	172.890 ± 2.524	0.264 ± 0.023	0.763 ± 0.002
DM20%C-PA	167.198 ± 1.411	0.237 ± 0.033	0.710 ± 0.004
DM20%C-CH	220.703 ± 2.386	0.303 ± 0.009	0.721 ± 0.002

One day after preparation, both drug-free and drug-loaded SLN and NLC-containing hydrogel formulations showed a narrow particle size distribution measured by LD analysis (d99%), which was completely in the nanometer range (Table XXIII and XXIV).

The presence of clotrimazole was not responsible for an increase in the mean particle size measured by PCS. For all tested formulations the mean particle size was lower than 300 nm. XG and CH hydrogels were responsible for a higher PI in comparison to HEC and PA hydrogels.

Sample D20%C-XG revealed a d99% higher than 1 μm, probably due to a poor effective dilution of XG hydrogel with double-distilled water.

5.6.2. Zeta potential of SLN and NLC

Determination of ζ was carried out in SLN and NLC-containing hydrogel formulations stored at room temperature. Tables XXV and XXVI show the ζ values of SLN and NLC formulations, respectively, one day after hydrogel preparation.

SLN and NLC were negatively charged when incorporated into XG, HEC and PA hydrogels. The same was not observed after incorporation into CH hydrogels.

On day 1 of storage at room temperature, clotrimazole-containing formulations, either SLN or NLC, showed a lower ζ than drug-free formulations.

Table XXV: Zeta potential of SLN-containing hydrogel formulations on day 1 of storage at 20°C.

Formulation	ζ
D10%-XG	-50.402 ± 1.082
D10%-HEC	-22.414 ± 0.153
D10%-PA	-21.290 ± 0.058
D10%-CH	45.881 ± 0.100
D10%C-XG	-40.900 ± 2.835
D10%C-HEC	-9.600 ± 0.231
D10%C-PA	-12.301 ± 0.346
D10%C-CH	41.498 ± 0.577
D20%-XG	-30.000 ± 1.054
D20%-HEC	-14.399 ± 0.252
D20%-PA	-15.004 ± 0.058
D20%-CH	39.500 ± 0.451
D20%C-XG	-39.323 ± 2.203
D20%C-HEC	-18.711 ± 0.289
D20%C-PA	-19.701 ± 1.100
D20%C-CH	28.214 ± 1.026

Table XXVI: Zeta potential of NLC-containing hydrogel formulations on day 1 of storage at 20°C.

Formulation	ζ
DM20%-XG	-17.500 ± 0.404
DM20%-HEC	-10.732 ± 0.361
DM20%-PA	-12.222 ± 0.603
DM20%-CH	36.901 ± 0.321
DM20%C-XG	-40.600 ± 2.800
DM20%C-HEC	-11.532 ± 0.208
DM20%C-PA	-19.818 ± 0.200
DM20%C-CH	35.500 ± 0.550

5.6.3. DSC studies

In order to assess interactions between lipid nanoparticles and the gel forming polymer, as well as investigate the solid state of SLN and NLC particles, DSC measurements were carried out. The samples (pure SLN and NLC aqueous dispersions and SLN and NLC-containing hydrogels) were heated from 25°C to 85°C and the respective melting enthalpies were recorded.

The components used for the preparation of the hydrogels do not melt at this temperature range (25°C-85°C). Therefore, it is possible to determine the crystallinity of SLN and NLC after their incorporation into the different developed semi-solid systems by DSC measurements. The melting peaks of pure SLN and NLC aqueous dispersions and of SLN and NLC incorporated into hydrogels were obtained on day 1 after production.

Figures 5.60 and 5.61 show the DSC curves of clotrimazole-free and clotrimazole-loaded SLN containing 10% of lipid matrix, respectively, as pure aqueous dispersion and when incorporated into four different hydrogels recorded after 1 day of storage at room temperature.

The melting point recorded for SLN containing 10% of lipid matrix (D10% and D10%C) as pure aqueous dispersion did not change significantly after incorporation into the four different hydrogels. It could be detected an increase from 60°C to 61°C when D10% was incorporated into HEC hydrogels.

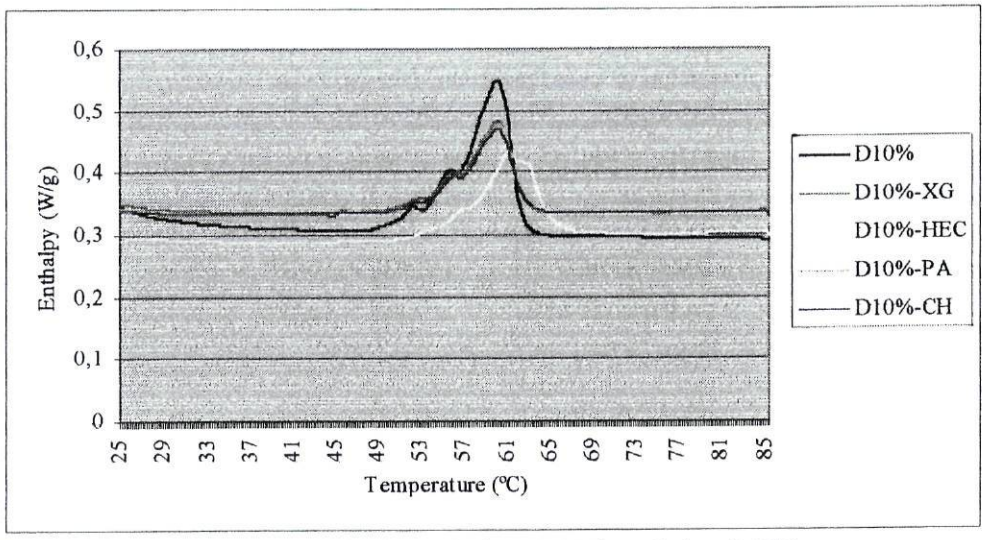

Figure 5.60: DSC curves of clotrimazole-free SLN formulation D10% as pure aqueous dispersion and when incorporated into four different hydrogels recorded after 1 day of storage at 20°C.

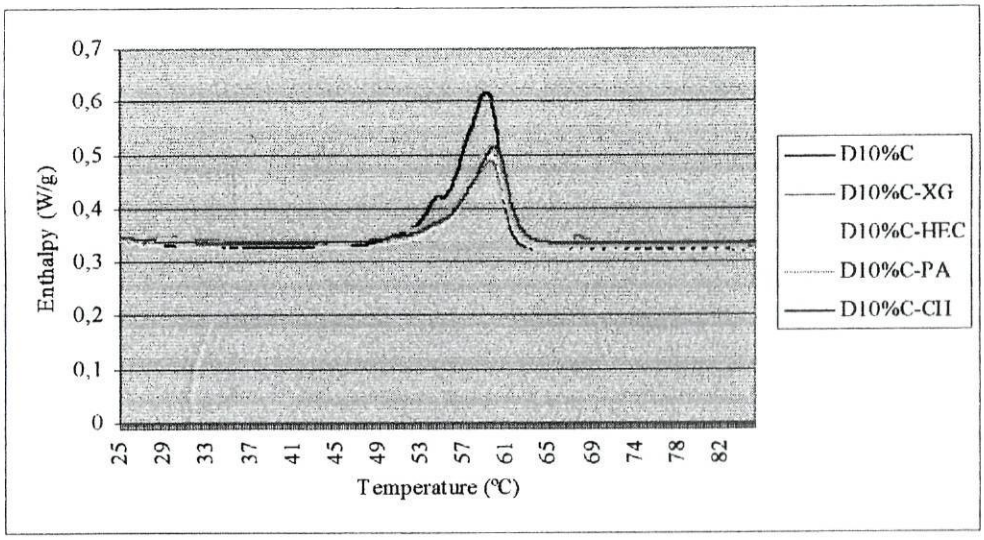

Figure 5.61: DSC curves of clotrimazole-loaded SLN formulation D10%C as pure aqueous dispersion and when incorporated into four different hydrogels recorded after 1 day of storage at 20°C.

Figures 5.62 and 5.63 show the DSC curves of clotrimazole-free and clotrimazole-loaded SLN containing 20% of lipid matrix, respectively, as pure aqueous dispersion and when incorporated into four different hydrogels recorded after 1 day of storage at room temperature.

It could also be observed that the melting point recorded for SLN containing 20% of lipid matrix (D20% and D20%C) as pure aqueous dispersion did not change after incorporation into four different hydrogels. In fact, the presence of clotrimazole did not change thermal behaviour of the formulations when incorporated into hydrogels.

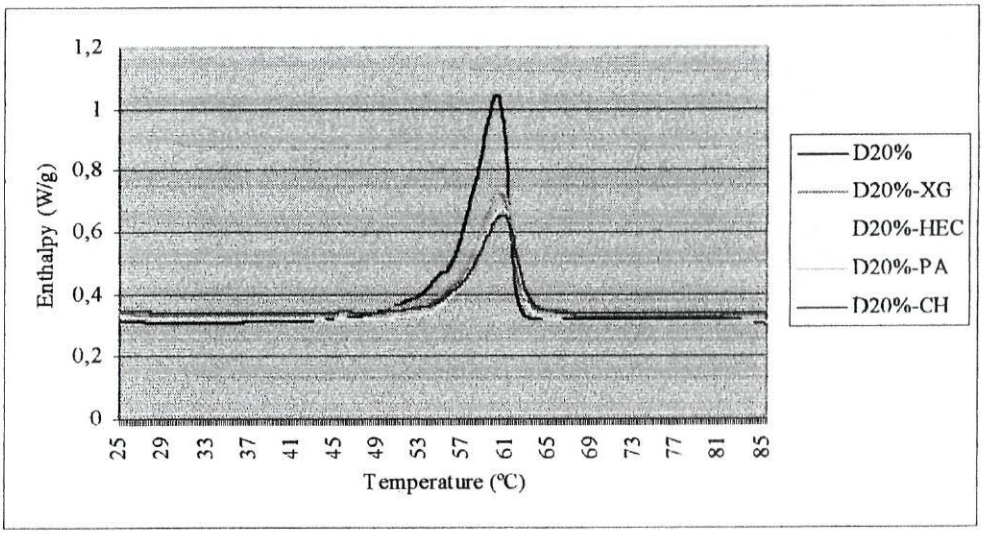

Figure 5.62: DSC curves of clotrimazole-free SLN formulation D20% as pure aqueous dispersion and when incorporated into four different hydrogels recorded after 1 day of storage at 20°C.

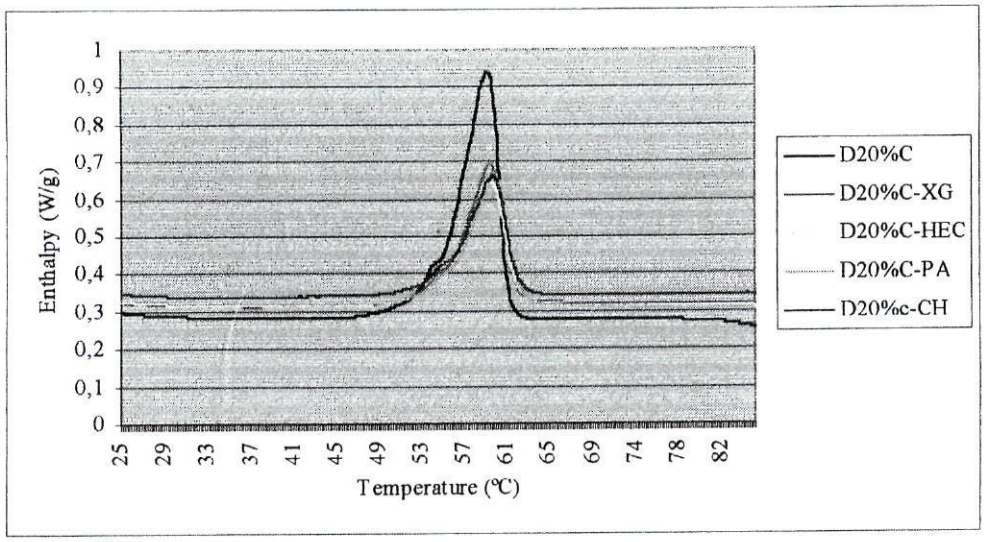

Figure 5.63: DSC-curves of clotrimazole-loaded SLN formulation D20%C as pure aqueous dispersion and when incorporated into four different hydrogels recorded after 1 day of storage at 20°C.

Figures 5.64 and 5.65 show the DSC curves of clotrimazole-free and clotrimazole-loaded NLC containing 20% of lipid matrix, respectively, as pure aqueous dispersion and when incorporated into four different hydrogels recorded after 1 day of storage at room temperature.

The melting point recorded for NLC containing 20% of lipid matrix as pure drug-free aqueous dispersion (DM20%) increased from 59°C to 60°C after incorporation into four different hydrogels. When the clotrimazole-loaded NLC formulation (DM20%C) was incorporated into HEC, PA and CH hydrogels an increase from 58°C to 60°C was observed. Nevertheless, the same was not observed when DM20%C formulation was incorporated into XG hydrogels. In fact, the melting point of this later formulation remained approximately at 58°C.

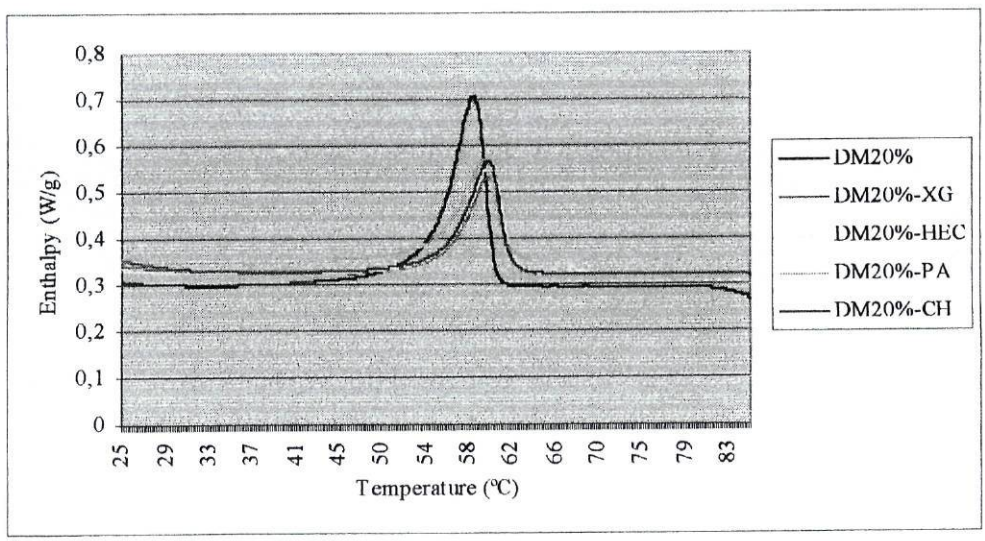

Figure 5.64: DSC curves of clotrimazole-free NLC formulation DM20% as pure aqueous dispersion and when incorporated into four different hydrogels recorded after 1 day of storage at 20°C.

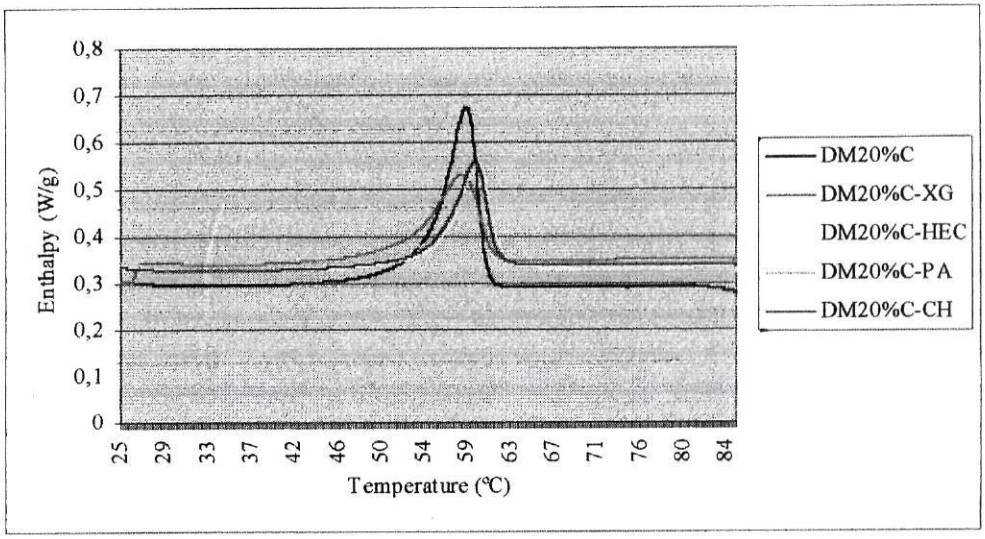

Figure 5.65: DSC curves of clotrimazole-loaded NLC formulation DM20%C as pure aqueous dispersion and when incorporated into four different hydrogels recorded after 1 day of storage at 20°C.

For both clotrimazole-free and clotrimazole-loaded SLN and NLC aqueous dispersions, lipid content of the hydrogel is always preserved. As figures show, the DSC curves of incorporated SLN and NLC aqueous dispersions into hydrogels revealed identical peaks compared to pure aqueous dispersions. This indicates that SLN and NLC particles remained chemically stable when incorporated and did not interfere with the gel forming polymer when stored at room temperature.

The decreased area under the curve observed for SLN and NLC-containing hydrogels is due to the lower solid lipid content of these samples in comparison to pure aqueous solid lipid dispersions. However, the melting enthalpy standardized on 1 g lipid remains constant.

To sum up, for all studied samples, either clotrimazole-free or clotrimazole-loaded, it could be observed that crystallinity of the solid matrix did not change significantly upon their incorporation into the four different hydrogels. Tables XXVII and XXVIII show the DSC results of clotrimazole-free and clotrimazole-loaded SLN and NLC aqueous dispersions, respectively, after 1 day of storage at 20°C.

Table XXVII: DSC results of clotrimazole-free SLN and NLC aqueous dispersions before and after incorporation into different four hydrogels recorded after 1 day of storage at 20°C.

Formulation	Melting point (°C)	Onset (°C)	Integral (mJ)	Enthalpy (J/g)	RI (%)
D10%	59.33	55.12	479.25	13.51	69.8
D10%-XG	59.01	56.15	772.22	8.38	43.3
D10%-HEC	60.18	56.12	724.66	8.93	46.2
D10%-PA	59.33	55.11	764.92	8.46	43.7
D10%-CH	59.27	55.16	775.00	8.35	43.2
D20%	59.46	55.53	330.87	33.67	87.0
D20%-XG	59.59	55.71	425.18	15.22	78.7
D20%-HEC	59.58	55.63	424.07	15.26	78.9
D20%-PA	59.52	55.68	423.23	15.29	79.0
D20%-CH	59.63	55.44	426.02	15.19	78.5
DM20%	58.04	54.22	623.07	17.88	46.2
DM20%-XG	59.14	55.74	521.45	12.41	64.2
DM20%-HEC	59.08	55.59	522.72	12.38	64.0
DM20%-PA	58.93	55.29	522.30	12.39	64.1
DM20%-CH	59.12	55.97	526.54	12.29	63.5

Table XXVIII: DSC results of clotrimazole-loaded SLN and NLC aqueous dispersions before and after incorporation into different four hydrogels recorded after 1 day of storage at 20°C.

Formulation	Melting point (°C)	Onset (°C)	Integral (mJ)	Enthalpy (J/g)	RI (%)
D10%C	58.95	54.65	411.36	15.86	81.2
D10%C-XG	59.08	56.22	737.88	8.77	45.3
D10%C-HEC	59.21	55.43	744.68	8.69	44.9
D10%C-PA	59.17	55.72	748.99	8.64	44.7
D10%C-CH	59.27	55.31	737.04	8.78	45.4
D20%C	59.07	54.97	339.08	32.85	84.9
D20%C-XG	59.14	55.07	424.07	15.26	78.9
D20%C-HEC	59.01	56.11	425.46	15.21	78.6
D20%C-PA	59.21	55,46	423.23	15.29	79.0
D20%C-CH	59.25	55.14	424.62	15.24	78.8
DM20%C	58.12	54.57	705.54	15.79	40.8
DM20%C-XG	58.81	55.42	563.21	11.49	59.4
DM20%C-HEC	58.87	55.17	566.16	11.43	59.1
DM20%C-PA	58.80	55.59	564.68	11.46	59.2
DM20%C-CH	58.76	55.18	568.15	11.39	58.9

5.7. Stability of developed hydrogel formulations

The stability of developed SLN and NLC-containing hydrogel formulations was evaluated concerning to particle size, ζ and crystalline status of lipid nanoparticles.

5.7.1. Particle size

For the analysis of physical stability of SLN and NLC incorporated into the hydrogels (e.g. nanoparticle aggregation), particle size has been evaluated. Aqueous dispersions were previously diluted with double-distilled water to weak opalescence and then LD diameter (d50%, d95% and d99%), PCS diameter and PI were determined.

5.7.1.1. SLN-containing hydrogel formulations

Figures 5.66 and 5.67 show the results after LD and PCS analysis, respectively, of clotrimazole-free and clotrimazole-loaded SLN containing 10% of lipid matrix incorporated into XG hydrogels, which were stored at room temperature during 3 months.

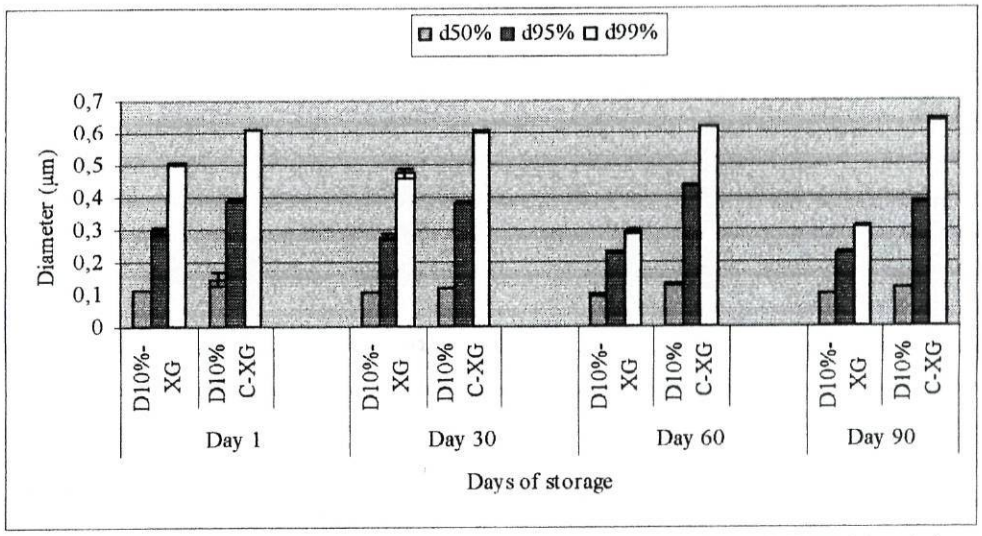

Figure 5.66: Particle size of clotrimazole-free and clotrimazole-loaded SLN formulations D10% and D10%C incorporated into XG hydrogels measured by LD (d50%, d95% and d99%), after 1, 30, 60 and 90 days of storage at room temperature (20°C).

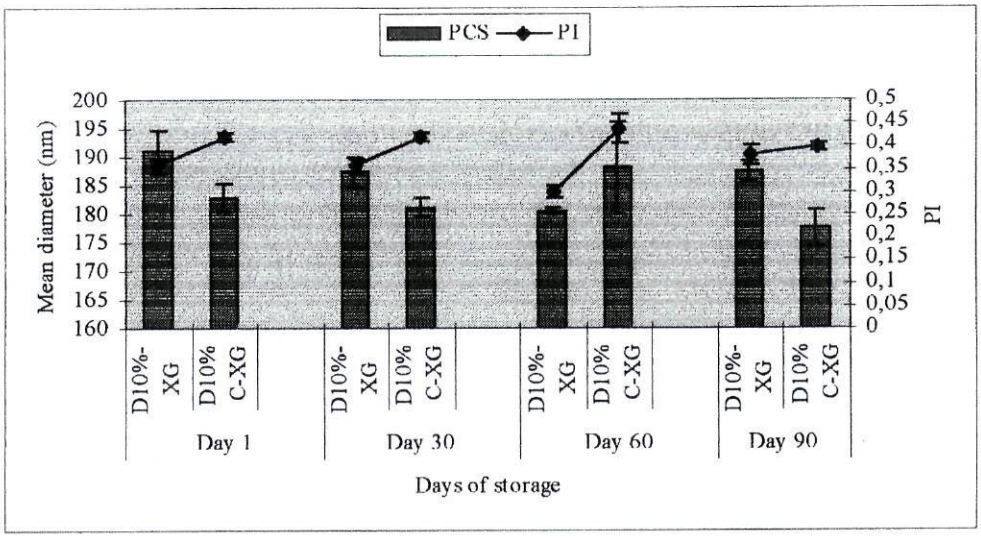

Figure 5.67: Mean particle size measured by PCS and PI of clotrimazole-free and clotrimazole-loaded SLN formulations D10% and D10%C incorporated into XG hydrogels, after 1, 30, 60 and 90 days of storage at room temperature (20°C).

Incorporation of D10% and D10%C into XG hydrogels did not result in aggregation of SLN. Upon incorporation of clotrimazole-free and clotrimazole-loaded SLN containing 10% of lipid matrix into XG hydrogels, 99% of volume distribution remained lower than 0.7 μm. For all formulations, 50% of volume distribution was lower than 100 nm. PCS analysis shows a mean particle size lower than 190 nm and a PI between 0.3 and 0.4 during 90 days of storage at room temperature.

Figures 5.68 and 5.69 show the results after LD and PCS analysis, respectively, of clotrimazole-free and clotrimazole-loaded SLN containing 10% of lipid matrix incorporated into HEC hydrogels, which were stored at room temperature during 3 months.

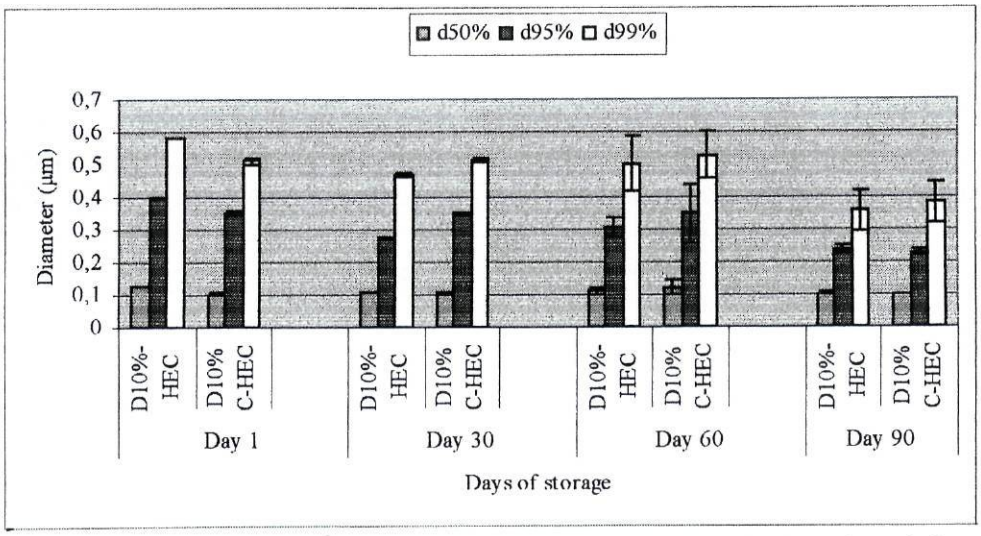

Figure 5.68: Particle size of clotrimazole-free and clotrimazole-loaded SLN formulations D10% and D10%C incorporated into HEC hydrogels measured by LD (d50%, d95% and d99%), after 1, 30, 60 and 90 days of storage at room temperature (20°C).

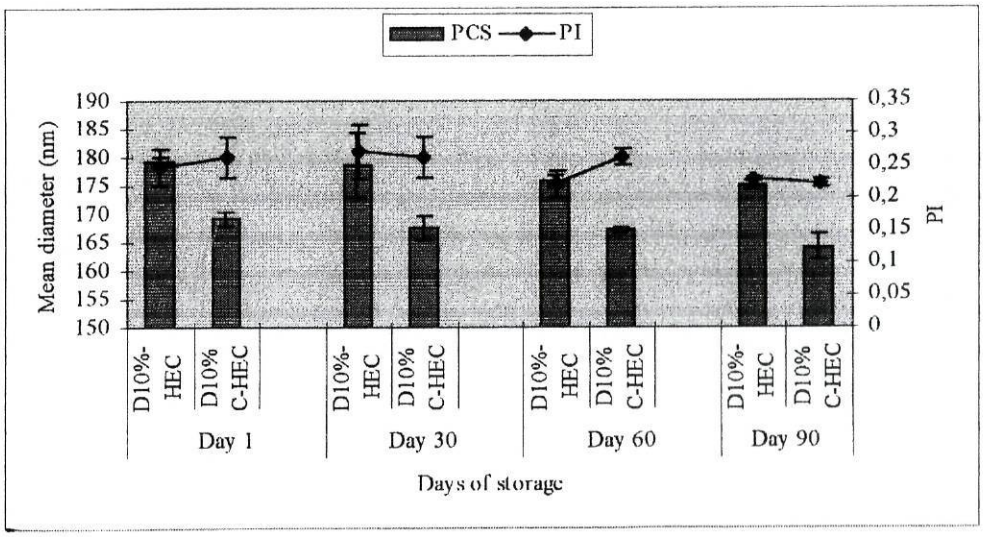

Figure 5.69: Mean particle size measured by PCS and PI of clotrimazole-free and clotrimazole-loaded SLN formulations D10% and D10%C incorporated into HEC hydrogels, after 1, 30, 60 and 90 days of storage at room temperature (20°C).

Incorporation of D10% and D10%C into HEC hydrogels did not result in aggregation of SLN. Upon incorporation of clotrimazole-free and clotrimazole-loaded SLN containing 10% of lipid matrix into HEC hydrogels, 99% of volume distribution remained lower than 0.6 μm. The presence of clotrimazole did not change significantly the particle size distribution. PCS data revealed a mean particle size of approximately 180 nm for clotrimazole-free SLN, while for clotrimazole-loaded SLN the mean particle size was 170 nm during 90 days of storage at room temperature. PI remained lower than 0.3 for both formulations.

Figures 5.68 and 5.65 show the results after LD and PCS analysis, respectively, of clotrimazole-free and clotrimazole-loaded SLN containing 10% of lipid matrix incorporated into PA hydrogels, which were stored at room temperature during 3 months.

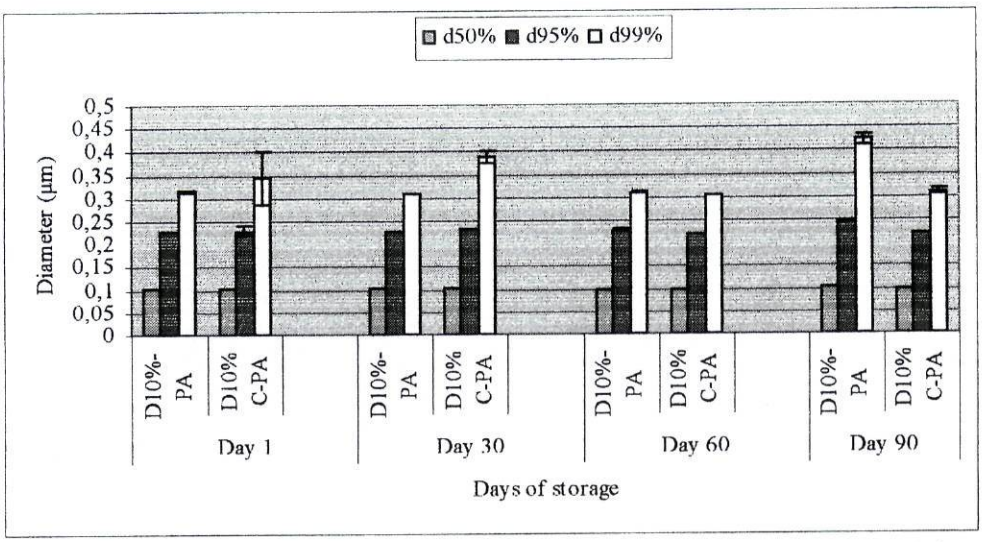

Figure 5.70: Particle size of clotrimazole-free and clotrimazole-loaded SLN formulations D10% and D10%C incorporated into PA hydrogels measured by LD (d50%, d95% and d99%), after 1, 30, 60 and 90 days of storage at room temperature (20°C).

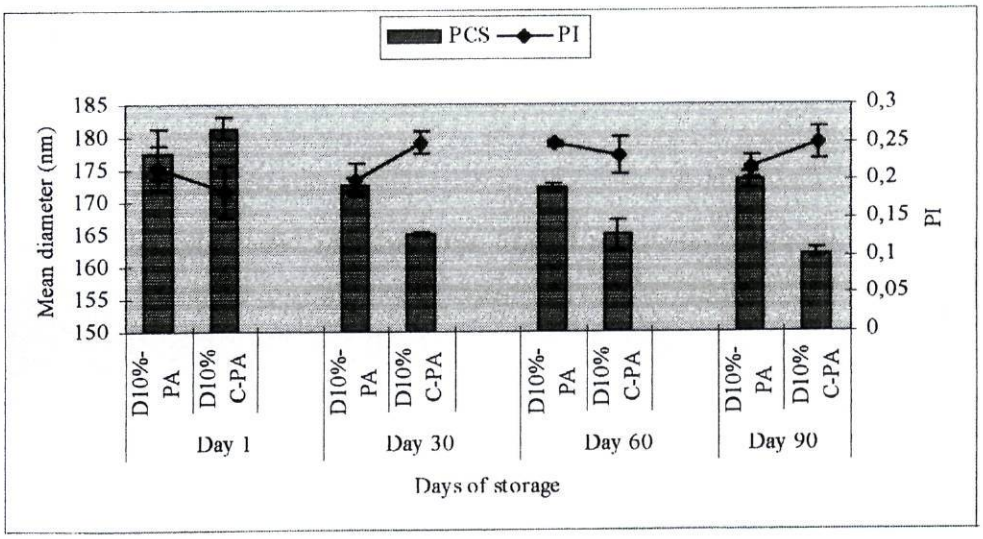

Figure 5.71: Mean particle size measured by PCS and PI of clotrimazole-free and clotrimazole-loaded SLN formulations D10% and D10%C incorporated into PA hydrogels, after 1, 30, 60 and 90 days of storage at room temperature (20°C).

Incorporation of D10% and D10%C into PA hydrogels did not result in aggregation of SLN. Upon incorporation of clotrimazole-free and clotrimazole-loaded SLN containing 10% of lipid matrix into PA hydrogels, 99% of volume distribution remained lower than 0.4 µm. It could not be observed any significant difference between clotrimazole-free and clotrimazole-loaded samples during 90 days of storage at room temperature. The mean particle size measured by PCS was lower 180 nm and the PI remained approximately 0.25.

Figures 5.66 and 5.67 show the results after LD and PCS analysis, respectively, of clotrimazole-free and clotrimazole-loaded SLN containing 10% of lipid matrix incorporated into CH hydrogels, which were stored at room temperature during 3 months.

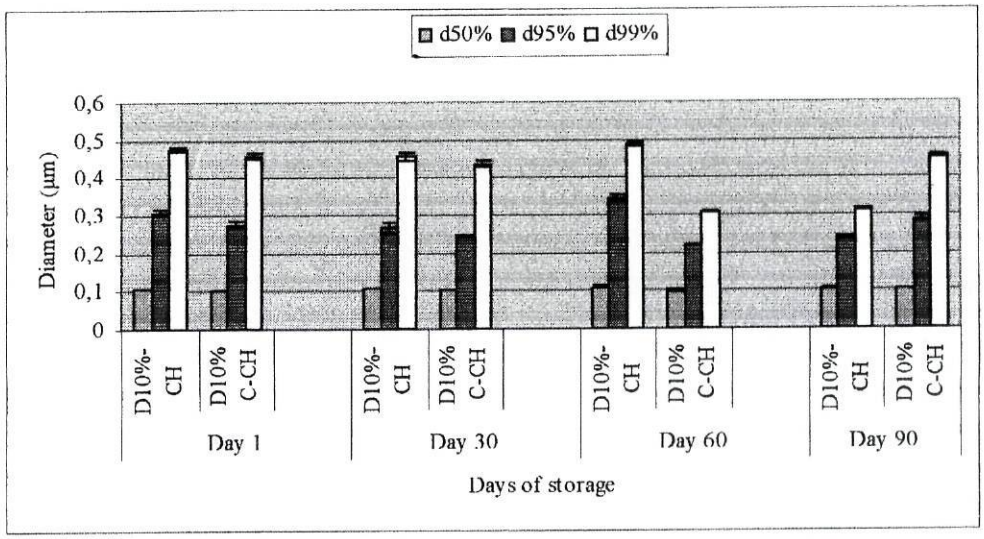

Figure 5.72: Particle size of clotrimazole-free and clotrimazole-loaded SLN formulations D10% and D10%C incorporated into CH hydrogels measured by LD (d50%, d95% and d99%), after 1, 30, 60 and 90 days of storage at room temperature (20°C).

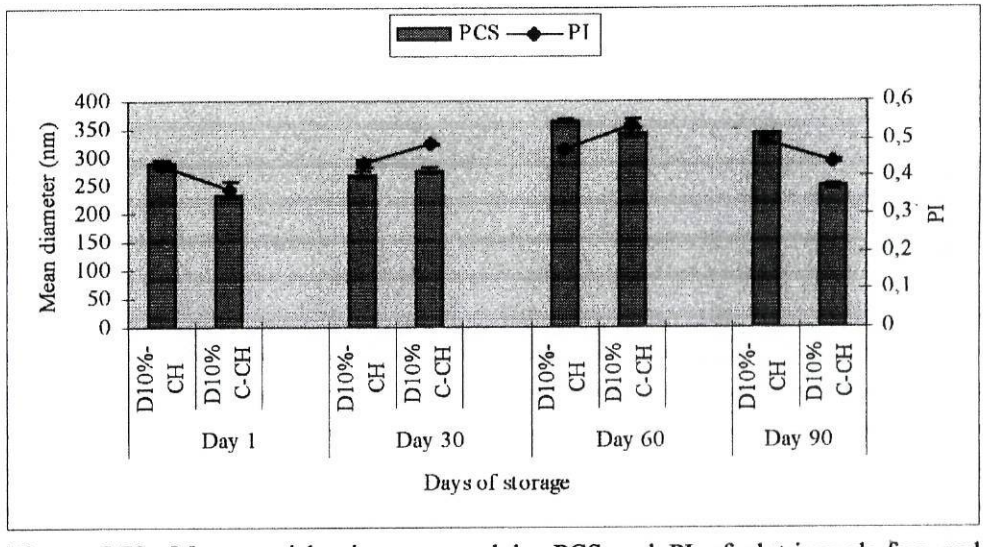

Figure 5.73: Mean particle size measured by PCS and PI of clotrimazole-free and clotrimazole-loaded SLN formulations D10% and D10%C incorporated into CH hydrogels, after 1, 30, 60 and 90 days of storage at room temperature (20°C).

The incorporation of D10% and D10%C into CH hydrogels increased the mean particle size of SLN in comparison to XG, HEC and PA hydrogels. From LD data, 99% of volume distribution remained below 0.5 µm, which is lower than the obtained after incorporation of these particles into XG. However, by PCS analysis a growth of particle size could be observed. The

mean particle size oscillated between 200 and 350 nm during 90 days of storage at room temperature and the PI remained between 0.4 and 0.5 during the same period of time.

Figures 5.74 and 5.75 show the results after LD and PCS analysis, respectively, of clotrimazole-free and clotrimazole-loaded SLN containing 20% of lipid matrix incorporated into XG hydrogels, which were stored at room temperature during 3 months.

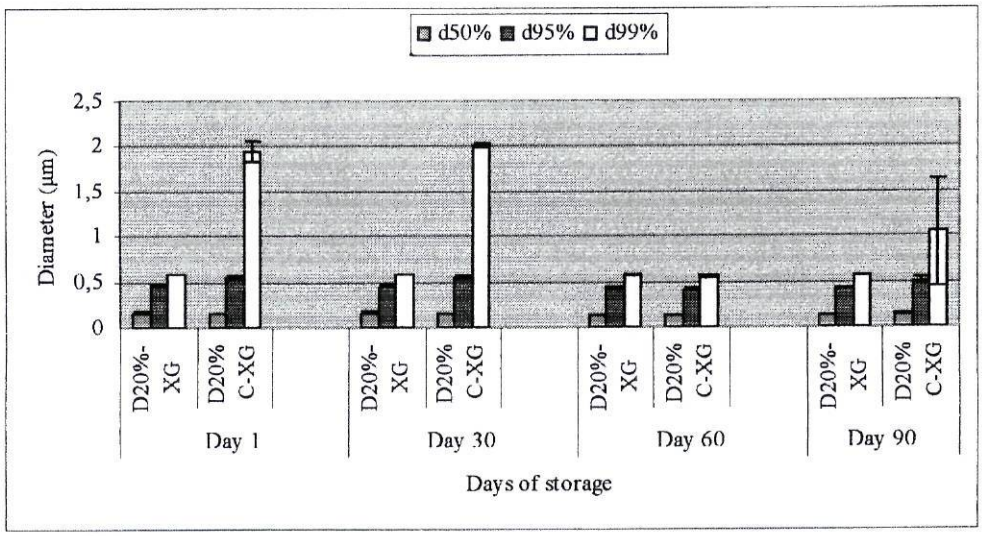

Figure 5.74: Particle size of clotrimazole-free and clotrimazole-loaded SLN formulations D20% and D20%C incorporated into XG hydrogels measured by LD (d50%, d95% and d99%), after 1, 30, 60 and 90 days of storage at room temperature (20°C).

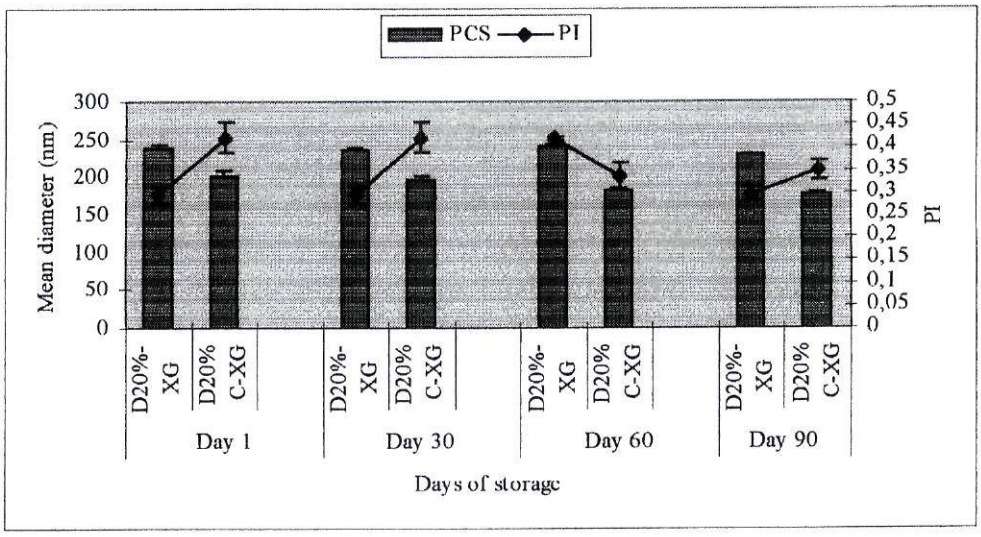

Figure 5.75: Mean particle size measured by PCS and PI of clotrimazole-free and clotrimazole-loaded SLN formulations D20% and D20%C incorporated into XG hydrogels, after 1, 30, 60 and 90 days of storage at room temperature (20°C).

Analysis of clotrimazole-free and clotrimazole-loaded SLN containing 20% of lipid matrix incorporated into XG hydrogels revealed peaks in the micrometer range. It could be observed that

99% of volume distribution remained lower than 2 µm. For all formulations 50% of volume distribution was lower than 500 nm. PCS analysis showed a mean particle size between 200 and 250 nm and a PI between 0.3 and 0.4 during 90 days of storage at room temperature.

Figures 5.76 and 5.77 show the results after LD and PCS analysis, respectively, of clotrimazole-free and clotrimazole-loaded SLN containing 20% of lipid matrix incorporated into HEC hydrogels, which were stored at room temperature during 3 months.

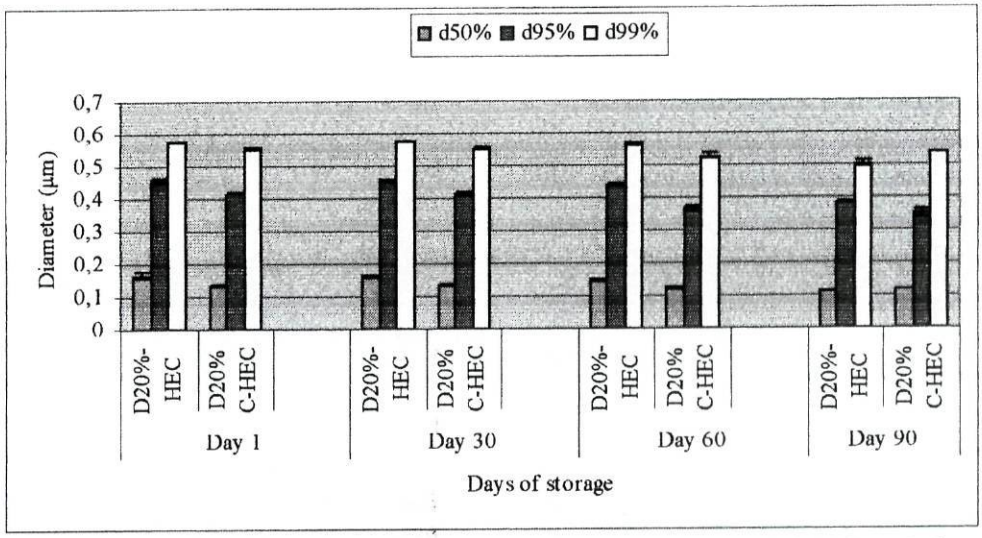

Figure 5.76: Particle size of clotrimazole-free and clotrimazole-loaded SLN formulations D20% and D20%C incorporated into HEC hydrogels measured by LD (d50%, d95% and d99%), after 1, 30, 60 and 90 days of storage at room temperature (20°C).

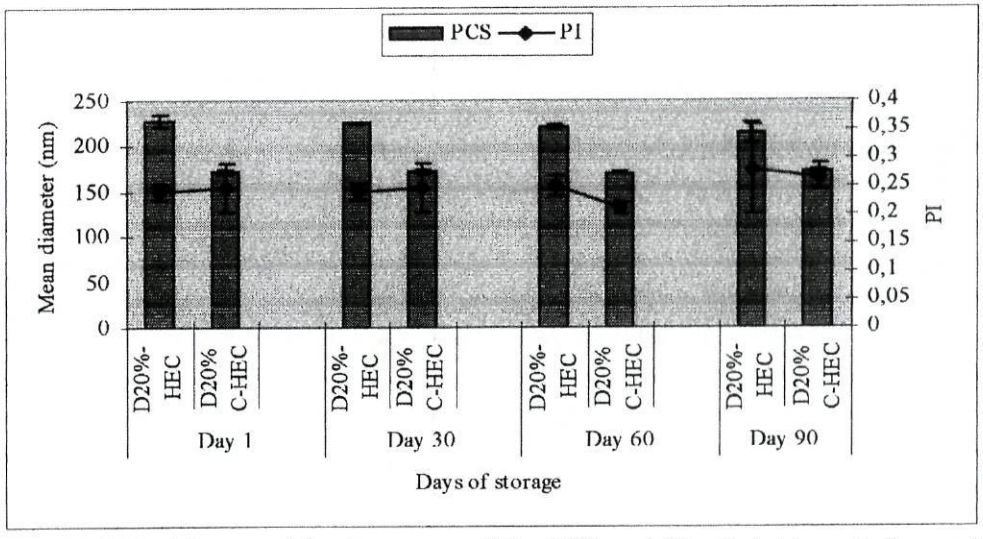

Figure 5.77: Mean particle size measured by PCS and PI of clotrimazole-free and clotrimazole-loaded SLN formulations D20% and D20%C incorporated into HEC hydrogels, after 1, 30, 60 and 90 days of storage at room temperature (20°C).

Upon incorporation of clotrimazole-free and clotrimazole-loaded SLN containing 20% of lipid matrix into HEC hydrogels, LD analysis did not exhibited peaks in the micrometer range. In fact, 99% of volume distribution was below 0.6 μm as obtained for samples with 10% of lipid matrix. The presence of clotrimazole did not change the particle size distribution. PCS data revealed a mean particle size of approximately 200 nm for SLN without drug and a PI of 0.35, while for drug-loaded SLN the mean particle size was 170 nm and the PI oscillated between 0.25 and 0.3 during 90 days of storage at room temperature.

Figures 5.78 and 5.79 show the results after LD and PCS analysis, respectively, of clotrimazole-free and clotrimazole-loaded SLN containing 20% of lipid matrix incorporated into PA hydrogels, which were stored at room temperature during 3 months.

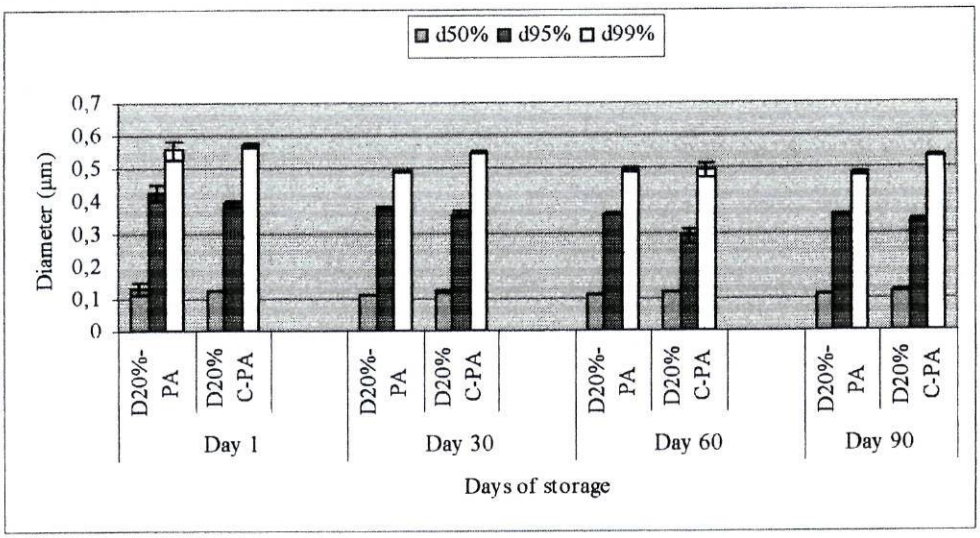

Figure 5.78: Particle size of clotrimazole-free and clotrimazole-loaded SLN formulations D20% and D20%C incorporated into PA hydrogels measured by LD (d50%, d95% and d99%), after 1, 30, 60 and 90 days of storage at room temperature (20°C).

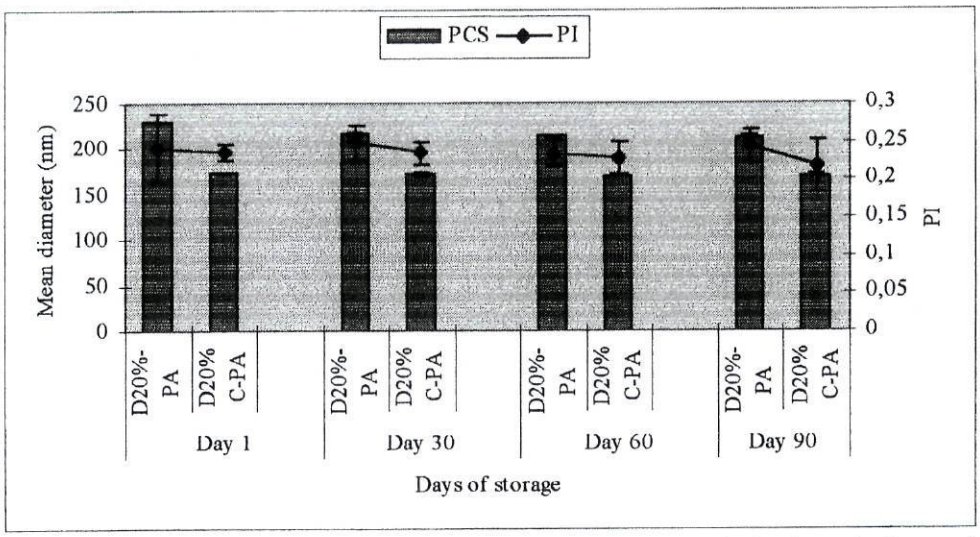

Figure 5.79: Mean particle size measured by PCS and PI of clotrimazole-free and clotrimazole-loaded SLN formulations D20% and D20%C incorporated into PA hydrogels, after 1, 30, 60 and 90 days of storage at room temperature (20°C).

Upon incorporation of clotrimazole-free and clotrimazole-loaded SLN containing 20% of lipid matrix into PA hydrogels, 99% of volume distribution remained lower than 0.6 μm. It could not be observed any significantly difference between samples without drug and clotrimazole-loaded during 90 days of storage at room temperature. The mean particle size measured by PCS remained approximately 230 nm for samples without drug, while it remained lower than 170 nm for samples with clotrimazole. PI oscillated between 0.2 and 0.25 for both formulations.

Figures 5.80 and 5.81 show the results after LD and PCS analysis, respectively, of clotrimazole-free and clotrimazole-loaded SLN containing 20% of lipid matrix incorporated into CH hydrogels, which were stored at room temperature during 3 months.

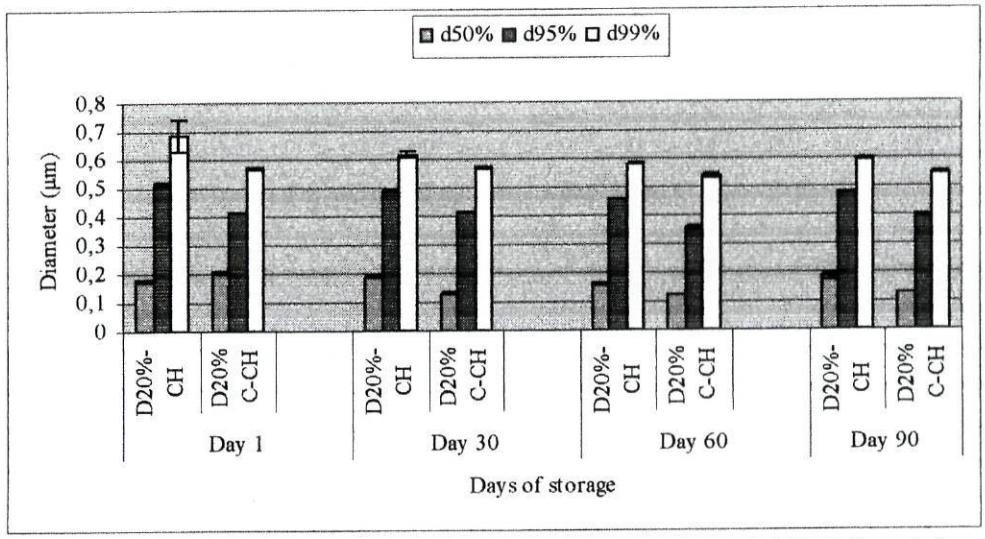

Figure 5.80: Particle size of clotrimazole-free and clotrimazole-loaded SLN formulations D20% and D20%C incorporated into CH hydrogels measured by LD (d50%, d95% and d99%), after 1, 30, 60 and 90 days of storage at room temperature (20°C).

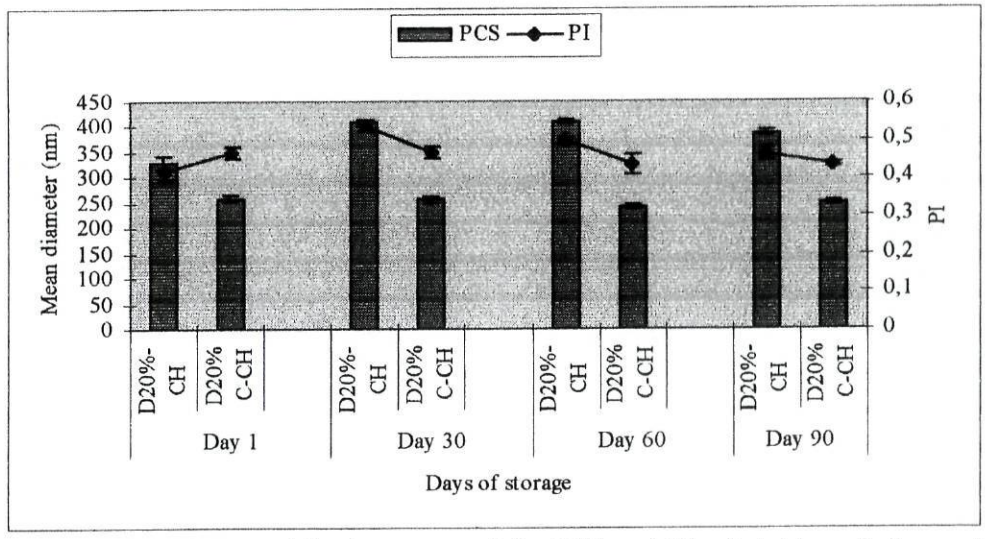

Figure 5.81: Mean particle size measured by PCS and PI of clotrimazole-free and clotrimazole-loaded SLN formulations D20% and D20%C incorporated into CH hydrogels, after 1, 30, 60 and 90 days of storage at room temperature (20°C).

The incorporation of D20% and D20%C into CH hydrogels increased the mean particle size of SLN in comparison to XG, HEC and PA hydrogels, as reported for SLN containing 10% of lipid matrix. From LD data, 99% of volume distribution remained below 0.7 μm, which is lower than the obtained after incorporation of these particles into XG. However, after PCS analysis it could be observed a growth in particle size. PCS data revealed a mean particle size of approximately 400 nm for SLN without drug and a PI higher than 0.5, while for SLN with clotrimazole the mean particle size was 250 nm and the PI was approximately 0.3 during 90 days of storage at room temperature during 3 months.

5.7.1.2. NLC-containing hydrogel formulations

Figures 5.82 and 5.83 show the results after LD and PCS analysis, respectively, of clotrimazole-free and clotrimazole-loaded NLC containing 20% of lipid matrix incorporated into XG hydrogels, which were stored at room temperature during 3 months.

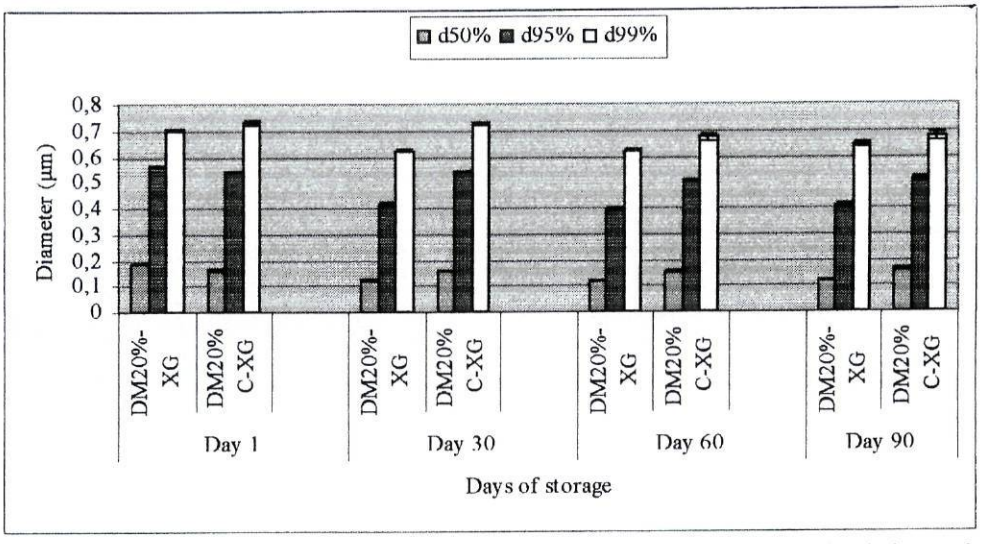

Figure 5.82: Particle size of clotrimazole-free and clotrimazole-loaded NLC formulations DM20% and DM20%C incorporated into XG hydrogels measured by LD (d50%, d95% and d99%), after 1, 30, 60 and 90 days of storage at room temperature (20°C).

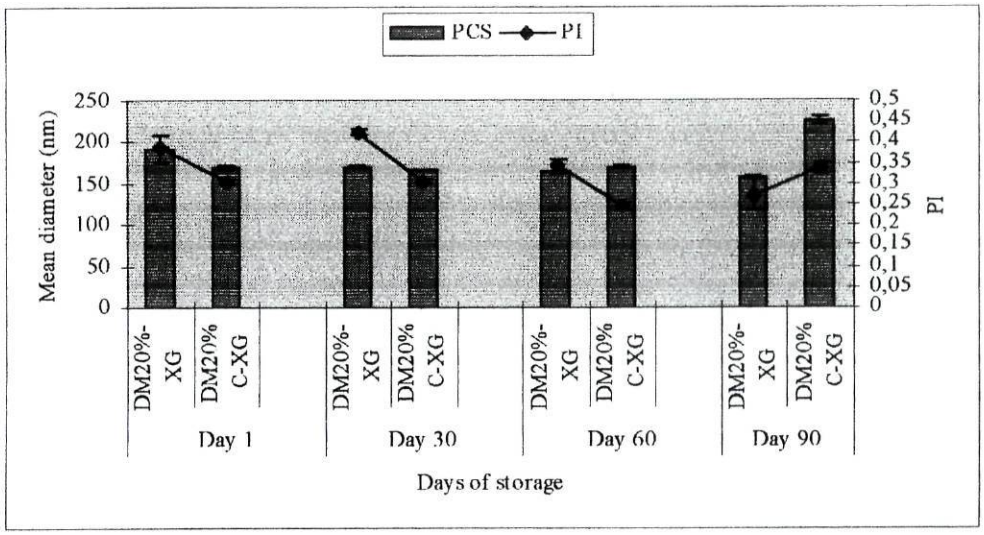

Figure 5.83: Mean particle size measured by PCS and PI of clotrimazole-free and clotrimazole-loaded NLC formulations DM20% and DM20%C incorporated into XG hydrogels, after 1, 30, 60 and 90 days of storage at room temperature (20°C).

Upon incorporation of clotrimazole-free and clotrimazole-loaded NLC containing 20% of lipid matrix into XG hydrogels, analysis by LD did not reveal peaks in the micrometer range. It could be observed that 99% of volume distribution remained lower than 0.7 μm and for all formulations 50% of volume distribution was lower than 200 nm. PCS analysis shows a mean particle size around 200 nm and a PI between 0.25 and 0.4 during 90 days of storage at room temperature.

Figures 5.84 and 5.85 show the results after LD and PCS analysis, respectively, of clotrimazole-free and clotrimazole-loaded NLC containing 20% of lipid matrix incorporated into HEC hydrogels, which were stored at room temperature during 3 months.

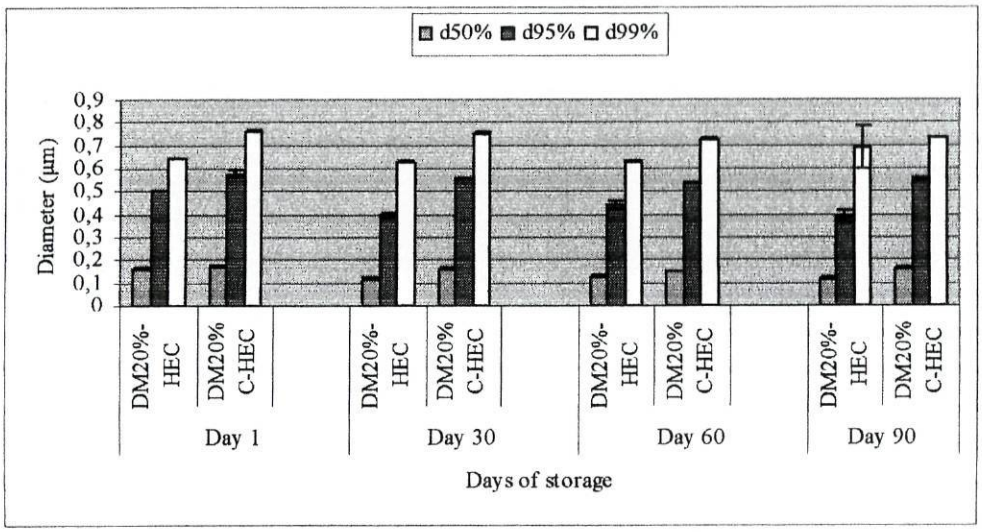

Figure 5.84: Particle size of clotrimazole-free and clotrimazole-loaded NLC formulations DM20% and DM20%C incorporated into HEC hydrogels measured by LD (d50%, d95% and d99%) after 1, 30, 60 and 90 days of storage at room temperature (20°C).

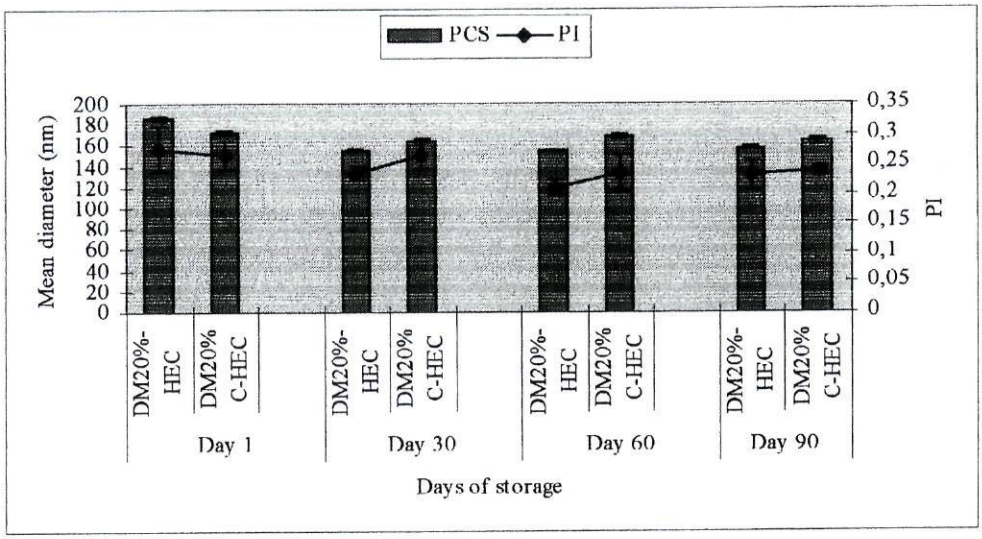

Figure 5.85: Mean particle size measured by PCS and PI of clotrimazole-free and clotrimazole-loaded NLC formulations DM20% and DM20%C incorporated into HEC hydrogels, after 1, 30, 60 and 90 days of storage at room temperature (20°C).

Upon incorporation of clotrimazole-free and clotrimazole-loaded NLC containing 20% of lipid matrix into HEC hydrogels, analysis by LD did not reveal peaks in the micrometer range. In fact, 99% of volume distribution was below 0.8 μm. The presence of clotrimazole did not change the particle size distribution. PCS data revealed a mean particle size of approximately 170 nm and a PI of 0.25 for both drug-free and drug-loaded formulations, during 90 days of storage at room temperature.

Figures 5.86 and 5.87 show the results after LD and PCS analysis, respectively, of clotrimazole-free and clotrimazole-loaded NLC containing 20% of lipid matrix incorporated into PA hydrogels, which were stored at room temperature during 3 months.

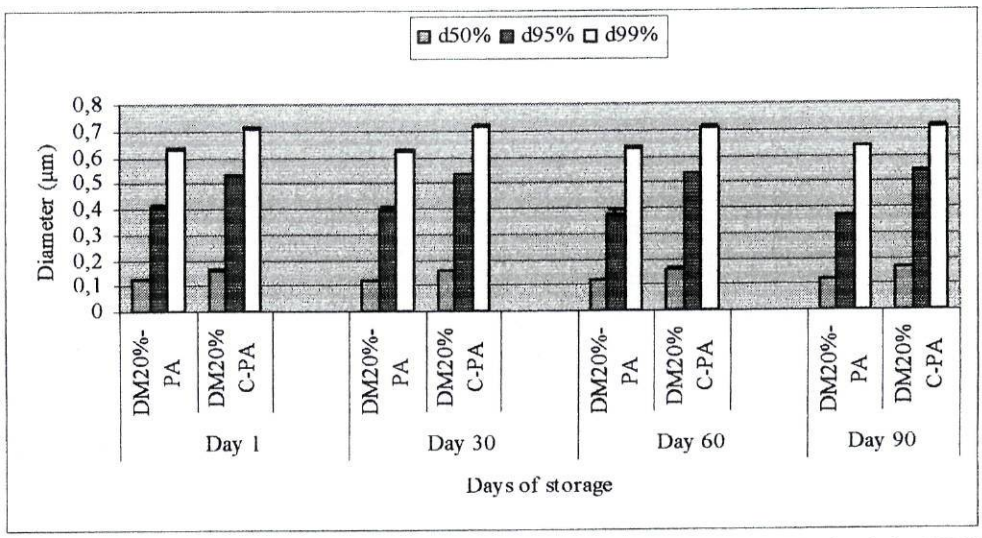

Figure 5.86: Particle size of clotrimazole-free and clotrimazole-loaded NLC formulations DM20% and DM20%C incorporated into PA hydrogels measured by LD (d50%, d95% and d99%), after 1, 30, 60 and 90 days of storage at room temperature (20°C).

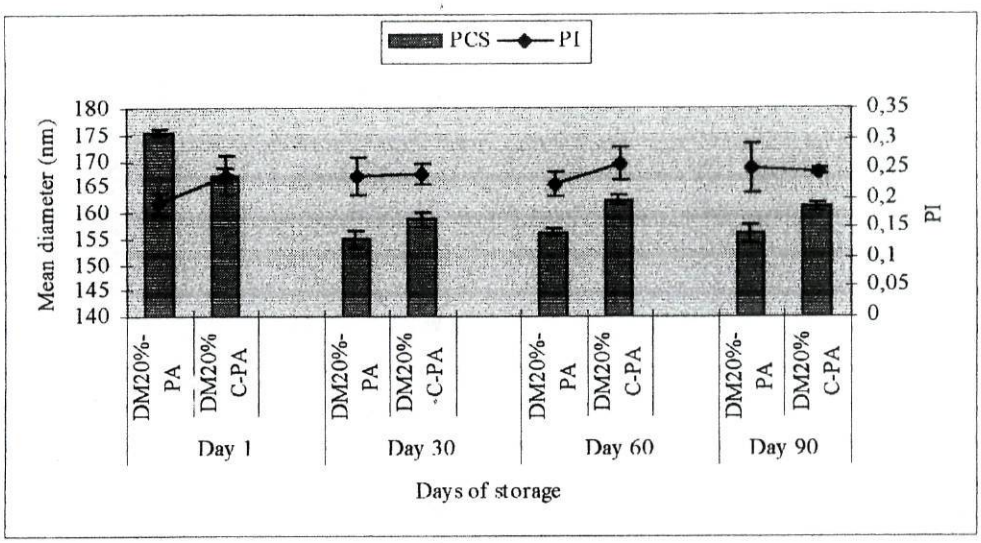

Figure 5.87: Mean particle size measured by PCS and PI of clotrimazole-free and clotrimazole-loaded NLC formulations DM20% and DM20%C incorporated into PA hydrogels, after 1, 30, 60 and 90 days of storage at room temperature (20°C).

Upon incorporation of clotrimazole-free and clotrimazole-loaded NLC containing 20% of lipid matrix into PA hydrogels, 99% of volume distribution remained lower than 0.7 μm. It could not be observed any significant difference between clotrimazole-free and clotrimazole-loaded samples during 90 days of storage at room temperature. The mean particle size measured by PCS remained below 175 nm and PI was approximately 0.25 for both formulations.

Figures 5.88 and 5.89 show the results after LD and PCS analysis, respectively, of clotrimazole-free and clotrimazole-loaded NLC containing 20% of lipid matrix incorporated into CH hydrogels, which were stored at room temperature during 3 months.

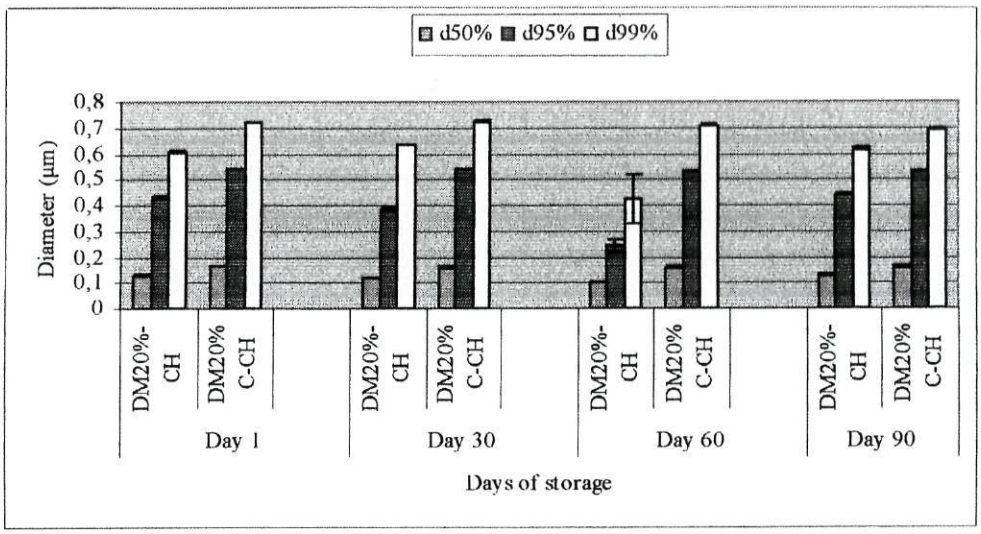

Figure 5.88: Particle size of clotrimazole-free and clotrimazole-loaded NLC formulations DM20% and DM20%C incorporated into CH hydrogels measured by LD (d50%, d95% and d99%), after 1, 30, 60 and 90 days of storage at room temperature (20°C).

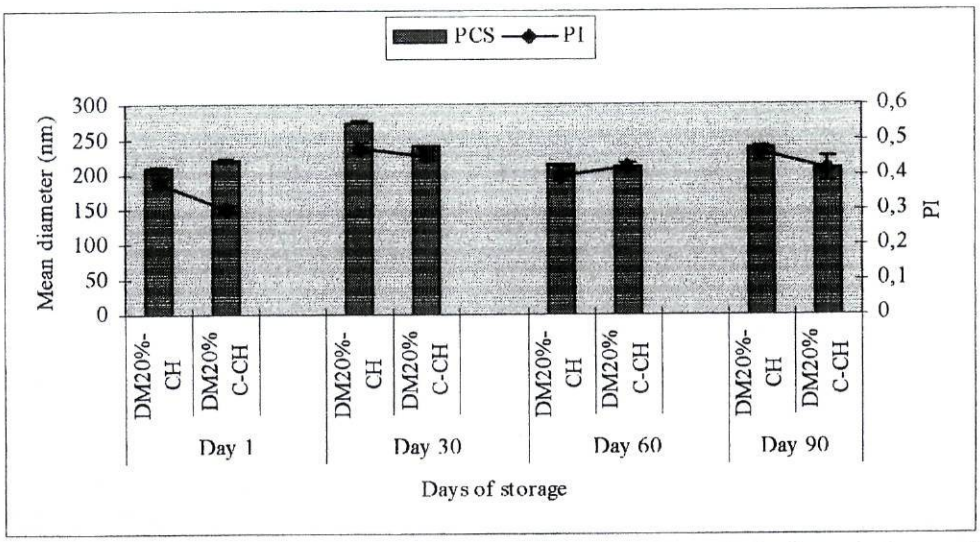

Figure 5.89: Mean particle size measured by PCS and PI of clotrimazole-free and clotrimazole-loaded NLC formulations DM20% and DM20%C incorporated into CH hydrogels after 1, 30, 60 and 90 days of storage at room temperature (20°C).

The incorporation of clotrimazole-free and clotrimazole-loaded NLC containing 20% of lipid matrix into CH hydrogels increased the mean particle size of NLC, in comparison to XG, HEC and PA hydrogels, as reported for SLN containing 10% and 20% of lipid matrix. From LD data, 99% of volume distribution remained approximately 0.7 μm, which is the same as the obtained after incorporation of these particles into XG. However, after PCS analysis a growth of particle size could be observed. PCS data revealed a mean particle size of between 200 and 300 nm and a PI between 0.3 and 0.5 for both drug-free and drug-loaded formulations during 90 days of storage at room temperature during 3 months.

Analysis of the different hydrogels developed in this study revealed no peak in the micrometer range, except for SLN formulations D20% and D20%C containing XG, probably caused by insoluble residues of this polysaccharide.

The lowest particle size obtained after incorporation of SLN and NLC into four different hydrogels was observed for SLN with the lowest lipid content (D10% and D10%C) when incorporated into PA hydrogels.

PA hydrogels were also responsible for the lowest PI value obtained for all tested formulations, while CH hydrogels showed the highest PI, especially for SLN samples containing 10% of lipid matrix.

CH was also responsible for the highest mean particle size for all tested SLN and NLC formulations. This result is probably due to the use of a solution of 4% (*m/V*) acetic acid in order to start gel formation of CH. The use of acetic acid might affect the ζ at the surface of SLN and NLC being responsible for particle aggregation.

5.7.2. Zeta potential of SLN and NLC

Figure 5.90 shows the ζ of clotrimazole-free and clotrimazole-loaded SLN formulations containing 10% of lipid matrix incorporated into XG, HEC, PA and CH hydrogels, measured on day 1 and day 90 after production and stored at room temperature.

Lipid nanoparticles remained negatively charged upon incorporation into XG, HEC and PA hydrogels. The same could not be observed when lipid nanoparticles were incorporated into CH hydrogels. In fact, the ζ of these later particles arose from -37 mV to 45.9 mV for samples without drug and from -11.3 mV to 41.5 mV for drug-loaded SLN formulations, one day after preparation.

The incorporation of D10% and D10%C SLN formulations into XG hydrogels revealed the highest ζ, either on day 1 or on day 90 of storage at room temperature. Incorporation of these particles into HEC and PA hydrogels showed similar ζ values.

In comparison to clotrimazole-free SLN containing 10% of lipid matrix, a decrease of ζ value could be observed for clotrimazole-loaded SLN formulations upon incorporation into four different hydrogels, both on day 1 and day 90 of storage at room temperature.

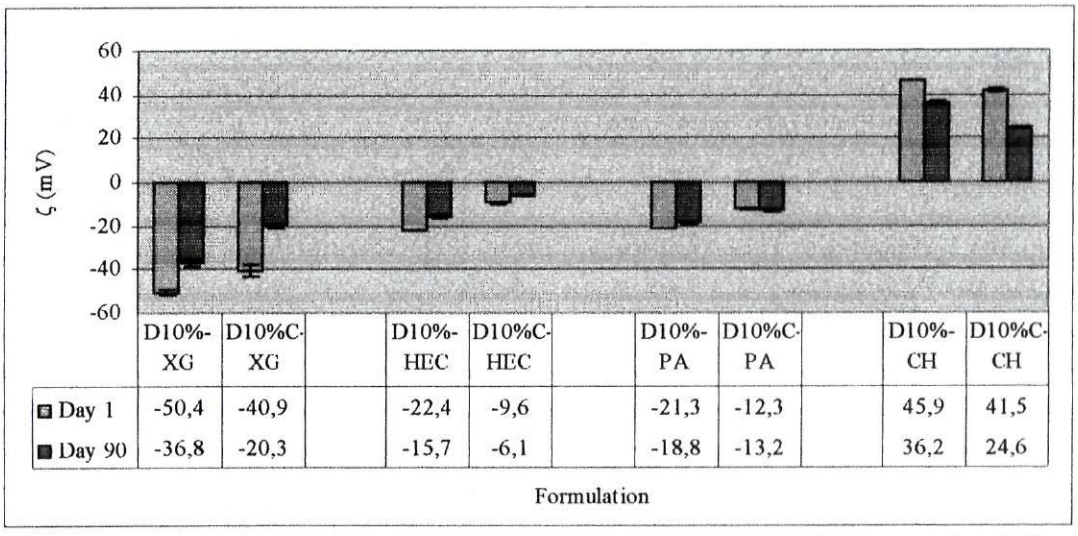

	D10%-XG	D10%C-XG	D10%-HEC	D10%C-HEC	D10%-PA	D10%C-PA	D10%-CH	D10%C-CH
Day 1	-50,4	-40,9	-22,4	-9,6	-21,3	-12,3	45,9	41,5
Day 90	-36,8	-20,3	-15,7	-6,1	-18,8	-13,2	36,2	24,6

Figure 5.90: Zeta potential of clotrimazole-free and clotrimazole-loaded SLN containing 10% of lipid matrix when incorporated into four different hydrogels, measured on day 1 and day 90 after production and stored at room temperature (20°C).

Figure 5.91 shows the ζ of clotrimazole-free and clotrimazole-loaded SLN formulations containing 20% of lipid matrix incorporated into XG, HEC, PA and CH hydrogels, measured on day 1 and day 90 after production and stored at room temperature.

The incorporation of D20% and D20%C SLN formulations into XG, HEC and PA hydrogels also revealed negatively charged, while when incorporated into CH hydrogels the ζ value was positive. The ζ of these later arose from -37 mV to 39.5 mV for drug-free particles and from -11.3 mV to 28.2 mV for drug-loaded SLN formulations, one day after preparation.

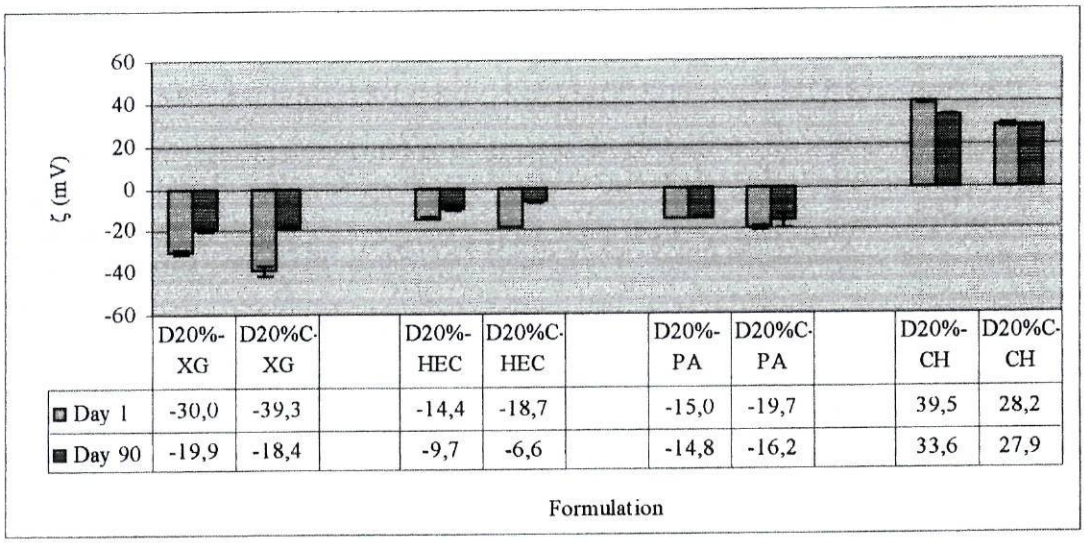

	D20%-XG	D20%C-XG		D20%-HEC	D20%C-HEC		D20%-PA	D20%C-PA		D20%-CH	D20%C-CH
Day 1	-30,0	-39,3		-14,4	-18,7		-15,0	-19,7		39,5	28,2
Day 90	-19,9	-18,4		-9,7	-6,6		-14,8	-16,2		33,6	27,9

Figure 5.85: Zeta potential of clotrimazole-free and clotrimazole-loaded SLN containing 20% of lipid matrix when incorporated into four different hydrogels, measured on day 1 and day 90 after production and stored at room temperature (20°C).

Figure 5.92 shows the ζ of clotrimazole-free and clotrimazole-loaded NLC formulations containing 20% of lipid matrix incorporated into XG, HEC, PA and CH hydrogels, measured on day 1 and day 90 after production and stored at room temperature.

As it could be expected, the incorporation of DM20% and DM20%C into XG, HEC and PA hydrogels also revealed particles negatively charged, while when incorporated into CH hydrogels the ζ value was positive. The ζ of these later arose from -37 mV to 36.8 mV for drug-free particles and from -11.3 mV to 32.5 mV for drug-loaded SLN formulations one day after preparation.

In comparison to SLN formulations with the same lipid content, all NLC formulations revealed lower ζ values on day 1 and 90 of storage at room temperature, except the D20%C when incorporated into XG hydrogels.

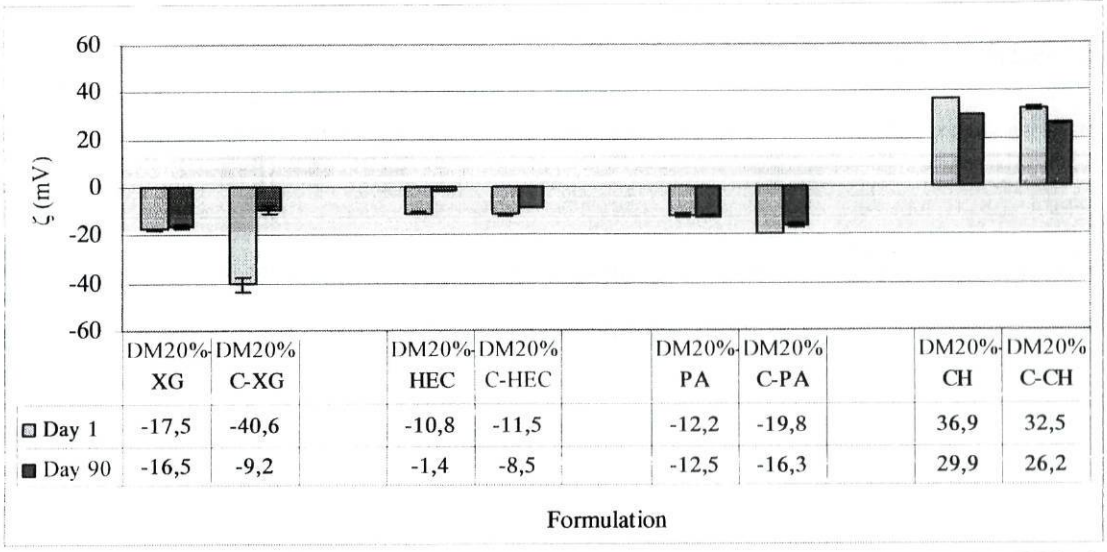

Figure 5.92: Zeta potential of clotrimazole-free and clotrimazole-loaded NLC containing 20% of lipid matrix when incorporated into four different hydrogels, measured on day 1 and day 90 after production and stored at room temperature (20°C).

As expected, for all tested formulations a decrease of ζ during the 90 days of storage could be observed. CH hydrogels were responsible for particles having a positive ζ value. These results are probably due to the cationic character of this bioadhesive polymer. Its positively charged amine groups are capable of neutralizing the negative charge at the surface of the particles changing their ζ. As a consequence of the positive value of ζ, aggregation is facilitated, as it could be observed after particle size analysis. In addition, one needs to use acetic acid in order to start gel formation of CH, which can also be a reason for the observed ζ.

In order to exhibit gel-forming properties, the carboxylic groups of PA have to be neutralized with NaOH. This neutralizing agent could enhance aggregation due to the action of sodium ions, which can reduce the ζ of the particles [322]. As a consequence of this lower ζ value, aggregation is facilitated. This phenomenon is well known for lipid nanoemulsions [97], as well as for SLN when incorporated into PA hydrogels [311]. However, the tested lipid nanoparticles made from *Dynasan*®116 and *Tyloxapol*® revealed no sensitivity to exposure of sodium ions.

In general terms, SLN and NLC aqueous dispersions can be incorporated into hydrogels consisting of more or less uncharged polymers without significant changes in the particle size characteristics and ζ values [107], which has been observed after incorporation of SLN and NLC aqueous dispersions into XG, HEC and PA. In the case of gel forming polymers with very polar groups, like CH, possible interactions between negative surface charge of lipid nanoparticles and polar groups of this polymer must be taken into account.

5.7.3. DSC studies

DSC studies during storage were performed in clotrimazole-containing samples, in order to evaluate the chemical stability of clotrimazole-loaded SLN and NLC into different hydrogels as a function of time.

Figure 5.93 shows the DSC curves of D10%C incorporated into XG hydrogel, obtained after 1 and 90 days of storage at room temperature.

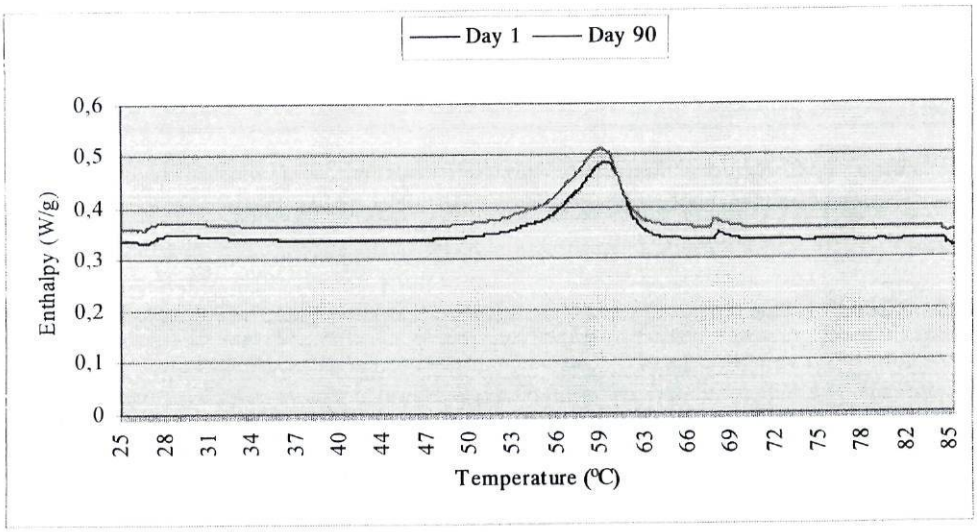

Figure 5.93: DSC curves of D10%C SLN formulation incorporated into XG hydrogel after 1 and 90 days of storage at room temperature (20°C).

Figure 5.94 shows the DSC curves of D10%C incorporated into HEC hydrogel, obtained after 1 and 90 days of storage at room temperature.

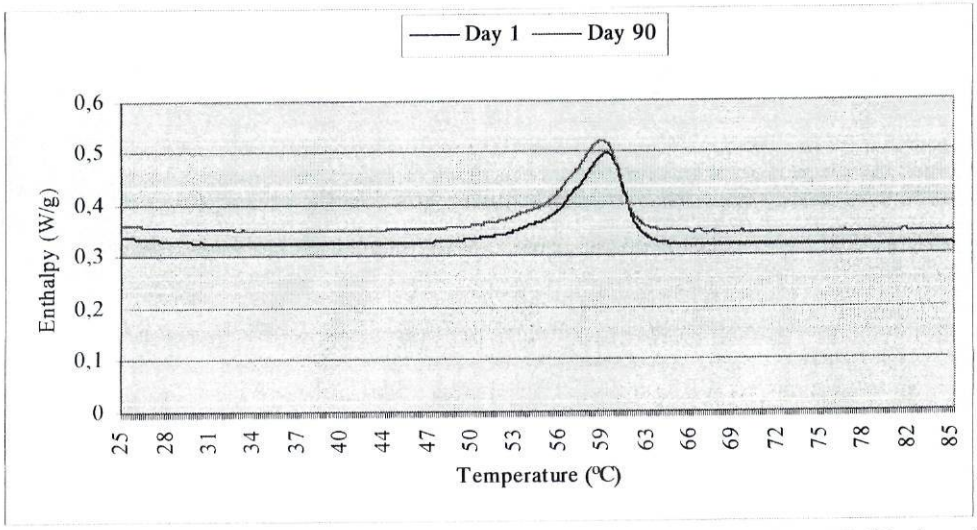

Figure 5.94: DSC curves of D10%C SLN formulation incorporated into HEC hydrogel after 1 and 90 days of storage at room temperature (20°C).

Figure 5.95 shows the DSC curves of D10%C incorporated into PA hydrogel, obtained after 1 and 90 days of storage at room temperature.

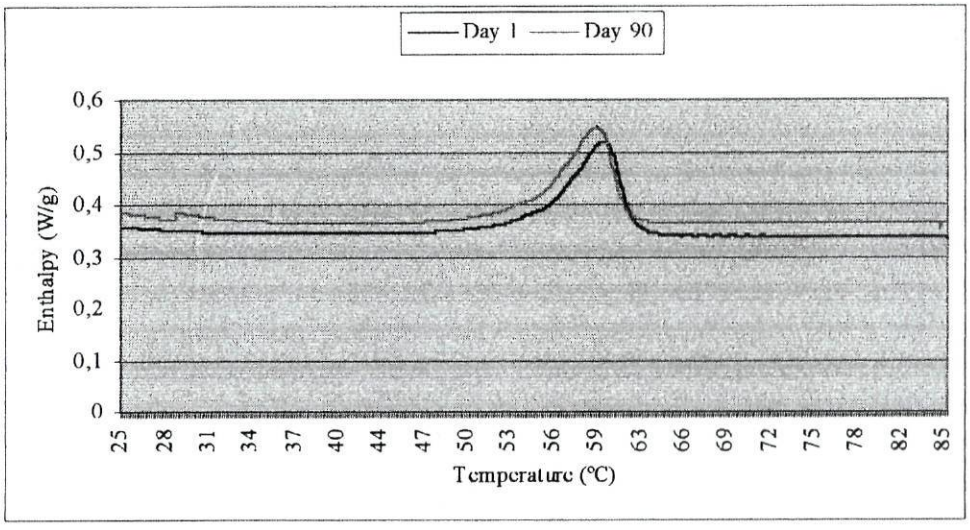

Figure 5.95: DSC curves of D10%C SLN formulation incorporated into PA hydrogel after 1 and 90 days of storage at room temperature (20°C).

Figure 5.96 shows the DSC curves of D10%C incorporated into CH hydrogel, obtained after 1 and 90 days of storage at room temperature.

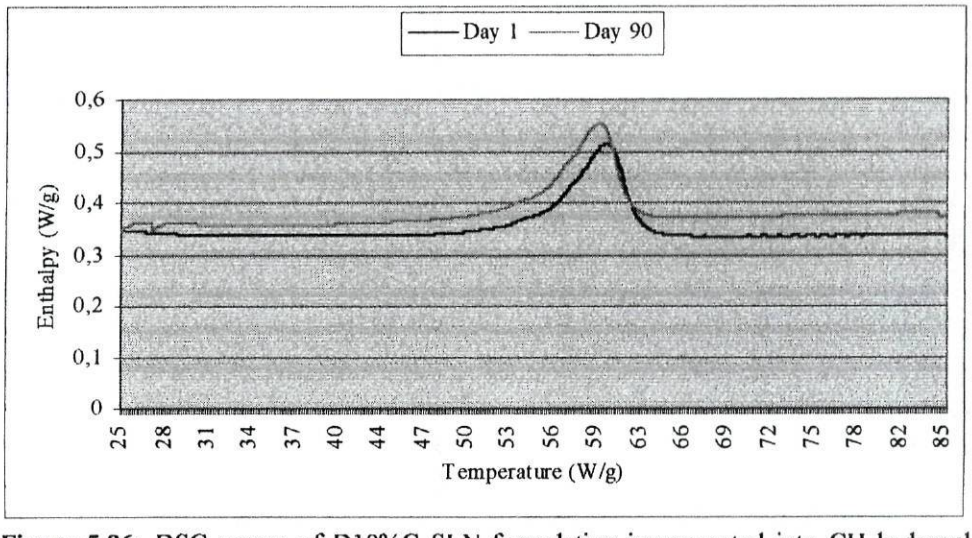

Figure 5.96: DSC curves of D10%C SLN formulation incorporated into CH hydrogel after 1 and 90 days of storage at room temperature (20°C).

Figure 5.97 shows the DSC curves of D20%C incorporated into XG hydrogel, obtained after 1 and 90 days of storage at room temperature.

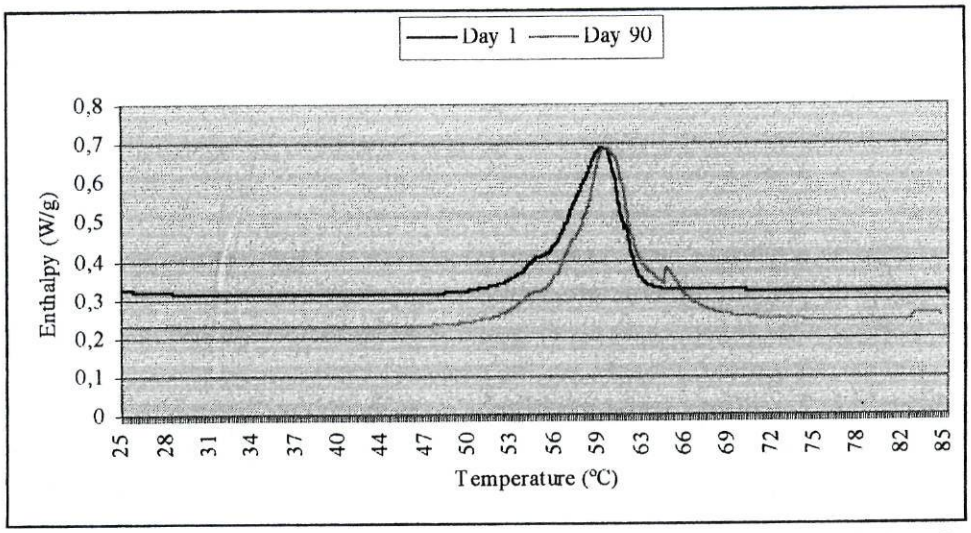

Figure 5.97: DSC curves of D20%C SLN formulation incorporated into XG hydrogel after 1 and 90 days of storage at room temperature (20°C).

Figure 5.98 shows the DSC curves of D20%C incorporated into HEC hydrogel, obtained after 1 and 90 days of storage at room temperature.

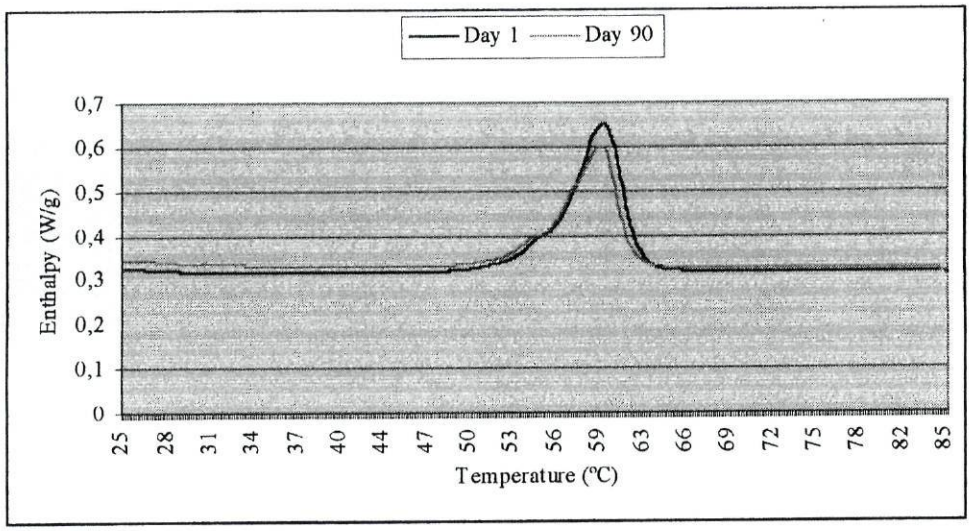

Figure 5.98: DSC curves of D20%C SLN formulation incorporated into HEC hydrogel after 1 and 90 days of storage at room temperature (20°C).

Figure 5.99 shows the DSC curves of D20%C incorporated into PA hydrogel, obtained after 1 and 90 days of storage at room temperature.

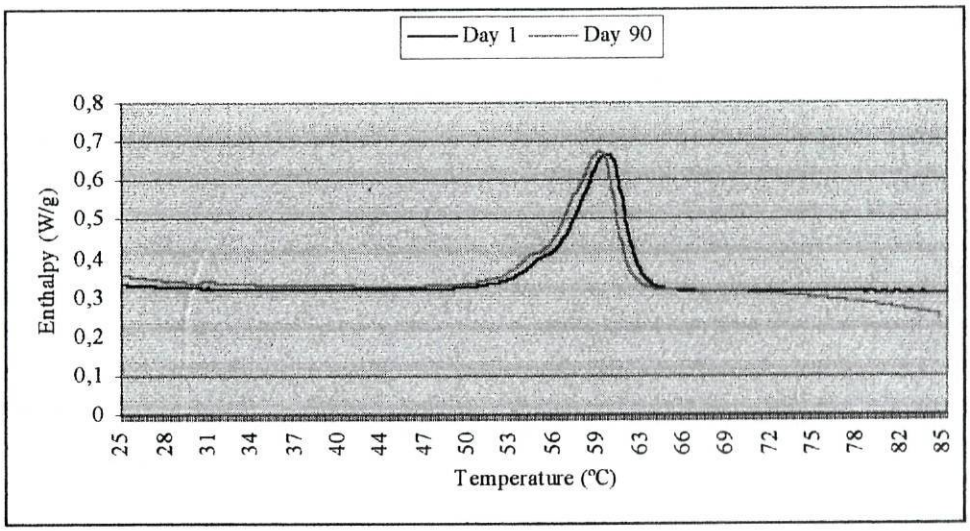

Figure 5.99: DSC curves of D20%C SLN formulation incorporated into PA hydrogel after 1 and 90 days of storage at room temperature (20°C).

Figure 5.100 shows the DSC curves of D20%C incorporated into CH hydrogel, obtained after 1 and 90 days of storage at room temperature.

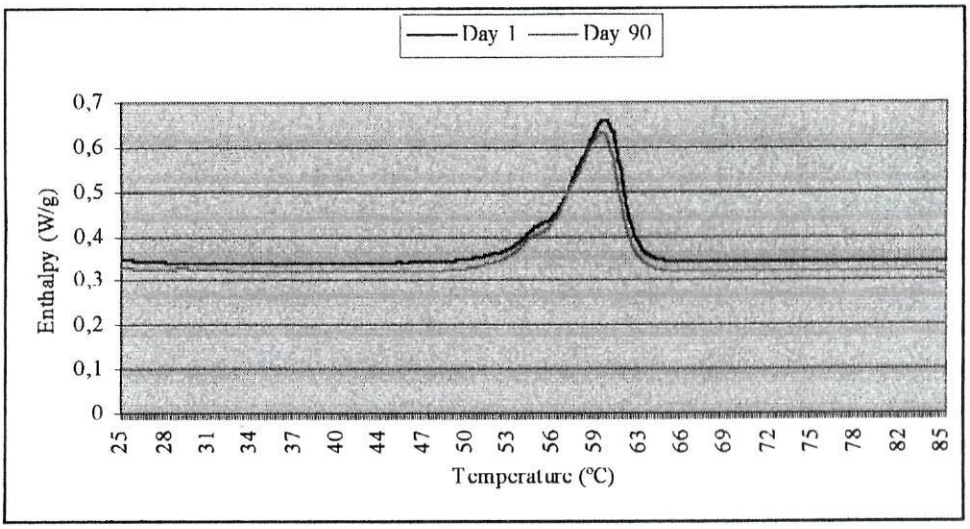

Figure 5.100: DSC curves of D20%C SLN formulation incorporated into CH hydrogel after 1 and 90 days of storage at room temperature (20°C).

Figure 5.101 shows the DSC curves of DM20%C incorporated into XG hydrogel, obtained after 1 and 90 days of storage at room temperature.

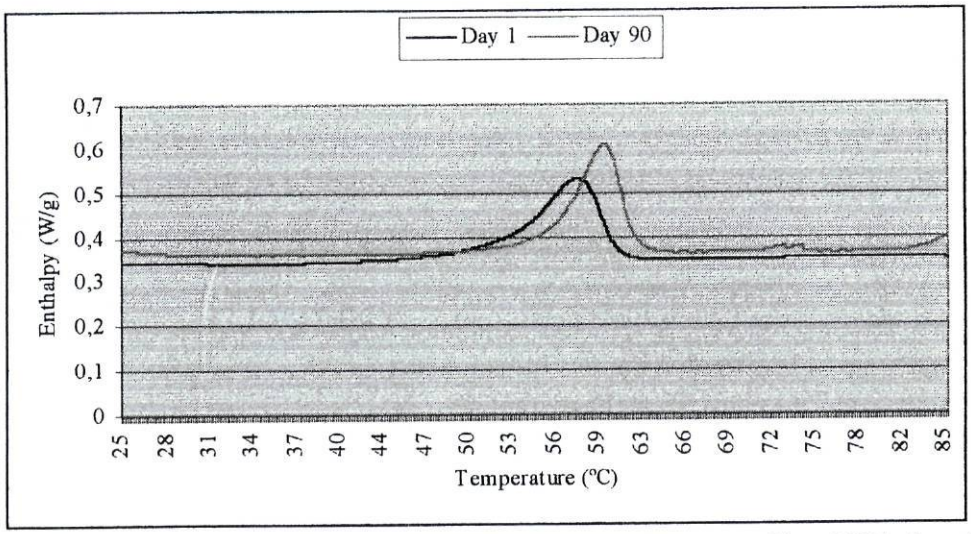

Figure 5.101: DSC curves of DM20%C NLC formulation incorporated into XG hydrogel after 1 and 90 days of storage at room temperature (20°C).

Figure 5.102 shows the DSC curves of DM20%C incorporated into HEC hydrogel, obtained after 1 and 90 days of storage at room temperature.

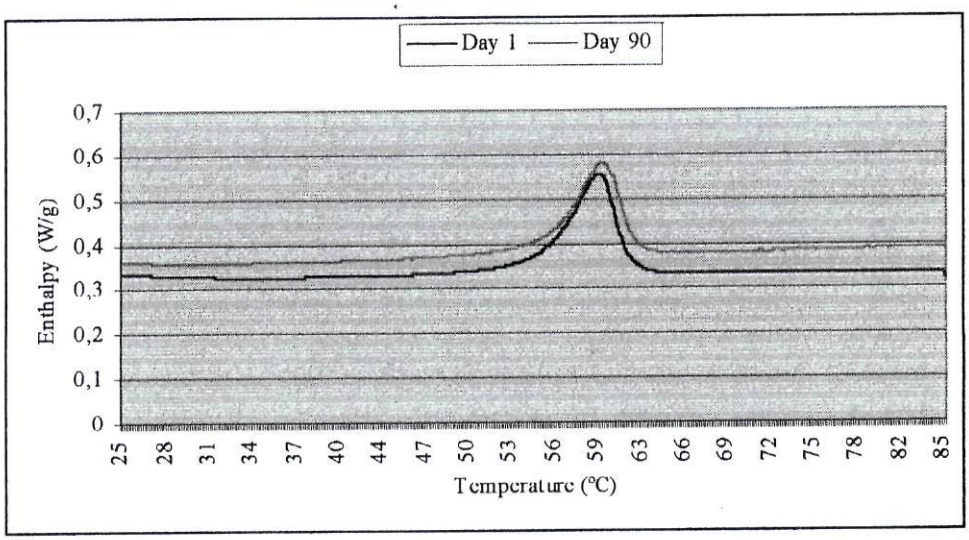

Figure 5.102: DSC curves of DM20%C NLC formulation incorporated into HEC hydrogel after 1 and 90 days of storage at room temperature (20°C).

Figure 5.103 shows the DSC curves of DM20%C incorporated into PA hydrogel, obtained after 1 and 90 days of storage at room temperature.

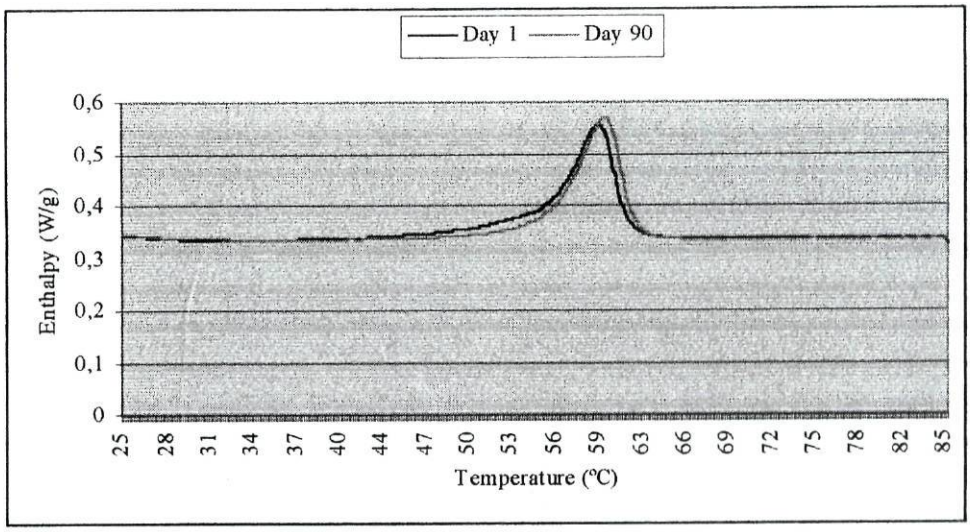

Figure 5.103: DSC curves of DM20%C NLC formulation incorporated into PA hydrogel after 1 and 90 days of storage at room temperature (20°C).

Figure 5.104 shows the DSC curves of DM20%C incorporated into CH hydrogel, obtained after 1 and 90 days of storage at room temperature.

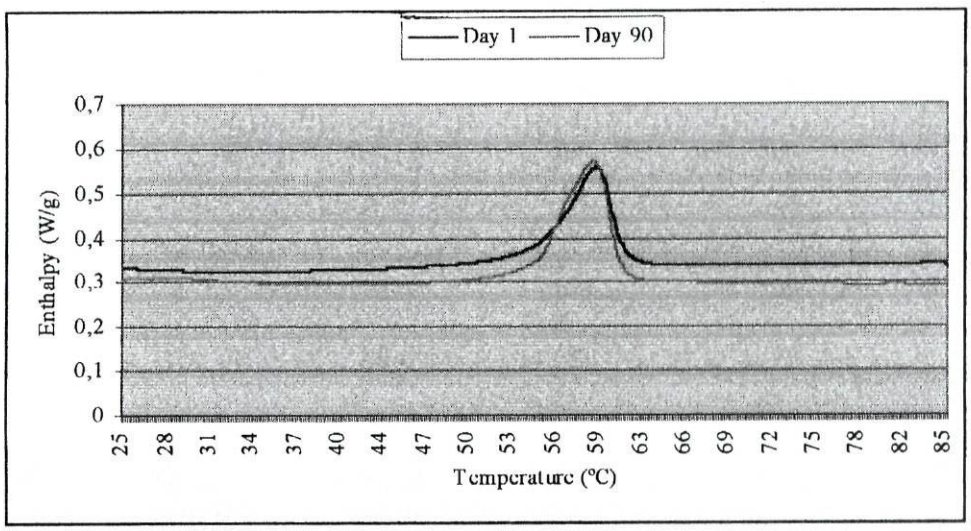

Figure 5.104: DSC curves of DM20%C NLC formulation incorporated into CH hydrogel after 1 and 90 days of storage at room temperature (20°C).

For all clotrimazole-loaded SLN and NLC formulations incorporated into different hydrogels it could be observed that during storage time the crystallinity of lipid matrix was practically constant. The melting enthalpy remained almost the same during 90 days of storage at room temperature, showing a melting event at 60°C.

To summarise, for all clotrimazole-loaded SLN and NLC containing hydrogels could be observed that crystallinity of the solid matrix remained practically constant during 90 days of storage at room temperature. Table XXIX shows the DSC results of clotrimazole-loaded SLN and NLC aqueous dispersions after their incorporation into different hydrogel formulations, obtained on day 1 and 90 after preparation.

Table XXIX: DSC results of clotrimazole-loaded SLN and NLC aqueous dispersions after their incorporation into different hydrogel formulations, obtained on day 1 and 90 after production.

Formulation	Days of storage	Melting point (°C)	Onset (°C)	Integral (mJ)	Enthalpy (J/g)	RI (%)
D10%C-XG	1	59.08	56.22	737.88	8.77	45.3
	90	59.57	55.25	746.39	8.67	44.8
D10%C-HEC	1	59.21	55.43	744.68	8.69	44.9
	90	61.38	60.60	745.53	8.68	44.9
D10%C-PA	1	59.17	55.72	748.99	8.64	44.7
	90	59.27	55.11	749.85	8.63	44.6
D10%C-CH	1	59.27	55.31	737.04	8.78	45.4
	90	59.32	55.19	738.73	8.76	45.3
D20%C-XG	1	59.14	55.07	424.07	15.26	78.9
	90	59.59	57.15	424.62	15.24	78.8
D20%C-HEC	1	59.01	56.11	425.46	15.21	78.6
	90	59.28	55.03	426.02	15.19	78.5
D20%C-PA	1	59.21	55.46	423.23	15.29	79.0
	90	59.37	55.19	423.79	15.27	78.9
D20%C-CH	1	59.25	55.14	424.62	15.24	78.8
	90	59.58	55.00	424.90	15.23	78.7
DM20%C-XG	1	58.81	55.42	563.21	11.49	59.4
	90	57.75	52.51	564.19	11.47	59.3
DM20%C-HEC	1	58.87	55.17	566.16	11.43	59.1
	90	53.18	51.36	567.15	11.41	59.0
DM20%C-PA	1	58.80	55.59	564.68	11.46	59.2
	90	58.77	56.13	565.67	11.44	59.1
DM20%C-CH	1	58.76	55.18	568.15	11.39	58.9
	90	58.97	54.89	569.15	11.37	58.8

5.8. Rheological properties of SLN and NLC aqueous dispersions and hydrogels

Conventional SLN and NLC aqueous dispersions contain about 10-20% (*m/m*) of lipid matrix and 80-90% (*m/m*) of water [48,81,113]. Therefore, their loading into a topical dosage form is limited. Hence drug loading is also limited. In addition, solid lipid particle liquid dispersions possess a low viscosity (approximately 100 mPa.s) and a yield value (Chapter IV, section 4.9) of practically zero [311]. Therefore, SLN and NLC aqueous dispersions usually have to be incorporated in convenient topical dosage forms, like hydrogels or creams, in order to obtain a topical application form having the desired semi-solid consistency [113,119].

Incompatibilities with hydrogel or cream ingredients may occur due to interactions between the gel forming polymer, emulsifying agents, lipid and drug. Aggregation of the solid nanoparticles is also possible, especially when using polar gel forming polymers, like charged polysaccharides [107]. The use of neutralizing agents, like NaOH, for preparation of polyacrylic acid gels can also affect particle size, as reported above. Electrolytes, like sodium ions, can reduce the ζ of the particles, leading to aggregation, which is well known also for lipid nanoemulsions [97]. All these phenomena are able to affect the semi-solid consistency of the topical formulation and, therefore, its rheological status.

The rheological status of a semi-solid drug carrier system is a very important physical parameter to study in the development process of a potential new drug delivery system for topical use [302]. Rheological measurements provide essential information on different aspects concerning semi-solid preparations, such as application and performance on skin. Furthermore, drug release from semi-solid vehicles is influenced by their rheological behaviour.

Rheometry might be particularly useful for the characterization of the viscoelastic properties of SLN and NLC aqueous dispersions and of SLN and NLC-containing hydrogels. Therefore, in the present work, an oscillation frequency sweep test was carried out for all developed SLN and NLC aqueous dispersions. In addition, continuous shear investigations were performed in all developed hydrogel formulations, in order to evaluate the shear rate as a function of shear stress.

5.8.1. Oscillation frequency sweep test

When performing oscillation measurements first the linear viscoelastic region has to be determined by a stress sweep at a constant frequency. As reported in Chapter IV, stress sweep is a dynamic test where the complex modulus G* is measured as a function of stress at a constant frequency. The range of stress over which G* is independent of the applied stress is called the linear viscoelastic region. Over the linear region the structure of the dispersion remains intact. Being in the viscoelastic region for all tested formulations 5 Pa was chosen as stress amplitude in the following studies.

In order to get information about the viscous and elastic behaviour of the investigated systems and the network structure formed by particle-particle interactions an oscillation frequency sweep test has to be performed. This test provides a fingerprint of a viscoelastic system under non-destructive conditions [320]. The shape of the material function curves reveals structural characteristics of the system. Therefore, in the present work this test was performed over a frequency range from 0 to 10 Hz at constant stress amplitude of 5 Pa.

Figures 5.105 and 5.106 show the results of the oscillation frequency sweep test of clotrimazole-free and clotrimazole-loaded SLN formulations containing 10% of lipid matrix, respectively, after 1 day of storage at room temperature.

As it can be observed in both figures, the storage modulus G' (elastic component) is grater than the loss modulus G'' (viscous component) over the measured frequency range, which indicates the presence of a gel-like structure. Both parameters show a strong dependence on the applied frequency, i.e. they increase with the increase of the frequency. The presence of clotrimazole increased the magnitude of viscosity (η*).

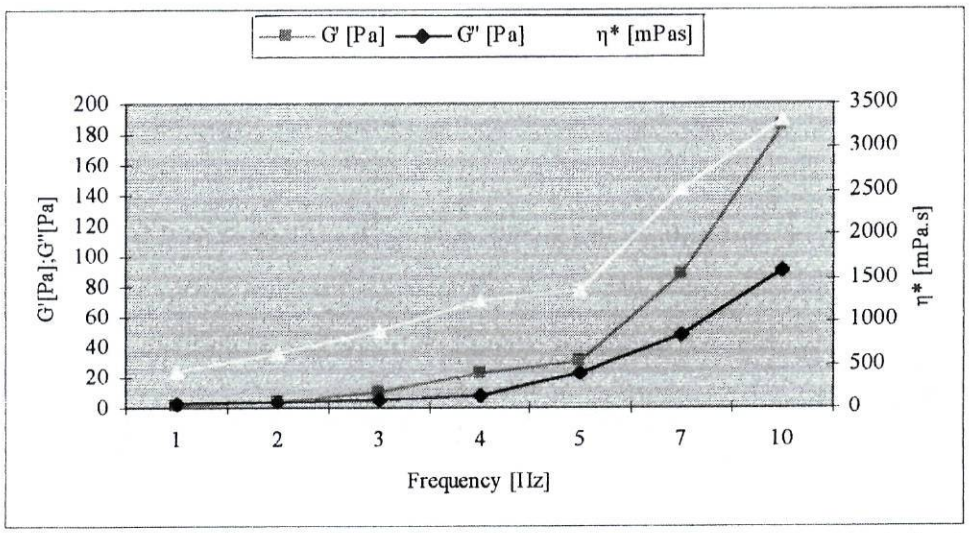

Figure 5.105: Storage modulus (G'), loss modulus (G'') and complex viscosity (η*) of clotrimazole-free SLN formulation D10%, as a function of the frequency at a constant stress amplitude of 5 Pa.

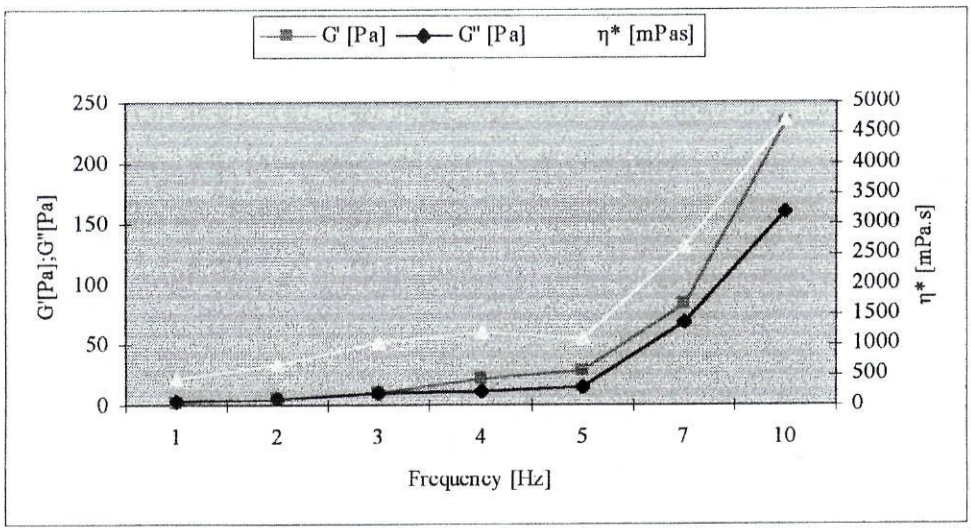

Figure 5.106: Storage modulus (G'), loss modulus (G'') and complex viscosity (η*) of clotrimazole-loaded SLN formulation D10%C, as a function of the frequency at a constant stress amplitude of 5 Pa.

Figures 5.107 and 5.108 show the results of the oscillation frequency sweep test of clotrimazole-free and clotrimazole-loaded SLN formulations containing 20% of lipid matrix, respectively, after 1 day of storage at room temperature.

Both figures also evidence the storage modulus G' (elastic component) far grater than the loss modulus G'' (viscous component) over the measured frequency range, indicating the presence of a gel-like structure. The loss modulus G'' shows weak dependence on the applied frequency, i.e. it remains practically the same over the frequency range, while the storage modulus G' is more dependent on the applied frequency, especially when clotrimazole is present. The viscosity (η^*) decreases with increasing frequency.

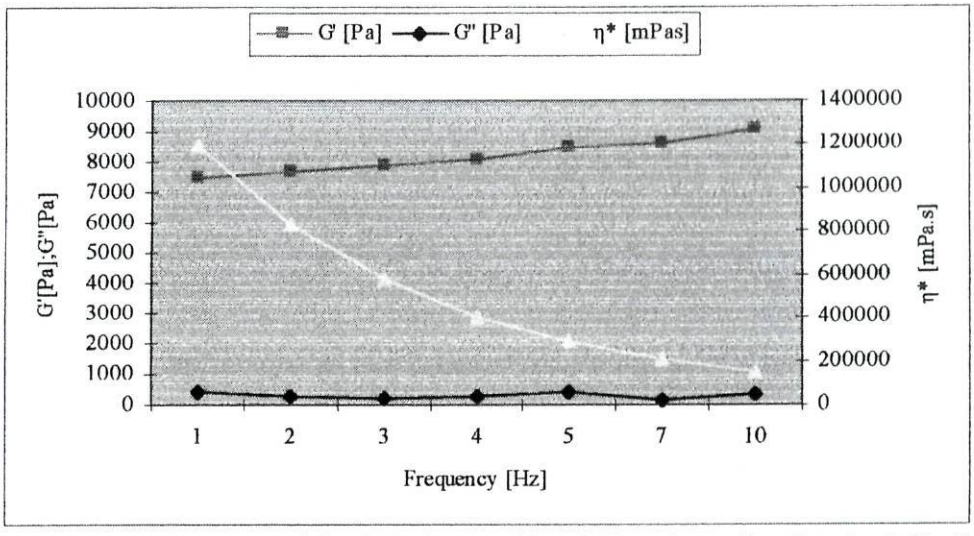

Figure 5.107: Storage modulus (G'), loss modulus (G'') and complex viscosity (η^*) of clotrimazole-free SLN formulation D20%, as a function of the frequency at a constant stress amplitude of 5 Pa.

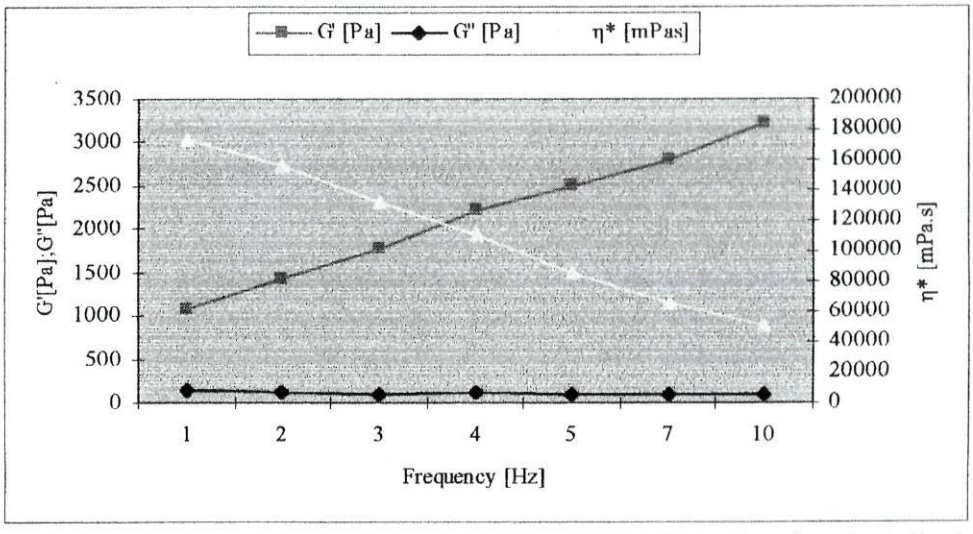

Figure 5.108: Storage modulus (G'), loss modulus (G'') and complex viscosity (η^*) of clotrimazole-loaded SLN formulation D20%C, as a function of the frequency at a constant stress amplitude of 5 Pa.

Figures 5.109 and 5.110 show the results of the oscillation frequency sweep test of clotrimazole-free and clotrimazole-loaded NLC formulations containing 20% of lipid matrix, respectively, after 1 day of storage at room temperature.

With regard to NLC formulations, the presence of clotrimazole in the lipid matrix was more emphasized than clotrimazole-loaded SLN formulations prepared with the same lipid content. Regarding drug-free NLC, the storage modulus G' appeared not so far from the loss modulus G'' over the measured frequency range, while clotrimazole-loaded NLC seemed to have a gel-like structure because G' and G'' are far grater from each other during the same frequency range. The increase of the applied frequency was followed by an increase in viscosity (η*) for drug-free NLC formulations and a decrease in viscosity for drug-loaded NLC formulations.

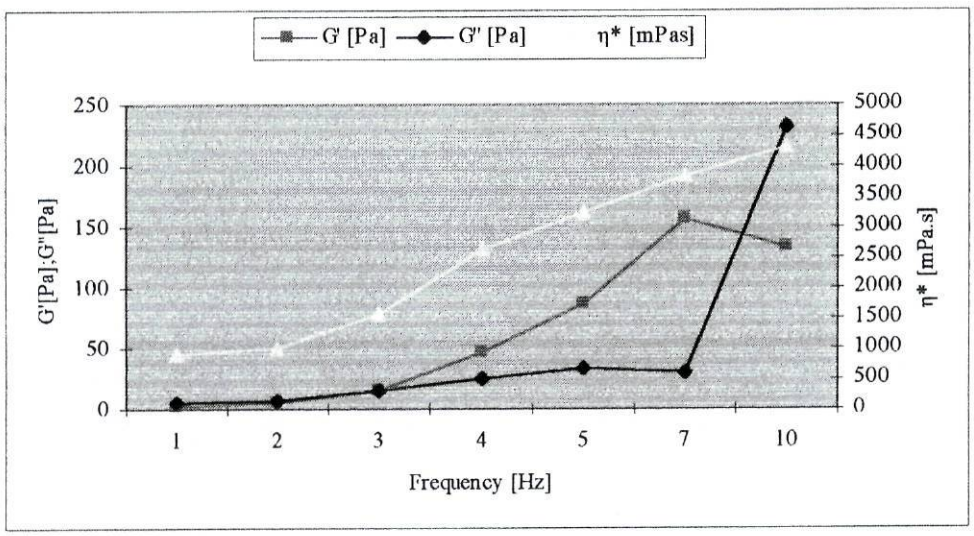

Figure 5.109: Storage modulus (G'), loss modulus (G'') and complex viscosity (η*) of clotrimazole-free NLC formulation DM20%, as a function of the frequency at a constant stress amplitude of 5 Pa.

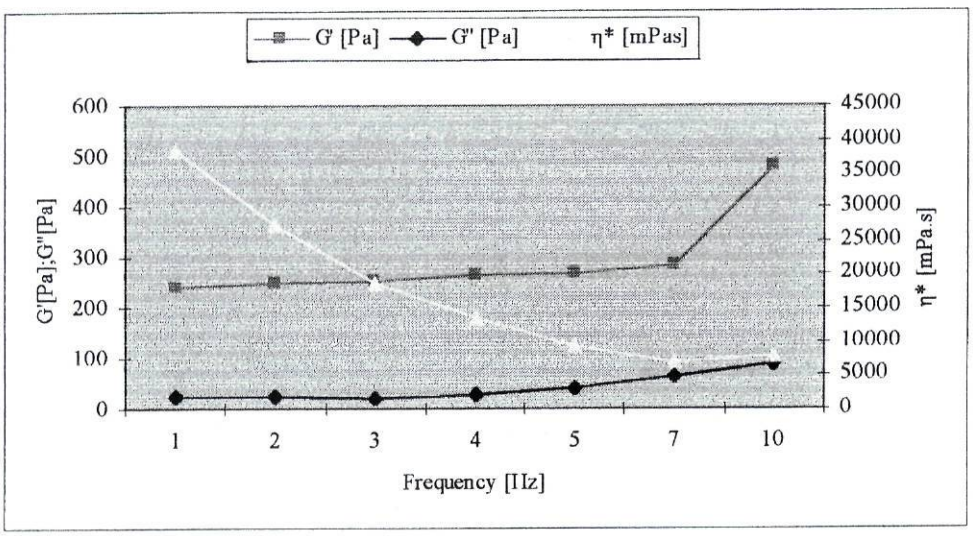

Figure 5.110: Storage modulus (G'), loss modulus (G'') and complex viscosity (η*) of clotrimazole-loaded NLC formulation DM20%C, as a function of the frequency at a constant stress amplitude of 5 Pa.

Lippacher showed that SLN dispersions possess higher elastic properties than emulsions of comparable lipid content [320]. In fact, if the storage modulus G' is higher by about one order of magnitude than the loss modulus G'', and if both parameters show weak dependence on the applied frequency, the system is more elastic than viscous in the investigated frequency range [320]. The decrease in viscosity observed by increasing the applied frequency is also typical for viscoelastic solids and can be found for standard topical dosage forms, like *Unguentum emulsificans aquosum* [113]. These results could be observed for SLN aqueous dispersions containing 20% of lipid matrix.

A completely different rheological behaviour, as a function of the frequency, could be detected with 10% and 20% SLN dispersions. SLN aqueous dispersions having less lipid content reveal a complex viscosity and both moduli much lower, which exhibit the much weaker structure of the system having a more liquid-like character. In addition G' and G'' are more dependent on the applied frequency than SLN aqueous dispersions having higher lipid content. Concerning to NLC aqueous dispersions, a typical viscoelastic behaviour could be observed for drug-loaded systems.

To summarize, it was found that increasing the lipid concentration leads to a dramatic change in the rheological properties. In the present study, the viscoelastic properties were found to be comparable to standard dermal preparations, as reported earlier [113]. Therefore, semi-solid SLN aqueous dispersions appear a promising topical dosage form, especially when they are formulated with high lipid content.

5.8.2. Continuous shear rheometry

The rheological behaviour of hydrogels containing either SLN or NLC was evaluated after one week of storage at room temperature.

Figures 5.111 and 5.112 show the flow curves of developed XG hydrogels containing clotrimazole-free and clotrimazole-loaded SLN and NLC formulations, respectively.

The incorporation of lipid particles into XG hydrogels resulted in flow curves with plastic characteristics, where the shear rate increases by increasing shear stress. Ascending and descending flow curve overlap, showing no time effects like e.g. thixotropy. Lipid particles in the semi-solid system tend to align with increasing shear stress, which is alleviating the flow. This phenomenon was more emphasized for DM20% and D10%C, while SLN with higher lipid content (D20% and D20%C) revealed less dependency upon the applied shear stress.

The presence of clotrimazole increased the magnitude of the recorded shear rate during the experiment.

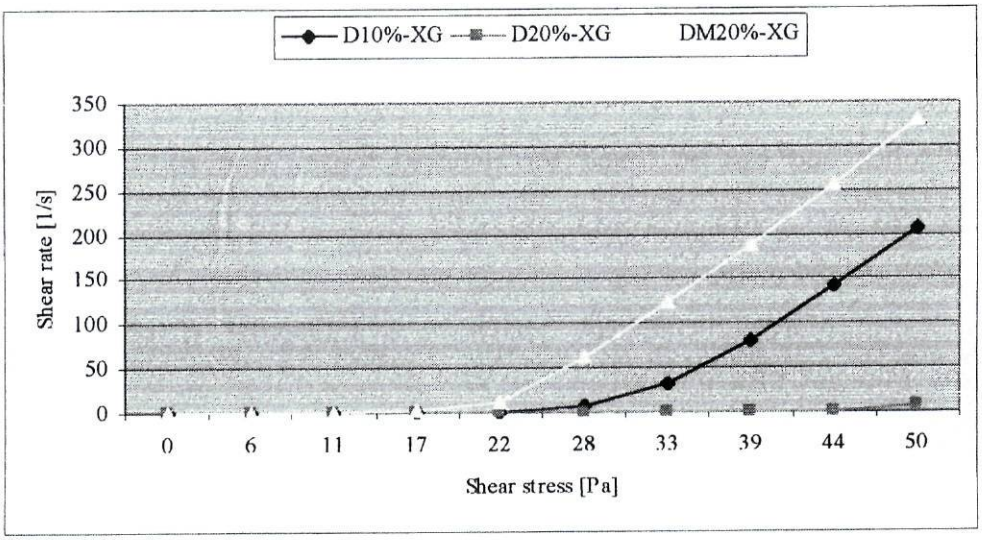

Figure 5.111: Shear rate of XG hydrogels containing clotrimazole-free lipid nanoparticles D10%, D20% and DM20%, as a function of shear stress.

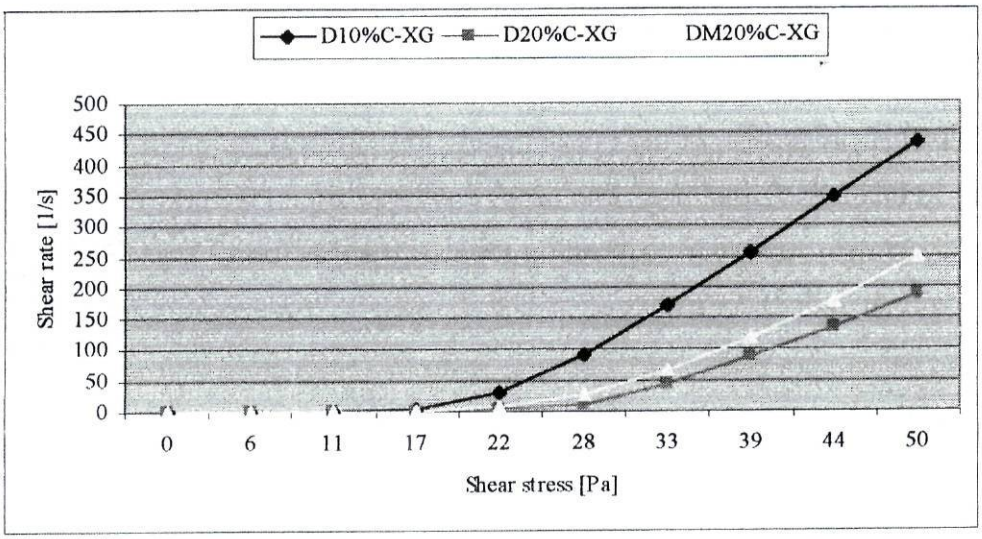

Figure 5.112: Shear rate of XG hydrogels containing clotrimazole-loaded lipid nanoparticles D10%C, D20%C and DM20%C, as a function of shear stress.

Figures 5.113 and 5.114 show the flow curves of the developed HEC hydrogels containing clotrimazole-free and clotrimazole-loaded SLN and NLC formulations, respectively.

The flow curves of HEC hydrogels containing D20%, D20%C, DM20% and DM20%C also revealed plastic characteristics. Nevertheless, the incorporation of D10% and D10%C into HEC hydrogels appeared to be responsible for a more pseudoplastic behaviour with a yield value almost zero, due to their lower lipid content. The increase of lipid content showed less dependency upon the applied shear stress.

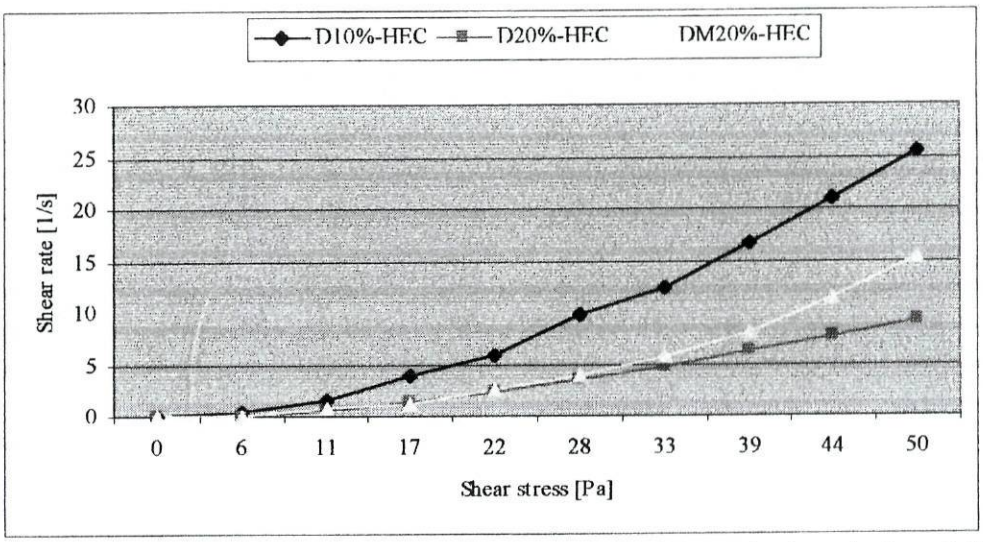

Figure 5.113: Shear rate of HEC hydrogels containing clotrimazole-free lipid nanoparticles D10%, D20% and DM20%, as a function of shear stress.

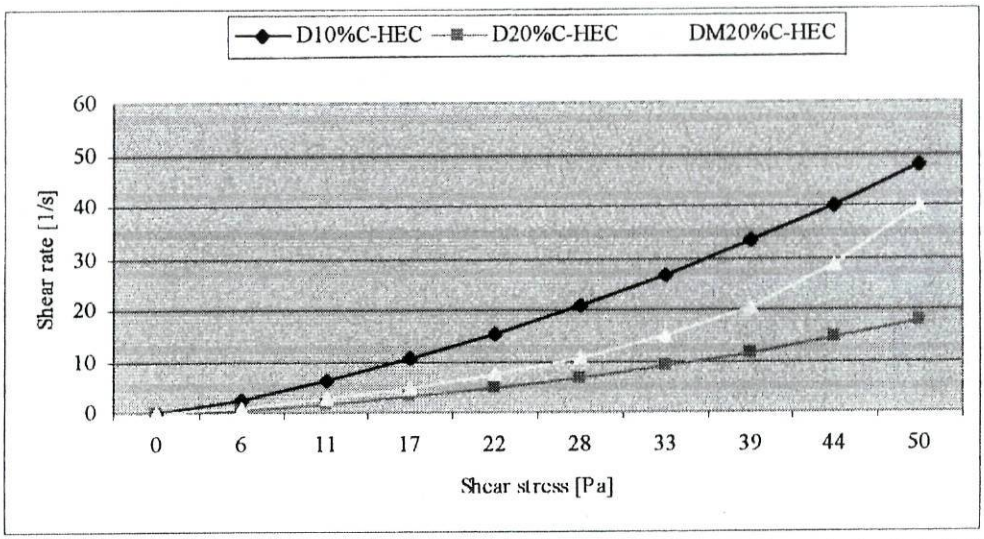

Figure 5.114: Shear rate of HEC hydrogels containing clotrimazole-loaded lipid nanoparticles D10%C, D20%C and DM20%C, as a function of shear stress.

Figures 5.115 and 5.116 show the flow curves of developed PA hydrogels containing clotrimazole-free and clotrimazole-loaded SLN and NLC formulations, respectively.

The incorporation of SLN and NLC aqueous dispersions into PA hydrogels was responsible for a significant increase in yield value especially for SLN formulations. Unlike SLN containing 10% of lipid content (D10% and D10%C) and NLC formulations (DM20% and DM20%C) the ascending and descending curve of SLN containing 20% of lipid content did not overlap, showing thixotropy. NLC formulations (DM20% and DM20%C) revealed more dependency upon the applied shear stress.

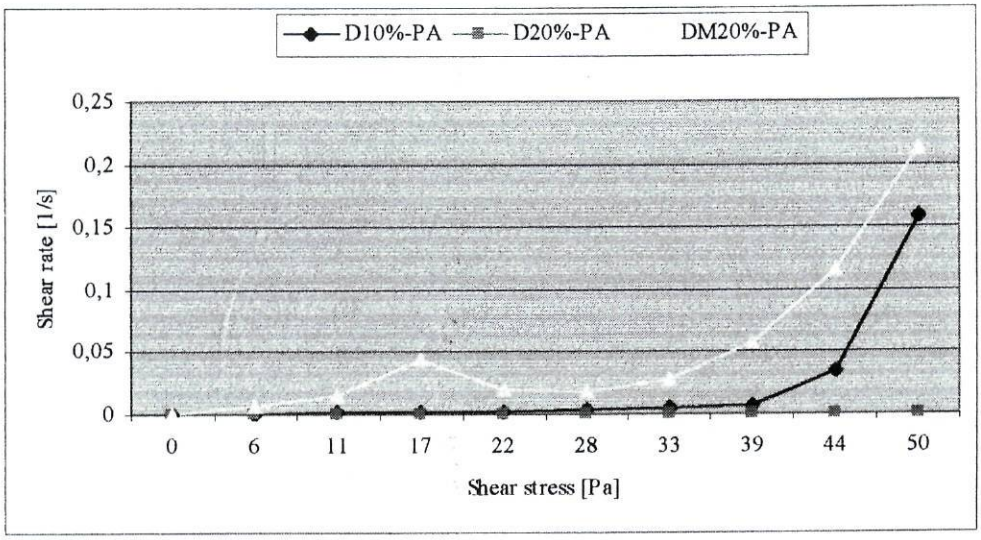

Figure 5.115: Shear rate of PA hydrogels containing clotrimazole-free lipid nanoparticles D10%, D20% and DM20%, as a function of shear stress.

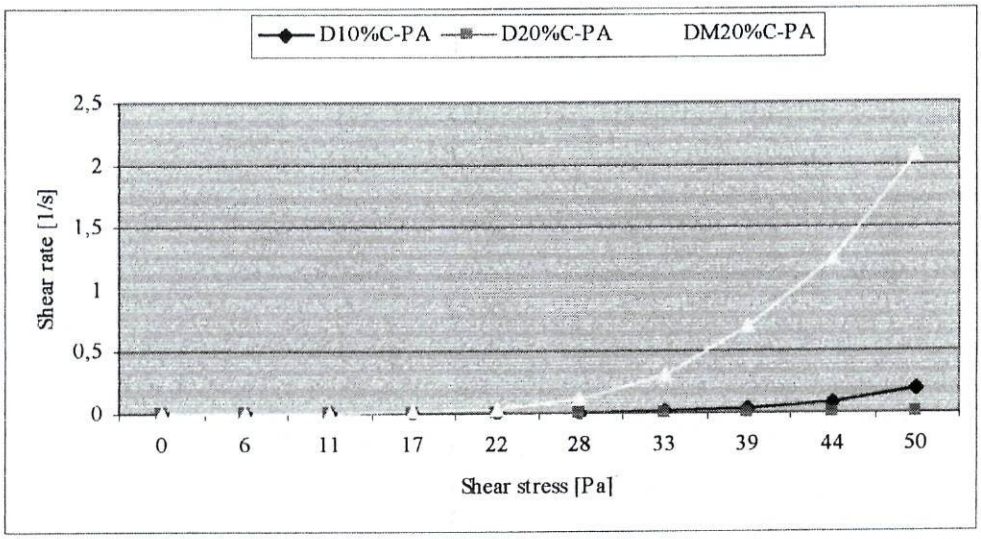

Figure 5.116: Shear rate of PA hydrogels containing clotrimazole-loaded lipid nanoparticles D10%C, D20%C and DM20%C, as a function of shear stress.

Figures 5.117 and 5.118 show the flow curves of developed CH hydrogels containing clotrimazole-free and clotrimazole-loaded SLN and NLC formulations, respectively.

Concerning to CH hydrogels, a more pseudoplastic behaviour with a yield value of approximately zero was observed for formulations containing NLC or SLN with lower lipid content. The presence of drug into SLN containing 20% of lipid matrix revealed a more plastic behaviour, probably due to the higher mean particle size observed after PCS analysis of these systems.

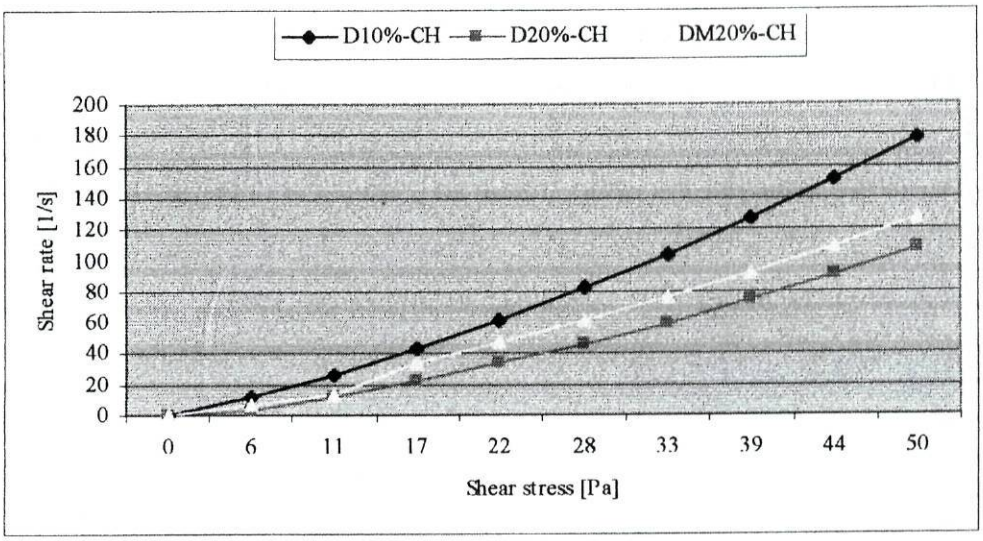

Figure 5.117: Shear rate of CH hydrogels containing clotrimazole-free lipid nanoparticles D10%, D20% and DM20%, as a function of shear stress.

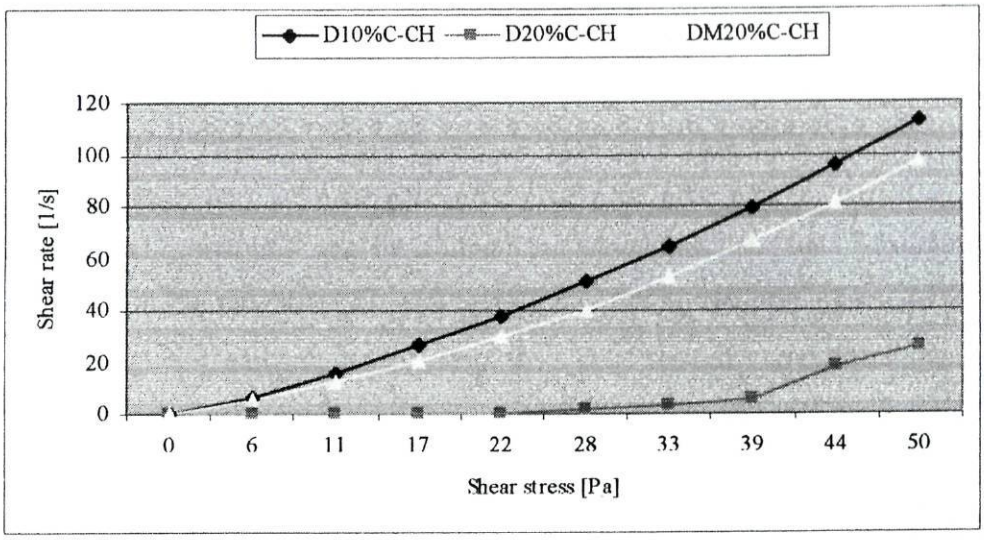

Figure 5.118: Shear rate of CH hydrogels containing clotrimazole-loaded lipid nanoparticles D10%C, D20%C and DM20%C, as a function of shear stress.

In conclusion, the increase of the hydrogel lipid content leads to different flow characteristics. For hydrogels with higher lipid content, thixotropy could be observed.

HEC and CH hydrogels are more liquid and they might not have a good consistency for topical administration. On the contrary, XG and PA hydrogels containing SLN and NLC revealed better rheological properties. Therefore, it can be envisaged that the combination of these later gel forming agents with SLN and NLC aqueous dispersions might comprise a novel drug delivery system for topical administration.

5.9. Occlusive properties of SLN and NLC aqueous dispersions and hydrogels

It is well known that occlusion effect enhances the penetration of drugs through the *stratum corneum*, due to an increase in hydration of this layer [27]. For dermatological preparations occlusion is mainly achieved by using liquid and semi-solid paraffin [174]. However, these formulations feel greasy and have a glossy appearance. To overcome these drawbacks SLN-containing topical formulations were suggested for this purpose [290].

Generally, nanoparticles are adhesive (i.e. they tend to adhere to cells and surfaces) and due to the film of nanoparticles formed on the surface of the skin, SLN possess occlusive properties [47,174,187,309]. This phenomenon offer the possibility to enhance the efficacy of drugs [174].

The occlusivity can be quantitatively evaluated *in vitro* by a filter test and *in vivo* by measurement of the transepidermal water loss (TEWL). For SLN the first systematic occlusion study was performed by Wissing *et al.*, which have investigated the influence of the chemical nature of the lipid, the crystallinity of the lipid matrix and the particle size on occlusion effect [47].

In the present work, the occlusive effect of SLN and NLC aqueous dispersions and hydrogels containing SLN and NLC was analysed by the de Vringler *in vitro* test [290]. The dependency of occlusion factor F was determined as a function of the following factors: (i) number of homogenization cycles applied for sample preparation; (ii) used sample mass in the experiment; (iii) lipid formulation type (SLN or NLC); (iv) presence of clotrimazole and (v) type of hydrogel (XG, HEC, PA and CH). The occlusion factor F has been determined as a function of time, i.e. after 6, 24 and 48 hours of storage, at 32°C and 50% of relative humidity. Every experiment was carried out in triplicate.

5.9.1. Dependency upon the number of homogenization cycles

In order to study the dependency of the occlusion factor F upon the number of homogenization cycles, 200 mg of D10%, D20% and DM20% aqueous dispersions were applied at the surface of a filter, as described in Chapter IV, section 4.10. A visible film formation on top of the filter paper could be observed during the experiment. SLN and NLC aqueous dispersions applying 1 to 5 homogenization cycles were prepared, physicochemically characterized and their occlusion factor was determined after 6, 24 and 48 hours of incubation time.

Figures 5.119, 5.120 and 5.121 show the relationship between the occlusion factor F, the number of homogenization cycles and the particle size for D10%, D20% and DM20% aqueous

dispersions, respectively. According to the obtained results, the dependency of the occlusion factor F upon the particle size is perfectly clear. For all tested formulations it could be observed the increase of F with the decrease of the size of the lipid particles measured by PCS.

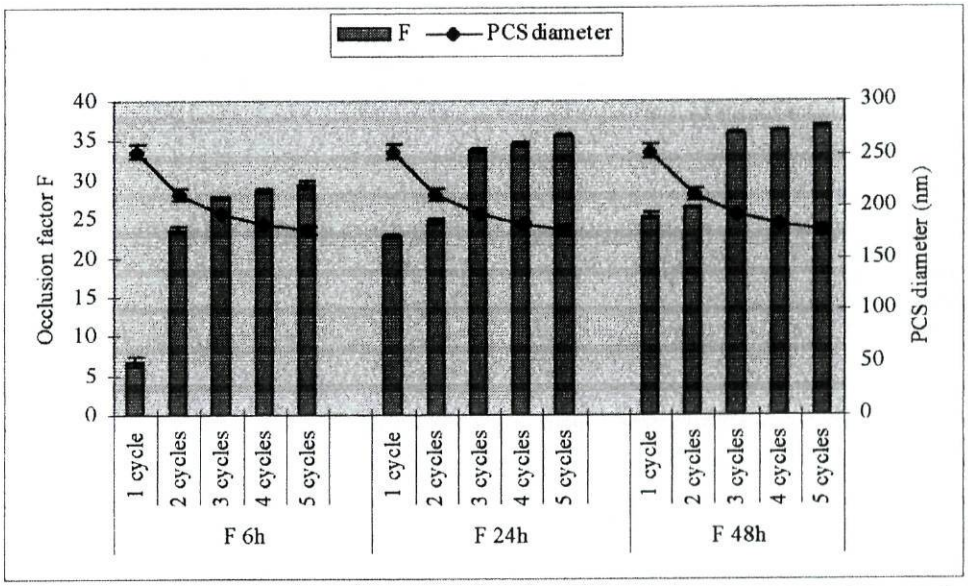

Figure 5.119: Effect of the number of homogenization cycles on occlusion factor F for D10% clotrimazole-free SLN aqueous dispersion.

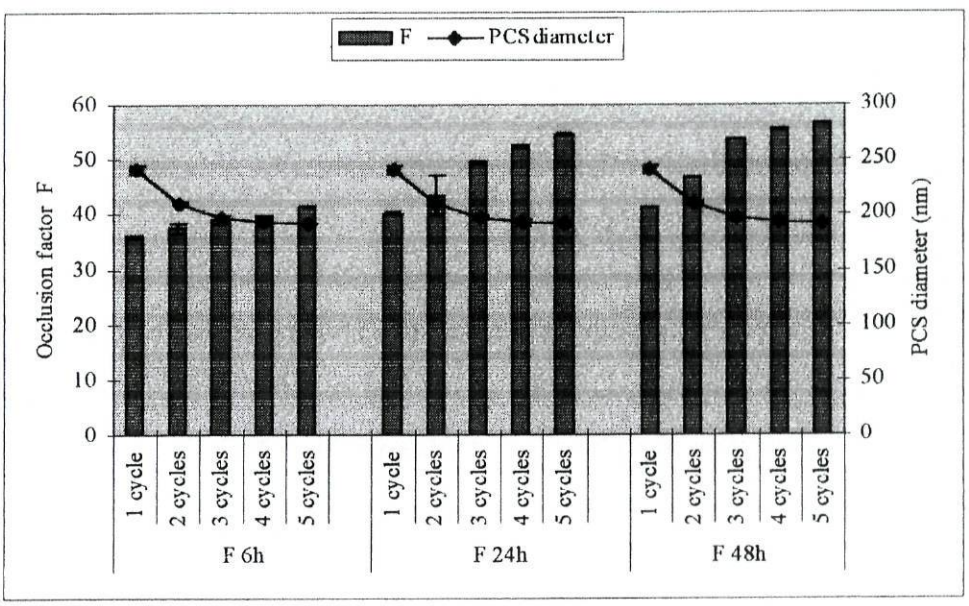

Figure 5.120: Effect of the number of homogenization cycles on occlusion factor F for D20% clotrimazole-free SLN aqueous dispersion.

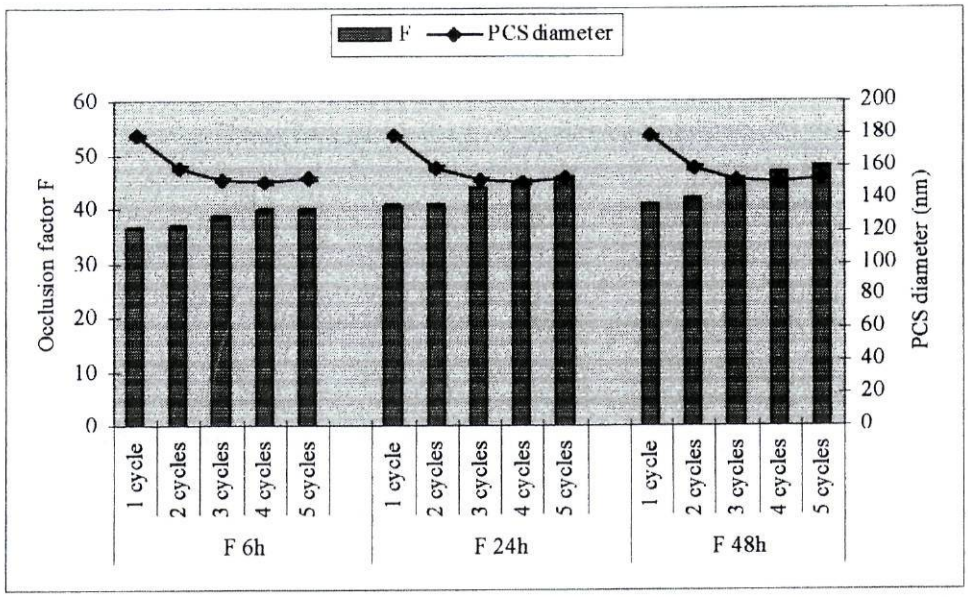

Figure 5.121: Effect of the number of homogenization cycles on occlusion factor F for DM20% clotrimazole-free NLC aqueous dispersion.

The obtained results reveal that smaller particles show higher occlusion properties, which is in agreement to the results obtained by Wissing *et al.* [47]. Increasing homogenization cycles from 1 to 3, particle size decreased and occlusion factor increased significantly. From cycle 3 onwards the decrease in particle size was almost neglected. In addition, the occlusion factor from cycle 3 to 5 remained fairly constant.

It has been shown by electron microscopy that after evaporation of the water from an aqueous dispersion of SLN, a continuous film is formed at the surface [114].

The first model for the film formation by SLN on the skin was developed by Müller and Dingler, assuming a hexagonal packing of the particles in a monolayer [187]. Figure 5.122 shows a comparison between 2 μm and 200 nm lipid particles, in correct size relationship. In hexagonal packing, about 76% of the surface is covered while 24% is uncovered, meaning that the uncovered surface is identical for both microparticles and nanoparticles. However, the holes in between the microparticles are relatively large and favour the hydrodynamic evaporation of water. In contrast, only tiny nanosized pores exist in the monolayer of lipid nanoparticles. From the pore dimensions, evaporation of water is hydrodynamically unfavourable. The pores are reminiscent of the occurrence of capillary condensation in silica gel. Water condensates in these pores due to their small size and reduced vapour pressure. Thus, the pores in the lipid nanoparticles film would rather attract than lose water.

It has been earlier reported by Wissing *et al.* that particles in the micrometer range do not show pronounced occlusive effect [47]. For these particles, the occlusion factor F remained under 15 throughout the duration of the de Vringler *in vitro* test. This was due to the fact that

these particles formed a film on the filter paper with larger pores. Particles in the nanometer range revealed an occlusion factor which was 2 to 3 times as high as the factor obtained by particles in the micrometer range. For particles with a size ranging from 200 to 400 nm, there was only a slight decrease in occlusive effect. However, for particles of 600 nm and more, the occlusion factor strongly decreased. From these observations it could stated that for having high occlusivity, mean particle sizes of 400 nm are appropriate [181]. In the present study, particles having a mean size lower than 300 nm were obtained and used for determining the occlusion factor. It could be observed that these small nanoparticles showed a pronounced occlusive effect.

Regarding the time dependency of the occlusive effect, it was reported that for particles having a mean diameter between 200 and 400 nm, the occlusion factor remains fairly constant throughout the experiment [47]. This was supported by findings that film formation takes place within the first hour. After film formation is completed, water evaporation should remain at a constant rate.

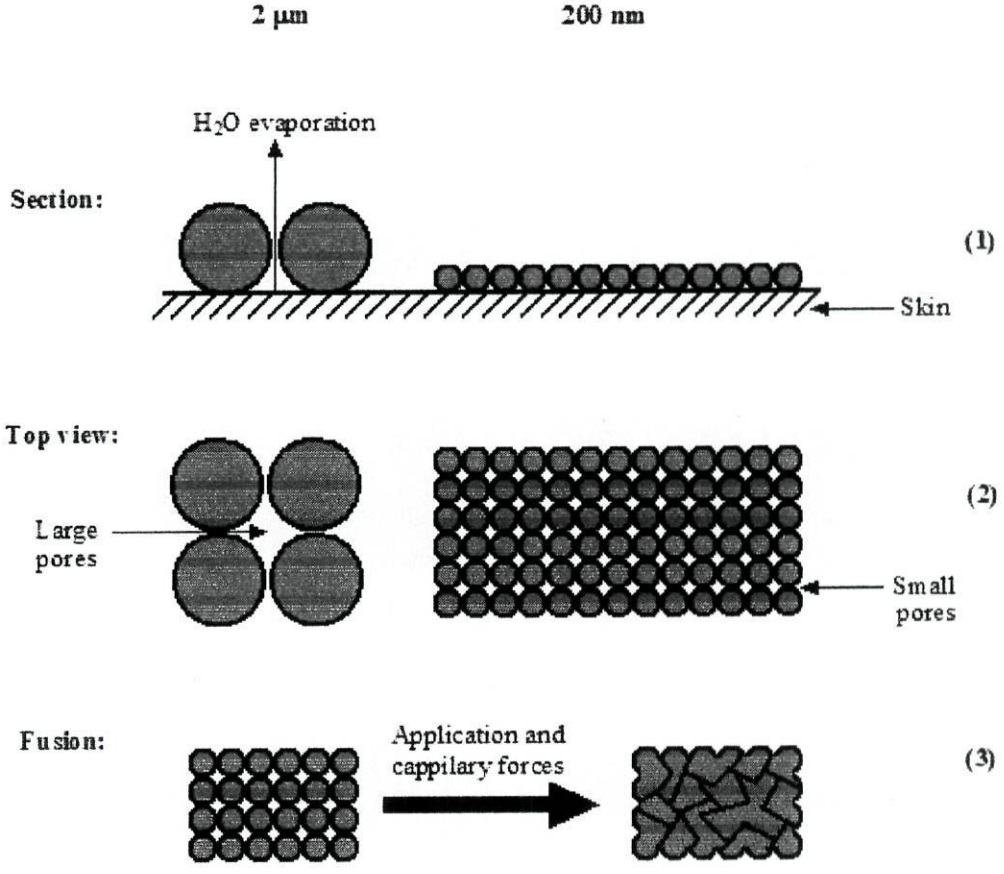

Figure 5.122: Model of film formation on the skin for 2 µm and 200 nm lipid particles. The film is shown as section (1), from the top (2) and as a new model of fusion of the nanoparticles to a pore-less film (3). (Adapted from Müller *et al.* [27]).

5.9.2. Dependency upon applied sample mass

Figure 5.123 shows the dependency of the occlusion factor upon sample mass. For this study, samples of 100, 150 and 200 mg, i.e. 5.3 mg/cm^2, 8 mg/cm^2 and 10.6 mg/cm^2, respectively, of the DM20% NLC formulation were applied to the membrane.

As reported by Wissing *et al.* for SLN formulations, F was more pronounced for higher sample quantities applied to the membrane [47].

The difference of the occlusion factor F between sample sizes of 5.3 mg/cm^2 and 8 mg/cm^2 was greater than the difference between sample sizes of 8 mg/cm^2 and 10.6 mg/cm^2. After 48 h of incubation time F was approximately 11% higher using a sample size of 8 mg/cm^2 in comparison to 5.3 mg/cm^2, while the difference between 10.6 mg/cm^2 and 8 mg/cm^2 was only approximately 4%. This is due to the fact that the denseness of the particles on the filter is already relatively high at higher sample volume [47].

According to Müller *et al.* a critical value has to be reached, in order to enable film formation due to particle fusion [27]. Thus, probably, a sample size of 100 mg is not enough to cover the filter paper with NLC in order to obtain a sufficient occlusive effect.

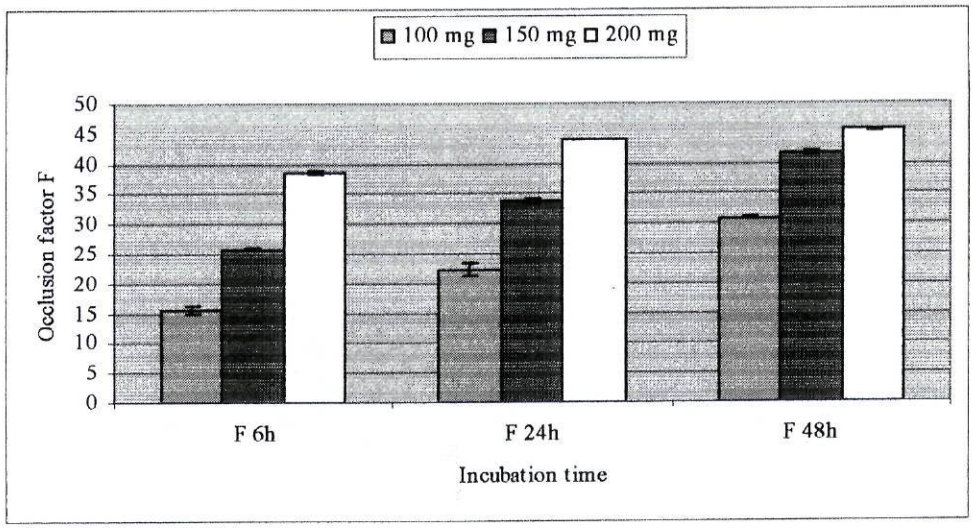

Figure 5.123: Effect of the applied sample mass of NLC aqueous dispersions containing 20% of lipid matrix on occlusion factor F.

5.9.3. Dependency upon lipid formulation type and presence of clotrimazole

Figure 5.124 shows the effect of the lipid formulation type (SLN and NLC) and the presence of clotrimazole on occlusion factor F.

This study was carried out in order to compare the occlusivity of SLN with different lipid content (10 and 20% *m/m*), as well as SLN and NLC with the same lipid content (20% *m/m*). For these *in vitro* tests, 200 mg of D10%, D10%C, D20%, D20%C, DM20% and DM20%C aqueous dispersions were applied at the surface of the filter.

As it could be expected, SLN with higher lipid content (20% *m/m*) were responsible for the highest occlusion factor, either for both drug-free or for drug-loaded formulations (approximately 53.8% for D20% and 50.3% for D20%C) after 48 h of incubation time. NLC formulations revealed an occlusion factor lower than SLN formulations with the same lipid content (approximately 45.5% for DM20% and 43.7% for DM20%C) after the same period of incubation. SLN containing 10% of lipid matrix showed a F of 35.9% for D10% sample and of 33.7% for D10%C, after 48h of incubation time.

These results can be explained by the solid content of the tested formulations. In fact, the higher lipid content makes difficult the hydrodynamic conditions for evaporation of water. Therefore, SLN containing 20% of lipid F exhibited the highest value. For the same lipid content, NLC formulations showed a lower F value, due to the presence of a liquid core inside their lipidic structure, which can enhance or facilitate water evaporation.

It has been found that the occlusion factor strongly depends on the degree of crystallinity of the lipid matrix, i.e. this effect is directly proportional [47,49]. In general, crystalline lipid particles are required to obtain a high occlusion factor and non-crystalline lipid nanoparticles, i.e. supercooled melts have no occlusive properties.

According to these observations, NLC seems to be less crystalline in comparison to SLN with the same lipid content, because the former have an oil liquid core. Therefore, NLC must be responsible for a lower occlusion factor F.

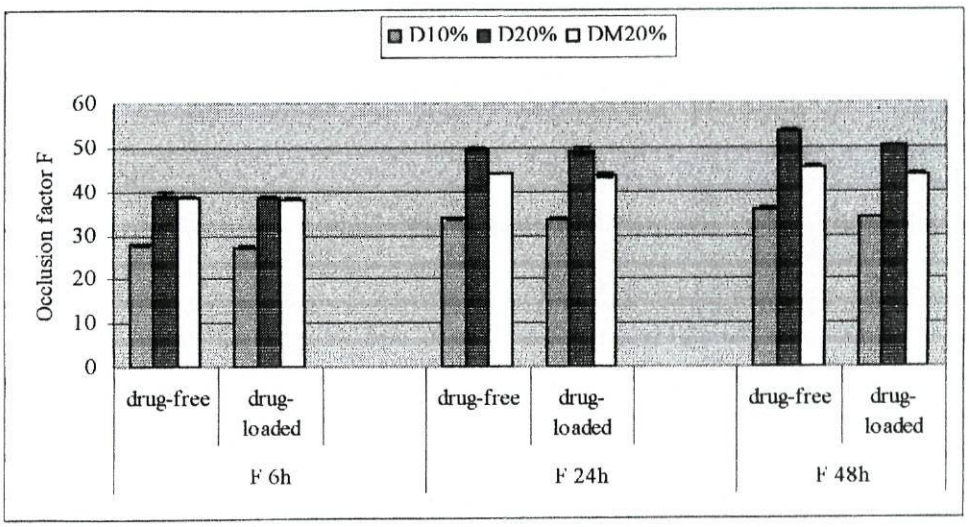

Figure 5.124: Effect of the lipid formulation (D10%, D20% and DM20%) and presence of clotrimazole on occlusion factor F.

5.9.4. Dependency upon hydrogel type

Incorporation of SLN and NLC into topical formulations (creams, ointments, emulsions or hydrogels) can be performed to create supersaturated systems as reported earlier [27]. The increase in saturation solubility will lead to an increased diffusion pressure of drug into the skin. It might also be advantageous to combine solid lipid aqueous dispersions with topical formulations [8-10,229]. It has been recently observed by an *in vivo* study that addition of 4% of SLN to a conventional O/W cream leaded to an increase of skin hydration of 31% after 4 weeks [181].

Figure 5.125 shows the effect of the type of hydrogel on occlusion factor F, observed in the present study. As described before, four different hydrogels (XG, HEC, PA and CH) were prepared, 200 mg of each was applied at the surface of the filter and the respective occlusion factor was determined after 6, 24 and 48 h of incubation time.

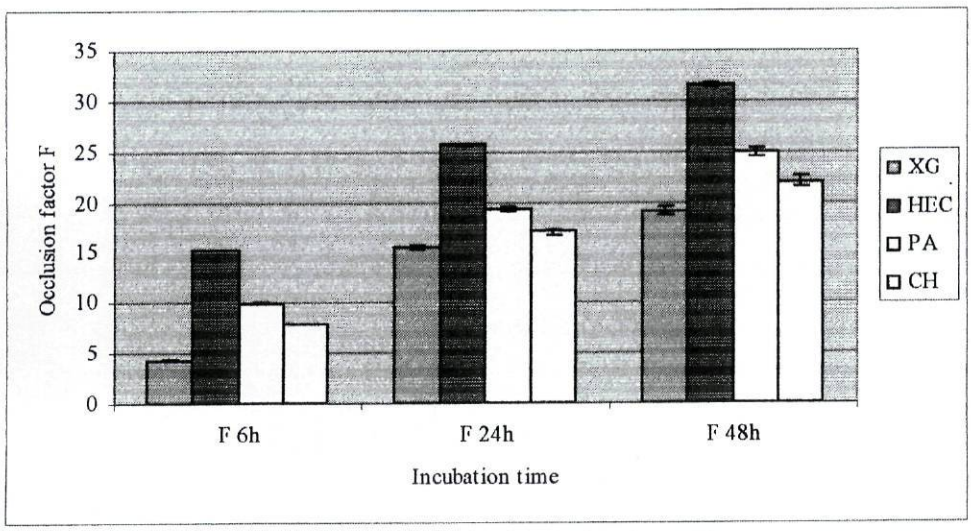

Figure 5.125: Effect of the type of hydrogel on occlusion factor F.

After 48 h it was observed that HEC hydrogels were responsible for the highest occlusion factor F (approximately 31.6%). PA revealed an occlusion factor F of approximately 25% and CH of approximately 22%. XG was responsible for the lowest obtained value (approximately 19.1%).

In order to compare the occlusion factor F of the same hydrogels containing solid lipid aqueous dispersions, NLC containing 20% of lipid matrix were incorporated into the different hydrogels. 200 mg of each sample was applied at the surface of the filter and the respective occlusion factor was determined after 6, 24 and 48 h of incubation time.

Figure 5.126 shows the effect of the type of hydrogel on occlusion factor F for NLC formulation containing 20% of lipid matrix. Obtained results are in agreement with the occlusion effect observed for the different hydrogels (Figure 5.125). HEC was responsible for the highest occlusivity, while XG was responsible for the lowest value. However, when lipid particles were present the differences between the values obtained for occlusion factor F decreased, as expected. These results confirm the importance of solid lipid particles to enhance the occlusivity of topical formulations.

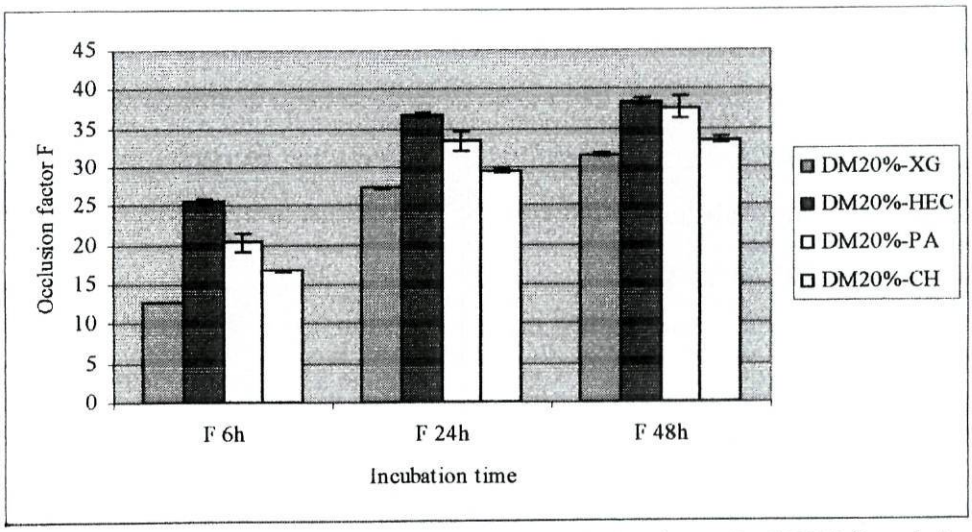

Figure 5.126: Effect of the type of hydrogel on occlusion factor F of NLC formulation containing 20% of lipid matrix.

When incorporated into topical formulations either SLN or NLC enhance the occlusive effect, due to their adhesive properties and the formation of a thin layer of densely packed nanoparticles. The dimensions of the spaces between the particles are very small, obstructing air circulation in these spaces and minimizing evaporation of water from the skin. Increased diffusion pressure and occlusive effect should distinctly enhance drug concentration in the skin or even drug penetration and systemic absorption.

Decisive for the fate of clotrimazole is whether it is located in the SLN matrix or outside, i.e. distributed in the hydrogel. In the first case it is possible to localize the drug in the upper regions of skin. In the second one, even if using drug-free or drug-loaded SLN or NLC, occlusive effect of these particles govern the penetration of incorporating agents and enhanced penetration predominates [174].

It has been found that either SLN or NLC form films after application to the skin as a consequence of water evaporation, which leads to particle fusion and film formation (Figure 5.116) [116]. Clotrimazole is localized in this film, thus penetration can be controlled. The small

particle size ensures close contact with *stratum corneum* and should increase the amount of drug penetrating into the viable skin.

The principle of supersaturation can be used to explain the increase of drug penetration from topical microemulsions and, therefore, from solid lipid aqueous dispersions when applied to the skin. When topical formulations saturated with drug are applied to the skin, water from the skin diffuses into the semi-solid system resulting in a decrease of saturation solubility of the drug. The uptake of water by the topical formulation leads to supersaturation of the drug, obligating this later not to leave the system [27]. In an *in vitro* situation drugs crystals would be formed, while *in vivo* the only way to leave the topical formulation is to penetrate the skin.

Figure 2.9 (Chapter II) explains the triggered drug release and supersaturation effect from NLC aqueous dispersions. Similar supersaturation systems can be created by incorporating drug-loaded SLN and NLC in traditional hydrogels or creams saturated with drug [27,160]. During storage on the shelf, the drug remains inside the lipid nanoparticles, preserving their lipidic structure and, therefore, preserving drug accommodation. Application to the skin leads to an increase in temperature and water loss. This phenomenon initiates the transition to more stable lipid modifications in the lipid nanoparticles leading to drug expulsion. The drug is being expelled into the dispersion being already saturated with drug and thus leading to supersaturation.

The obtained results in the present study confirmed that the degree of occlusivity of solid lipid aqueous dispersions correlates with particle size, lipid concentration, degree of crystallinity of lipid matrix and type of topical formulation. Therefore, when developing a new topical formulation based on SLN and NLC, it should be adjusted exactly to the desired degree of occlusion, on a controlled way.

CHAPTER VI

CONCLUSIONS AND FUTURE TRENDS

CHAPTER VI

CONCLUSIONS AND FUTURE TRENDS

Drug delivery to the skin presents unique opportunities but also obstacles due to the particular skin structure, physiology and barrier properties. Aiming to improve dermatological formulations, attempts are being made to design new topical drug delivery systems, i.e. particulate carriers that will enable a drug to reach the desired pharmaceutical site of action. One of the main possibilities is the use of based lipid carriers, such as SLN and NLC [6,7].

The materials used for preparation of SLN and NLC are excipients already present in cosmetic and pharmaceutical products accepted by the regulatory authorities. In fact, the full range of GRAS substances and substances of recognized GRAS status is available [259]. These substances also include compounds with surface activity or surfactants suitable for SLN and NLC stabilization. Therefore, based on the *in vitro* cytotoxicity and the *in vivo* toxicity data, either SLN or NLC appear to be very well tolerated drug carrier systems [12,13,84,102].

SLN and NLC possess a number of features advantageous for topical route [6,7]. The small particle size ensures a close contact to the *stratum corneum* and may increase the amount of incorporated agent penetrating into the viable skin. Due to their solid matrix, sustained drug release is possible and they can also be incorporated into semi-solid dosage forms. Furthermore, occlusive properties, as a result of a film formation on the skin surface, and chemical stabilization of incorporated drugs have also been reported [7,174,187].

With regard to the present work, pre-formulation studies were conducted in order to select the best lipid (or lipids) for incorporating clotrimazole in stable SLN and NLC formulations, as well as in order to select the emulsifying agent and the production conditions.

To ensure the success of the incorporation process, the drug needs to be solubilized in the melted lipid, both at high and low temperatures. Therefore, the solubility of clotrimazole was screened by mixing the drug in different concentrations (1%, 5%, 10% and 20%, *m/m*) with 15 different lipids and melting the mixtures at 90°C. Solubility was determined visually and microscopically either at 90°C or at room temperature (20°C), in order to evaluate the presence/absence of crystals of drug in the mixtures. *Dynasan*®116, *Softisan*®154, *Witepsol*®H5, *Witepsol*®S55, *Witepsol*®E75 and *Imwitor*®191 were selected for SLN preparation containing 20% (*m/m*) of lipid matrix with different emulsifying agents (*Tween*®80, *Span*®85, *Lipoid*®S75, *Lutrol*®F68, *Tego Care*®450, *Tyloxapol*® and *Lanette*®N), at 90°C using a homogenization pressure of 500 bar and 3 homogenization cycles.

After particle size analysis by LD (d99%) on day 1 and day 7 of storage at room temperature, *Dynasan*®116 seemed to be the best lipid for the preparation of SLN using *Tyloxapol*® as emulsifying agent, since the lowest d99% was obtained and maintained during one week of storage at room temperature (20°C). Therefore, *Dynasan*®116 and *Tyloxapol*® were selected, respectively, as the lipid and the emulsifying agent for preparation of SLN and NLC containing 5% (*m/m*) of clotrimazole (with regard to the lipid matrix), at 90°C using a homogenization pressure of 500 bar and 3 homogenization cycles.

Three different clotrimazole-free and clotrimazole-loaded SLN and NLC formulations, having distinct lipid concentrations (SLN 10%, SLN 20% and NLC 20%) were developed and characterized by LD, PCS, ζ, DSC and x-ray diffraction. The E.E., drug loading capacity and drug release profile were also determined after preparation.

All developed clotrimazole-containing SLN and NLC formulations revealed E.E. higher than 64% and loading capacities higher than 2.5%. Both clotrimazole-free and clotrimazole-loaded SLN and NLC aqueous dispersions showed a narrow particle size distribution measured by LD (d99%) and the presence of clotrimazole did not increase the mean particle size measured by PCS. NLC formulations revealed a lower PI (< 0.182), i.e. a narrow size distribution, in comparison to SLN formulations with the same lipid content (< 0.241). The former also showed a smaller mean particle size (approximately 180 nm). Concerning to the determination of ζ, drug-free samples showed values between -17 mV and -37 mV, while drug-loaded samples showed values between -8 mV and -11 mV. Drug-free NLC formulations also showed lower ζ values in comparison to SLN samples. With regard to the evaluation of crystallinity of SLN and NLC, DSC and x-ray diffraction data indicated the presence of a crystalline matrix. In comparison to SLN with the same lipid content, NLC formulations evidenced lower lipid crystallinity, due to the existence of a liquid core. By x-ray diffraction studies, SLN formulations showed the characteristic peaks for β'/β modifications, while none of NLC formulations displayed any characteristic peaks in their x-ray patterns, revealing their lower lipid crystallinity, in agreement with the obtained DSC data. Although NLC formulations displayed a thermal event in DSC heating runs, they were more amorphous in comparison to SLN formulations. Therefore x-ray patterns did not show the characteristic β'/β modifications.

Long term stability of SLN and NLC developed formulations was also assessed. Samples were stored at 4°C, 20°C and 40°C and physicochemically characterized during a period of three months. The E.E. and the drug loading capacity were evaluated for a period of 21 days in samples stored at room temperature (20°C).

Physicochemical stability of the developed SLN and NLC formulations was carried out regarding the following factors: lipid concentration, presence of clotrimazole and storage temperature during three months of the study. All samples were physicochemically stable at the different temperatures. SLN formulation with 10% (*m/m*) of lipid matrix stored at 40°C showed lower particle sizes. All formulations revealed a slightly decreased of ζ values during storage time. However, aqueous dispersions remained in the nanometer range during 3 months of storage at room temperature. Moreover, the presence of clotrimazole did not interfere neither with the particle size nor with the chemical stability of the investigated systems.

For all investigated formulations E.E. higher than 50% were observed after 21 days of storage at room temperature (20°C). For SLN formulations, the sample with lower lipid content (10%, *m/m*) revealed a lower E.E. (approximately 57%) in comparison to the sample with 20% (*m/m*) of lipid content (approximately 59%). On the contrary, NLC formulation revealed the highest value (approximately 67%), due to the existence of the liquid core, which is responsible for more imperfections in the lattice, offering more space to accommodate clotrimazole molecules. Moreover, the oil compartment solubilizes clotrimazole increasing the drug content in the solid lipid system.

Obtained results confirmed the higher loading capacity of NLC formulations (approximately 3.5%, *m/m*), in comparison to SLN with the same lipid content (approximately 2.3%, *m/m*). For SLN formulations, the sample with lower lipid content (10%, *m/m*) revealed a higher loading capacity (approximately 3%, *m/m*) in comparison to the sample with 20% (*m/m*) of lipid content (approximately 2.3%, *m/m*). Thus, the presence of a liquid lipid in the carrier enhances both E.E. and drug loading capacity.

Concerning to drug loss during storage time, it was observed that NLC formulation lost only 6% of incorporated clotrimazole after 21 days of storage at room temperature, while SLN formulations slowed higher drug loss. SLN formulations containing 10% (*m/m*) of lipid matrix lost 10% and SLN formulations containing 20% (*m/m*) of lipid matrix lost 12% of incorporated drug.

With regard to the release profile investigations, results revealed that clotrimazole was more quickly released from samples containing lower lipid concentration. NLC formulation was also responsible for the highest percentage of drug released (almost double in comparison to SLN formulations with the same lipid content). After 1 hour, the percentage of drug released from the NLC formulation was almost 10% (*m/m*). SLN formulations containing 10% (*m/m*) of lipid matrix revealed 7% (*m/m*) of drug released, while SLN formulations containing 20% (*m/m*) of lipid matrix revealed 4% (*m/m*) after the same period. The obtained release profiles are related to

the different drug incorporation and release mechanism models. NLC formulation is responsible for a more easily release due to their liquid core, where clotrimazole is less tightly incorporated, while in SLN formulations the drug is seizure in the solid core. SLN formulation containing 10% (*m/m*) of lipid matrix corresponds to the drug-enriched shell model, while SLN formulation containing 20% (*m/m*) of lipid matrix corresponds to the drug-enriched core model. A more quickly release was observed for SLN formulation corresponding to the drug-enriched shell model.

SLN and NLC aqueous dispersions were incorporated into four different hydrogels: XG, HEC, PA and CH. Twelve different clotrimazole-free and clotrimazole-loaded formulations were developed and physicochemically characterized, concerning to particle size (by PCS and LD), ζ (by PCS) and crystalinity and interactions between components (by DSC). Long term stability of SLN and NLC containing hydrogels was also assessed by PCS, LD and DSC, during a period of three months at room temperature (20°C).

Particle size characterization of SLN and NLC after their incorporation into different hydrogels revealed no peak in the micrometer range, except for both clotrimazole-free and clotrimazole-loaded SLN formulations containing 20% (*m/m*) of lipid matrix incorporated into XG hydrogels. This was probably caused by insoluble residues of this polysaccharide. The lowest particle size was observed for SLN containing 10% (*m/m*) of lipid matrix incorporated into PA hydrogels. These hydrogels were also responsible for the lowest PI value obtained for all SLN and NLC formulations after incorporation into the different hydrogels. The highest PI was obtained using CH hydrogels, especially for SLN samples containing 10% of lipid matrix. CH was also responsible for the highest mean particle size for all tested SLN and NLC formulations. This result is probably due to the polar character of this polymer and to the use of acetic acid for starting the gel formation process of CH. The use of acetic acid might affect the ζ at the surface of SLN and NLC and might be responsible for particle aggregation.

With regard to physicochemical stability investigations, it could be observed that XG, HEC and PA hydrogels were not responsible for aggregation of SLN or NLC after their incorporation into the semi-solid systems. On the contrary, CH hydrogels showed particle aggregation. However, using this polymer particle size remained below 1 μm. During storage at room temperature a decrease of ζ could be observed. For both clotrimazole-free and clotrimazole-loaded SLN and NLC aqueous dispersions, the lipid content in the hydrogel was preserved. Concerning to thermal analysis, DSC curves of SLN and NLC aqueous dispersions incorporated into hydrogels revealed identical peaks compared to the correspondent aqueous dispersions. This

result indicates that SLN and NLC particles did not interfere with the gel forming agent when stored at room temperature (20°C).

In order to evaluate the performance of semi-solid preparations on the skin, rheological measurements were carried out. An oscillation frequency sweep test was performed for all developed SLN and NLC aqueous dispersions. In addition, continuous shear investigations were performed in all hydrogel formulations, evaluating the shear rate as a function of shear stress.

Viscoelastic properties of SLN and NLC aqueous dispersions were found to be comparable to conventional topical formulations. It was found that increasing the lipid concentration leads to a dramatic change in the rheological properties. SLN formulations revealed a presence of a gel-like structure because the storage modulus "G'" was greater than the loss modulus "G''". This difference was more emphasized for SLN formulations containing 20% (*m/m*) of lipid matrix.

Concerning to the presence of clotrimazole, the influence of drug in viscoelastic properties of SLN and NLC aqueous dispersions was more emphasized for NLC formulation than for SLN formulation with the same lipid content. Regarding to clotrimazole-free NLC formulations, the storage modulus "G'" appeared not so far from the loss modulus "G''" over the measured frequency range, while clotrimazole-loaded NLC formulations appeared to have a gel-like structure because "G'" and "G''" were grater from each other during the same frequency range.

With regard to continuous shear rheometry, the incorporation of SLN and NLC aqueous dispersions into XG hydrogels resulted in flow curves with plastic characteristics. HEC hydrogels with 20% (*m/m*) of lipid containing SLN and NLC aqueous dispersions seemed to be responsible for a more plastic behaviour, while samples having less lipid content revealed a more pseudoplastic-like behaviour. PA hydrogels containing SLN with 20% (*m/m*) of lipid matrix showed thixotropy and NLC formulations prepared with the same lipid content revealed more dependency upon the applied shear stress. Concerning to CH hydrogels, these later revealed a more pseudoplastic-like behaviour when containing NLC formulations and SLN formulations with less lipid content. The presence of drug into SLN containing 20% (*m/m*) of lipid matrix revealed a more plastic behaviour.

To summarize, thixotropy was observed for systems having higher lipid content. Increasing the lipid content leaded to different flow characteristics. HEC and CH hydrogels are more fluid and they might not have a good consistency for topical administration. In comparison to XG hydrogels, SLN and NLC aqueous dispersions containing PA hydrogels revealed less dependency upon the applied shear stress.

It could be shown that physical properties, like physical state of the dispersed lipid phase, have a great impact on the formation of a semi-solid gel structure within lipid particle

dispersions. By employing viscoelastic measurements, it could be demonstrated that the existence of a solid particle matrix with a particle size in nanometer range is a prerequisite to form a semisolid dispersion having the appropriate consistency for topical administration.

Occlusive properties of SLN and NLC aqueous dispersions and hydrogels containing SLN and NLC were analysed by the de Vringler *in vitro* test. The dependency of the occlusion factor (F) was determined with regard to the number of homogenization cycles used for preparation of nanoparticles, sample mass applied, nanoparticle formulations (SLN or NLC), presence of clotrimazole and hydrogel type (XG, HEC, PA or CH). The occlusion factor was determined as a function of time.

The dependency of occlusion factor upon the particle size was clearly visible. For all tested formulations it could be observed the increase of occlusion factor with the decrease of particle size measured by PCS. The increase of the number of homogenization cycles from 1 to 3 leaded to a significant decrease of particle size. From cycle 3 onwards the decrease of particle size was almost neglected. Furthermore, the occlusion factor from cycle 3 to 5 remained practically constant.

The dependency of the occlusion factor upon the applied sample mass was determined for NLC formulations. It was found that occlusion factor was more pronounced for a higher mass of sample, as reported by Wissing *et al.* for SLN formul□tions [47].

In order to compare the occlusive properties between SLN and NLC aqueous dispersions, the occlusion factor was determined for all formulations. SLN with higher lipid content (20% *m/m*) were responsible for the highest occlusion factor for both clotrimazole-free and clotrimazole-loaded formulations. NLC formulations revealed an occlusion factor lower than SLN formulations with the same lipid content, while SLN containing 10% (*m/m*) of lipid matrix showed the lowest occlusion factor. The higher lipid content turn difficult the hydrodynamic conditions for evaporation of water. Therefore, the highest value of occlusion factor was observed for SLN containing 20% (*m/m*) of lipid. For the same lipid content, NLC formulations showed an occlusion factor value lower than SLN due to the existence of a liquid core inside their lipidic structure, which can enhance or facilitate water evaporation.

In order to compare the occlusion factor of nanoparticle aqueous dispersions containing hydrogels, NLC containing 20% (*m/m*) of lipid matrix were incorporated into four different hydrogels. HEC hydrogel was responsible for the highest occlusivity, while XG was responsible for the lowest value. Moreover, the occlusion factor obtained for NLC containing PA hydrogels was slightly higher than for NLC containing CH hydrogels. However, as expected, when lipid particles were incorporated into hydrogels the differences between the values of occlusion factor

decreased. These results confirm the importance of solid lipid particles to enhance the occlusivity and skin hydration of topical formulations.

In conclusion, the results obtained in the present work clearly reveal that SLN and NLC are able to carry clotrimazole for topical drug delivery. It could be demonstrated that these systems have appropriate particle size and ζ, high E.E. and loading capacity for clotrimazole, which are dependent on the percentage of lipid matrix, and present a controlled release profile of the drug. Moreover, it is possible to prepare and characterize semi-solid systems based on hydrogels containing SLN and NLC having the desire physicochemical properties for the improvement of clotrimazole delivery in topical formulations. The gel forming agent is an important factor for optimizing the rheological and occlusive properties of semi-solid systems.

According to the present investigation, some of the developed formulations might be selected as promising drug delivery systems for topical administration of clotrimazole. Thus, NLC formulation containing 20% (*m/m*) of lipid matrix might be more advantageous for clotrimazole delivery, in comparison to the developed SLN formulations. With regard to semi-solid formulations, PA hydrogel might be the best vehicle for incorporation of NLC formulation containing 20% (*m/m*) of lipid matrix.

The purpose of using lipid nanoparticles for topical drug delivery has further fields to be exploited. With regard to physicochemical characterization of lipid nanoparticles, other techniques should be employed in future investigations. These techniques include the electron microscopy that, in contrast to PCS and LD, provides direct information about the shape of the lipid particles [7] and the atomic force microscopy (AFM), which allows the observation of *in situ* processes occurring at the interfaces. Therefore, AFM can be used to image the morphological structure of lipid particles [93]. Transmission electron microscopy (TEM) can be employed for visualizing the colloidal particle size [323] and the Infrared and Raman spectroscopies are useful tools for investigating the structural properties of the lipids [324]. Both nuclear magnetic resonance (NMR) and electron spin resonance (ESR) are sensitive methods which can be employed for the detection of the presence of different colloidal species, such as liposomes or micelles that can be formed during the production process of SLN and NLC aqueous dispersions [7].

SLN have been found to modulate drug release into the skin [56] and to improve drug delivery to particular skin layers *in vitro* [57]. Further studies will be developed in order to assess the *in vivo* pharmacokinetic of clotrimazole-loaded SLN and NLC aqueous dispersions and the passage of the drug across the different strata of the skin. For this purpose, the performance of

SLN and NLC might be evaluated by the *in vitro* Transpore™ test proposed by Diffey *et al.* [325], which has relevance regarding to *in vitro/in vivo* correlations [179].

These systems can be incorporated into topical dosage forms for dermal and mucosal drug delivery, maintaining their colloidal particle size. Further investigations should also be conducted in order to evaluate the large scale production of semi-solid SLN and NLC dispersions and the influence of scaling up on the colloidal structure of the carriers and gel structure.

Concerning laboratory and industrial production of SLN and NLC aqueous dispersions, these systems can be prepared by HPH using piston-gap homogenizers [5,6]. For very expensive compounds, the use of an *Avestin B3* apparatus is recommended having a batch volume as small as 3 ml dispersion [48]. The *Micron Lab 40* can be considered as the standard machine for laboratory scale, where the batch size is 40 ml in the discontinuous version and approximately 200-500 ml in the continuous version [326].

For topical products, a large batch is usually in the range of 100 kg up to 1000 kg. Such quantities can be easily realized using a *Gaulin 5.5* (150 kg dispersion per hour) or a *Rannie 118* going up to 2000 kg/h (*APV Systems*, Unna, Germany [17]). These homogenizers are accepted in production lines even for parenteral production. In addition, they are low cost equipments and, therefore are used in pharmaceutical industry [327].

REFERENCE LIST

REFERENCE LIST

1. Ehrlich, P., in: Collected Studies on Immunity, Vol. 2, Wiley and Sons, New York, 1906, pp. 442.

2. Müller, R.H., Colloidal carriers for controlled drug delivery and targeting. Modification, characterisation and in vivo distribution, Wissenschaftliche Verlagsgesellschaft Stuttgart, CRC Press Boca Raton, 1991.

3. Speiser, P., Lipidnanopellets als Trägersystem für Arzneimittel zur peroralen Anwendung, European Patent EP 0167825, 1990.

4. Müller, R.H., Feste Lipidnanopartikel (SLN), in Pharmazeutische Technologie: Moderne Arzneiformen, Müller, R.H. and Hildebrand, G.E. ed., Wissenschaftliche Verlagsgesellschaft Stuttgart, 1998, pp. 357-366.

5. Müller, R.H., Mehnert, W., Lucks, J.-S., Schwarz, C., zur Mühlen, A., Weyhers, H., Freitas, C., Rühl, D., Solid lipid nanoparticles (SLN) – an alternative colloidal carrier system for controlled drug delivery, Eur. J. Pharm. Biopharm. 41 (1995) 62-69.

6. Müller, R.H., Mäder, K., Gohla, S., Solid lipid nanoparticles (SLN) for controlled drug delivery – A review of the state of art., Eur. J. Pharm. Biopharm. 50 (2000) 161-177.

7. Mehnert, W., Mäder, K., Solid lipid nanoparticles – Production, characterization and applications, Adv. Drug Deliv. Rev. 47 (2001) 165-196.

8. Mehnert, W., zur Mühlen, A., Dingler, A., Weyhers, H., Müller, R.H., Solid Lipid Nanoparticles – ein neuartiger Wirkstoff-Carrier für Kosmetika und Pharmazeutika, I. Mitteilung: Systemeigenschaften, Herstellung und Scaling-up, Pharm. Ind. 59 (1997) 423-427.

9. Mehnert, W., zur Mühlen A., Dingler, A., Weyhers, H., Müller, R.H., Solid lipid nanoparticles (SLN) – ein neuartiger Wirkstoff-Carrier für Kosmetika und Pharmazeutika. II. Wirkstoff-Inkorporation, Freisetzung und Sterilizierbarkeit, Pharm. Ind. 59 (1997) 511-514.

10. Mehnert, W., zur Mühlen, A., Dingler, A., Weyhers, H., Müller, R.H., Solid Lipid Nanoparticles – ein neuartiger Wirkstoff-Carrier für Kosmetika und Pharmazeutika, III. Mitteilung: Langzeitstabilität, Gefrier- und Sprühtrocknung, Toxizität, Anwendung in Kosmetika und Pharmazeutika, Pharm. Ind. 59 (1997) 614-619.

11. zur Mühlen, A., Mehnert, W., Drug release and release mechanism of prednisolone loaded solid lipid nanoparticles, Pharmazie 53 (1998) 552-555.

12. Schöler, N., Zimmermann, E., Katzfey, U., Hahn, H., Müller, R.H., Liesenfeld, O., Effect of solid lipid nanoparticles (SLN) on cytokine production and the viability of murine peritoneal macrophages, J. Microencapsul. 17 (2000) 639-650.

13. Schöler, N., Hahn, H., Müller, R.H., Liesenfeld, O., Effect of lipid matrix and size of solid lipid nanoparticles (SLN) on the viability and cytokine production of macrophages, Int. J. Pharm. 231 (2002) 167-176.

14. Olbrich, C. Entwicklung optimierter Lipidcarrier und ihre Untersuchung in biologischen Systemen, PhD Thesis, Freie Universität Berlin, 2002.

15. Cavalli, R., Caputo, O., Carlotti, M.E., Trotta, M., Scarnecchia, C., Gasco, M.R., Sterilization and freeze-drying of drug-free and drug-loaded solid lipid nanoparticles, Int. J. Pharm. 148 (1997) 47-54.

16. Schwarz, C., Mehnert, W., Lucks, J.S., Müller, R.H. Solid lipid nanoparticles (SLN) for controlled drug delivery. I. Production, characterization and sterilization, J. Control. Release 30 (1994) 83-96.

17. Schneppe, T., Entwicklung und Qualifizierung einer Pilotanlage zur GMP- und QM-gerechten Herstellung von festen Lipid-Nanopartickeln, PhD Thesis, Freie Universität Berlin, 1998.

18. Gohla, S., Dingler, A., Scaling up feasibility of the production of solid lipid nanoparticles (SLN™), Pharmazie 56 (2001) 61-63.

19. Schwarz, C., Feste Lipid nanopartickel: Herstellung, Charaterisierung, Arzneistoffinkorporation und Freisetzung, Sterilisation und Lyophilisation, PhD Thesis, Freie Universität Berlin, 1995.

20. Schwarz, C., Mehnert, W., Freeze-drying of drug-free and drug-loaded solid lipid nanoparticles (SLN), Int. J. Pharm. 157 (1997) 171-179.

21. Freitas, C., Müller, R.H., Spray-drying of solid lipid nanoparticles (SLN™), Eur. J. Pharm. Biopharm. 46 (1998) 145-151.

22. Zimmermann, E., Müller, R.H., Mäder, K., Influence of different parameters on reconstitution of lyophilized SLN, Int. J. Pharm. 196 (2000) 211-213.

23. Bocca, C., Caputo, O., Cavalli, R., Gabriel, L., Miglietta, A., Gasco, M.R., Phagozytic uptake of fluorescent stealth and non-stealth solid lipid nanoparticles, Int. J. Pharm. 175 (1998) 185-193.

24. Cavalli, R., Bocca, C., Miglietta, A., Caputo, O., Gasco, M.R., Albumin adsorption on stealth and non-stealth solid lipid nanoparticles, STP Pharma Sci. 9 (1999) 183-189.

25. Podio, V., Zara, G.P., Carazzone, M., Cavalli, R., Gasco, M.R., Biodistribution of stealth and non-stealth solid lipid nanospheres after intravenous administration to rats, J. Pharm. Pharmacol. 52 (2000) 1057-1063.

26. Radtke, M., Müller, R.H., NLC™ Nanostructured lipid carriers: the new generation of lipid drug carriers, New Drugs 2 (2001) 48-52.

27. Müller, R.H., Radtke, M., Wissing, S.A., Solid lipid nanoparticles (SLN) and nanostructured lipid carriers (SLN) in cosmetic and dermatological preparations, Adv. Drug Deliv. Rev. 54 (2002) S131-S155.

28. Müller, R.H., Radtke, M., Wissing, S.A., Nanostructured lipid matrices for improved microencapsulation of drugs, Int. J. Pharm. 242 (2002) 121-128.

29. Radtke, M., Nanostructured lipid carriers (NLC): Untersuchungen zur Struktur, Wirkstoffinkorporation und Stabilität, PhD Thesis, Freie Universität Berlin, 2003.

30. Gasco, M.R., Solid lipid nanospheres from warm micro-emulsions, Pharm. Tech. Eur. 9 (1997) 52-58.

31. Almeida, A.J., Runge, S., Müller, R.H., Peptide-loaded solid lipid nanoparticles (SLN): influence of production parameters, Int. J. Pharm. 149 (1997) 255-265.

32. Domb,A.J., Long acting injectable oxytetracycline-liposphere formulation, Int. J. Pharm. 124 (1995) 271-278.

33. Lim, S.-J., Kim, C.-K., Formulation parameters determining the physicochemical characteristics of solid lipid nanoparticles loaded with all-trans retinoic acid, Int. J. Pharm. 243 (2002) 135-146.

34. Domb, A.J., Long acting injectable oxytetracycline-liposphere formulation, Int. J. Pharm. 124 (1995) 271-278.

35. Westesen, K., Bunjes, H., Do nanoparticles prepared from lipids solid at room temperature always possess a solid lipid matrix?, Int. J. Pharm. 115 (1995) 129-131.

36. Bunjes, H., Westesen, K., Koch, M.H.J., Crystallization tendency and polymorphic transitions in triglyceride nanoparticles, Int. J. Pharm. 129 (1996) 159-173.

37. Heiati, H., Phillips, N.C., Tawashi, R., Evidence for phospholipids bilayer formation in solid lipid nanoparticles formulated with phospholipid and triacylglyceride, Pharm. Res. 13 (1996) 1406-1410.

38. Heiati, H., Tawashi, R., Shivers, R.R., Phillipps, N.C., Solid lipid nanoparticles as drug carriers. I. Incorporation and retention of the lipophilic prodrug 3'-azido-3'-deoxythymidine palmitate, Int. J. Pharm. 146 (1997) 123-131.

39. Heiati, H., Tawashi, R., Phillips, N.C., Solid lipid nanoparticles as drug carriers. II. Plasma stability and biodistribution of solid lipid nanoparticles containing the lipophilic prodrug 3'-azido-3'-deoxythymidine palmitate in mice, Int. J. Pharm. 174 (1998) 71-80.

40. Heiati, H., Tawashi, R., Phillips, N.C., Drug retention and stability of solid lipid nanoparticles containing azidothymidine palmitate after autoclaving storage and lyophilization, J. Microencapsul. 15 (1998) 173-184.

41. zur Mühlen, A., Schwarz, C., Mehnert, W., Solid lipid nanoparticles (SLN) for controlled drug delivery – Drug release and release mechanism, Eur. J. Pharm. Biopharm. 45 (1998) 149-155.

42. Müller, R.H., Olbrich, C., Solid lipid nanoparticles: phagocytic uptake, in vitro cytotoxicity and in vitro biodegradation. 2nd Comunication, Drugs made in Germany 42 (1999) 75-79.

43. Schwarz, C., Mehnert, W., Solid lipid nanoparticles (SLN) for controlled drug delivery II. Drug incorporation and physicochemical characterization, J. Microencapsul. 16 (1999) 205-213.

44. Bunjes, H., Koch, M.H.J., Westesen, K., Effect of particle size on colloidal size solid triglycerides, Langmuir 16 (2000) 5234-5241.

45. Unruh, T., Bunjes, H., Westesen, K., Kocj, M.H., Investigations on the melting behaviour of triglyceride nanoparticles, Colloid. Polym. Sci. 279 (2001) 398-403.

46. Unruh, T., Westesen, K., Bösecke, P., Lindner, P., Koch, M.H.J., Self-assembly of tryglyceride nanocrystals in suspension, Langmuir 18 (2002) 1796-1800.

47. Wissing, S.A., Lippacher, A., Müller, R.H., 2001. Investigations on the occlusive properties of solid lipid nanoparticles (SLN), J. Cosmet. Sci. 52 (2001) 313-323.

48. Wissing, S.A., SLN als innovatives Formulierungskonzept für pflegende und protective dermale Zubereitungen, PhD Thesis, Free University of Berlin, 2002.

49. Wissing, S.A., Müller, R.H., The influence of the crystallinity of lipid nanoparticles on their occlusive properties, Int. J. Pharm. 242 (2002) 377-379.

50. zur Mühlen, A., Feste Lipid – Nanopartikel mit prolongierter Wirkstoffliberation: Herstellung, Langzeitsabilität, Charakterisierung, Freisetzungsverhalten und Mechanismen, PhD Thesis, Free University of Berlin, 1996.

51. Müller, R.H., Rühl, D., Runge, S.A., Biodegradation of solid lipid nanoparticles as a funtion of lipase incubation time, Int. J. Pharm. 144 (1996) 115-121.

52. Müller, R.H., Rühl, D., Runge, S., Schulze-Forster, K., Mehnert, W., Cytotoxicity of solid lipid nanoparticles as a funtion of the lipid matrix and the surfactant, Pharm. Res. 14 (1997) 458-462.

53. Westesen, K., Bunjes, H., Koch, M.H.J., Physicochemical characterization of lipid nanoparticles and evaluation of their drug loading capacity and sustained release potential, J. Control Release 48 (1997) 223-236.

54. Ahlin, P., Kristl, J., Šmid-Kobar, J., Optimization of procedure parameters and physical stability of solid lipid nanoparticles in dispersions, Acta Pharm. 48 (1998) 259-267.

55. Unruh, T., Bunjes, H., Westesen, K., Observation of size-dependent melting in lipid nanoparticles, J. Phys. Chem. 103 (1999) 10373-10377.

56. Jenning, V., Feste Lipid-Nanopartikel (SLN) als Trägersystem für die dermale Applilkation von Retinol, PhD Thesis, Freie Universität Berlin, 1999.

57. Maia C.S., Mehnert, W., Schläfer-Korting, M., Solid lipid nanoparticles as drug carriers for topical glucocorticoids, Int. J. Pharm. 196 (2000) 165-167.

58. Bunjes, H., Koch, M.H.J., Westesen, K., Effect of particle size on colloidal size solid triglycerides, Langmuir 16 (2000) 5234-5241.

59. Zimmermann, E., Müller, R.H., Electrolyte- and pH-stabilities of aqueous solid lipid nanoparticles (SLN™) dispersions in artificial gastrointestinal media, Eur. J. Pharm. Biopharm. 52 (2001) 203-210.

60. Olbrich, C., Kayser, O., Müller, R.H., Enzymatic degradation of Dynasan 114 SLN – effect of surfactants and particle size, J. Nanoparticle Res. 4 (2002) 121-129.

61. Olbrich, C., Kayser, O., Müller, R.H., Lipase degradation of Dynasan 114 and 116 solid lipid nanoparticles (SLN) – effect of surfactants, storage time and crystallinity, Int. J. Pharm. 237 (2002) 119-128.

62. Siekmann, B., Westesen, K., Submicron-sized parenteral carrier systems based on solid lipids, Pharm. Pharmacol. Lett. 1 (1992) 123-126.

63. Westesen, K., Siekmann, B., Koch, M.H.J., Investigations on the physical state of lipid nanoparticles by synchroton radiation X-ray diffraction, Int. J. Pharm. 93 (1993) 189-199.

64. Siekmann, B., Westesen, K., Melt-homogenized solid lipid nanoparticles stabilized by the nonionic surfactant tyloxapol. I. Physicochemical characterization and lyophilization, Pharm Phrmacol. Lett. 3 (1994) 194-197.

65. Siekmann, B. Westesen, K., Investigations on solid lipid nanoparticles prepared by precipitation in o/w emulsions, Eur. J. Pharm. Biopharm. 43 (1996) 104-109.

66. Westesen, K., Siekmann, B., Investigation of the gel formation of phospholipid-stabilized solid lipid nanoparticles, Int. J. Pharm. 151 (1997) 35-45.

67. Olbrich, C., Müller, R.H., Enzymatic degradation of SLN – effect of surfactants and surfactant mixtures, Int. J. Pharm. 180 (1999) 31-39.

68. Ahlin, A., Sentjurc, M., Strancar, J., Kristl, J., Location of lipophilic substances and ageing of solid lipid nanoparticles studied by EPR, STP Pharma Sci. 10 (2000) 125-132.

69. Ahlin, P., Kristl, J., Šentjurc, M., Štrancar, J., Pečar, S., Influence of spin probe structure on its distribution in SLN dispersions, Int. J. Pharm. 196 (2000) 241-244.

70. Jenning, V., Gohla, S., Comparison of wax and glyceride solid lipid nanoparticles (SLN®), Int. J. Pharm. 196 (2000) 219-222.

71. Miglietta, A., Cavalli, R., Bocca, C., Gabriel, L., Gasco, M.R., Cellular uptake and cytotoxicity of solid lipid nanospheres (SLN) incorporating doxorrubicin or paclitaxel, Int. J. Pharm. 210 (2000) 61-67.

72. Cavalli, R., Caputo, O., Gasco, M.R., Preparation and characterization of solid lipid nanospheres containing paclitaxel, Eur. J. Pharm. Biopharm. 10 (2000) 305-309.

73. Bunjes, H., Drechsler, M., Koch, M.H., Westesen, K., Incorporation of the model drug ubidecarenone into solid lipid nanoparticles, Pharm. Res. 18 (2001) 287-293.

74. Reithmeier, H., Herrmann, J., Göpferich, A., Development and characterization of lipid microparticles as a drug carrier for somatostatin, Int. J. Pharm. 218 (2001) 133-143.

75. Jenning, J., Gohla, S.H., Encapsulation of retinoids in solid lipid nanoparticles (SLN®), J. Microencapsul. 18 (2001) 149-158.

76. Wissing, S.A., Müller, R.H., The development of an improved carrier system for sunscreens formulations based on crystalline lipid nanoparticles, Int. J. Pharm. 242 (2002) 373-375.

77. Kristl, J., Volk, B., Ahlin, P., Gombač, K., Šentjurc, M., Interactions of solid lipid nanoparticles with model membranes and leukocytes studied by EPR, Int. J. Pharm. 256 (2003) 133-140.

78. Ahlin, P., Kristl, J., Pečar, S., Štrancar, J., Šentjurc, M., The effect of lipophilicity of spin-labelled compounds on their distribution in solid lipid nanoparticles dispersions studies by electron paramagnetic resonance, J. Pharm. Sci. 92 (2003) 58-66.

79. Souto, E.B., Wissing, S.A., Müller, R.H., Barbosa, C.M., HEC and Carbopol hydrogels containing clotrimazole loaded SLN, Rev. Port. Farm. LII Suppl. (2003) 25.

80. Souto, E.B., Wissing, S.A., Müller, R.H., Barbosa, C.M., Incorporation of clotrimazole in SLN - Evaluation of drug-lipid interaction, Rev. Port. Farm. LII Suppl. (2003) 117.

81. Souto, E.B., Wissing, S.A., Barbosa, C.M., Müller, R.H., Preparation of clotrimazole-loaded NLC and SLN, Proc. Intern. Symp. Control. Rel. Bioact. Mater. 30 (2003) 321.

82. Souto, E.B., Wissing, S.A., Barbosa, C.M., Müller, R.H., Preparation of topical formulations containing an antimycotic agent, Proc. Intern. Symp. Control. Rel. Bioact. Mater. 30 (2003) 322.

83. Eldem, T., Speiser, P., Altorfer, H., Polymorphic behavior of sprayed lipid micropellets and its evaluation by differential scanning calorimetry and scanning electron microscopy, Pharm. Res. 8 (1991) 178-184.

84. Weyhers, H., Feste Lipid Nanopartikel (SLN) für die gewebsspezifische Arzneistoffapplikation, Herstellung, Charakterisierung oberflächenmodifizierter Formulierungen, PhD Thesis, Freie Universität Berlin, 1995.

85. Dingler, A., Feste Lipif-Nanopartickel als kolloidale Wirkstoffträgersysteme zur dermalen Applikation, PhD Thesis, Freie Universität Berlin, 1998.

86. Radomska, A., Dobrucki, R., Müller, R.H., Chemical stability of the lipid matrices of solid lipid nanoparticles (SLN) development of an analytical method and determination of long-term stability, Pharmazie 54 (1999) 903-909.

87. Wang, J.-X., Sun, X., Zhang, Z.-R., Enhanced brain targeting by synthesis of 3'-5'-dioctanoyl-5-fluoro-2'-deoxyuridine and incorporation into solid lipid nanoparticles, Eur. J. Pharm. Biopharm. 54 (2002) 285-290.

88. Schubert, M.A., Müller-Goymann, C.C., Solvent injection as a new approach for manufacturing lipid nanoparticles – evaluation of the method and process parameters, Eur. J. Pharm. Biopharm. 55 (2003) 125-131.

89. Cavalli, R., Gasco, M.R., Morel, S., Behaviour of timolol incorporated in lipospheres in the presence of series of phosphate esters, STP Pharma Sci. 2 (1992) 514-518.

90. Cavalli, R., Peira, E., Caputo, O., Gasco, M.R., Solid lipid nanoparticles as carriers of hydrocortisone and progesterone complexes with β-cyclodextrins, Int. J. Pharm. 182 (1999) 59-69.

91. Trotta, M., Debernardi, F., Caputo, O., Preparation of solid lipid nanoparticles by a solvent emulsification-diffusion technique, Int. J. Pharm. 257 (2003) 153-160.

92. Müller, R.H., Maaβen, S., Weyhers, H., Mehnert, W., Phagocytic uptake and cytotoxicity of solid lipid nanoparticles (SLN) sterically stabilized with poloxamine 908 and poloxamer 407, J. Drug Target. 4 (1996) 161-170.

93. zur Mühlen, A., zur Mühlen, E., Niehus, H., Mehnert, M., Atomic force microscopy studies of solid lipid nanoparticles, Pharm. Res. 13 (1996) 1411-1416.

94. Müller, R.H., Maaβen, S., Weyhers, H., Specht, F., Lucks, J.S., Cytotoxicity of magnetite-loaded polylactide, polylacttide/glycolide particles and solid lipid nanoparticles, Int. J. Pharm. 138 (1996) 85-94.

95. Müller, R.H., Maaβen, S., Schwarz, C., Mehnert, W., Solid lipid nanoparticles (SLN) as potential carrier for human use: interaction with human granulocytes, J. Control. Release 47 (1997) 261-269.

96. Freitas, C., Müller, R.H., Effect of light and temperature on zeta potential and physical stability in solid lipid nanoparticles (SLN™) dispersions, Int. J. Pharm. 168 (1998) 221-229.

97. Freitas, C., Müller, R.H., Stability determination of solid lipid nanoparticles (SLN™) in aqueous dispersion after addition of electrolyte, J. Microencapsul. 16 (1999) 59-71.

98. Freitas, C., Müller, R.H., Correlation between log-term stability of solid lipid nanoparticles (SLN™) and crystallinity of the lipid phase, Eur. J. Pharm. Biopharm. 47 (1999) 125-132.

99. Müller, R.H., Olbrich, C., Solid lipid nanoparticles: phagocytic uptake in vitro cytotoxicity and in vitro biodegradation. 1st Comunication, Pharm. Ind. 61 (1999) 462-467.

100. Pinto, J.F., Müller R.H., Pellets as carriers of solid lipid nanoparticles (SLN) for oral administration of drugs, Pharmazie 54 (1999) 506-509.

101. Videira, M.A., Almeida, A.J., Botelho, M.F., Santos, A.C., Gomes, C., Pedroso Lima, J.J., Lymphatic uptake radiolabelled solid lipid nanoparticles administered by the pulmonary route, Eur. J. Nuclear Medicine 26 (1999) PS-462.

102. Schöler, N., Zimmermann, E., Katzfey, U., Hahn, H., Müller, R.H., Liesenfeld, O., Preserved solid lipid nanoparticles (SLN) at low concentrations do cause neither direct nor indirect cytotoxic effects in peritoneal macrophages, Int. J. Pharm. 196 (2000) 235-239.

103. Jenning, V., Thünemann, A.F., Gohla, S.H., Characterization of a novel solid lipid nanoparticle carrier system based on binary mixtures of liquid and solid lipids, Int. J. Pharm. 199 (2000) 167-177.

104. Jenning, V., Gysler, A., Schäfer-Korting M., Gohla S., Vitamin A loaded solid lipid nanoparticles for topical use: occlusive properties and drug targeting to the upper skin, Eur. J. Pharm. Biopharm. 49 (2000) 211-218.

105. Olbrich, C., Müller, R.H., Tabatt, K., Kayser, O., Schulze, C., Schade, R., Stable biocompatible adjuvants – a new type of adjuvant based on solid lipid nanoparticles: a study on cytotoxicity, compatibility and efficacy in chicken, ATLA 30 (2002) 443-458.

106. Jenning, V., Mäder, K., Gohla, S., Solid lipid nanoparticles (SLN™) based on binary mixtures of liquid and solid lipids: a ^{1}H-NMR study, Int. J. Pharm. 205 (2000) 15-21.

107. Jenning, V., Schäfer-Korting, M., Gohla, S., Vitamin A-loaded solid lipid nanoparticles for topical use: drug release properties, J. Control Release 66 (2000) 115-126.

108. Olbrich, C., Bakowsky, U., Lehr, C.-M., Müller, R.H., Kneuer, C., Cationic solid-lipid nanoparticles can efficiently bind and transfect plasmid DNA, J. Control. Release 77 (2001) 345-355.

109. Demirel, M., Yzan, Y., Müller, R.H., Kilic, F., Bozan, B., Formulation and in vitro-in vivo evaluation of piribedil solid lipid micro- and nanoparticles, J. Microencapsul. 18 (2001) 359-371.

110. Videira, M.A., Botelho, M.F., Santos, A.C., Gouveia, L.F., Pedroso Lima, J.J., Almeida, A.J., Lymphatic uptake of pulmonary delivered radiolabelled solid lipid nanoparticles, J. Drug. Target. 10 (2002) 607-613.

111. Lukowski, G., Pflegel P., Electron diffraction of solid lipid nanoparticles loaded with aciclovir, Pharmazie 52 (1997) 642-643.

112. Lukowski, G., Kasbohm, J., Pflegel, P., Illing, A., Wulff, H., Crystallographic investigation oof cetylpalmitate solid lipid nanoparticles, Int. J. Pharm. 196 (2000) 201-205.

113. Lippacher, A., Müller, R.H., Mäder, K., Preparation of semisolid drug carriers for topical application based on solid lipid nanoparticles, Int. J. Pharm. 214 (2001) 9-12.

114. Wissing, S.A., Müller, R.H., Solid lipid nanoparticles (SLN) – a novel carrier for UV blockers, Pharmazie 56 (2001) 783-786.

115. Sznitowska, M., Gajewska, M, Janicki, S., Radwanska, A., Lukowski, G., Bioavailability of diazepam from aqueous-organic solution, submicron and solid lipid nanoparticles after rectal administration in rabbits, Eur. J. Pharm. Biopharm. 52 (2001) 159-163.

116. Wissing, S.A., Müller, R.H., A novel sunscreen system based on tocopherol acetate incorporated into solid lipid nanoparticles, Int. J. Cosmet. Sci. 23 (2001) 233-243.

117. Wissing, S.A., Müller, R.H., Solid lipid nanoparticles as carrier for sunscreens: in vitro release and in vivo skin penetration, J. Control. Release 81 (2002) 225-233.

118. Souto, E.B., Wissing, S.A., Müller, R.H., Barbosa, C.M., NLC as new carrier systems for dermal and cosmetic preparations, Congresso Nacional dos Farmacêuticos, Lisbon 27th to 29th Nov 2003.

119. Lippacher, A., Müller, R.H., Mäder, K., Semisolid SLN™ dispersions for topical application: influence of formulation and production parameters on viscoelastic properties, Eur.J. Pharm. Biopharm. 53 (2002) 155-160.

120. Gasco, M.R., Cavalli, R., Carlotti, M.E., Timolol in lipospheres, Pharmazie 47 (1992) 119-121.

121. Gasco, M.R., Morel, S., Carpigno, R., Optimization of the incorporation of desoxycortisone acetate in lipospheres, Eur. J. Pharm. Biopharm. 38 (1992) 7-10.

122. Cavalli, R., Caputo, O., Gasco, M.R., Solid lipospheres of doxorubicin and idarubicin, Int. J. Pharm. 89 (1993) R9-R12.

123. Morel, S., Gasco, M.R., Cavalli, R., Incorporation in lipospheres of [D-Trp-6]LHRH, Int. J. Pharm. 105 (1994) R1-R3.

124. Cavalli, R. Morel, S., Gasco, M.R., Chetoni, P., Saettone, M.F., Preparation and evaluation in vitro of colloidal lipospheres containing pilocarpine as ion pair, Int. J. Pharm. 117 (1995) 243-246.

125. Cavalli, R., Marengo, E., Rodriguez, L., Gasco, M.R., Effect of some experimental factors on the production process of solid lipid nanoparticles, Eur. J. Pharm. Biopharm. 43 (1996) 110-115.

126. Morel, S., Ugazio, E., Cavalli, R., Gasco, M.R., Thymopentin in solid lipid nanoparticles, Int. J. Pharm. 132 (1996) 259-261.

127. Cavalli, R., Caputo, O., Marengo, E., Pattarino, F., Gasco, M.R., The effect of the components of microemulsions on both size and crystalline structure of solid lipid nanoparticles (SLN) containing a series of model molecules, Pharmazie 53 (1998) 392-396.

128. Morel, S., Terreno, E., Ugazio, E., Aime, S., Gasco, M.R., NMR relaxometric investigations of solid lipid nanoparticles (SLN) containing gadolinium (III) complexes, Eur. J. Pharm. Biopharm. 45 (1998) 157-163.

129. Yang, S., Zhu J., Lu, Y., Liang, B., Yang, C., Body distribution of camptpthecin solid lipid nanoparticles after oral administration, Pharm. Res. 16 (1999) 751-757.

130. Marengo, E., Cavalli, R., Caputo, O., Rodriguez, L., Gasco, M.R., Scale-up of the preparation process of solid lipid nanospheres. Part I, Int. J. Pharm. 205 (2000) 3-13.

131. Cavalli, R., Gasco, M.R., Barresi, A.A., Rovero, G., Evaporative drying of aqueous dispersions of solid lipid nanoparticles, Drug Dev. Ind. Pharm. 27 (2001) 919-924.

132. Chen, D.-B., Yang, T.-Z., Lu, W.-L., Zhang Q., In vitro and in vivo study of two types of long-circulating solid lipid nanoparticles containing paclitaxel, Chem. Pharm. Bull. 49 (2001) 1444-1447.

133. Zhang, Q., Yie, G., Li, Y., Yang, Q., Nagai, T., Studies on the cyclosporin A loaded stearic acid nanoparticles, Int. J. Pharm. 200 (2000) 153-159.

134. Yang, A.C., Lu, L.F., Cai, Y., Zhu, J.B., Liang, B.W., Yang, C.Z., Body distribution in mice of intravenously injected camptothecin solid lipid nanoparticles and targeting effect on brain, J. Control. Release 59 (1999) 299-307.

135. Ugazio, E., Cavalli, R., Gasco M.R., Incorporation of cyclosporine A in solid lipid nanoparticles (SLN), Int. J. Pharm. 241 (2002) 341-344.

136. Zara, G.P., Cavalli, R., Fundaro, A., Bargoni, A., Caputo, O., Gasco, M.R., Pharmacokinetics of doxorrubicin incorporated in solid lipid nanospheres (SLN), Pharmacol. Res. 40 (1999) 281-286.

137. Fundaro A., Cavalli R., Bargoni A., Vighetto D., Zara G.P., Gasco M.R. - Non-stealth and stealth solid lipid nanoparticles (SLN) carrying doxorubicin: pharmacokinetics and tissue distribution after i.v. administration to rats, Pharmacol. Res. 42 (2000) 337-343.

138. Cavalli, R., Zara, G.P., Caputo, O., Bargoni, A., Fundaro, A., Gasco, M.R., Transmucosal transport of tobramycin incorporated in solid lipid nanoparticles (SLN) after duodenal administration to rats. Part I – A pharmacokinetic study, Pharmacol. Res. 42 (2000) 541-545.

139. Bargoni, A., Cavalli, R., Zara, G.P., Fundaro, A., Caputo, O., Gasco, M.R., Transmucosal transport of tobramycin incorporated in solid lipid nanoparticles (SLN) after duodenal administration to rats. Part II – Tissue distribution, Pharmacol. Res. 43 (2001) 497-502.

140. Cavalli, R., Bargoni, A., Porio, V., Muntoni, E., Zara, G.P., Gasco, M.R., Duodenal administration of solid lipid nanoparticles loaded with different percentages of tobramicin, J. Pharm. Sci. 92 (2003) 1085-1094.

141. Siekmann, B., Westesen, K., Preparation and physicochemical characterization of aqueous dispersions of coenzyme Q_{10} nanoparticles, Pharm. Res. 12 (1995) 201-208.

142. Sjöström, B., Bergenståhl, B., Preparation of submicron drug particles in lecithin-stabilized o/w emulsions. I. Model studies of the precipitation of cholesteryl acetate, Int. J. Pharm. 88 (1992) 53-62.

143. Lukowski, G., Werner, U., Pflegel, P., Surface investigation and drug release of drug-loaded solid lipid nanoparticles, Proc. 2nd World Meeting APGI/APV, Paris, 573-574, 1998.

144. Lukowski, G., Werner, U., Investigation of surface and drug release of solid lipid nanoparticles loaded with acyclovir, Intern. Symp. Control. Rel. Bioact. Mater. 25 (1998) 425-428.

145. Fukui, H., Koike, T., Saheki, A., Sonoke, S., Yoshikaw, H., Sasaki, H., Tomii, Y., Seki, S., Characteristics of NS-718, a low-dose therapeutic system for amphotericin B with lipid nano-sphere (LNS®), Proc. Intern. Symp. Control. Rel. Bioact. Mater. 25, 1998, 388-389.

146. Hossain, M.A., Maesaki, S., Razzaque, M.S., Tomono, K., Taguchi, T., Kohno, S., Attenuation of nephrotoxicity by a novel lipid nanosphere (NS-718) incorporating amphotericin B, J. Antimicrob. Chemother. 46 (2000) 263-268.

147. Lukowski, G., Hölzle, D., Structural investigations of drug incorporation in solid lipid nanoparticles, Proc. 4th World Meeting APV/APGI, Florence, 2002, 1455-1456.

148. Shahgaldian, P., Quattrocchi, L., Gualbert, J., Coleman, A.W., Goreloff, P., AFM imaging of calixarene based solid lipid nanoparticles in gel matrices, Eur. J. Pharm. Biopharm. 55 (2003) 107-113.

149. Shahgaldian, P., Gualbert, J., Aïssa, K., Coleman, A.W., A study of the freeze-drying conditions of calixarene based solid lipid nanoparticles, Eur. J. Pharm. Biopharm. 55 (2003) 181-184.

150. Shahgaldian, P., Da Silva, E., Coleman, A.W., Rather, B., Zaworotko, M.J., Para-acyl-calix-arene based solid lipid nanoparticles (SLNs): a detailed study of preparation and stability parameters, Int. J. Pharm. 253 (2003) 23-38.

151. Gualbert, J., Shahgaldian, P., Coleman, A.W., Interactioms of amphiphilic calyx[4]arene-based Solid Lipid Nanoparticles with bovine serum albumin, Int. J. Pharm. 257 (2003) 69-73.

152. Sjöström, B., Kaplun, A., Talmon, Y., Cabane, B., Structures of nanoparticles prepared from oil-in-water emulsions, Pharm. Res. 12 (1995) 39-48.

153. Ugazio, E., Marengo, E., Pellizzaro, C., Coradini, D., Peira, E., Daidone, M.G., Gasco, M.R., The effect of formulation and concentration of cholesteryl butyrate solid lipid nanospheres (SLN) on NIH-H460 cell proliferation, Eur. J. Pharm. Biopharm 52 (2001) 197-202.

154. Dubes, A., Parrot-Lopez, H., Abdelwahed, W., Degobert, G., Fessi, H., Shahgaldian P., Coleman, A.W., Scanning electron microscopy and atomic force microscopy imaging of solid lipid nanoparticles derived from amphiphilic cyclodextrins, Eur. J. Pharm. Biopharm. 55 (2003) 279-282.

155. Dubes, A., Parror-Lopez, H., Shahgaldian, P., Coleman, A.W., Interfacial interactions between amphiphilic cyclodextrins and physiologically relevant cations, J. Colloid Interface Sci. 259 (2003) 103-111.

156. Müller, R.H. Runge, S., Ravelli, V., Pharmaceutical cyclosporin formulation of improved biopharmaceutical performance and improved physical quality and stability and process for producing same. Deutsche Patentanmeldung 198 19 273 A1, 1998.

157. Runge, S.A., Feste Lipidnanopartikel (SLN®) alss kolloidaler Arzneistoffträger für die orale applikation von cyclosporin A, Ph.D Thesis, Freie Universitär Berlin, 1998.

158. Penkler, L., Müller, R.H., Runge, S., Ravelli, V., Pharmaceutical cyclosporin formulation with improved biopharmaceutical properties, improved physical quality and greater stability, and method for producing said formulation. PCT application PCT/EP99/02892, 1999.

159. Olbrich, C., Runge, S.A., Mehnert, W., Thünemann A.F., Müller R.H., Entrapment efficiency and biodegradation of cyclosporine loaded solid lipid nanoparticles (SLN) for peroral administration, Proc. 3rd World Meeting APV/APGI, Berlin, 2000, 425-426.

160. Radtke, M., Müller, R. H., Novel concept of topical cyclosporine delivery with supersaturated SLN™ creams, Intern. Symp. Control. Rel. Bioact. Mater. 28 (2001) 470-471.

161. Radtke, M., Müller, R. H., Stability study of creams containing cyclosporine SLN™, Proc. Intern. Symp. Control. Rel. Bioact. Mater. 28 (2001) 472-473.

162. Fresta, M., Bucolo, C., Maltese, A., Mangiafico, S., Puglisi, G., Pegylated solid lipid nanospheres as ophthalmic delivery systems of dexamethasone, Proc. 4th World Meeting APGI/APV, Florence, 2002, 941-942.

163. Wissing, S.A., Mäder, K., Müller, R.H., Prolonged efficacy of the insect lemon oil by incorporation into solid lipid nanoparticles (SLN™), Proc. 3rd World Meeting APGI/APV, Berlin, 2000, 439-440.

164. Yaziksiz-Iscan, Y., Wissing, S.A., Müller, R.H., Hekimoglu, S., Different production methods for solid lipid nanoparticles (SLN) containing the insect repellent DEET. Proc. 4th World Meeting APGI/APV, Florence, 2002, 789-790.

165. Yaziksiz-Iscan, Y., Hekimoglu, S., Sargon, M.F., Kas, S., Hincal, A.A., In vitro release and skin permeation of DEET incorporated solid lipid nanoparticles in various vehicles, Proc. 4th World Meeting APGI/APV, Florence, 2002, 1183-1184.

166. Olbrich, C., Kayser, O., Lamprecht, A., Kneuer, C., Lehr, C.M., Müller, R.H., Interactions of fluorescent solid lipid nanoparticles (SLN) with macrophage-like cells visualized by CLSM, Proc. 3rd World Meeting APV/APGI, Berlin, 2000, 331-332.

167. Ambarkhane, A.V., Gala, H.J., Patravale, V.B., Submicron Lipopearls of nimesulide, Abstract Book 4th Internation Symposium on Innovations in Pharmaceutical Sciences and Technology 2000, p.52.

168. Videira, M., Azevedo, A.F., Almeida, A.J., Entrapment of a high molecular weight protein into solid lipid nanoparticles (SLN), Proc. 2nd World Meeting APGI/APV, Paris, 1998.

169. Videira, M., Almeida, A.J., Müller, R.H., Incorporation of paclitaxel in SLN: Assessment of drug-lipid interaction, Proc. 3rd World Meeting APGI/APV, Berlin, 2000.

170. Müller, R.H., Mäder, K., Lippacher, A., Jenning, V., Fest-flüssig (halbfeste) Lipidpartikle und Verfahren zur Herstellung hochkonzentrierter Lipidpartikeldispersionen. PCT application PCT/EP00/04565.

171. Wissing, S.A., Mäder, K., Müller, R.H., Solid lipid nanopartices (SLN™) as a novel carrier system offering prolonged release of the perfume Allure (Chanel), Proc. Int. Symp. Control. Rel. Bioact. Mater. 27 (2000) 311-312.

172. Müller, R.H., zur Mühlen, A., Freitas, A., Mehnert, W., Solid lipid nanoparticles (SLN) for intravenous drug delivery, Proc. Intern. Symp. Control. Rel. Bioact. Mater. 23 (1996) 184-185.

173. Schütt, D.H., Kaiser, Stamm, I., Kubis, A., E., Müller, R.H., New generation of cosmetic products based on solid lipid nanoparticles (Lipopearls™), Proc. 2nd World Meeting APGI/APV, Paris, 585-586, 1998.

174. Jenning, V., Hildebrand, G. E., Gysler, A., Schäfer-Korting, M., Gohla, S., Solid lipid nanoparticles (SLN™) for topical application: occlusive properties, Intern. Symp. Control. Rel. Bioact. Mater. 26 (1999) 405-406.

175. Jenning, V., Lippacher, A., Gohla, S.H., Rheologic properties of SLN-containing dermal preparations, Proc. 3rd Word Meeting APGI/APV, Berlin, 713-714, 2000.

176. Ahlin, P., Kristl, J., Šentjurc, M., EPR study of loading capacity and location of spin-labeled lipophilic substances in different SLN, Proc. Intern. Symp. Control. Rel. Bioact. Mater. 25, 1998, 334-335.

177. Lippacher, A., Müller, R.H., Mäder, K., Investigations on semi-solid SLN™ dispersions made from solid-liquid mixtures by means of ERS and rheometry, Proc. Intern. Symp. Control. Rel. Bioact. Mater. 27, 2000, 325-326.

178. Lippacher, A., Pharmazeutisch-technologische Characterisierung von flüssigen und halbfesten SLN Dispersionen für die topische Applikation, PhD Thesis, 2000.

179. Wissing, S.A., Müller, R.H., Solid lipid nanoparticles (SLN) as sunscreens: advantages over conventional emulsion based systems, Proc. Intern. Symp. Control. Rel. Bioact. Mater. 28 (2001) 522-523.

180. Wissing, S.A., Müller, R.H., In vitro and in vivo skin permeation of sunscreens from solid lipid nanoparticles (SLN™), supercooled melts and emulsions, Proc. 4th World Meeting APGI/APV, Florence, 2002, 1135-1136.

181. Wissing, S.A., Müller, R.H., Cosmetic applications for solid lipid nanoparticles (SLN), Int. J. Pharm. 254 (2003) 65-68.

182. Dingler, A., Hildebrand, G., Niehus, H., Müller, R.H., Cosmetic anti-aging formulation based on vitamin E-loaded solid lipid nanoparticles, Intern. Symp. Control. Rel. Bioact. Mater. 25 (1998) 433-434.

183. Dingler, A., Blum, R.P., Niehus, H., Müller, R.H., Gohla, S., Solid lipid nanoparticles (SLN/Lipopearls) – a pharmaceutical and cosmetic carrier for the application of vitamin E in dermal products, J. Microencapsul. 16 (1999) 751-767.

184. Olbrich, C., Kayser, O., Müller, R.H., Tributyrin, a potent anticancer agent retains its biological activity after incorporation in solid lipid nanoparticles (SLN), Proc. Intern. Symp. Control. Rel. Bioact. Mater. 26 (1999) 935-936.

185. Müller, R.H., Dingler, A., Feste Lipid-Nanopartikel (Lipopearls™) als neuartiger Carrier für kosmetische und dermatologische Wirkstoffe, Pharm. Zeit. Dermo. 49 (1998) 11-15.

186. Yaziksiz-Iscan, Y., Wissing, S.A., Hekimoglu, S., Müller, R.H., Development of a novel carrier system for vitamin K using solid lipid nanoparticles (SLN™), Proc. 4th World Meeting APGI/APV, Florence, 2002, pp. 787-888.

187. Müller, R.H., Dingler, A., The next generation after the liposomes: solid lipid nanoparticles (SLN™, Lipopearls™) as dermal carrier in cosmetics, Eurocosmetics 7/8 (1998) 19-26.

188. Henry, K.W., Nickels, J.T., Edlind, T.D., Upregulation of ERG genes in Candida species by azoles and other sterol biosynthesis inhibitors, Antimicrob. Agents Chemother. 44 (2000) 2693-2700.

189. Appleton, S.S., Candidiasis: pathogenisis, clinical characteristics and treatment, J. Calif. Dent. Assoc. 28 (2000) 942-948.

190. Remington's Pharmaceutical Sciences, 18th Ed.

191. Niedner, R., Ziegenmeyer, J., Dermatika: Therapeutischer Einsatz, Pharmakologie und Pharmazie, Wissenschaftliche Verlagsgeselschaft mbH Stuttgart, 1992.

192. Carola, R., Harley,J., Noback C.R., Human anatomy and physiology, McGraw Hill, 2nd Ed, 1992, pp. 122-139.

193. Beck, T.,Wree, A., Die Haut, Pharmazeutische Zeitung 51/52 (1994) 68-73.

194. Heymann, E., Haut, Haar und Kosmetik, Wissenschaftliche Verlagsgesellschaft mbH, Stuttgart, 1994.

195. Wright, N.A., The Cell Proliferation Kinetics of the Epidermis, in: Biochemistry and Physiology of the Skin, Goldsmith, L.A., ed., Oxford University Press, New York/Oxford, 1983.

196. Mathias, C.G.T., Clinical and Experimental Aspects of Cutaneous Irritation, in: Dermatotoxicity, Marzulli, F.N. and Maibech, M.I., eds., 2nd Ed., Washington/New York/London, 1983.

197. Idson, B., Lazarus, J., Semisolids, in: The Theory and Practice of Industrial Pharmacy, Lachman, L., Lieberman, H.A., Kanig, J.L. eds., Lea & Febiger, Philadelphia, 1986.

198. Flynn, G.L., Clinical supplies to dermal diffusion and delivery principles, in: Encyclopedia of Pharmaceutical Technology, Swarbrick, J., and Boylan, J.C., eds., Marcel Dekker, New York/Basel, Vol. 3, 1988, pp. 457-503.

199. Gregoriades, G. (ed.) Liposomes as drug Carrier, John Wiley & Sons, Chichester-New York-Brisbane-Toronto-Singapore, 1989.

200. Barbosa C.M.G., Desenvolvimento e caracterização de formulações lipossómicas de monofosfato de vidarabina para o tratamento da hepatite B crónica., PhD Thesis, Faculdade de Farmácia Universidade do Porto, 1995.

201. Schubert, R., Liposomen in Arzneimitteln, in: Pharmazeutische Technologie: Moderne Arzneiformen, Müller, R.H., Hildebrand, G. eds., Wissenschaftliche Verlagsgesellschaft mbH, Stuttgart, 1998, pp. 219-242.

202. New York Acad. Sci.; The use of liposomes in biology and medicine. Conference Proceedings, 1977.

203. Schubert, R., Liposomes in topical application and their mode of action in the skin, Arch. Pharm, 324 (1991) 627-633.

204. Lasch, J., Bouwstra, J., Interactions of external lipids (lipid vesicles) with the skin, J. Liposome Res. 5 (1995) 543-569.

205. Foldvari, M., Gesztes, A., Mezei, M., Dermal drug delivery by liposome encapsulation: clinical and electromicroscopical studies, J. Microencapsul 7 (1990) 479-489.

206. Hofland, H.E.J., Bouwstra, J.A., Spies, F., Boddé, E., Nagelkerke, J.F., Cullander, C., Junginger, H.E., Interactions between non-ionic surfactant vesicles and human stratum corneum in vitro, J. Liposome Res. 5 (1995) 241-263.

207. Wohlrab, W., Lasch, J., The effect of liposomal incorporation of topically applied hydrocortisone on its serum concentration and urinary excretion, Dermatol. Mon. Schr. 175 (1989) 348-352.

208. Cevc, G., Blume, G., Lipid vesicles penetrate into skin owing to the transdermal osmotic gradients and hydration force, Biochim. Biophys. Acta 1104 (1992) 226-232.

209. Arunothayanun, P., Craig, D.Q.M., Uchegbu, I.F., Florence, A.T., An investigation into the phase behaviour of polyhedral niosomes using high sensitivity differential scanning calorimetry, Proc. Int. Symp. Control. Rel. Bioact. Mater. 24 (1997) 977-978.

210. Schreier, H., Bouwstra, J., Liposomes and niosomes as topical drug carriers: dermal and transdermal drug delivery, J. Control. Release 30 (1994) 1-15.

211. Schubert, R., Liposomen in Arzneimitteln, in: Pharmazeutische Technologie: Moderne Arzneiformen, Müller, R.H., Hildebrand, G. eds., Wissenschaftliche Verlagsgesellschaft mbH, Stuttgart, 1997, pp. 167-186.

212. Theis, H., Göhring, S., Einsatz von Sphingolipiden in Hautpflegeprodukten, SÖFW 121 (1995) 343-348.

213. Haße, A., Keipert, S., Development and characterization of microemulsions for ocular application, Eur. J. Pharm. Biopharm. 43 (1997) 179-183.

214. Wendorff, A., Keipert, S., Optimierte Verfügbarkeit von β-Rezeptorenblockern aus einem Mikroemulsionssystem zur okularen Anwendung, PhD Thesis, Brandenburg-Berlin, 1999.

215. Pouton, C.W., Formulation of self-emulsifying drug delivery systems, Adv. Drug. Del. Rev. 25 (1997) 47-58.

216. Attwood, D., Microemulsions, in: Colloidal drug delivery systems, Kreuter, J., ed., Marcel Dekker Inc., New York, Basel, Hong Kong, 1994, pp. 31-71.

217. Kreilgaard, M., Influence of microemulsions on cutaneous drug delivery, Adv. Drug Deliv. Rev. 54 (2002) S77-S98.

218. Paolino, D., Ventura, C.A., Nistico, S., Puglisi, G., Fresta, M., Lecithin microemulsions for the topical administration of ketoprofen: percutaneous adsorption through human skin and in vivo human skin tolerability, Int. J. Pharm. 244 (2002) 21-31.

219. Rangarajan, M., Zatz, J.L., Effect of formulation on the topical delivery of alpha-tocopherol, J. Cosmet. Sci. 54 (2003) 131-174.

220. Trotta, M., Ugazio, E., Peira, E., Pulitano, C., Influence of ion pairing on topical delivery of retinoic acid from microemulsions, J. Control. Release 86 (2003) 315-321.

221. Kutz, G., Bielh, P., Waldmann-Laue, M., Jackwerth, B., Zur Auswahl von O/W-Emulgatoren für den Einsatz in Hautpflegeprodukten, SÖFW 123 (1997) 145-150.

222. Gohla, S., Multiple Emulsionen vom Typ Wasser-in-öl-in-Wasser (W/O/W) in Kosmetika, in: Pharmazeutische Technologie: Moderne Arzneiformen, Müller, R.H., Hildebrand, G.E., Hrsg, Wissenschaftliche Verlagsgesellschaft mbH, Stuttgart, 1997, pp. 143-154.

223. Marty, J.J., Oppenheim, R.C., Speiser, P., Nanoparticles – A new colloidal drug delivery system, Pharm. Acta Helv. 53 (1978) 17-23.

224. Hausberger, A.G., Kenley, R.A., DeLuca, P.P., Gamma irradiation effects on molecular weight and in vitro degradation of poly(D,L-lactide-co-glycolide) microparticles, Pharm. Res. 12 (1995) 851-856.

225. Smith, A., Hunneyball, J.M., Evaluation of poly(lactic acid) as biodegradable drug delivery system for parenteral administration, Int. J. Pharm. 30 (1986) 215-220.

226. Eldem, T., Speiser, P., Hincal, A., Optimization of spray-dried and congealed lipid micropellets and characterization of their surface morphology by scanning electron microscopy, Pharm. Res. 8 (1991) 47-54.

227. Domb, A.J., Liposheres for controlled delivery of substances, USP Patent, 1993, USS 188837.

228. Domb, A.J., Liposphere parenteral delivery system, Proc. Intern. Symp. Control. Rel. Bioact. Mater. 20 (1993) 346-347.

229. Müller, R.H., Lucks J.S., Arzneistoffträger aus festen Lipidteilchen, Feste Lipidnanosphären (SLN). European Patent EP0605497B1, 1996.

230. Gasco, M.R., Methods for producing solid lipid microspheres having a narrow size distribution, USP Patent 5 250 236 (1993).

231. Siekmann, B., Westesen, K., Submicron lipid suspensions (Solid lipid nanoparticles) versus lipid nanoemulsions: similarities and differences, in: Submicron Emulsions in Drug Targeting and Delivery, Benita, S. ed., Harwood Academic Publishers, Amsterdam, 1998, pp. 205-218.

232. Souto, E.B., Aspectos tecnológicos da preparação de micro e nanopartículas biodegradáveis, Faculdade de Farmácia, Universidade do Porto, 2003.

233. Schwarz, C., Mehnert, W., Müller, R.H., Influence of production parameters of solid lipid nanoparticles (SLN) on the suitability for intravenous injection, Eur. J. Pharm. Biopharm. 40 (1994) 24S.

234. Maa, Y.F., Hsu, C.C., Performance of sonication and microfluidization for liquid-liquid emulsification, Pharm. Dev. Technol. 4 (1999) 233-240.

235. Fessi, H., Puisieux, F., Devissaguet, J.P., Eur. Patent 274 961 (1987).

236. Quintanar-Gerrero, D., Fessi, H., Alléman, E., Doelker, E., Pseudilatex preparation using a novel emulsion-diffusion process involving direct displacement of partially-water-miscible solvents by distillation, Int. J. Pharm. 188 (1999) 155-164.

237. Müller, R.H., Jenning, V., Deutsche Patentenmeldung 199 38 371.5, 2000.

238. Barrow, G. M., Physikalische Chemie, Bohmann Vieweg Verlag Braunschweig, 6. Auflage 1984.

239. Sato, K., Crystallization of fats and fatty acids, in: Garti, N., Sato, K. (Eds), Crystallization and Polymorphism of Fats and Fatty Acids, Surfactant Science Series, Vol. 32, Marcel Dekker, New York, 1988, pp. 267-303.

240. Weiner, A. L., Lipids in pharmaceutical dosage forms, in: Swarbrick, J., Boylan, J. C., Encyclopedia of pharmaceutical technology, Marcel Dekker Inc. New York, 1993.

241. Larsson, K., Classification of glyceride crystal forms, Acta Chem. Scand. 20 (1966) 2255-2260.

242. Sato, K., Ueno, S., Yano, J., Molecular interactions and kinetic properties of fats, Pro. Lipid Res. 38 (1999) 91-116.

243. Hagemann, J. W., Thermal behaviour and polymorphism of acylglycerides, in: Crystallization and polymorphism of fats and fatty acids, Marcel Dekker Inc. New York und Basel, 1988, 9-95.

244. Hernqvist, L., Crystal structures of fats and fatty acids, in: Crystallization and polymorphism of fats and fatty acids, Garti, N., Sato, K., Hrsg., Marcel Dekker Inc. New York and Basel, 1988, 97-137.

245. Müller, B.W., Suppositorien, Wissenschaftliche Verlagsgesellschaft mbH, Stuttgart, 1986.

246. Vadnera, K., in: Encyclopedia of pharmaceutical technology, Swarbrick, J. and Boylan, J., Marcel Dekker Inc., New York, 1993, pp. 337-352.

247. Larsson, K., Fette, Seifen, Anstrichm. 74, (1972) 136-142.

248. Westesen, K., Novel lipid based-colloidal dispersions as potential drug administration systems – expectations and reality, Colloid. Polym. Sci. 278 (2000) 608-618.

249. Voigt, R., Pharmazeutischen Technologie, Ullstein Mosby GmbH Berlin, 7. Auflage 1993.

250. Sasol Germany GmbH, Oleochemicals Catalogue, Arthur-Imhausen-Str. 92, D-Witten, Deutschland.

251. Fiedler, H. P., Lexikon der Hilfsstoffe für Pharmazie, Kosmetik und angrenzender Gebiete, Edition Cantor Verlag Aulendorf, 4. Auflage, 1996.

252. European Pharmacopoeia, 4th Ed.

253. Hüls AG, Catalogue, Postfach 1269, D-Witten, Deutschland.

254. Kibbe A.H. (Ed), Handbook of Pharmaceutical Excipients, 3rd Ed., 2000.

255. Gattefossé AG, Pharmaceutical excipients guide, Haupstr. 435, Weil am Rhein, Deutschland.

256. Weidlich, H. A., Gattefossé AG, persönliche Mitteilung, 1999.

257. Caelo GmbH, Caesar and Loretz, D-Hilden, Deutschland.

258. IUPAC (International Union of Pure and Applied Chemistry), Division of Physical Chemistry, Manual of Symbols an Terminology for Physicochemical Quantities and Units, Appendix II part I, Butterworths London, 1972, S. 611.

259. Food additives - GRAS substances, Food Drug Cosmetic Law Reports, Chicago, 1994.

260. Martindale, The Extra Pharmacopoeia, 34th Ed.

261. ICI Surfactants, Essen, Germany.

262. BASF AG, Pharmaceutical excipients guide, Carl-Bosch-Straße 38, D-67056 Ludwigshafen, Deutschland.

263. Bauer, K. H., Frömming, K. H., Führer, C., Pharmazeutische Technologie, Thieme Verlag Stuttgart, 4. Auflage 1993

264. Lipoid KG, Catalogue, D-Ludwigschafen, Germany.

265. Goldschmidt, Catalogue 2002, Essen, Germany.

266. Pena, L. E., Gel Dosage Forms: Theory, Formulation and Processing, in: Topical Drug Delivery Formulations, Osborne, D. W., Amann, A.H., eds., Marcel Dekker, Inc, New York, Basel, 1990.

267. Sigma Aldrich, Catalogue, D-Deisenhofen, Germany.

268. BF Goodrich, Catalogue, USA.

269. Illum, L., Chitosan and its use as pharmaceutical excipient, Pharm. Res. 15 (1998) 1326-1331.

270. Singla, A.K., Chawala, M., Chitosan: some pharmaceutical ad biological aspects – an update, J. Pharm. Pharmacol. 53 (2001) 1047-1067.

271. Austen, P.R., Chitin solvents and solubility parameters. in: Chitin, Chitosan and Related Enzimes, Zikakis, J.P. ed., Academic, New York, 1984, pp. 277.

272. Hoogerheide, J.G., Wyka, E., Clotrimazole, in: Analyical Profiles of Drug Substances, Florey, K., ed., Vol. 11, Academic Press Inc., 1982, pp. 225-255.

273. Greenberg, H.L., Shwayder, T.A., Bieszk, N., Fivenson, D.P., Clotrimazole/betamethasone dipropionate: A review of costs and complications in the treatment of common cutaneous fungal infections, Ped. Dermatol. 19 (2002) 78-81.

274. Huy, N.T., Kamei, K., Yamamoto, T., Kondo, Y., Kanaori, K., Takano, R., Tajima, K., Hara, S., Clotrimazole binds to heme and enhances heme-dependent hemolysis, J. Biol. Chem. 277 (2002) 4152-4158.

275. Mselle, J., Use of topical clotrimazole in human keratomycosis, Ophthalmologica, 215 (2001) 357-360.

276. Saleh, A.S., Al-Hedaithy, First report of human infection due to the fungus Triadelphia pylvinata, J. Clin. Microbiol. 39 (2001) 3386-3389.

277. Smith, E.B., Brenenman D.L., Griffith, R.F., et al. Double-blind comparison of naftifine cream and clotrimazole/betamethasone dipropionate cream in the treatment of tinea pedis, J. Am. Acad. Dermatol. 26 (1992) 125-127.

278. Fernández-Torres, B., Vásquez-Veiga, H., Llovo, X., Peiro Jr., M., Guarro, J., In vitro susceptibility to itraconazole, clotrimazole, ketocolazole and terbinafine of 100 isolates of Tichophyton rubrum, Chemotherapy 46 (2000) 390-394.

279. Rosen, T., Elewski, B.E., Failure of clotrimazole-betamethasone dipropionate cream in treatment of Microsporum canis infections, J. Am. Acad. Dermatol. 32 (1995) 1050-1051.

280. Kast, C.E., Valenta, C., Leopold, M., Bernkop-Schnürch, A., Design and in vitro evaluation of a novel bioadhesive vaginal drug delivery system for clotrimazole, J. Control. Release 81 (2002) 347-354.

281. Duhm, B., Maul, W., Medenwald, H., Patzschke, K., Wegner, L.A., Oberste-Lehn, H., Pharmacokinetics of bis-phenyl-(2-chloro-phenyl)-1-imidazolyl-methane-(14 C) following topical administration, Arzneimittelforsch. 22 (1972) 1276-1280.

282. Kráčmar, J., Sotolongo, M.A., Kráčmarová, J., Ultraviolet spectrophotometry in drug control. XXI. Follow-up on the effects of substitution and solvents in new medicinal substances with chromophores of benzene and pyridine rings in the molecules, Cesk. Farm. 26 (1977) 345-353.

283. Jahnke, I.S., The theory of high-pressure homogenisation, in: Müller, R.H., Böhm B.H.L. (eds.), Dispersion techniques for laboratory and industrial scale processing, Wissenschaftliche Verlagsgesellschaft mbH, Stuttgart, 2001.

284. Zimmermann, I., Possibilities and limitations of laser light scattering techniques for particle size analysis, in: Müller, R.H., Mehnert, W. (eds.), Particle and surface characterisation methods, Medpharm, Scientific Publishers, Stuttgart, 1997.

285. Müller, R.H., Polydispersität elektrophoretische Beweglichkeit hochdisperser Systeme, PhD Thesis, University of Kiel, Germany, 1983.

286. Clas, S.-D., Dalton, C.R., Hancock, B.C., Differential scanning calorimetry: applications in drug development, PSTT 2 (1999) 311-320.

287. Ford, J.L., Timmins, P., Pharmaceutical thermal analysis, Ellis Horwood Ltd. Chichester, 1989.

288. Heurtault, B., Saulnier, P., Pech, B., Proust, J.-E., Benoit, J.-P., Physico-chemical stability of colloidal lipid particles, Biomaterials 24 (2003) 4283-4300.

289. Siekmann, B., Westesen, K., Thermoanalysis of the recrystallization process of melt-homogenized glyceride nanoparticles, Colloids Surface B 3 (1994) 159-175.

290. de Vringer, T., de Ronde, H.A.G., Preparation and Structure of a water-in-oil cream containing lipid nanoparticles, J. Pharm. Sci. 84 (1995) 466-472.

291. Hunter, R.T., Foundations of colloid science, Oxford University press, Oxford, 1986.

292. Krischner, H., Einführung in die Röntgenfeinstrukturanalyse, Vieweg Verlag Braunschweig, 4. Auflage, 1990.

293. Thoma, K., Serno, P., Precht, D., Röntgendiffraktometrischer Nachweis der Polymorphie, Pharm. Ind. 45 (1983) 420-425.

294. Garti, N., Effects of surfactants on crystallization and polymorphic transformation of fats and fatty acids, in: Crystallization and Polymorphism of Fats and Fatty Acids, Surfactant Science Series, Garti, N., Sato, K., eds, Vol. 32, Marcel Dekker, New York, 1988, pp. 267-303.

295. Fiese, E.F., Hagen, T.A., Pre-formulation, in: The Theory and Practice of Industrial Pharmacy, Lachman, L., Lieberman, H.A., Kanig, J.L. eds., Lea & Febiger, Philadelphia, 1986.

296. Rücker, A., Neugebauer, M., Willems, G.G., Instrumentelle pharmazeutische Analytik, 2. Auflage, Wissenschaftliche Verlagsgesellschaft mbH, Stuttgart, 1992, pp. 57-100.

297. Skoog, D.A., Leary, J.J., Instrumentelle Analytik, Springer Verlag, Berlin, 1996.

298. Franz, T.J., Percutaneous absorption. On the relevance of in vitro data, Invest. Dermatol. 64 (1975) 190-195.

299. Barry, B.W., Drugs and the Pharmaceutical Sciences, Dermatological Formulations-Percutaneous Absorption, in: Rheology of Dermatological Vehicles, Marcel Dekker, vol.18 (1983), pp. 351-396.

300. Ceulemans, J., van Santvliet, L., Ludwig, A., Evaluation of continuous shear and creep rheometry in the physical characterisation of ointments, Int. J. Pharm. 176 (1999) 187-202.

301. Eros, I., Rheologische Untersuchung einiger neuerer emulsions Salbengrundlagen, Pharmazie 31 (1976) 241-246.

302. Wood, J.H., Pharmaceutical rheology, in: The Theory and Practice of Industrial Pharmacy, Lachman, L., Lieberman, H.A., Kanig, J.L. eds., Lea & Febiger, Philadelphia, 1986, pp.123-145.

303. Stricker, H., Physikalische Pharmazie, Auflage, wissenschaftliche Verlagsgesellschaft mbH Stuttgart, 1987.

304. Barry, B.W., Warburton, B., Some rheological aspects of cosmetics, J. Soc. Cosmet. Chem. 19 (1968) 725-744.

305. Eccleston, G.M., Barry, B.W., Davis, S.S., Correlation of viscoelastic functions for pharmaceutical semisolids: comparison of creep and oscillatory tests for oil-in-water creams stabilized by mixed emulsifiers, J. Pharm. Sci. 62 (1973) 1954-1961.

306. Martin, A., Rheology, in: Physical Pharmacy, 4th Ed., Martin, A., ed., Lea & Febinger, Philadelphia, 1993, pp. 453-476.

307. Reich, G., Rheologie, in :Herzfeldt, C.-D., Kreuter, J., (Hrsg.), Grundlagen der Arzneiformenlehre Galenik 2, 1. Auflage, Springer-Verlag Berlin Heidelberg New York, 1999, pp. 275-301.

308. Stieß, M., Mechanische Verfahrenstechnik 1, Springer-Verlag Berlin Heidelberg New York, 1995, pp.59-62.

309. de Vringer, T., Topical preparation containing a suspension of solid lipid particles, European Patent N°. 91200664, 1992.

310. Müller, R.H., Böhm, B.H.L., Nanosuspensions, in: Emulsions and nanosuspensions for the formulation of poorly soluble drugs, Müller, R.H., Benita, S., Böhm, B., eds., Medpharm, Stuttgart, 1998.

311. Freitas, C., Feste Lipid Nanopartikel (SLN): Mechanismen der physikalischen Destabilisierung und Stabilisierung, PhD Thesis, Freie Universität Berlin, 1998.

312. Yoshino, H., Kobayashi, M., Samejima, M., Influence of the fatty acid composition on the properties and polymorphic transition of fatty suppository bases, Chem. Pharm. Bull. 31 (1983) 237-246.

313. Müller, R.H., Heinemann, S., Fat emulsions for parenteral nutrition. II. Characterization and physical stability of Lipofundin MCT/LCT, Clinical Nutrition, 12 (1993) 298-309.

314. Müller, R.H., Zetapotential und Partikelladung in der Laborpraxis, APV paperback series, Vol. 37, Wissenschaftliche Verlagsgesellschaft mbH Stuttgart, Germany, 1996.

315. Müller, R.H., Heinemann, S., Fat emulsions for parenteral nutrition. III. Lipofundin MCT regimens for TPN with low and medium electrolyte load, Int. J. Pharm. 101 (1994) 175-189.

316. Bunjes, H., Siekmann, B., Westesen, K., Submicron lipid suspensions (Solid lipid nanoparticles) versus lipid nanoemulsions: similarities and differences, in: Submicron Emulsions in Drug Targeting and Delivery, Benita, S. ed., Harwood Academic Publishers, Amsterdam, 1998, pp. 175-204.

317. Boistelle, R., Fundamentals of nucleation and crystal growth, in: Crystallization and Polymorphism of Fats and Fatty Acids, Surfactant Science Series, Garti, N., Sato, K., eds.,Vol. 32, Marcel Dekker, New York, 1988, pp. 189-226.

318. Müller, R.H., Schwarz, C., zur Mühlen, A., Mehnert, W., Incorportion of lipophilic drugs and drug release profiles of solid lipid nanoparticles, Proc. Int. Symp. Control. Rel. Bioact. Mater. 21 (1994) 146-147.

319. Olbrich, C., Mehnert, W., Müller, R.H., Development of an in vitro degradation assay for solid lipid nanoparticles, Proc. 2nd World Meeting APGI/APV, Paris, pp. 627-628.

320. Lippacher, A., Müller, R.H., Mäder, K., Investigations on the viscoelastic properties of lipid based colloidal drug carriers, Int. J. Pharm. 196 (2000) 227-230.

321. Lippacher, A., Müller R.H., Mäder, K., Semisoid SLN™ dispersions for topical application: influence of formulation and production parameters on viscoelastic properties, Eur. J. Pharm. Biopharm. 53 (2002) 155-160.

322. Müller, B.W., Lucks, J.S., Stampa, B., Müller R.H., Effect of anti-floculants on suspension stability and size distribution, Pharm. Ind. 52 (1990) 789-793.

323. Wissing, S.A., Lippacher, A., Müller-Goymann, C.C., Müller, R.H., Highly concentrated solid lipid nanoparticles (SLN): Production and transmission electron microscopy (TEM) investigations, Proc. 4th World Meeting APGI/APV, Florence, 2002, 811-812.

324. Kobayashi, M., Vibrational spectroscopy aspects of polymorphism and phase transition of fats and fatty acids, in: Crystallization and Polymorphism of Fats and Fatty Acids, Garti, N., Sato, K., eds., Marcel Dekker Inc., New York, Basel, 1988, pp. 139-188.

325. Diffey, B.L., Farr, P.M., Sunscreen protection against UVB, UVA and blue light: an in vivo and in vitro comparison, Br. J. Dermatol. 124 (1991) 258-263.

326. Hildebrand, G.E., Dingler, A., Runge, S.A., Müller, R.H., Medium scale production of solid lipid nanoparticles (SLN), Int. Symp. Control. Release Bioact. Mater. 25 (1998) 968-969.

327. Müller, R.H., Dingler, A., Runge, S.A., Schneppe, T., Gohla, S., Large scale production of solid lipid nanoparticles (SLN™) and nanosuspensions (DissoCubes™), in: Wise, D., ed., Handbook of Pharmaceutical Controlled Release Technology, Marcel Dekker, New York, 2000, pp. 359-376.